การเตรียมอินดิเคเตอร์กระดาษอเนกประสงค์จากไดแอเซทิลีนลิพิด

นายวัชชรินทร์ งามพึงพิศ

วิทยานิพนธ์นี้เป็นส่วนหนึ่งของการศึกษาตามหลักสูตรปริญญาวิทยาศาสตรดุษฎีบัณฑิต
สาขาวิชาปิโตรเคมี
คณะวิทยาศาสตร์ จุฬาลงกรณ์มหาวิทยาลัย
ปีการศึกษา 2555
ลิขสิทธิ์ของจุฬาลงกรณ์มหาวิทยาลัย

PREPARATION OF MULTI-PURPOSED PAPER INDICATORS FROM DIACETYLENE LIPIDS

Mr. Watcharin Ngampeungpis

A Dissertation Submitted in Partial Fulfillment of the Requirements
for the Degree of Doctor of Philosophy Program in Petrochemistry
Faculty of Science
Chulalongkorn University
Academic Year 2012

Thesis Title	PREPARATION OF MULTI-PURPOSED PAPER INDICATORS FROM DIACETYLENE LIPIDS
By	Mr. Watcharin Ngampeungpis
Field of Study	Petrochemistry
Thesis Advisor	Associate Professor Mongkol Sukwattanasinitt, Ph.D.
Thesis Co-advisor	Gamolwan Tumcharern, Ph.D.

Accepted by the Faculty of Science, Chulalongkorn University in Partial Fulfillment of the Requirements for the Doctoral Degree

.....Dean of the Faculty of Science
(Professor Supot Hannongbua, Dr. rer. nat.)

THESIS COMMITTEE

.....Chairman
(Assistant Professor Warinthorn Chavasiri, Ph.D.)

.....Thesis Advisor
(Associate Professor Mongkol Sukwattanasinitt, Ph.D.)

.....Thesis Co-advisor
(Gamolwan Tumcharern, Ph.D.)

.....Examiner
(Associate Professor Nuanphun Chantarasiri, Ph.D.)

.....Examiner
(Assistant Professor Varawut Tangpasuthadol, Ph.D.)

.....External Examiner
(Assistant Professor Rakchart Traiphol, Ph.D.)

วัชชรินทร์ งามพึงพิศ : การเตรียมอินดิเคเตอร์กระดาษอเนกประสงค์จากไดแอเซทิลีนลิพิด. (PREPARATION OF MULTI-PURPOSED PAPER INDICATORS FROM DIACETYLENE LIPIDS) อ.ที่ปรึกษาวิทยานิพนธ์หลัก : รศ.ดร.มงคล สุขวัฒนาสินิทธิ์, อ.ที่ปรึกษาวิทยานิพนธ์ร่วม : ดร.กมลวรรณ ธรรมเจริญ, 138 หน้า.

ได้สังเคราะห์ไดแอเซทิลีนที่มีหมู่ปลายเป็นเบตาอะลานีนเอทิลเอสเทอร์และไดเบตาอะลานีนเอทิล เอสเทอร์ด้วยวิธีเอไมด์คัปปลิงโดยใช้อีดีซีและเอชโอบีทีเป็นสารคัปปลิง ไดแอเซทิลีนที่สังเคราะห์ได้สามารถนำไปเคลือบบนกระดาษกรองโดยวิธีการจุ่มแล้วฉายด้วยแสงยูวี 254 นาโนเมตร จากนั้นนำไปศึกษาสมบัติการเป็นอินดิเคเตอร์ 4 ประเภท ได้แก่ อินดิเคเตอร์ตรวจวัดปริมาณรังสียูวี อินดิเคเตอร์ตรวจวัดอุณหภูมิ อินดิเคเตอร์ตรวจชนิดตัวทำละลายและอินดิเคเตอร์ตรวจวัดความชื้น โดยอาศัยการบันทึกภาพการเปลี่ยนสีและแปลงเป็นค่าสีอาร์จีบีเพื่อนำไปสร้างเป็นกราฟระหว่างเปอร์เซ็นต์สีน้ำเงินและแดงเทียบกับตัวแปรอิสระที่สนใจ เช่น เวลาและอุณหภูมิ ซึ่งกำหนดจุดตัดระหว่างกราฟเปอร์เซ็นต์สีน้ำเงินและสีแดงเป็นจุดเปลี่ยนสีของอินดิเคเตอร์ พบว่าความว่องไวในการตรวจวัดปริมาณรังสียูวีและอุณหภูมิของอินดิเคเตอร์ สามารถปรับเปลี่ยนได้จากการเปลี่ยนหมู่ปลายจากคาร์บอกซิลิกไปเป็นเบต้าอะลานีนเอทิลเอสเทอร์และไดเบต้าอะลานีนเอทิลเอสเทอร์และการเปลี่ยนความยาวของสายโซ่แอลิฟาติก จากการเปรียบเทียบหมู่ฟังก์ชันที่แตกต่างกัน ความว่องไวของการตรวจวัดความร้อนไม่ขึ้นกับความว่องไวในการตรวจวัดปริมาณรังสียูวี แสดงถึงการเปลี่ยนสีด้วยรังสียูวีเกิดจากกลไกอื่นนอกจากกลไกแบบการเปลี่ยนสีโดยความร้อนที่เหนี่ยวนำด้วยแสง นอกจากนี้ได้ศึกษาอินดิเคเตอร์อาร์เรย์ที่เตรียมจากพอลิไดแอเซทิลีน 6 ชนิด เพื่อใช้ในการตรวจวัดและจำแนกตัวทำละลายอินทรีย์ พบว่าอาร์เรย์ที่ได้มีความถูกต้องในการจำแนกชนิดของตัวทำละลายค่อนข้างต่ำคือประมาณ 74 เปอร์เซ็นต์ สำหรับอินดิเคเตอร์ตรวจวัดความชื้นสามารถเตรียมได้จากไดแอเซทิลีนที่มีหมู่ปลายเป็นกรดคาร์บอกซิลิก ได้แก่ ทีซีดีเอ และ พีซีดีเอ โดยอาศัยหลักการเปลี่ยนสีโดยเบสซึ่งเตรียมโดยการเคลือบแบ่งส่วนของไดแอเซทิลีนและโพแทสเซียมคาร์บอเนต ส่วนสีน้ำเงินของพอลิไดแอเซทิลีนเปลี่ยนเป็นสีแดงที่ความชื้นสัมพัทธ์ 62% โดยเริ่มจากรอยต่อระหว่างสองส่วนที่เวลา 3 ชม. และเปลี่ยนเป็นสีแดงทั่วทั้งส่วนของพอลิไดแอเซทิลีนภายใน 24 ชม. การเปลี่ยนสีที่ขึ้นกับเวลานี้ เหมาะสำหรับการนำไปพัฒนาเพื่อใช้งานจริงกับผลิตภัณฑ์ที่ว่องไวต่อความชื้นซึ่งมักมีการป้องกันความชื้นอยู่แล้ว แต่อาจมีโอกาสสัมผัสความชื้นเกินข้อจำกัดโดยไม่เจตนา

สาขาวิชา ปิโตรเคมี ลายมือชื่อนิสิต .....

ปีการศึกษา 2555 ลายมือชื่อ อ.ที่ปรึกษาวิทยานิพนธ์หลัก .....

ลายมือชื่อ อ.ที่ปรึกษาวิทยานิพนธ์ร่วม .....

5273847923 : MAJOR PETROCHEMISTRY
KEYWORDS : POLYDIACETYLENE / SENSORS / RGB / THERMOCHROMISM / PHOTOCHROMISM / SOLVATOCHROMISM / HUMIDITY

WATCHARIN NGAMPEUNGPIS : PREPARATION OF MULTI-PURPOSED PAPER INDICATORS FROM DIACETYLENE LIPIDS. ADVISOR : ASSOC. PROF. MONGKOL SUKWATTANASINITT, Ph.D., CO-ADVISOR : GAMOLWAN TUMCHARERN, Ph.D., 138 pp.

Diacetylenes with β-alanine ethyl ester and di-β-alanine ethyl ester were synthesized by amide coupling method using EDC and HOBt as coupling reagents. The diacetylene were fabricated onto filter paper and polymerized by 254 nm UV light. The prepared devices were intended to be used as indicators *i.e.* UV-dose, temperature, solvent and humidity indicators. The color transitions of the indicators were determined from their color images using the RGB color system in which the crossing point of %B and %R curves from their plots against the independent variables such as time and temperature. The sensitivity of UV and temperatures can be tuned by converting carboxylic acid head group to β-alanine ethyl ester and di-β-alanine ethyl ester and varing the number of aliphatic chain length. Comparing between different functional groups, the thermal sensitivity was not always in line with the UV sensitivity that demonstrated other mechanisms beyond the photo-induced thermochromism for the blue-to-red color transition induced by UV light. The attempt in constructing an indicator array from 6 PDAs for detection and classification of organic solvents gave relatively low classification accuracy of 74%. The diacetylene carboxylic acid could be used as humidity sensing materials via an alkalinochromism effect by a zone coating of the diacetylene and K_2CO_3. The blue PDA zone turned red at 62% RH with time dependence starting from the PDA/ K_2CO_3 interface at 3 h and completed within 24 h. This time dependent colorimetric transition is very attractive for real applications where the moisture-protected products are usually unintentionally exposed to the ambient humidity for an unknown period of time.

Field of Study : Petrochemistry Student's Signature .....
Academic Year : 2012 Advisor's Signature .....
Co-advisor's Signature .....

ACKNOWLEDGEMENTS

I would like to express my appreciation to my advisor, Associated Professor Dr. Mongkol Sukwattanasinitt and my co-advisor Dr. Gamolwan Tumcharern for their invaluable suggestion, generousness and extremely encouragement during the course of this research. This research is impossible to succeed without their helpfulness. Moreover, I have learned many things from my advisor such as attitude, creativeness, logic and kindness to students. He supported me to do the things that gave me the new experiences such as going to research in Japan, attending the Sci & Tech initiative and Sustainability contest until getting the award. I appreciate him and I try to remember to the things that he taught me for using in my life.

I would like to show gratitude to Assistant Professor Dr. Warinthorn Chavasiri, chairperson of dissertation defense committee, for their kind attention and recommendations. I also would like to thank Assistant Professor Dr. Paitoon Rashatasakhon, Assistant Professor Dr. Sumrit Watcharasindhu and Dr. Anawat Ajavakom for his attention and suggestion during our group meeting.

I would like to express my sincere gratitude to Dr. Prompong Pienpinijthum from Sensor Research Unit, Department of Chemistry, Faculty of Science, Chulalongkorn University for SEM data.

My appreciation is also given to many people in our research group; Dr. Warathip Siripornnoppakhun for PCA data and valuable advice, Mr. Chaiwat Phollookin and Dr.Thirawat Sirijindalert for training and suggestion in this research; Miss Kanokthorn Boonkitpattarakul and Miss Nattaporn Kimpitak for their helpfulness; and everyone in MAPS Group for a great friendships and encouragement;

I would like to thanks Chulalongkorn Universitiy and my financial support from the Thailand Graduate Institute of Science and Technology (TGIST) from NSTDA.

Finally, I would like to express my thankfulness to my beloved parents who always stand by my side during both of my pleasant and hard time.

CONTENTS

Page

Page

LIST OF TABLES

Page

Page

Page

Page

LIST OF FIGURES

Page

Page

Page

Page

Page

Page

Page

Page

LIST OF SCHEMES

Page

LIST OF ABBREVIATIONS

PDA	Polydiacetylene
PCDA	10,12-pentacosadiynoic acid
TCDA	10,12-tricosadiynoic acid
NDDA	6,8-nonadecadiynoic acid
ODDA	5,7-octadecadiynoic acid
EPCDP	Ethyl-3-pentacosa-10,12-diynoylamidopropanoate
ETCDP	Ethyl-3-tricosa-10,12-diynamidopropanoate
ENDDP	Ethyl-3-nonadeca-6,8-diynamidopropanoate
EODDP	Ethyl-3-octadeca-5,7-diynamidopropanoate
EPCDPP	Ethyl-3-(3-pentacosa-10,12-diynamidopropanamido) propanoate
ETCDPP	Ethyl-3-(3-tricosa-10, 12-diynamidopropanamido)propanoate
ENDDPP	Ethyl-3-(3-nonadeca-6,8-diynamidopropanamido)propanoate
EODDPP	Ethyl-3-(3-octadeca-5, 7-diynamidopropanamido)propanoate
EDC	1-Ethyl-3-(3-dimethylaminopropyl)carbodiimide
HOBt	1-Hydroxybenzotriazole hydrate
NMR	Nuclear magnetic resonance spectroscopy
DSC	Differential scanning calorimetry
SEM	Scanning electron microscopy
℃	Degree celsius
g	Gram
mL	Millilitre
µW	Microwatt
µL	Microlitre
mM	Millimolar
nm	Nanometre
µm	micrometre
min	Minute
%	Percent

CHAPTER I

INTRODUCTION

1.1 Background and statements of problems

Due to their unique optical and electrical properties associated with extensively delocalized π-electron networks and intrinsic conformational restrictions, conjugated polymers have been widely investigated for applications as indicators and sensors for detection of environmental condition. Particularly, their change of electronic absorption and emission properties have been gracefully applied to the design of efficient sensors [1,2].

Polydiacetylene (PDA) is a promising class of conjugated polymer successfully used as many sensors. PDAs can be produced by UV or γ-irradiation of crystalline or semicrystalline states obtained from molecular self-assembled diacetylene (DA) monomers without the need for chemical initiators or catalysts. The polymers possess unique colorimetric properties useful for sensing applications. Various types of stimuli such as temperature, organic solvent, mechanical stress, molecular recognition, pH and UV light can cause color change of PDAs. The color transition property can be tuned via rational design of supramolecular interactions among the polymeric side chains [3-5] PDAs have also been prepared in the forms of various nanostructures such as vesicles, tubes, and ribbons [6-11]. The formation of nanovesicles allows the preparation of homogeneously dispersed PDA vesicle sols resulting in several noteworthy chemical and biological sensing systems [12]. However, the aqueous sols have short shelf life and are not suitable for portable and tag-on applications. Fabrication of PDAs as solid state sensors or indicators in the form of gel [13] thin film [14,15] and electrospun fiber [16] have recently been reported. The preparation methods for these forms of PDAs generally require additional polymer matrix and equipment setup. Recently, white paper has been demonstrated as a very promising supporting material for portable and disposable multi-sensing devices because it is omnipresent, inexpensive and easy to be stored, transported and handled [17,18]. In our research group, we have also recently reported

the use of filter paper as a support for fabrication of PDA based colorimetric sensors of solvents, surfactants and VOCs [19-21].

UV-Vis absorption measurement is a common method for determination of colorimetric response percentage (%CR) for solution samples [9,15,22] but this technique does not generally give reliable values for opaque solid materials. CCD imaging technology has turned photography into a readily processable digital form [23]. The capability to capture wide area of image of digital imaging is also the advantage, in comparison with the reflective spectroscopic instrument, that produce more reliable color analysis of rough surface samples such as paper. For examples, it has recently been used along with the RGB color system to record and evaluate colorimetric sensors [17] including PDA films [19-21,24-25]. Despite these successes in quantifying colorimetric responses of solid state PDAs, there has not yet been proposition of the degree of color change that should represent the color transition point of PDA. In this research, a utilization of webcam and RGB values to quantify the color transition PDAs on paper support along with mathematical formula to use RGB values in specifying the color transition temperatures PDA paper based indicators. The technique developed in this work should provide practical guidelines for systematic and comparison of chromic properties of PDAs toward the development of economical and reliable multi-purposed paper indicators from diacetylenes.

1.2 Theory

1.2.1 Polydiacetylene

A polydiacetylene (PDA) is an ene-yne conjugated polymer comprising of double and triple bonds in its backbone. It can be prepared by a topological 1,4-addition polymerization of diacetylene monomer by UV light or γ-rays as shown in Figure 1.1.

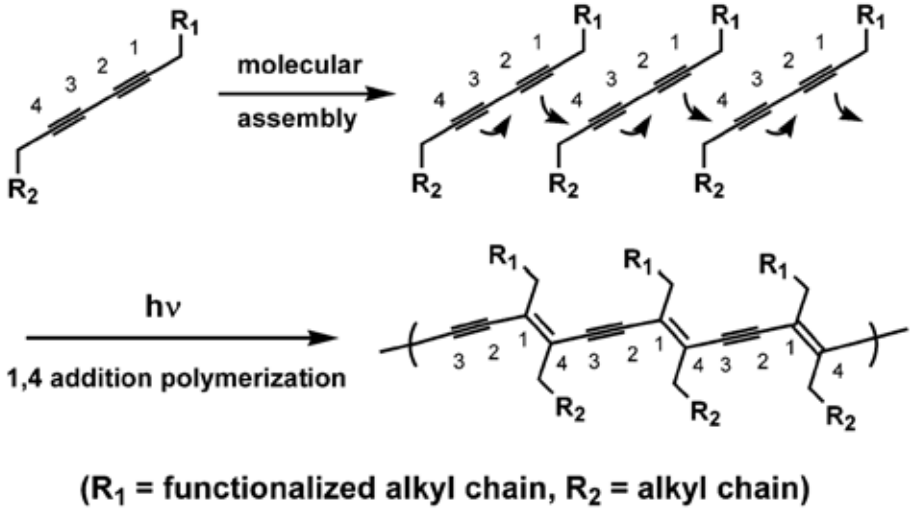

Figure 1.1 Phototopopolymerization of diacetylene monomers. [26].

Topological polymerization is a polymerization which requires specific prealignment of the monomer usually found in solid state crystal [*27*]. For topological polymerization of diacetylenes, the distance (d) between the corresponding tripple bonds of the adjacent monomers and the orientation angle (θ) relative to the translation axis should be ~5 Å and ~45º, respectively [28-29].

1.2.2 Polydiacetylene forms

There are numerous forms, which PDA can be structured: bulk single crystal, Langmuir monolayer film, multilayer film, nano tube and vesicle.

1.2.2.1 Polydiacetylene vesicles

The vesicle is one of the most widely used forms of polydiacetylene for sensor applications. It is water filled spherical assembly of lipid bilayer. The formation of vesicle is thermodynamically driven so that the hydrophobic surface of the lipid molecules is not exposed to water. Only the hydrophilic head group of the lipid is exposed to water inside and outside of the bilayer membrane. A number of lipids containing diyne unit can self assemble into vesicle that have the right packing parameters for topological polymerization to form PDA vesicles (Figure 1.2). In the form of vesicle, PDA can be homogeneously dispersed in an aqueous media to form a sol type colloid, which is convenient for further characterization, fabrication and applications. The most studied diacetylene lipids are 10,12-pentacosadiynoic acid

(PCDA). The interest in these lipid vesicles is mainly related to the development into bio- [30] and chemosensors [31].

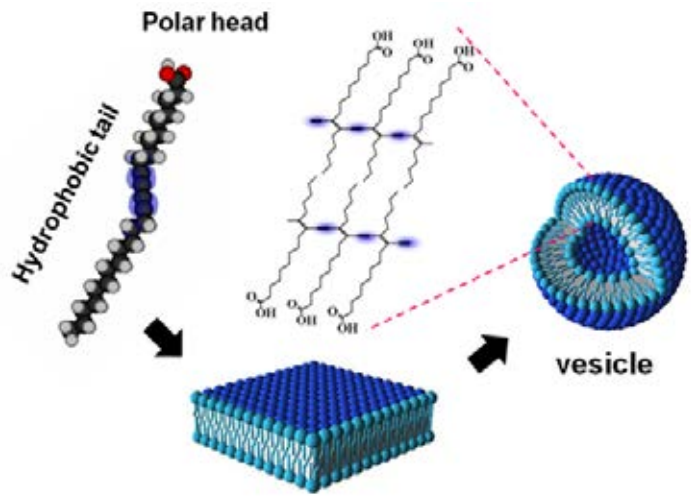

Figure 1.2 Structure and formation of a PDA lipid vesicle.

1.2.2.2 Polydiacetylene films

It is widely accepted that the sensing process of PDA of diacetylene lipids is initiated at the lipid head group. Intuitively, the most desirable form of PDA for sensing applications is thin film as it can maximize sensing area and it is easy to be developed into simple to use device. Several techniques have been utilized for making different types of thin films on the surface of substrates.

Langmuir-Blodgett film can generate an ideal highly ordered monolayer assembly of lipid molecules at water/air interface. The monolayer can be transferred onto solid substrate by horizontal or vertical deposition (Figure 1.3). The monolayer Langmuir-Blodgett film is however often fragile and difficult to prepare in large area. The number of layers can be increased by repeating the transferring process with a newly generated monolayer. Hence, it can be quite bothersome to prepare a multilayer film as the preparation of each new monolayer requires a slow surface compression and the transferring step needs adroit attention. This type of PDA film is one of the most interesting form of PDA in research but the development of the technique for practical mass production remains elusive [32].

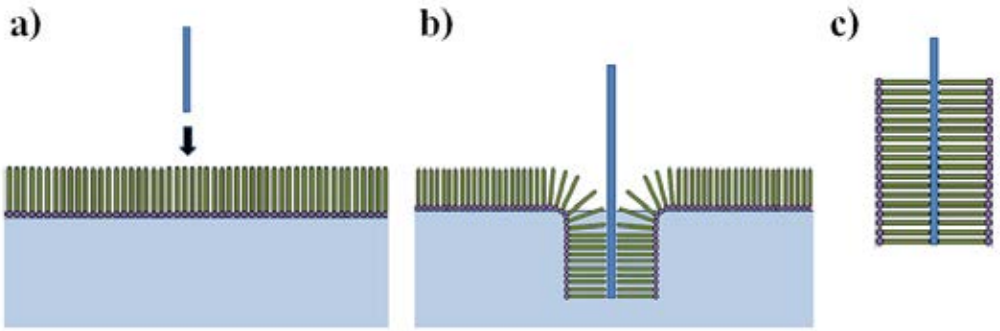

Figure 1.3 Preparation of Langmuir Blodgett film a) floating of condensed monolayer film on the water subphase, b) film deposition, c) monolayer films on the substrate.

1.2.2.3 Polydiacetylene electrospun fibers

Electrospinning has proved to be an efficient method for forming long polymer fibers with diameters in the range from nanometers to several micrometers as shown in Figure 1.4. In this technique, a high voltage is applied to a conductive capillary attached to a reservoir containing a polymer solution as shown in Figure 1. A charged polymer jet is ejected from the surface of the polymer solution when the charge imbalance exceeds the surface tension of the polymer solution. Polymer fibers are formed when the jet stream, driven by the electrostatic force, moves to the grounded screen collector [33].

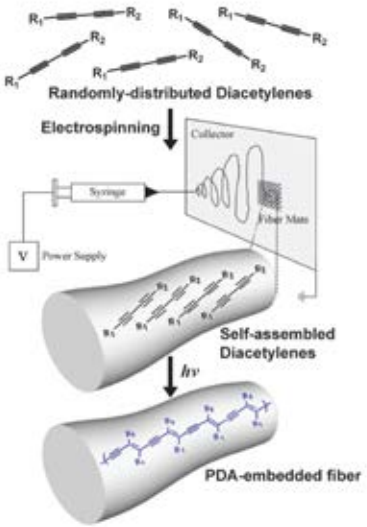

Figure 1.4 A schematic representation of the preparation of polymer fibers embedded with PDA supramolecules using the electrospinning technique, followed by irradiation with UV light.

1.2.3 Colorimetric properties of polydiacetylene

PDAs usually appear as deep colored materials that exhibit interesting colorimetric properties. Optical absorption in polydiacetylene occurs via an electronic $\pi \rightarrow \pi^*$ transition within the linear π-conjugated polymer backbone. Upon polymerization, frequently the first chromogenically interesting state of PDA appears blue in color. The exposure of PDA to environmental perturbations, such as temperature, UV light, pH, solvent, mechanical stress and ligand-receptor interactions, induce a significant shift in absorption from low to high energy bands of the visible spectrum, so the polydiacetylene transforms from blue ($\lambda_{max} \sim 630$ nm) to red ($\lambda_{max} \sim 540$ nm). These perturbations alter the polymer side chain orientation that inturn change the backbone strain and torsion, thus changing the electronic states and the corresponding optical absorption.

The most investigated PDAs are those having blue color, which can change their color to red corresponding to the shift of the maximum absorption peak from as a result of reduction of the effective conjugation length. The color transition can be induced by several external stimuli

1.2.3.1 Colorimetric Response (CR)

The color transition of the polymerized vesicles was monitored by measuring the absorbance differences between the vesicles before and after stimulation by an interesting parameter. This information is often converted to a percentage, termed the Colorimetric Response (CR) [34].

A quantitative value for the extent of blue-to-red color transition is given by the colorimetric response (%CR) which is defined as

$$\%CR = (PB_0\text{-}PB)/PB_0 \times 100$$

Where $PB = A_{blue}/(A_{blue}+A_{red})$, A_{blue} and A_{red} are the absorbance of the blue and the red phase at 630 and 540 nm, respectively. The visible absorbance was measured by a temperature controlled UV-vis spectrometer. PB_0 is the initial percent blue of the vesicle solution and film before heated. All blue-colored PDA vesicle solution and film samples were heated from 10 to 90 ℃.

1.2.4 RGB color model

According to development of paper based colorimetric respond of polydiacetylene is a simple method and suitable to use as a sensors application, since evaluate the results into a quantitative analysis can be collected by using the RGB color model. The RGB color model is an additive color model in which red, green, blue color are added together in various component ratio to reproduce a broad array of colors as shown in Figure 1.5. The name of the model comes from the initials of the three additive primary colors, red, green, and blue. The main purpose of the RGB color model is for the sensing, representation, and display of images. The RGB color model was used to descript how much of each red, green, and blue color is included in the photographic images [35].

For the basic of the RGB value(R, G, B), the color is black when the intensity of each component is zero (0, 0, 0) and the color is white when the intensity of each component is full (255, 255, 255). When the intensities are the same, the result is a shade of gray, darker or lighter depending on the intensity.

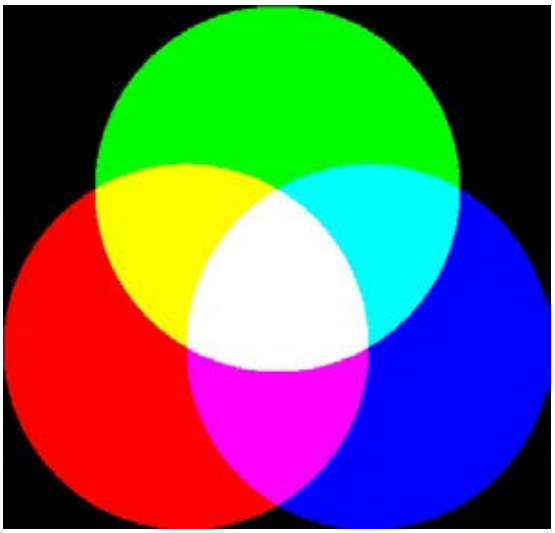

The RGB color model.

1.3 Literature surveys on applications of polydiacetylenes

1.3.1 Thermochromism

Thermochromism, the color transition upon the increase of temperature, is one of the interesting chromic properties of polydiacetylenes both for its applications and fundamental understanding. Thermochromism in polydiacetylenes arises from the conformational changes of the conjugated backbone from planar to non-planar due to movement of the side chains. The color transition is thus resulted from the increase of energy gap between the HOMO and LUMO level. The color transition of polydiacetylenes is driven by the relief of mechanical strain in their structures [36].

For polydiacetylene vesicles, hydrogen bonding between the head groups of the lipid monomers is usually responsible for the planarity of the conjugated backbone. Thermal energy can break or weaken the hydrogen bonding between the head groups resulting in random movement of the side chains and lower the planarity of the backbone and hence the average conjugation length of π-electrons along the polymer backbone inducing the color change from blue to red.

In 1998, Okada *et al.* [9] studied the self-assembly in vesicles form of diacetylene containing carboxylic in hydrophilic head group and its derivatives which various alkyl chain length within the chain and between diacetylene and carboxyl group (Figure 1.6) in water media. Then polymerized by UV-irradiation 254 nm and studied the thermochromic properties monitoring by UV-vis spectrometer. It was found that polydiacetylene which have the short alkyl chain length between diacetylene and carboxyl group (compound 3 and 4) were more sensitive to the thermal changes than long alkyl chain length (compound 1 and 2).

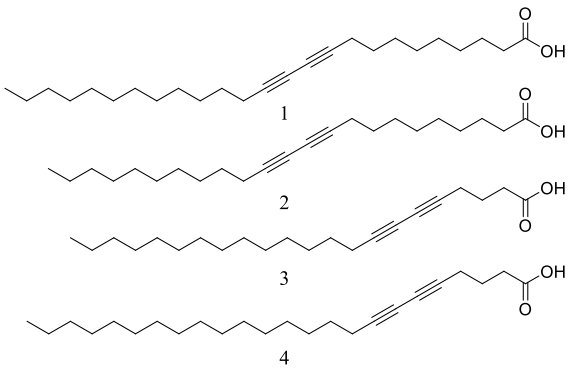

Figure 1.6 Structure of diacetylene monomers used in investigations of thermochromism in vesicles.

In 2005, Kim *et al.* [26] reported the colorimetric reversibility of polydiacetylene supramolecules, derived from a variety of functionalized diacetylenic lipids as shown in Figure 1.7. Polydiacetylene vesicles prepared from PCDA-mBzA 1, bearing terminal m-carboxyphenylamido groups. They studied the effects of (1) internal amide groups, (2) headgroup aromatic interactions, (3) lengths of the hydrophobic alkyl chains, and (4) terminal carboxylic groups on the colorimetric reversibility of polydiacetylene. The results demonstrate that well developed hydrogen-bonding and aromatic interactions between headgroups are essential for complete recovery of the length of the conjugated π-electron chain following thermal stimulus.

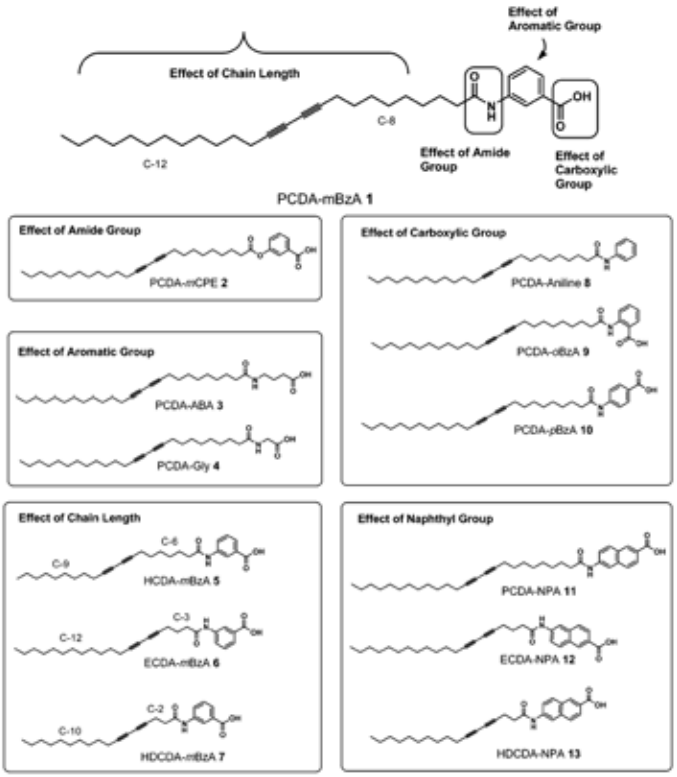

Figure 1.7 Structures of diacetylene lipids investigated for thermochromism.

In 2007, Fujita *et al.* [37] proposed that molecular modeling to seek a stable conformation of PDA prepared from G*n*s in the gel state which is useful in predicting the effective conjugation length (ECL) in PDA where the odd-even number of alkyl

chains (*n*) is a key factor for determining the blue and red phases of the PDAs (See in Figure1.8).

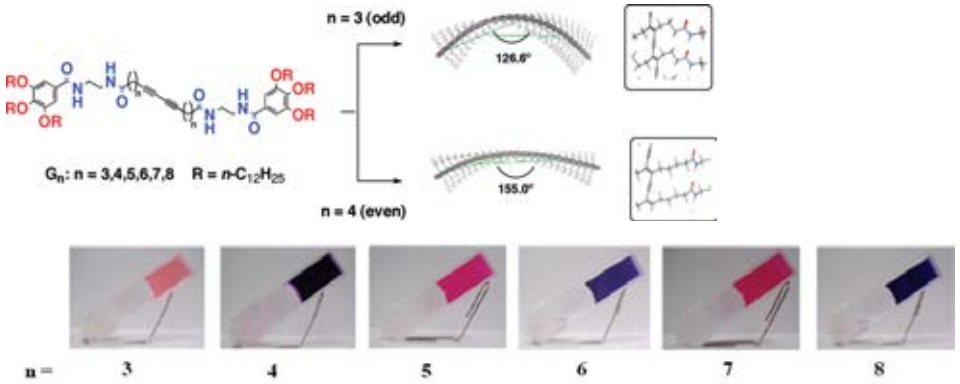

Figure 1.8 Chemical structure of G_n and the optimized conformation of 24 mers of (upper) polyG_3 and (lower) polyG_4.

In 2010, Wacharasindhu *et al.* [4] synthesized Mono- and diamides derivatives of 10, 12-pentacosadiynoic acid (PCDA) from condensation of PCDA with various aliphatic and aromatic diamines. The color transition temperatures and thermochromic reversibility of the polymers are varied depended on the number of amide groups and the structure of the aliphatic and aromatic linkers. The phenylenediamide and polymethylenediamide PCDA derivatives give polydiacetylenes with complete thermochromic reversibility, while the polydiacetylenes obtained from 1,2-cyclohexylene and glycolic chain diamide derivatives exhibited irreversible thermochromism, whereas the polymers attained from the aromatic monoamide analogues are partially reversible. The variation of the linkers also allows the color transition temperature of the polydiacetylene to be tuned in the range of 20 °C to over 90 °C (See in Figure 1.9).

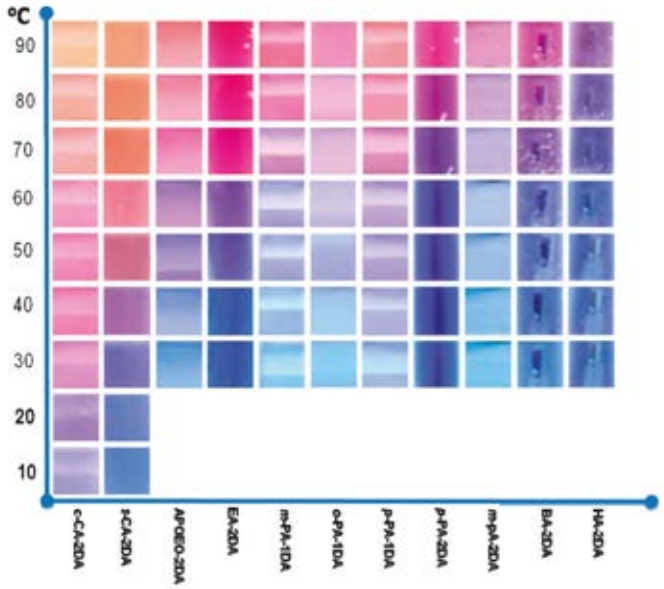

Figure 1.9 Color of PDA sols recorded by photography during the heating process displaying the variation of color transition temperature.

In 2010, Phollookin *et al.* [5] investigated a series of bisdiynamide lipids containing various lengths of methylene spacer (m=2, 3 and 4) between the diynes and the diamide headgroup and number of methylene units (n = 6 and 9) in their hydrophobic tails are synthesized. The color transitions from blue to red during heating-cooling cycles of the PDA sols are photographically recorded and monitored byUV-vis absorption spectroscopy. The bisdiynamide PDAs exhibit excellent thermochromic reversibility and the color transition temperature can be tuned between 25-55 °C by the variation of m and n values as shown in Figure 1.10. The decrease of n value enhances the thermal sensitivity resulting in lower color transition temperature, the effect of m value is not as straightforward. Moreover, temperature indicators can be obtained by applying a screen printing ink formulated from the bisdiynamide monomer on plastic substrates followed by UV irradiation to generate desired patterns of thermochromically reversible PDAs.

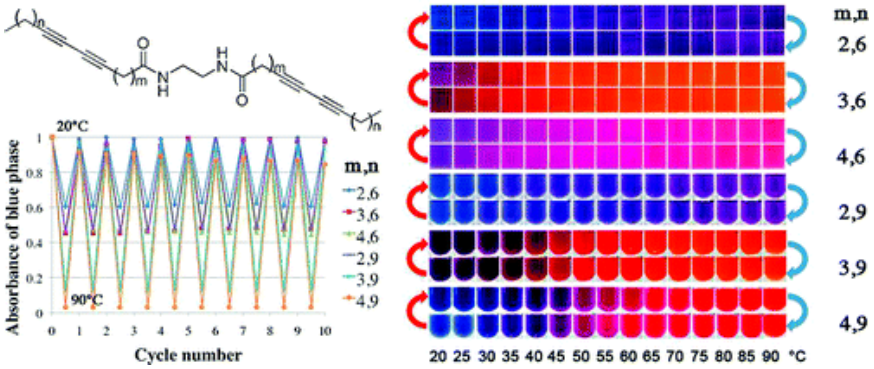

Figure 1.10 Structure of diacetylene monomers, their color transition and reversibility in vesicles solution.

In 2012, Ampornpun *et al.* [38] reported that two series of symmetrical (Sx) and unsymmetrical (Uy) diacetylene monomers containing diamide groups with different methylene units are successfully prepared (See in Figure 1.11). Photopolymerization of their nanovesicles dispersed in water is carried out by irradiation at 254 nm affording blue sols of the corresponding PDAs. The degree of thermochromic reversibility (%DR) of the PDA sols are determined using UV−vis spectroscopy in order to probe effects of the number of the methylene units, x and y , within the linker and hydrophobic tail, respectively. The complete color reversibility (%DR > 89%) is observed only when x is an even number while partially reversible or irreversible thermochromism (%DR < 65%) is displayed in the case of odd x number. For the Uy series, the color recovering ability within the heating and cooling process increases along with the y number; %DR = 3, 62, and 90% for y = 0, 4, and 16, respectively. This work is the first direct demonstration of the roles of number of methylene units within the diacetylene monomers on the thermochromic reversibility of their PDAs that provide additional dimensions for rational molecular design in the development of PDA thermal sensors.

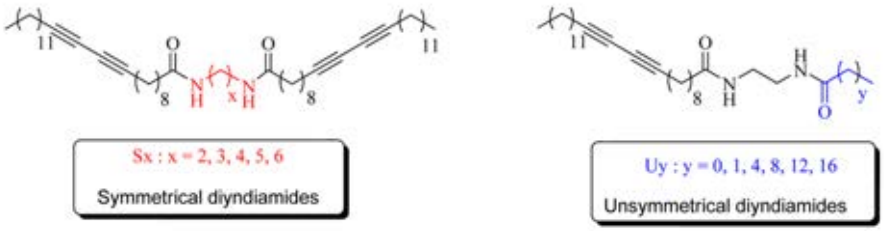

Figure 1.11 Structure of investigated diacetylene monomers: symmetrical diyndiamides (Sx) and unsymetrical diyndiamide monomers (Uy).

In 2013, Chanakul *et al.* [39] reported polydiacetylene (PDA)/ZnO nanocomposites are prepared by using three types of monomers with different alkyl chain length, 5, 7-hexadecadiynoic acid, 10, 12-tricosadiynoic acid, and 10,12-pentacosadiynoic acid. The monomers dispersed in aqueous medium spontaneously assemble onto the surface of ZnO nanoparticles, enhanced by strong interfacial interactions. All nanocomposites show reversible blue/purple color transition upon multiple heating/cooling cycles, while the irreversible blue/red color transition is observed in the systems of pure PDAs (Figure 1.12). The shortening of alkyl side chain in PDA/ZnO nanocomposites leads to a systematic decrease in their color transition temperatures.

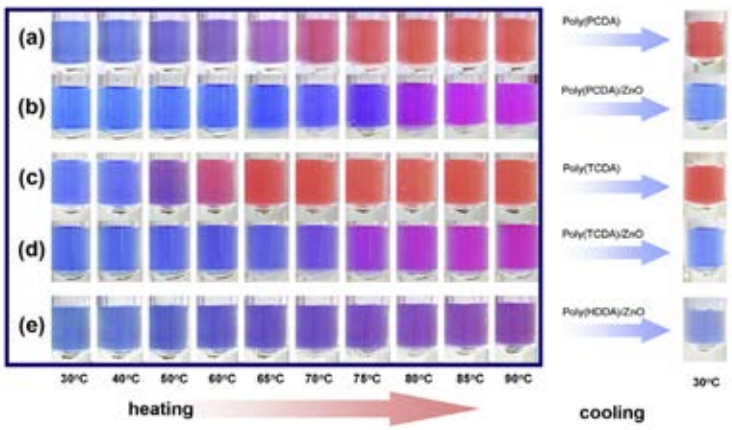

Figure 1.12 Color photographs of the aqueous suspensions of (a) pure poly(PCDA), (b) poly(PCDA)/ZnO nanocomposite, (c) pure poly(TCDA), (d) poly(TCDA)/ZnO nanocomposite, and (e) poly(HDDA)/ZnO nanocomposite taken upon increasing temperature from 30 to 90 °C, followed by cooling to room temperature.

1.3.2 Photochromism

Photochromism were chromic properties that material can change color by irradiation of UV light or γ-rays. The mechanism of color transition of PDA by photo is not clear. There are groups of diacetylene monomer had affect on the colorimetric transition as reported by several researchers.

In 1985, Kanetake *et al.* [40] investigated the change of absorption spectra by UV light irradiation (photo-chromism) and by thermal annealing (thermo-chromism) have been investigated on vacuum-deposited polydiacetylene (12-8 PDA) films. The

results are compared with those of the Langmuir-Blodgett films of the same 12-8 PDA. It is suggested that the blue-to-red colour conversion of these films is associated with a isomeric transformation of the polymer backbone structures. The films also show a remarkable colour change by a visible laser-beam irradiation.

In 1987, Tokura [41] reported that the photoinduced change in absorption spectra has been measured on poly(10, 12-pentacosadiynoic acid) (PDA-12,8) films for various photon energies and light intensities. The observed photochromic behaviors indicate that photoexcited electron-hole pairs in polymer backbone chains relax into a metastable state which develops into clusters with a local change in bond structure via a temperature independent and self-activated multiple excitation process produced by light irradiation.

In 1989, Wenzel and Atkinson [42] investigated that the thermochromic and proposed visible photochromic properties of poly(10, 12-pentacosadiynoic acid) (PDA-12,8) are examined by resonance Raman (RR) and Fourier transform infrared (FTIR) spectroscopies. Irradiation at 532 nm of water-cooled (0.5 ℃) samples of the blue-colored material produces no chromatic changes. A chromatic change to the red-colored material is induced by 532-nm radiation, however, when the PDA-12,8 is not cooled. No evidence supporting a visible photochromic change in PDA-12,8 is found, and it is proposed that the previously reported chromatic properties derive from thermal effects. RR results also show that no change occurs in the distribution of electron density along the PDA-12,8 backbone when chromatic effects are induced.

In 1997, Peng [43] investigated the photochromism in polydiacetylene crystals. It is considered that the photochromism is the result of phase structural conversion during photoexcitation excitonic relaxation process, and its dependence on the energy and density of incident photons can be explained correctly. They claimed that he electronic excitation state is unaffected by localized heating of laser irradiation. If this conversion is mainly caused by localized heating, the change of color will spread to surrounding nonirradiated region because of very high thermal conductivity of polydiacetylene crystals.

In 1999, Huo *et al.* [44] studied a new diacetylene compound (PDATAZ), which readily formed a complementary hydrogen bonding self-assembly at the air-water interface or in the solid state with barbituric acid (BA) or cyanuric acid (CA). It

was found that the chromatic property of polydiacetylenes is determined by whether the polymer chain is capable of adopting a linear chainlike shape. With the continuous increase of the length of the polymer chain, the original linear polyenyne backbone starts to “self-fold” to a “zigzag” structure due to the free rotation of single bonds within the polymer chain. The efficient π-electron delocalization along the polyenyne backbone is interrupted by this process, leading to a chromatic change from the blue to red form of polydiacetylenes. If there are strong intermolecular interactions existing between the polar groups of the side chains, such as the complementary hydrogen-bonding network between the triaminotriazine (TAZ) moiety of the diacetylene amphiphile and its complementary components, the movement of the side chains is restricted and the folding process of the polymer backbone is inhibited. The polymer backbone is able to maintain its extended chainlike conformation, leading to only the blue form absorption band.

In 2004, Song *et al.* [45] reported the design, preparation, and characterization of self-assembling functional bolaamphiphilic polydiacetylenes (BPDAs) inspired by nature’s strategy for membrane stabilization. The conjugated polymers can be engineered to display a range of radiation-, thermal-, and pH-induced colorimetric responses (Figure 1.13). They observed dramatic nanoscopic morphological transformations accompanying charge-induced chromatic transitions, suggesting that both side-chain disordering and main-chain rearrangement play important roles in altering the effective conjugation lengths of the poly(ene-yne).

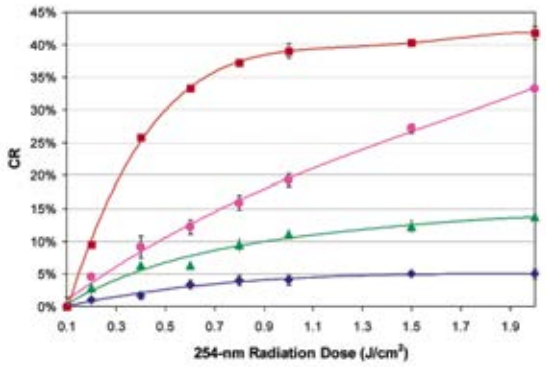

Figure 1.13 Radiation dose-induced colorimetric response of BPDAs: BPDA-1 (green triangle); BPDA-2 (pink circle); BPDA-3 (blue diamond); BPDA-4 (red square). Error bars indicate the standard deviation of six replicate experiments.

In 2006, Yuan *et al.* [46] revealed that a photoinduced chromatic transition from blue to red for the polydiacetylene 10, 12-pentacosadiynoic acid produces an obvious change in the ultraviolet–visible absorption and fluorescence emission spectra. A two-dimensional micropattern has been realized on the basis of this change and imaged with a confocal fluorescence microscope. The results indicate that the conformational change of alkyl side chains constricted by hydrogen-bonded head groups imposes strain on the polymer backbone and finally leads to a drastic decrease in the π-electron-conjugation length.

In 2010, Sung *et al.* [47] reported highly ordered lamellar polydiacetylene nanocomposites synthesized by assembling polydiacetylene and azobenzene through a ready solution process. The trans-to-cis transition of azobenzene under UV light may induce a conformation change of PDA with color changes through pulling on its side chains as shown in Figure 1.14. Lengths of the side chains play a critical role for the transfer efficiency of the conformation change from azobenzene to PDA.

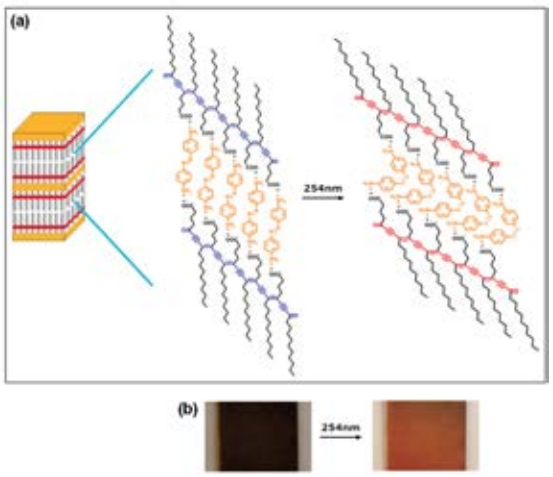

Figure 1.14 PDA nanocomposite films with ordered lamellar mesostructure derived from 4,4′-azodianiline and 5,7-octadecadiynoic acid. (a) Schematic illustration of trans-to-cis transition in azobenzene under UV irradiation and chromatism of complexed PDA. (b) Photographs of blue and red films during the above process.

1.3.3 Solvatochromism

Solvatochromism is the ability of a chemical substance to change color due to a change in solvent polarity. The molecularly ordered states of supramolecular PDAs

can be influenced also by the presence of organic solvents as investigated by many researchers.

In 2007, Kim *et al*. [31] have developed the efficient sensors for the detection of volatile organic compounds (VOCs) based on conjugated polymer-embedded electrospun fibers. The observation of an organic solvent induced, blue-to-red color transition of PDA embedded electrospun fibers suggests that the colorimetric response might vary in an organic solvent-dependent manner on the structure of diacetylene monomer. They show different colorimetric responses upon exposure to the 4 organic solvents such as chloroform, tetrahydrofuran (THF), ethyl acetate (EA), or *n*-hexane as illustrated in Figure 1.15.

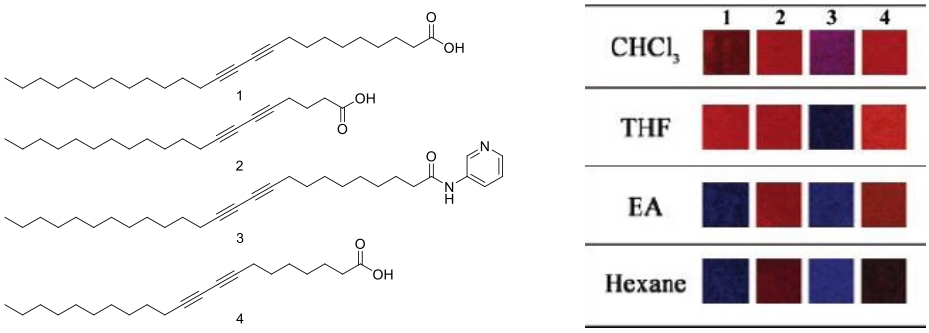

Figure 1.15 Photographs of the PDA-embedded electrospun fiber mats prepared with diacetylene monomers **1-4** after exposure to organic solvent.

In 2008, A. Potisatityuenyong and co worker [3] conduced extensively investigation poly-10,12-pentacosadiynoic acid (poly(PCDA)) vesicle solution in the aspect of thermochromism, solvatochromism and alkalinochromism. In the case of solvatochromic and alkalinochromic experiment, UV-vis absorption and observation by eye show the similar pattern, blue to red color transformation. The decreasing and increasing in absorbance of red and blue phase without peak shifting indicate directly to quantitative conversion between blue and red vesicle. Solvatochromism and alkalinochromism involve hydrogen bond breaking turning the blue vesicle into red color. The author proposed the mechanism of color transition of PCDA as shown in Figure 1.16.

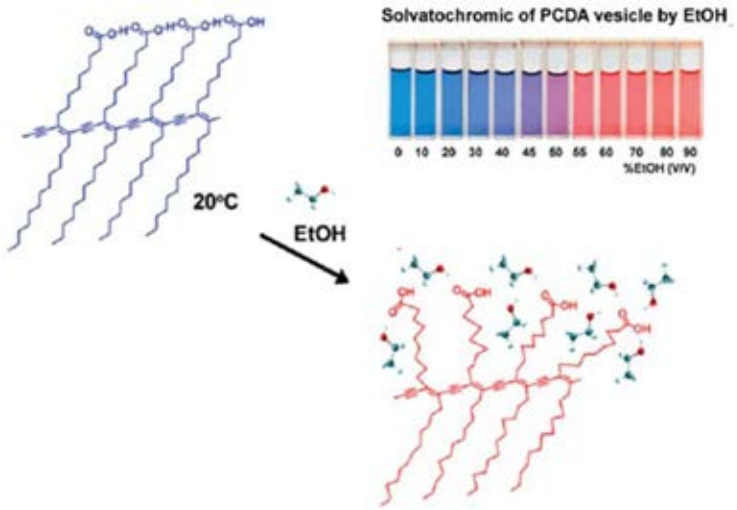

Figure 1.16 Proposed side-chain movements in the chromic transitions of poly(PCDA) vesicles upon organic solvent.

In 2009, Yoon *et al*. [48] have generated the electrospun fiber mats from PDA-embedded polymer matrix that can be used to detect volatile organic compounds (VOCs). The results display the different color patterns of the fiber mats derived from different combinations of PDA-ABA 1 and PCDA-AN 2 as illustrated in Figure 1.17.

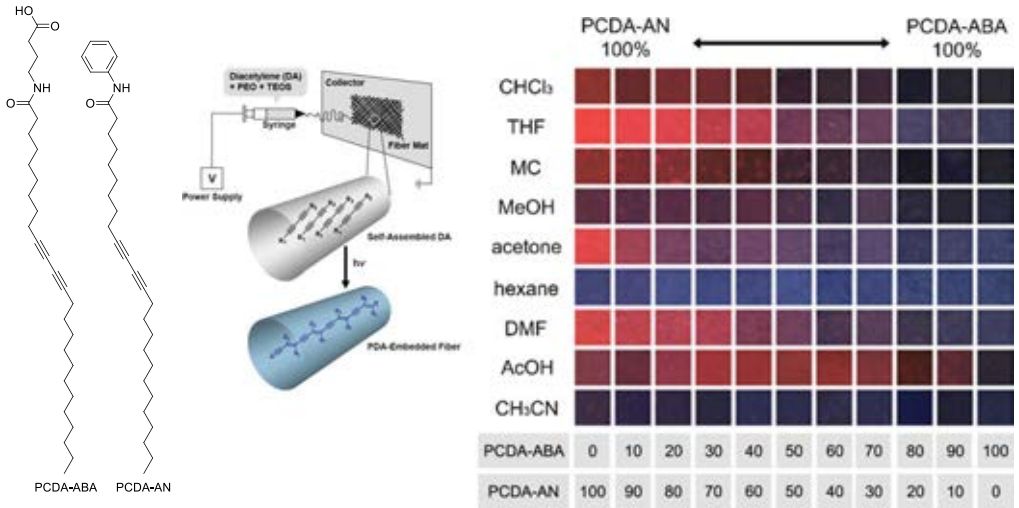

Figure 1.17 Schematic representation of the preparation of PDA-embedded electrospun microfibers and photographs of the polymerized PDA-embedded electrospun fiber mats after exposure to organic solvents at 25 ºC for 30 s.

In 2010, H. Jiang and colleagues [49] have also reported the development of a novel polydiacetylene (PDA)-based sensitive colorimetric microarray sensor for the detection and identification of volatile organic compounds. PDA-embedded polymer matrix films as the multi-layer PDA-based micro patterns (Figure 1.18) could be prepared by the spin-coating method combined with the sol–gel process. Polydimethylsiloxane Sylgard 184 (PDMS) was employed to enhance the stability of the PDA films when dipped in VOCs, especially chlorinated solvent.

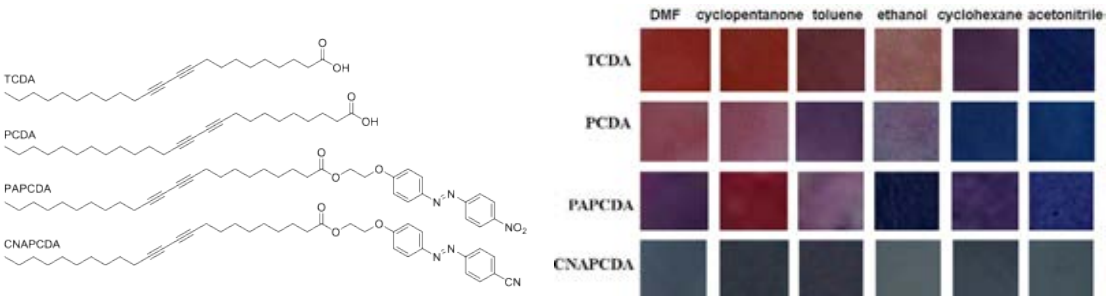

Figure 1.18 photographs of the PDA-embedded polymer matrix films derived from TCDA, PCDA, PAPCDA and CNAPCDA after dipped in organic solvents at room temperature.

In 2010, S. Wu and colleagues [50] investigated the effects of solvents on structure of micelle-like assemblies of an azo chromophore-functionalized polydiacetylene (polyAzoDA) and polymerized tricosa-10,12-diynoic acid (polyTDA). They used the mixtures of water with glycol, DMSO, ethanol and THF to observe blue-to-red color changes of polydiacetylenes. They found that the colors of polyTDA and polyAzoDA change at certain contents of organic solvents. The results in Figure 1.19 exhibit the strength of the polyTDA-solvent interaction in the following order: THF>ethanol> DMSO>glycol. According to the results, THF is a solvent which can effected on blue-to-red color transitions of polyAzoDA in THF/water mixtures. However, they do not observe color transitions in the other solvents/water mixtures. The authors have proposed that the stability to several solvents of polyAzoDA caused by the H- and J-like aggregates of azo chromophores in polyAzoDA.

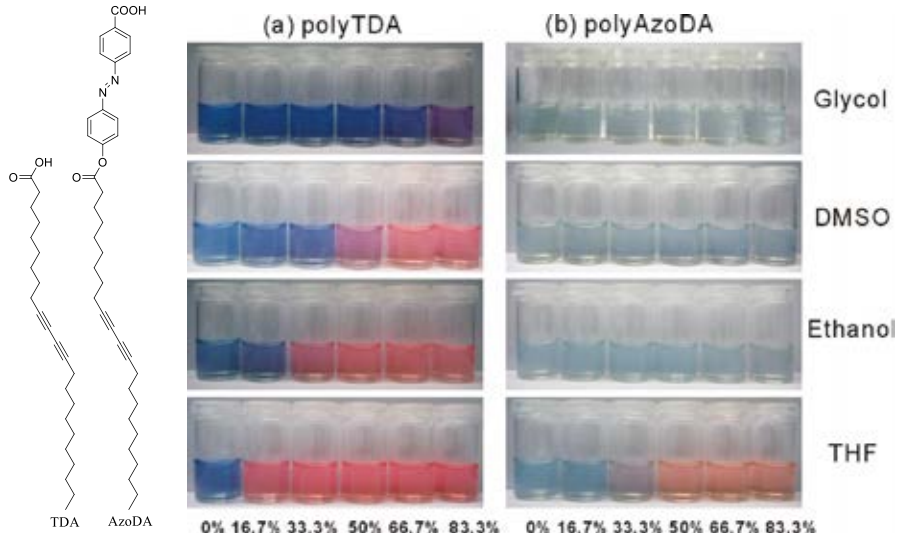

Figure 1.19 Photographs of micelle dispersions in different water-solvent mixtures. At increasing solvent content, the color of (a) polyTDA and (b) polyAzoDA changes from blue to purple/red depending on type of solvent and its relative content, respectively.

In 2011, Pumtang et al. [19] reported the synthesis of a novel series of diacetylene acids from the condensation of pentacosa-10,12-diynylamine (PCDAmine) and dicarboxylic acid or its anhydrides. One of these diacetylene lipids, 4-(pentacosa-10,12-diynylamino)-4-oxobutanoic acid (PCDAS), is used in combination with pentacosa-10,12-diynoic acid (PCDA) for dropcasting on pieces of filter paper which are consequently irradiated by UV light to generate a paper based sensor array for solvent detection and identification. Upon the exposure to various types of organic solvents, the blue colored sensors colorimetrically respond to give different shades of colors between blue to red (Figure 1.20). The color patterns of the sensor array are recorded as RedGreenBlue (RGB) values and statistically analyzed by principal component analysis (PCA). The PCA score plot reveals that the array is capable of identifying eleven common organic solvents.

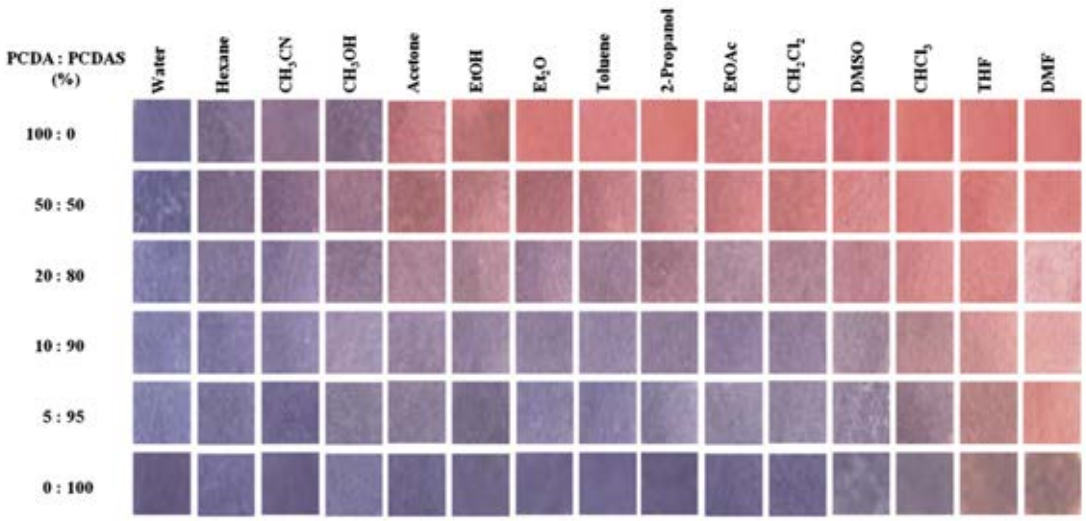

Figure 1.20 Array of cropped photographic images of PDAs on filter paper fabricated from PCDA and PCDAS responding to various organic solvents.

In 2012, Eaidkong *et al.* [21] reported detection and identification of VOCs by paper-based polydiacetylene (PDA) colorimetric sensor array. They were prepared from eight diacetylene monomers, six of which are amphiphilic and the other two are bolaamphiphilic. To fabricate the sensors, monomers are coated onto a filter paper surface using the drop-casting technique and converted to PDAs by UV irradiation. The PDA sensors show solvent induced irreversible color transition upon exposure to VOC vapors as shown in Figure 1.21. When combined into a sensing array, the color change pattern as measured by RGB values and statistically analyzed by principal component analysis (PCA) is capable of distinguishing 18 distinct VOCs in the vapor phase. The PCA score and loading plots also allow the reduction of the sensing elements in the array from eight to three PDAs that are capable of classifying 18 VOCs.

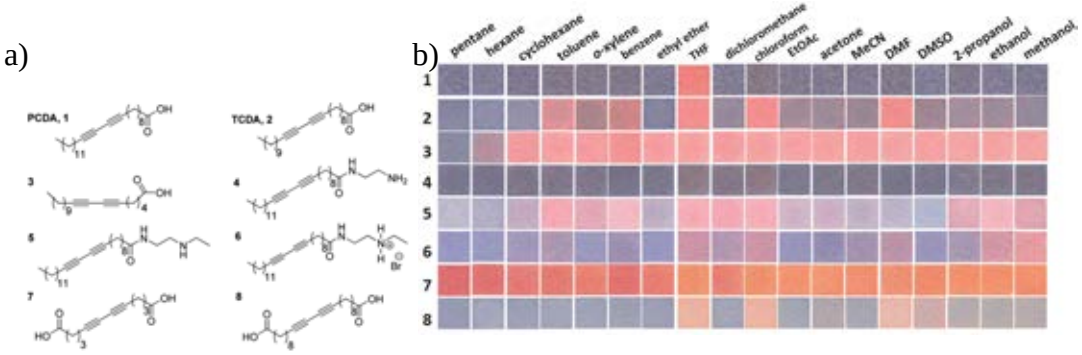

Figure 1.21 a) Structure of diacetylene monomers b)Scanned images of the paper-based PDA sensor array prepared from 1–8 exposed to various saturated vapors of volatile organic solvents.

1.3.4 Alkalinochromism and Acidochromism

Alkalinochromism and acidochromism were chromic properties that material can change color by deprotonation in case of alkalinochromism and protonation in case of acidochromism. Either alkalinochromism or acidochromism, the role of head group of diacetylene monomer had directly impact on the colorimetric transition as reported by several researchers.

In 1998, Cheng and coworkers [51] had been synthesized and studied the colorimetric response in various pH solutions of a series of amino acid-derivatized 10, 12-pentacosadiynoic acid. The result showed a different colorimetric response based on type of head groups. For example, Glu-PDA which has dicarboxylic head group changed the color from blue to red at pH 6 by deprotonation of the carboxylic group. The protonation of the tertiary amine head group of DMAP-PDA changed its color at pH 5. His-PDA which has both of carboxylic and imidazole changed the color at pH below 0 and pH 8-9 (Figure 1.22).

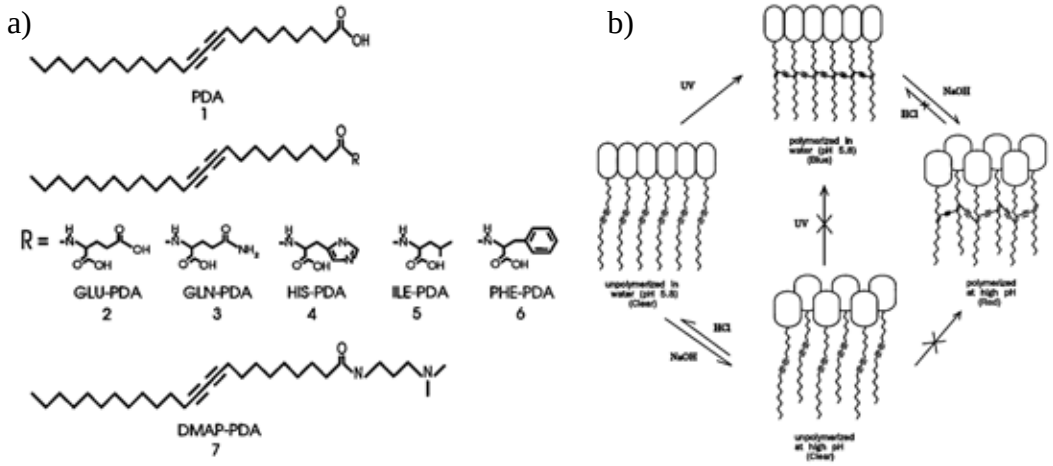

Figure 1.22 a) Structure of the diacetylene lipid 10,12-pentacosadiynoic acid (**1**) and its derivatives: lipids **2-6**, amino acids derivatives; lipid **7**, 3-(dimethylamino)propylamine (DMAP) derivative. b) Schematic diagram of amino acid-derivatized polydiacetylene liposomes in a chromatic transition.

In 1999, Jonas *et al.* [59] studied a novel system based on hydrazide derivatives of single chain diacetylene lipids which are 10,12-Tricosadiynohydrazide (THY) and 10,12-Pentacosadiynohydrazide (PHY). These materials showed an unusual aggregation and polymerization behavior in organic solution, in contrast to the parent carboxylic acids. In addition, these hydrazide lipids undergo an unprecedented reversible color change (blue/red) in polymerized vesicles when the pH of the surrounding aqueous medium is cycled between acidic and basic conditions. This unusual behavior is attributed to the unique hydrogen-bonding pattern of the hydrazide head group (Figure 1.23).

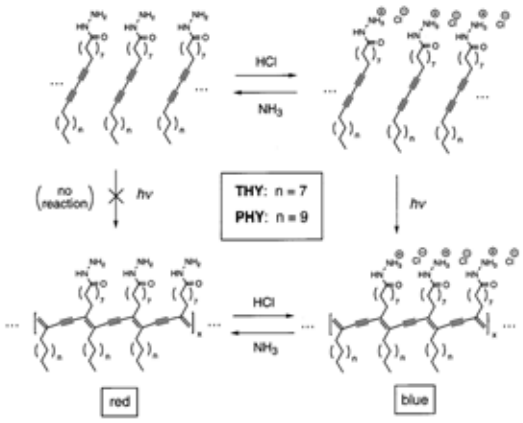

Figure 1.23 Schematic representations of the polymerization behavior and colorimetric changes of the diacetylene hydrazides PHY and THY in the presence of HCl or NH_3.

In 2011, Charoenthai *et al.* [52] investigated that the colorimetric response of the polydiacetylene (PDA) vesicles prepared by 10,12-tricosadiynoic acid (TCDA), 10,12-pentacosadiynoic acid (PCDA) and N-(2-aminoethyl)pentacosa-10,12-diynamide (AEPCDA) were stimulated by temperature, ethanol and pH. They found that a shorter side chain of poly(TCDA) yields weaker inter- and intra-chain dispersion interactions in the bilayers compared to the system of poly(PCDA). The color transition of poly(TCDA) and poly(PCDA) vesicles occured when increasing of pH to ~9 and ~10, respectively (Figure1.24). The poly(AEPCDA) vesicles, on the other hand, change color upon decreasing pH to ~0.

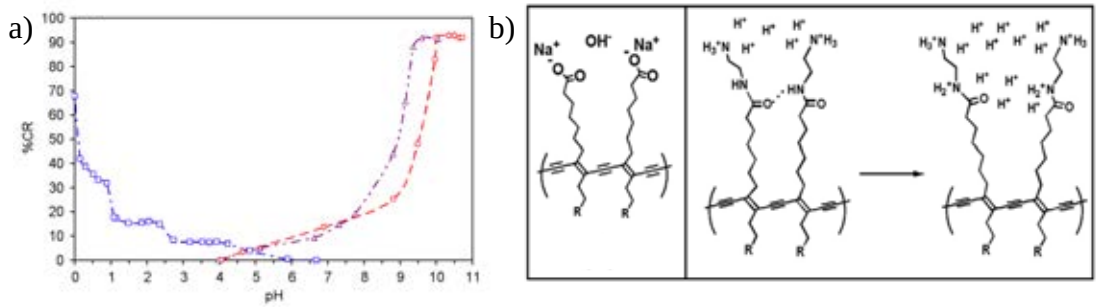

Figure 1.24 a) The colorimetric responses (%CR) of the vesicles were plotted as a function of pH. Symbols are (O) poly(PCDA), (Δ) poly(TCDA) and (□) poly(AEPCDA). b) The charged species of head groups of poly(PCDA) in high pH region and poly(AEPCDA) in low pH region.

1.3 Objectives and scope of the research

The objectives of this thesis are synthesis of diacetylene monomers containing β-alanine ethyl ester and di-β-alanine ethyl ester for use as indicator for detection of temperature, UV doses, organic solvent and humidity. To achieve the objectives, the work scopes are shown as following;

1) To synthesize and characterize amide and diamide derivatives from 10, 12-pentacosadiynoic acid (PCDA), 10, 12-tricosadiynoic acid (TCDA), 6, 8-nonadecadiynoic acid (NDDA) and 5,7-octadecadiynoic acid (ODDA)

2) To prepare polydiacetylene indicator on the filter paper

3) To test the sensitivity of the indicators for detection of temperature, UV doses, organic solvent and humidity.

CHAPTER II

EXPERIMENTAL

2.1 General Information

2.1.1 Chemicals and materials

1. 10,12-Pentacosadynoic acid (PCDA), GFS, USA
2. 10,12-tricosadiynoic acid (TCDA), GFS, USA
3. 6,8-nonadecadiynoic acid (NDDA), GFS, USA
4. 5,7-octadecadiynoic acid (ODDA), GFS, USA
5. Ethyl-3-aminopropanoate hydrochloride, Aldrich, Germany
6. 3-Aminopropionic acid, Fluka, Switzerland
7. 1-Hydroxybenzotriazole hydrate (HOBt•H_2O), Aldrich, Germany
8. 1-Ethyl-3-(3-dimethylaminopropyl)carbodiimide (EDC), Fluka, Switzerland
9. Diethylether (Et_2O), reagent grade, Lab-Scan, Ireland
10. Chloroform ($CHCl_3$), AR grade, Lab-Scan, Ireland
11. Dichloromethane (CH_2Cl_2), commercial grade, Lab-Scan, Ireland
12. Hexane, commercial grade, Lab-Scan, Ireland
13. Ethyl acetate (EtOAc), commercial grade, Lab-Scan, Ireland
14. Tetrahydrofuran (THF), AR grade, Lab-Scan, Ireland
15. Methanol (CH_3OH), commercial grade, Lab-Scan, Ireland
16. Sodium hydroxide (NaOH), Merck, Germany
17. Hydrochloric acid (HCl), Merck, Germany
18. Magnesium sulfate ($MgSO_4$) anhydrous, Riedel-deHaën®, Germany
19. Silica gel 60, Merck, Germany

2.1.2 Apparatus and equipments

1. Rotary evaporator, R200, Buchi, Switzerland
2. Ultrasonicator, Elma, Germany
3. Magnetic stirrer, Fisher Scientific, USA
4. Hot plated magnetic stirrer, IKA, Germany

5. Pipette man (P20, P200 and P5000), Gilson, France
6. Pipette man (Le100 and Le1000), Nichiryo, Japan
7. Nuclear Magnetic resonance spectrometer (NMR) 400 MHz, Mercury 400, Varian, USA
8. Differential scanning calorimetry (DSC), NETZSCH DSC 204 F1, Germany
9. Scanning electron microscopy (SEM), JEOL, JEM-2100, Japan
10. Webcam, ICON228, 14M pixels
11. Labtop, Macbook pro, apple, USA
12. UV Lamp, TUV 15W/G15 T18 lamp, Philips, Holland.

2.2 Synthesis of diacetylene monomer

2.2.1 Synthesis procedure

β-Alanine ethyl ester diacetylene and di-β-alanine ethyl ester diacetylene, boc-protected β-alanine was synthesized by amide coupling synthesis [53]. β-Alanine (0.71 g, 8 mmol) was dissolved in NaOH solution (1.0 M, 20 mL) and t-butanol (10 mL) of was then added. The solution of Boc_2O in t-butanol (15 mL) was added dropwise to obtain a clear solution and was stirred for 12 h. After removing the solvent by rotary evaporator, the mixture was adjusted to pH 2 by HCl solution (2.0 M) and then extracted with ethyl acetate (5 × 25mL). The combined organic layer was separated, dried over anhydrous $MgSO_4$ and filtered. The filtrate was evaporated to give Boc-protected β-alanine as white powder (1.27 g, 6.69 mmol, 83% yield).

The di-β-alanine ethyl ester was prepared by first dissolving boc-β-alanine (1.50 g 7.93 mmol) and $HOBt.H_2O$ (1.60 g, 11.91mmol) in CH_2Cl_2 (15 mL). Then, 1-Ethyl-3-(3-dimethyllaminopropyl) carbodiimide hydrochloride (EDC) (2.28 g, 11.91 mmol) in CH_2Cl_2 (20 mL) was added. The mixture was stirred for 1 h before β-alanine ethyl ester hydrochloride (1.46 g, 9.52 mmol) and triethylamine (4.40 mL) in CH_2Cl_2 (15 mL) were then added at 0 ℃ and stirred for 3 h. The reaction mixture was evaporated by rotary evaporator and was extracted by ethyl acetate 20 mL. The organic layer was consecutively washed by deionized water (2 × 10mL), HCl (10 mL), saturated $NaHCO_3$ (10 mL) and water (10 mL). The organic layer was dried by $MgSO_4$ anhydrous and was evaporated to obtain crude Boc-di-β-alanine ethyl ester

product (60%) as a white solid. The product was deprotected by trifluoroacetic acid after stirring for 2 h and freeze dried to give the desired di-β-alanine ethyl ester product in quantitative yield.

Ethyl 3-(pentacosa-10,12-diynoylamido)propanoate (EPCDP): 10,12-Pentacosadiynoic acid (0.38 g, 1.0 mmol) and 1-hydroxybenzotriazole hydrate (HOBt•H_2O; 0.20 g, 1.5 mmol) were stirred to dissolve in CH_2Cl_2 (3 mL). The solution was then added with a solution of 1-ethyl-3-(3-dimethylaminopropyl)carbodiimide (EDC; 0.29 g, 1.5 mmol) in CH_2Cl_2 (5 mL) and stirred for 1 h. The mixture of ethyl 3-aminopropanoate hydrochloride (0.18 g, 1.2 mmol) and triethylamine (0.56 mL, 4.0 mmol) in CH_2Cl_2 (5 mL) was added dropwise into the mixture at 0 ℃. The resulting mixture was stirred at room temperature for 3 h. The mixture was evaporated and the crude product was eluted through a silica gel column using hexane and ethyl acetate (1:1 v/v) as the eluent. After the solvent removal, ethyl-3-pentacosa-10, 12-diynamidopropanoate (EPCDP) was obtained as a white solid (0.41 g, 87% yield). M.p. (DSC): 72.6 °C; ^{1}H NMR (400 MHz, $CDCl_3$) δ 6.03 (s, 1H), 4.16 (q, *J* = 7.0 Hz, 2H), 3.58 – 3.44 (m, 2H), 2.53 (t, *J* = 6.0 Hz, 2H), 2.24 (t, *J* = 7.0 Hz, 4H), 2.14 (t, *J* = 8.0 Hz, 2H), 1.43 – 1.13 (m, 31H), 0.88 (t, *J* = 6.5 Hz, 3H).; ^{13}C NMR (101 MHz, $CDCl_3$) δ 172.6, 172.4, 77.2, 77.0, 64.9, 64.9, 60.3, 36.3, 34.4, 33.7, 31.5, 29.2, 29.0, 28.9, 28.8, 28.7, 28.7, 28.5, 28.4, 28.3, 28.0, 27.9, 25.2, 22.2, 18.8, 18.8, 13.8, 13.7; Anal. Found: C 76.08, H 10.42, N 2.99 (Calcd. for $C_{30}H_{51}NO_3$: C 76.06, H 10.85, N 2.96).

Ethyl 3-tricosa-10,12-diynamidopropanoate (ETCDP): The compound was synthesized and purified according to the above procedure using 10,12-tricosadiynoic acid (0.35 g, 1.0 mmol), β-alanine ethyl ester hydrochloride (0.18 g, 1.2 mmol), HOBt•H_2O (0.20 g, 1.5 mmol), EDC (0.29 g, 1.5 mmol) and triethylamine (0.56 mL, 4.0 mmol). The desired product, ETCDAP, was obtained as a white solid (0.41 g, 91% yield). M.p. (DSC): 63.3°C; ^{1}H NMR (400 MHz, $CDCl_3$) δ 6.03 (s, 1H), 4.16 (q, *J* = 7.0 Hz, 2H), 3.64 – 3.33 (m, 2H), 2.53 (t, *J* = 6.0 Hz, 2H), 2.24 (t, *J* = 7.0 Hz, 4H), 2.14 (t, *J* = 8.0 Hz, 2H), 1.51 (s, 4H), 1.42 – 1.09 (m, 27H), 0.88 (t, *J* = 7.0 Hz, 3H); ^{13}C NMR (101 MHz, $CDCl_3$) δ 172.6, 172.4, 77.2, 77.0, 64.9, 64.8, 60.3, 36.3, 34.3, 33.7, 31.4, 29.1, 29.0, 28.9, 28.8, 28.7, 28.6, 28.5, 28.4, 28.3, 27.9, 27.9, 25.2, 22.2,

18.8, 18.8, 13.8, 13.7; Anal. Found: C 75.49, H 10.61, N 3.17 (Calcd. for $C_{28}H_{47}NO_3$: C 75.46, H 10.63, N 3.14).

Ethyl 3-nonadeca-6,8-diynamidopropanoate (ENDDP). The compound was synthesized and purified according to the above procedure using 6,8-nonadecadiynoic acid (0.30 g, 1.1 mmol), β-alanine ethyl ester hydrochloride (0.20 g, 1.3 mmol), HOBt•H_2O (0.22 g, 1.6 mmol), EDC (0.31 g, 1.6 mmol) and triethylamine (0.91 mL, 6.5 mmol). The desired product, ENDDP, was obtained as a white solid (0.42 g, 98%yield); M.p. (DSC): 47.5°C; ^{1}H NMR (400 MHz, $CDCl_3$) δ 6.08 (s, 1H), 4.15 (q, *J* = 7.0 Hz, 2H), 3.57 – 3.44 (m, 2H), 2.52 (t, *J* = 6.0 Hz, 2H), 2.33 – 2.07 (m, *J* = 27.0, 14.5, 7.5 Hz, 6H), 1.72 – 1.66 (m, 2H), 1.51 (tt, *J* = 14.5, 7.0 Hz, 4H), 1.29 (dd, *J* = 24.5, 17.0 Hz, 17H), 0.87 (t, *J* = 6.5 Hz, 3H); ^{13}C NMR (101 MHz, $CDCl_3$) δ 172.8, 172.6, 77.9, 77.5, 65.9, 65.3, 60.8, 60.5, 36.8, 36.1, 35.0, 34.2, 32.0, 29.6, 29.6, 29.4, 29.2, 28.9, 28.4, 28.0, 24.9, 24.0, 22.8, 19.3, 19.1, 14.3, 14.2; Anal. Found: C 73.45, H 10.23, N 3.70 (Calcd. for $C_{24}H_{39}NO_3$: C 73.99, H 10.09, N 3.60).

Ethyl 3-octadeca-5,7-diynamidopropanoate (EODDP). The compound was synthesized and purified according to the above procedure using 5,7-heptadecadiynoic acid (0.15 g, 0.54 mmol), β-alanine ethyl ester hydrochloride (0.10 g, 0.65 mmol), HOBt•H_2O (0.11 g, 0.81 mmol), EDC (0.15 g, 0.81 mmol) and triethylamine (0.45 mL, 3.25 mmol), The desired product, EODDP, was obtained as a white solid (0.16 g, 80%yield). M.p. (DSC): 66°C; ^{1}H NMR (400 MHz, $CDCl_3$) δ 6.07 (s, 1H), 4.16 (q, *J* = 7.0 Hz, 2H), 3.57 – 3.45 (m, 2H), 2.53 (t, *J* = 6.0 Hz, 2H), 2.36 – 2.20 (m, 6H), 1.91 – 1.75 (m, *J* = 7.0 Hz, 2H), 1.54 – 1.46 (m, *J* = 15.0, 7.0 Hz, 2H), 1.43 – 1.17 (m, *J* = 25.0, 17.5 Hz, 17H), 0.87 (t, *J* = 6.5 Hz, 3H); ^{13}C NMR (101 MHz, $CDCl_3$) δ 172.7, 172.1, 78.1, 77.5, 66.4, 65.2, 60.8, 35.2, 35.0, 34.2, 32.0, 29.7, 29.6, 29.4, 29.2, 29.0, 28.4, 24.2, 22.8, 19.3, 18.8, 14.3, 14.2; Anal. Found: C 73.60, H 10.34, N 3.90 (Calcd. for $C_{23}H_{37}NO_3$: C 73.56, H 9.93, N 3.73).

Ethyl 3-(3-pentacosa-10,12-diynamidopropanamido) propanoate (EPCDPP). This was synthesized according to the above general procedure from 10, 12-pentacosadiynoic acid (0.64 g, 1.70 mmol), di-β-alanine ethyl ester (0.45 g, 2.38 mmol), HOBt•H_2O (0.34 g, 2.55 mmol), EDC (0.48 g, 2.55 mmol) and triethylamine (1.42 mL, 10.21 mmol), purified by column chromatography with hexane and ethyl acetate (1:1 v/v) as white solid (0.61 g, 66%yield). M.p. (DSC) 121°C; ^{1}H NMR (400

MHz, $CDCl_3$) δ 6.31 (s, 1H), 6.19 (s, 1H), 4.16 (q, *J* = 7.0 Hz, 2H), 3.57 – 3.46 (m, 2H), 2.52 (t, J = 6.0 Hz, 2H), 2.43 – 2.32 (m, 2H), 2.23 (t, J = 7.0 Hz, 4H), 2.14 (t, *J* = 7.5 Hz, 2H), 1.54 – 1.45 (m, 4H), 1.29 (dd, *J* = 25.0, 17.5 Hz, 31H), 0.88 (t, *J* = 7.0 Hz, 3H); ^{13}C NMR (101 MHz, $CDCl_3$) δ 173.4, 172.6, 171.8, 77.7, 77.6, 65.4, 65.4, 61.0, 36.9, 35.7, 35.5, 35.0, 34.2, 32.0, 29.8, 29.7, 29.7, 29.6, 29.5, 29.3, 29.3, 29.2, 29.0, 29.0, 28.9, 28.5, 28.4, 25.8, 22.8, 19.3, 19.3, 14.3, 14.2; Anal. Found: C 72.83, H 10.30, N 5.29 (Calcd. for $C_{33}H_{56}N_2O_4$: C 72.75, H 10.36, N 5.14).

Ethyl 3-(3-tricosa-10, 12-diynamidopropanamido)propanoate (ETCDPP). This was synthesized according to the above general procedure from 10, 12-tricosadiynoic acid (0.58 g, 1.70 mmol), di-β-alanine ethyl ester (0.67 g, 2.34 mmol), HOBt•H_2O (0.34 g, 2.51 mmol), EDC (0.48 g, 2.51 mmol) and triethylamine (1.40 mL, 10.0 mmol), purified by column chromatography with hexane and ethyl acetate (1:1 v/v) as white solid (0.61 g, 70%yield) M.p. (DSC): 119°C; ^{1}H NMR (400 MHz, $CDCl_3$) δ 6.31 (s, 2H), 6.19 (s, 1H), 4.16 (q, J = 7.0 Hz, 3H), 3.68 – 3.37 (m, 6H), 2.52 (t, J = 6.0 Hz, 2H), 2.43 – 2.29 (m, 2H), 2.24 (t, J = 7.0 Hz, 4H), 2.19 – 2.09 (m, 2H), 1.54 – 1.43 (m, 4H), 1.42 – 1.16 (m, 27H), 0.88 (t, J = 7.0 Hz, 3H); ^{13}C NMR (101 MHz, $CDCl_3$) δ 172.5, 172.4, 171.7, 78.1, 77.5, 66.3, 65.2, 60.9, 35.7, 35.6, 35.2, 35.1, 34.2, 32.0, 31.6, 29.8, 29.6, 29.6, 29.4, 29.2, 29.0, 28.4, 24.2, 22.8, 19.3, 18.8, 14.3, 14.2; Anal. Found: C, 72.06; H, 10.26; N, 5.44 (Calcd. for $C_{31}H_{52}N_2O_4$: C, 72.05; H, 10.14; N, 5.42).

Ethyl 3-(3-nonadeca-6,8-diynamidopropanamido)propanoate (ENDDPP). This was synthesized according to the above general procedure from 6, 8-nonadecadiynoic acid (0.36 g, 1.24 mmol), di-β-alanine ethyl ester (0.50 g, 1.74 mmol), HOBt•H_2O (0.25 g, 1.86 mmol), EDC (0.36 g, 1.86 mmol) and triethylamine (1.0 mL, 7.44 mmol), purified by column chromatography with hexane and ethyl acetate (1:1 v/v) as white solid (0.34 g, 60%yield); M.p. (DSC): 119.8°C; ^{1}H NMR (400 MHz, CD_3OD) δ 4.14 (q, *J* = 7.0 Hz, 2H), 3.47 – 3.37 (m, 4H), 2.52 (t, *J* = 6.5 Hz, 2H), 2.37 (t, *J* = 7.0 Hz, 2H), 2.31 – 2.13 (m, 6H), 1.75 – 1.60 (m, 2H), 1.57 – 1.44 (m, *J* = 13.5, 7.0 Hz, 4H), 1.44 – 1.20 (m, 19H), 0.90 (t, *J* = 6.5 Hz, 3H); ^{13}C NMR (101 MHz, CD_3OD) δ 175.9, 173.7, 173.4, 78.1, 77.4, 66.7, 66.3, 61.7, 37.1, 37.0, 36.6, 36.5, 36.4, 36.4, 35.0, 34.4, 33.0, 30.6, 30.6, 30.4, 30.2, 29.9, 29.5, 29.0,

26.1, 25.3, 23.7, 19.7, 19.5, 14.5, 14.4; Anal. Found: C, 70.45; H, 9.67; N, 6.05 (Calcd. for $C_{27}H_{44}N_2O_4$: C, 70.40; H, 9.63; N, 6.08).

Ethyl 3-(3-octadeca-5, 7-diynamidopropanamido)propanoate(EODDPP). This was synthesized according to the above general procedure from 5, 7-heptadecadiynoic acid (0.59 g, 2.14 mmol), di-β-alanine ethyl ester (0.86 g, 3.0 mmol), HOBt•H_2O (0.43 g, 3.21 mmol), EDC (0.61 g, 3.21 mmol) and triethylamine (1.78 mL, 12.84 mmol), purified by column chromatography with hexane and ethyl acetate (1:1 v/v) as white solid (0.58 g, 61%yield); M.p. (DSC): 134.4°C; ^{1}H NMR (400 MHz, CD_3OD) δ 4.15 (q, *J* = 7.0 Hz, 2H), 3.47 – 3.37 (m, 4H), 2.53 (t, *J* = 6.5 Hz, 2H), 2.37 (t, *J* = 6.5 Hz, 2H), 2.33 – 2.16 (m, 6H), 1.85 – 1.71 (m, 2H), 1.59 – 1.01 (m, *J* = 14.5, 7.5 Hz, 19H), 0.90 (t, *J* = 7.0 Hz, 3H); ^{13}C NMR (101 MHz, $CDCl_3$) δ 172.5, 172.4, 171.7, 78.1, 77.5, 66.3, 65.2, 60.9, 35.7, 35.6, 35.2, 35.1, 34.2, 32.0, 31.6, 29.8, 29.6, 29.6, 29.4, 29.2, 29.0, 28.4, 24.2, 22.8, 19.3, 18.8, 14.3, 14.2; Anal. Found: C, 69.79; H, 9.67; N, 6.01 (Calcd. for $C_{26}H_{42}N_2O_4$: C, 69.92; H, 9.48; N, 6.27).

2.3 Preparation of paper-based diacetylene indicator and thermal sensing study

A piece of filter paper (Whatman No.1) (1 × 5 cm^2) was dipped in adiacetylene monomer solution (10 mM) in CH_2Cl_2 and dried in the air for 2 h. Then, it was stored at 4 ℃ for overnight. Next, the indicators were irradiated by 254 nm UV light for specific periods of time depended on the time required for obtaining the maximum blue phase, typically 10 sec to 2 min. The indicators were attached on the outside of a glass beaker 600 mL filled with 400 mL of water. The beaker was gradually heated from 30 ℃ to 90 ℃ while their color images were monitored by webcam and the RGB values were determined from the centered crop area of 15 × 15 pixels by an image-processing program.

2.4 Preparation of paper-based diacetylene indicator and UV sensing study

A piece of filter paper (Whatman No.1) (1 × 5 cm^2) was dipped in a solution of diacetylene monomer with designated concentration (10 mM) in CH_2Cl_2 and dried in the air for 2 h. Then, it was stored at 4 ℃ for overnight. The indicators were irradiated by 254 nm UV light with the UV energy power of 1.4-1.5 mW/cm^2 for

various periods of time. Their color images of the indicators were recorded by a commercial scanner and the RGB values were determined from the centered crop area of 50 × 50 pixels by an image-processing program.

2.5 Preparation of paper-based diacetylene indicator and solvent sensing study

A piece of filter paper (Whatman No.1) (1 × 5 cm^2) was dipped in a solution of diacetylene monomer with designated concentration (10 mM) in CH_2Cl_2 and dried in the air for 2 h. Then, it was stored at 4 °C for overnight. A paper-based indicator was dipped into an organic solvent and surfactant tested at room temperature (~ 30 ºC) for 1 min. The indicator pieces were withdrawn from the solvent and allowed to dry in the air. Thirteen organic solvents were tested and deionized water was used for the blank test. The colors of the indicators were recorded by a commercial scanner (Epson Perfection V33) in 3 pieces for each solvent.

2.6 Preparation of paper-based polydiacetylene humidity indicator and humidity sensing study

2.6.1. Single coating of diacetylene carboxylate salts

The single coating of diacetylene carboxylate salts were prepared by using 0.2 M of carbonate salt solution (Na_2CO_3 and K_2CO_3) to dissolve diacetylene monomer (TCDA) and sonicated for 10 minutes to obtain milky solution. The solution was left overnight at room temperature. Then, the solution was dropped on the filter paper and dried at 100 °C for 10 minutes. Next, the paper was irradiated by UV light for 1 min.

2.6.2. Layer-by-layer coating of diacetylene carboxylic acid/carbonate salt

The layer-by-layer coating of diacetylene carboxylic acid/carbonate salt was prepared in two methods. In the first method, 20 μL of 5 mM of TCDA in CH_2Cl_2 was deposited on the filter paper by drop-casting technique and dried in room temperature for 10 minutes. 20 μL of a saturated carbonate solution (Na_2CO_3 or K_2CO_3) was dropped, dried at 100 °C and followed by irradiated with UV light for 1 minute. The second method exploited the opposite deposition sequences, 20 μL of the

saturated carbonate solution followed by 20 μL of 5 mM of TCDA. After the layer-by-layer deposition, the coated paper was irradiated with UV 254 nm for 1 min.

2.6.3 Zone coating of diacetylene carboxylic acid and carbonate salt

A filter paper strip was divided into 2 zones. The first zone was coated with carbonate salt and the second zone was coated with TCDA monomer. The filter paper strip was dipped into a saturated aqueous solution of the carbonate salt and dried at 100 °C. Then, the other end of the filter paper strip was dipped into a 5mM of TCDA solution in CH_2Cl_2 and the filter paper was dried in a desiccator for 10 minutes. The coated paper was irradiated with 254 nm UV light for 1 minute to generate a humidity indicator with blue PDA zone on one end and off-white zone of the carbonate salt on the other end. The dipping process was performed with care to make sure that these two zones are separated by 3 mm.

CHAPTER III

RESULTS AND DISCUSSION

This dissertation involved the study of diacetylene compounds with three types of functional groups including carboxylic acid, amide and diamide. Each series of the diacetylenes have four members with different number of methylene chains (Scheme 3.1). The results of the synthesis and utilization of these diacetylene compounds as sensing materials are reported and discussed in this chapter which is divided into 5 sections *i.e.* synthesis, UV indicators, thermochromic study, solvatochromic study and humidity indicators.

3.1 Synthesis of diacetylene monomers

The synthesis of the diacetylene monomers containing β-alanine ethyl ester and di-β-alanine ethyl ester were accomplished by condensing the commercially available diacetylene fatty acids (PCDA, TCDA, NDDA, ODDA) with β-alanine ethyl ester and di-β-alanine ethyl ester by using EDC and HOBt as coupling agents (Scheme 3.1, see section 2.2 for detail synthetic procedures). The monoamides (EPCDP, ETCDP, ENDDP, EODDP) were obtained in excellent yields (80-98%) and the diamides (EPCDPP, ETCDPP, ENDDPP, EODDPP) were also obtained in satisfactory yields (60-70%).

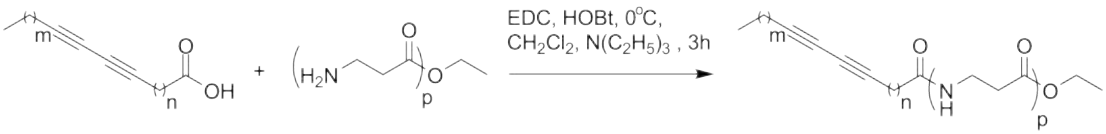

ODDA: m = 9, n = 3
NDDA: m = 9, n = 4
TCDA: m = 9, n = 8
PCDA: m = 11, n = 8

β-alanine ethyl ester: p = 1
di-β-alanine ethyl ester: p = 2

EODDP: m = 9, n = 3, p = 1 (80%)
ENDDP: m = 9, n = 4, p = 1, (98%)
ETCDP: m = 9, n = 8, p = 1, (91%)
EPCDP: m = 11, n = 8, p = 1, (87%)
EODDPP: m = 9, n = 3, p = 2 (61%)
ENDDPP: m = 9, n = 4, p = 2 (60%)
ETCDPP: m = 9, n = 8, p = 2 (70%)
EPCDPP: m = 11, n = 8, p = 2 (66%)

Scheme 3.1 Synthesis of diacetylenes containing amide and diamide head groups.

The ^{1}H NMR spectra of the diacetylene compounds comprising β-alanine ethyl ester in $CDCl_3$ were shown in Figure 3.1. These monomers have a characteristic quartet peak ~4.2 ppm corresponding to OCH_2 (*d'*) in the ethyl ester and triplet peak ~3.5 ppm belonging to NCH_2 in the amido group (*b'*). The signals of amido proton appeared as a singlet peak (*a'*) near 6.1 ppm and those of methylene proton c' appeared as triplet peak near 2.5 ppm. The chemical shift of the methylene protons between the amide and the diacetylene group were observed in the range of 1.4-2.5 ppm.

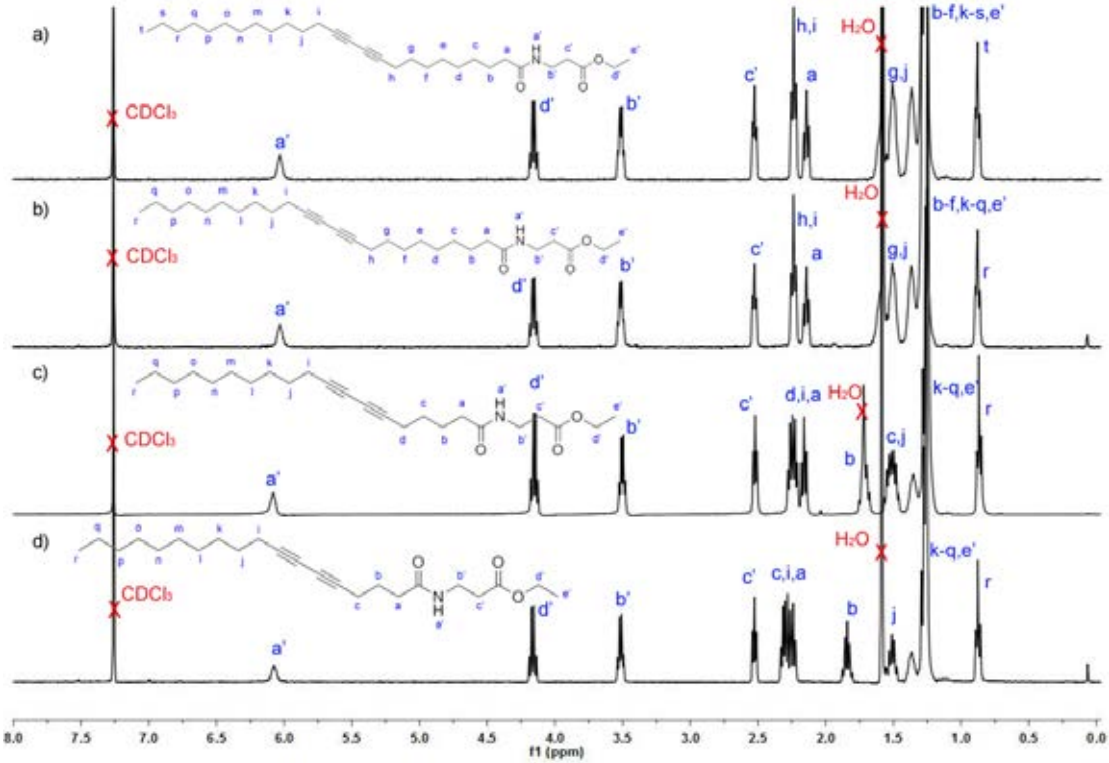

Figure 3.1 ^{1}H NMR spectra of mono-β-alanine ethyl ester diacetylene monomers a) EPCDP, b) ETCDP, c) ENDDP, d) EODDP in $CDCl_3$.

The ^{1}H NMR spectra of the diacetylene monomers containing di-β-alanine ethyl ester (Figure 3.2) have a characteristic quartet peak (*g'*) around 4.2 ppm and multiplet peak around 3.5 ppm corresponding to the methylene groups *b'* and *e'*. The signals near 6.2 and 6.4 ppm, corresponding to the amido N-H protons (*a'* and *d'*), and the signals in the range of 1.4-2.6 ppm matched the methylene proton between the amide and the diacetylene group.

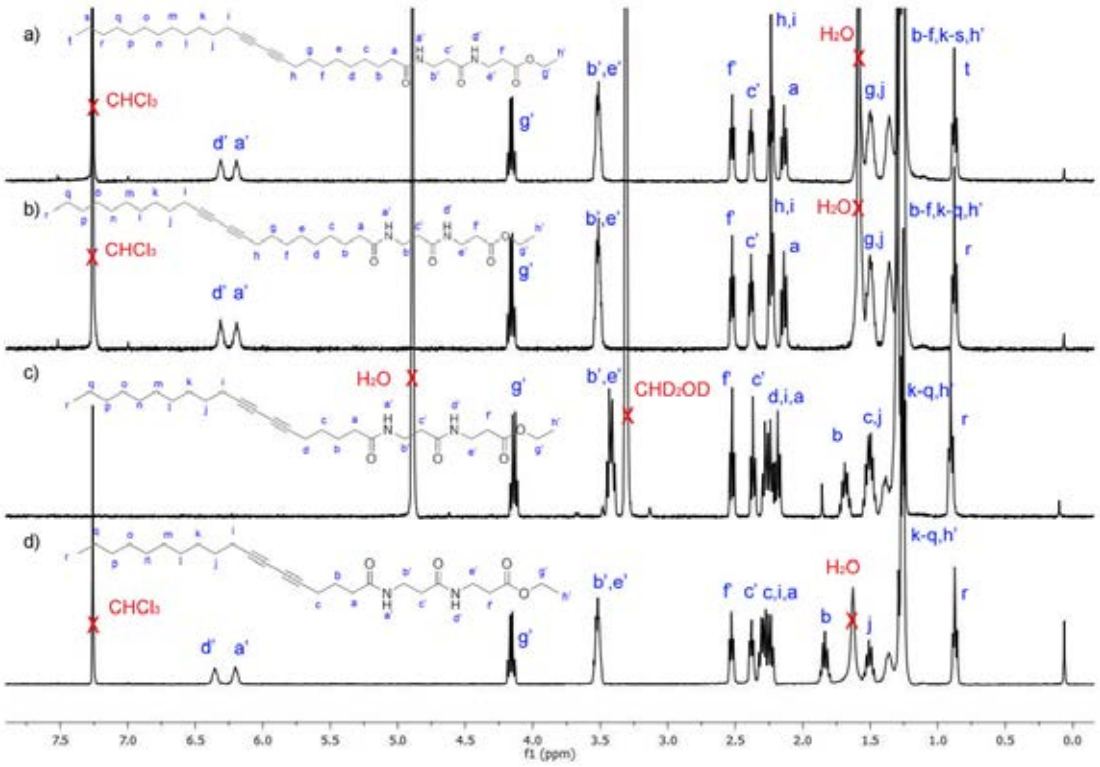

Figure 3.2 ^{1}H NMR spectra of dipropanamide diacetylene monomers a) EPCDPP in $CDCl_3$, b) ETCDPP in $CDCl_3$, c) ENDDPP in CD_3OD, d) EODDPP in $CDCl_3$

3.2 UV indicators

The UV sensing indicators were prepared from all 12 diacetylene monomers having 3 different head groups including carboxylic acid (PCDA, TCDA, NDDA, ODDA), β-alanine ethyl ester (EPCDP, ETCDP, ENDDP, EODDP), di-β-alanine ethyl ester (EPCDPP, ETCDPP, ENDDPP, ODDPP). Typically, the indicator was prepared by dipping a strip of filter paper (1 × 5 cm^2) in a CH_2Cl_2 solution of the diacetylene monomer (10 mM) followed by air dry and stored in a refrigerator before further sensing study.

3.2.1 UV sensing study

The white diacetylene coated paper strips were irradiated by 254 nm UV light with the intensity of 1.4-1.5 mW/cm^2 for various periods of time. The paper strips were periodically removed from the irradiation area and the color images were recorded by a commercial scanner. Each image of the indicator was taken from

individual sample. As shown in Figure 3.3, the color of all PDAs on the paper rapidly changed their color from white to blue or purple within 10 seconds. With prolong irradiation, the blue or purple PDAs gradually turned into red or orange color at different irradiation time depending on the structures of the diacetylene monomers. From the color images, the diacetylenes in the series of the same head group with shorter alkyl chain, either between the diyne and carboxyl group or in the lipid tail (lower n or m numbers), required shorter irradiation time to cause the blue-to-red color transition indicating their greater UV sensitivity. Furthermore, the diacetylene compounds with amide and diamide head groups are generally more sensitive than those with carboxylic acid head group.

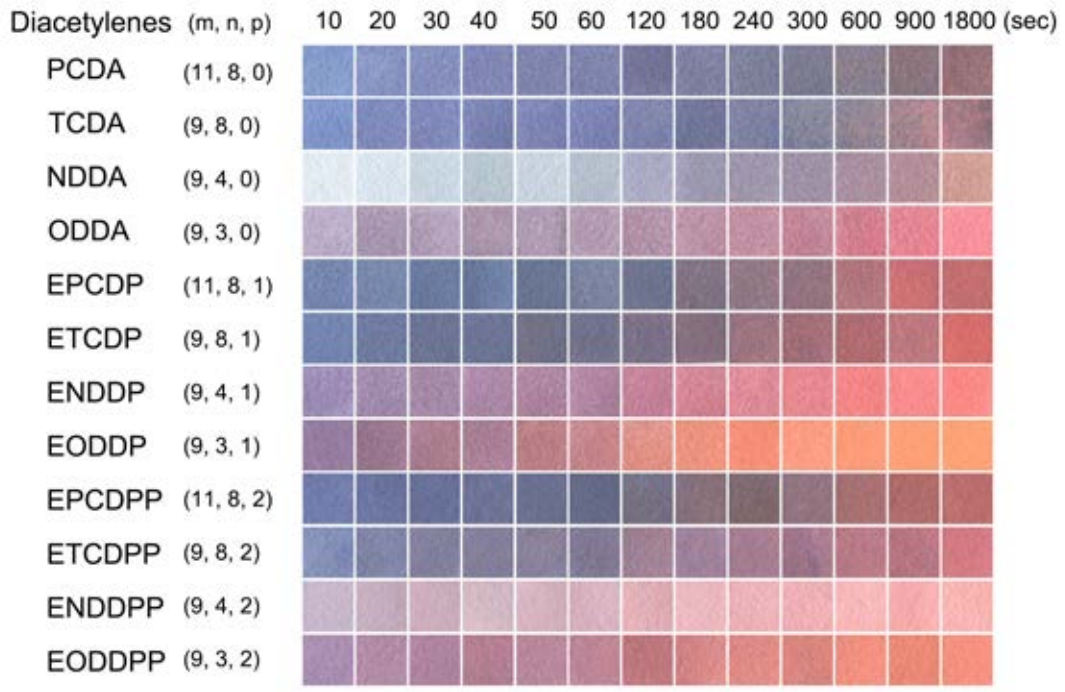

Figure 3.3 Color images of PDA indicators obtained at different UV irradiation times.

3.2.2 Determination of UV doses required for blue-to-red color transition

For the determination of the color transition of the paper-based polydiacetylene indicators, the color transition images of the indicators (Figure 3.3)

were converted to RGB values by image-processing program. The R, G and B values represent the extent of the red, green and blue components in the image. The values are varied from 0 to 255 that the greater the value is the higher the extent of the hue. For examples, the RGB coordinate of (0, 0, 0) is white and (255, 255, 255) is black.

For better comparison of the colorimetric responses, the effects from the background light and color depth were evened out by using the percentage value of each RGB component calculated according to the following equation shown below, instead of its absolute value.

$$\%R \text{ (or \%G or \%B)} = (R \text{ (}or\ G\ or\ B\text{)})/(R+G+B)\times 100$$

To obtain the UV dose (mJ/cm^2), the irradiation time (s) was multiplied by with the intensity (mW/cm^2) of the UV light. The plot of %R and %B against the UV dose clearly showed the increase of %R in the expense of %B while %G remained relatively constant (Figure 3.4). The small error bars in the plots confirmed high reproducibility of the indicator preparation and color measurement.

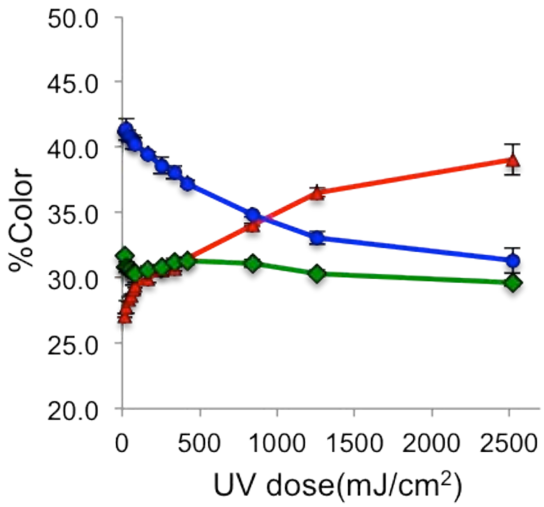

Figure 3.4 Plots of %R (▲), %G (◆) and %B (●) against UV doses of PDA indicators prepared from PCDA. Error bars represent standard deviations.

To apply the RGB values for the sensitivity evaluation, the UV dose required at the intersection between %R and %B curves was assigned as the color transition dose. As shown in Figure 3.5, the UV doses required for the blue-to-red color

transition of all diacetylene monomers can be easily determined from the crossing point. By visual observation, these color transition points correspond to purple color.

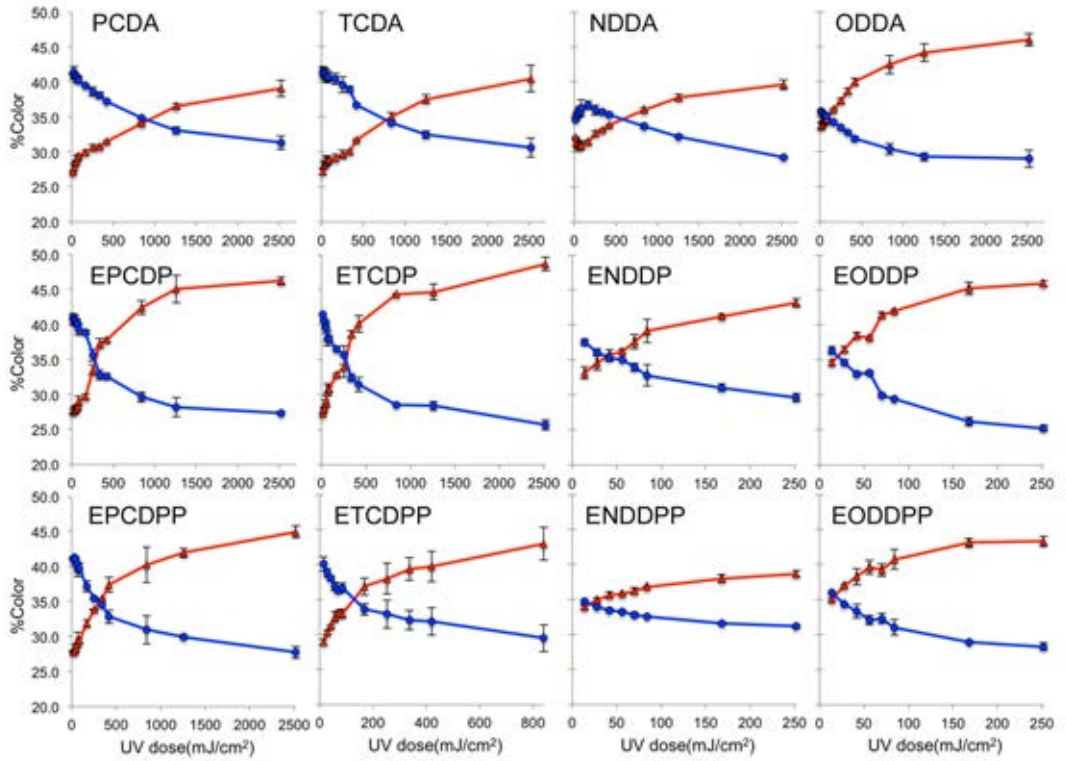

Figure 3.5 Plots of %R (▲) and %B (●) of the PDA indicators against UV irradiation doses. Error bars represent standard deviations.

The blue-to-red color transition doses determined from the intersection point of %R and %B are compiled in Table 3.1. The diacetylene that gives the lower dose required for the color transition is more UV sensitive. For examples, TCDA, ETCDP and ETCDPP required the exposure doses of 780±52 mJ/cm^2, 264±32 mJ/cm^2 and 130±9 mJ/cm^2, respectively, that represent the sensitivity order of TCDA < ETCDP < ETCDPP.

Table 3.1 UV doses required for blue-to-red color transition of the indicators prepared from various diacetylene compounds

Compound	UV dose (mJ/cm^2)	Compound	UV dose (mJ/cm^2)	Compound	UV dose (mJ/cm^2)
PCDA	918±19	EPCDP	276±17	EPCDPP	309±3
TCDA	780±52	ETCDP	264±32	ETCDPP	130±9
NDDA	586±24	ENDDP	39±11	ENDDPP	20±4
ODDA	98±22	EODDP	21±1	EODDPP	18±1

To realize the structure-activity relationships of the diacetylene compounds with their UV induced color transition, the data in Table 3.1 were plotted into a bar chart as shown in Figure 3.6. From the chart, there is a clear trend of the UV doses required for the color transition within the series of the same head group. The diacetylenes with shorter alkyl chain (lower n or m numbers), either between the diyne and carboxyl group or in the lipid tail, required lower UV doses in causing the blue-to-red color transition indicating their greater UV sensitivity. This result suggested a photo-induced thermochromism, which will be described in more details in section 3.3.

Comparing between the series of different head groups, the UV doses required for the color transition of the fatty acid series (PCDA, TCDA, NDDA and ODDA) are generally greater than those of the corresponding monopropanamide (EPCDP, ETCDP, ENDDP and EODDP) and dipropanamide (EODDPP, ENDDPP, ETCDPP and EPCDPP). The effects of the head group on the UV sensitivity are likely associated with the difference of orientation and strength of hydrogen bonding among the carboxylic acid and amido head groups in the molar self-assemblies of the diacetylene lipids. Since the blue-to-red transition of the amide series is faster in the UV irradiation, their molecular assemblies are probably more readily to undergo the conformational alteration during the topopolymerization process. Further details on the roles of the head groups on the color transition sensitivity will be discussed in the section 3.3 related to the thermochromism properties.

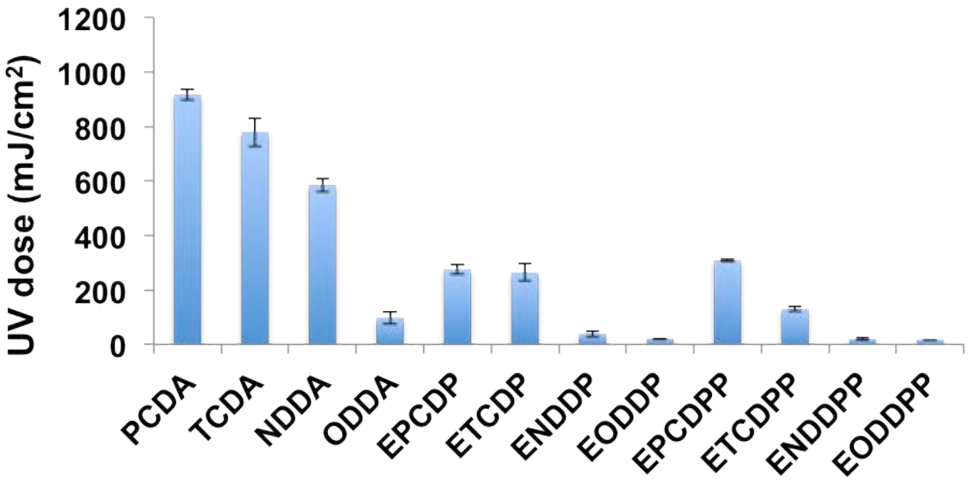

Figure 3.6 Bar chart of UV doses required for causing blue-to-red color transition of diacetylene-based paper sensors. The plots are the average data obtained from 3 independent samples with the error bars representing the standard deviation.

3.3.3 Morphology change of PDA upon UV irradiation

Scanning electron microscopy (SEM) of the blue and red PDA coated on cellulose fibers of the filter paper strips revealed interesting microscopic phenomena. The diacetylene containing carboxylic acid head group showed PDA film rupture upon the UV induced color transition from blue to red (Figure 3.7 a and d). However, no significant change was observed for the PDAs obtained from the diacetylene containing mono- and diamide head groups. The rupture denoted that the blue-to-red color transition was accompanied with a major and sudden change in the molecular assembly [54].

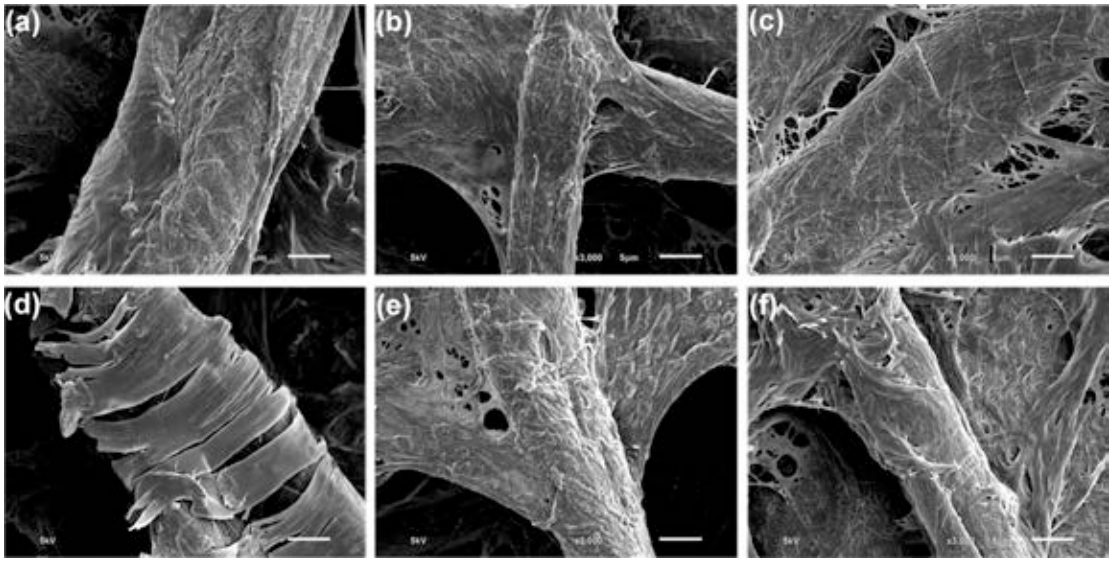

Figure 3.7 SEM (5 kV) micrographs of filter paper coated with blue PDAs (a) PCDA (b) EPCDP (c) EPCDPP and red PDAs of (d) PCDA (e) EPCDP (f) EPCDPP. The scale bars represent 5 μm.

3.3 Thermochromic study

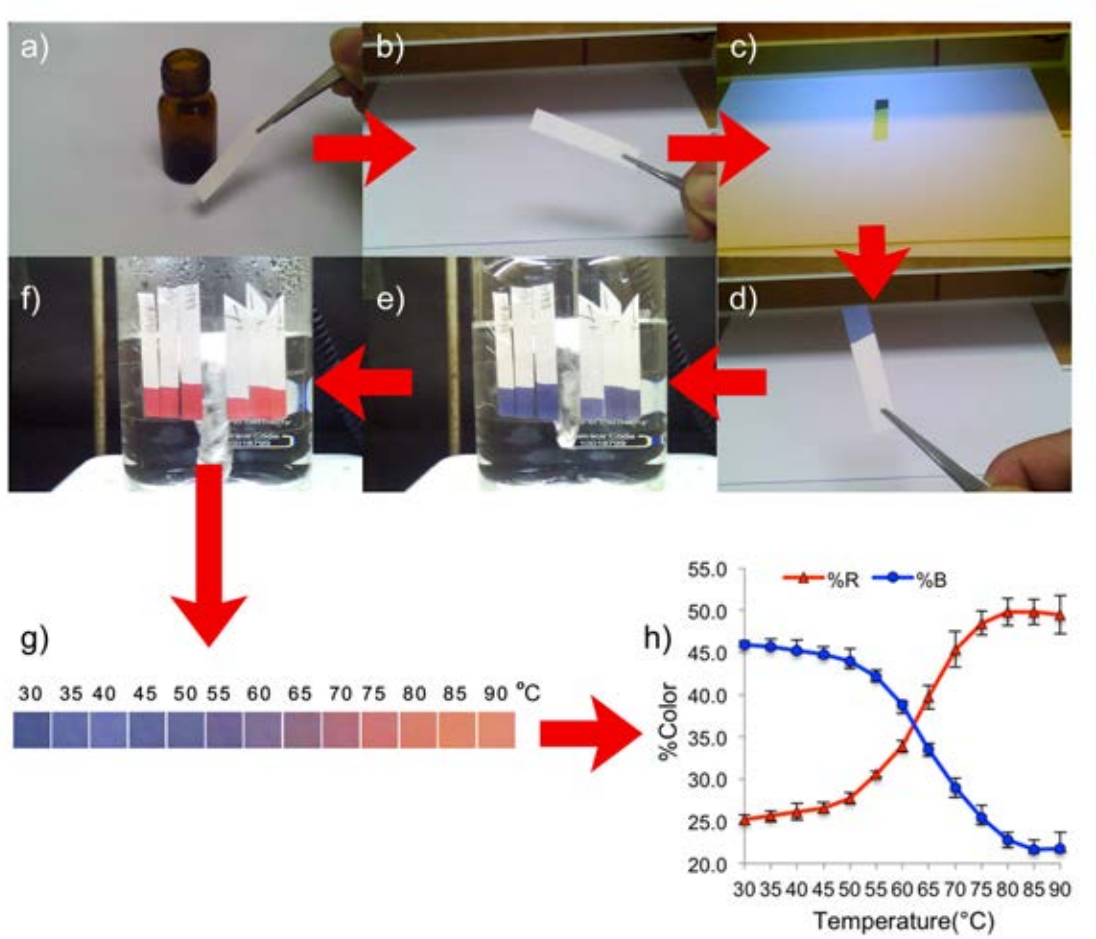

Scheme 3.2 Steps in preparation and thermal sensing study of paper-based PDA indicators: a) dip-coating, b) drying, c) UV irradiating, d) visualizing after UV irradiation, e) apparatus set-up for thermal sensing study before heating, f) indicators after heating, g) color images of indicators at various temperature and h) data processing for determination of color transition temperature.

3.3.1 Preparation of paper-based diacetylene indicator for thermal sensing study

For thermal sensing study, the indicators were prepared by a dip coating of filter paper with a diacetylene monomer followed by UV irradiation according to the scheme 3.2. Typically, a strip of filter paper was dipped into a solution of the diacetylene monomer in CH_2Cl_2. The dry paper strip was irradiated with 254 nm UV

light at room temperature to generate a blue paper-based PDA indicator (Table 3.2). The formation of blue color indicated a successful polymerization of the diacetylene monomer to its corresponding PDA. The irradiation period for each monomer was varied depending on their UV sensitivity that has been described earlier in section 3.2. After the photopolymerization process, the indicator was ready to be used in thermal sensing study.

Table 3.2 Irradiation time and color appearance of paper-based PDA indicators

Diacetylenes	Irradiation time	Color
PCDA	60	
TCDA	60	
NDDA	180	
ODDA	10	

Diacetylenes	Irradiation time	Color
EPCDP	30	
ETCDP	20	
ENDDP	10	
EODDP	10	

Diacetylenes	Irradiation time	Color
EPCDPP	10	
ETCDPP	10	
ENDDPP	10	
EODDPP	10	

3.3.2 Color transition of PDA indicator by temperature

The paper indicators were adhered to the side of the beaker 600 mL and they were heated from 30 ℃ to 90 ℃. The color images (Figure 3.9) of the indicators were recorded by a commercial webcam.

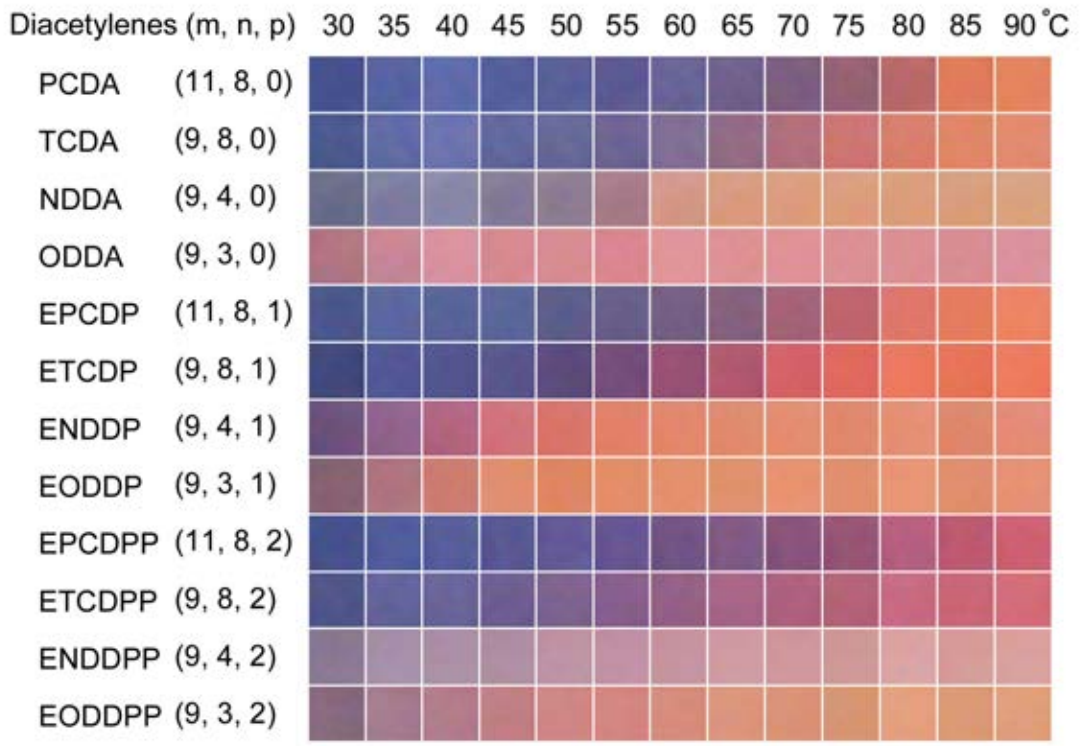

*m and n are the numbers of methylene groups while p is the the number of β-alanine units in the diacetylene monomers (see Scheme 3.1)

Figure 3.8 Color images of PDA indicators captured at different temperatures.

As shown in Figure 3.8, the color transition temperatures of the PDAs from the diacetylenes within the series of the same head group decrease with decreasing methylene chain length (n or m numbers) showing the higher thermal sensitivity that is in the same trend with the UV sensitivity of the diacetylenes. Furthermore, the PDAs with amide and diamide functional groups generally changed their color from blue to red at lower temperature than those with the same number of methylene groups but consisting of carboxylic acid functional group.

3.3.3 Determination of color transition temperatures

Using the RGB values according to the procedures described in section 3.2.3, the color transition temperatures were successfully determined from the color images of the indicators (similar to Figure 3.8). The plots of %R and %B against the

temperature gave the crossing point, assigned as the color transition temperatures (Figure 3.9).

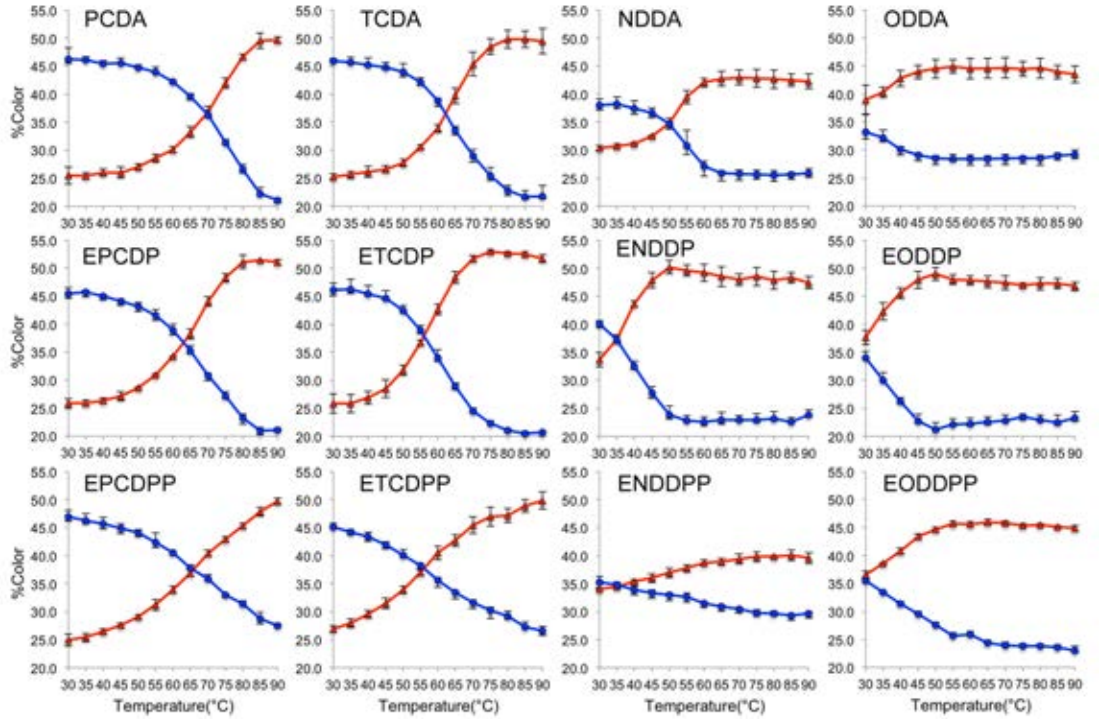

Figure 3.9 Plots of %R (▲) and %B (●) of the PDA indicators against temperature. Error bars represent standard deviations.

The color transition temperatures determined from the crossing point of %R and %B are listed in Table 3.3. The diacetylene that gives the lower temperature is more thermal sensitive. For examples, TCDA, ETCDP and ETCDPP changed their color from blue to red at 62.3±0.6 ℃, 56.4±0.7 ℃ and 55.6±0.8 ℃, respectively. The trends of the color transition temperatures determined from the RGB values are in good agreement with the trends of the color changes observed by naked eyes described in section 3.3.1.

Table 3.3 Color transition temperatures of the PDA indicators prepared from various diacetylene compounds

Compound	T (°C)
PCDA	69.7±0.9
TCDA	62.3±0.6
NDDA	49.6±1.2
ODDA	<30

Compound	T (°C)
EPCDP	63.1±0.6
ETCDP	56.4±0.7
ENDDP	34.5±0.9
EODDP	<30

Compound	T (°C)
EPCDPP	65.7±1.0
ETCDPP	55.6±0.8
ENDDPP	36.7±1.6
EODDPP	<30

The color transition temperatures of the PDAs were plotted as the red dots in Figure 3.10. The plot clearly shows the increase of temperature sensitivity with the decrease of the aliphatic chain length. In thermochromism, the role of the alkyl side chains on the temperature sensitivity has been attributed to the increase of their hydrophobic interaction, which in turn stabilizes the π-conjugated backbone [5,9,37]. The plot also shows that the color transition temperatures of the carboxylic acid series (PCDA, TCDA, NDDA and ODDA) are generally higher than those of the corresponding monoamide (EPCDP, ETCDP, ENDDP and EODDP) and diamide (EODDPP, ENDDPP, ETCDPP and EPCDPP). These quantitative results are well correlated with the color changes observed by eyes (Figure 3.8). The effects of the head group on the thermal sensitivity are related to the strength of hydrogen bonding among the polar head groups in the molecular self-assemblies of the diacetylene lipids[2,44]. The higher color transition temperatures of the carboxylic acid series thus suggest that the hydrogen bonding of the carboxylic head groups is stronger than that of the amide head groups.

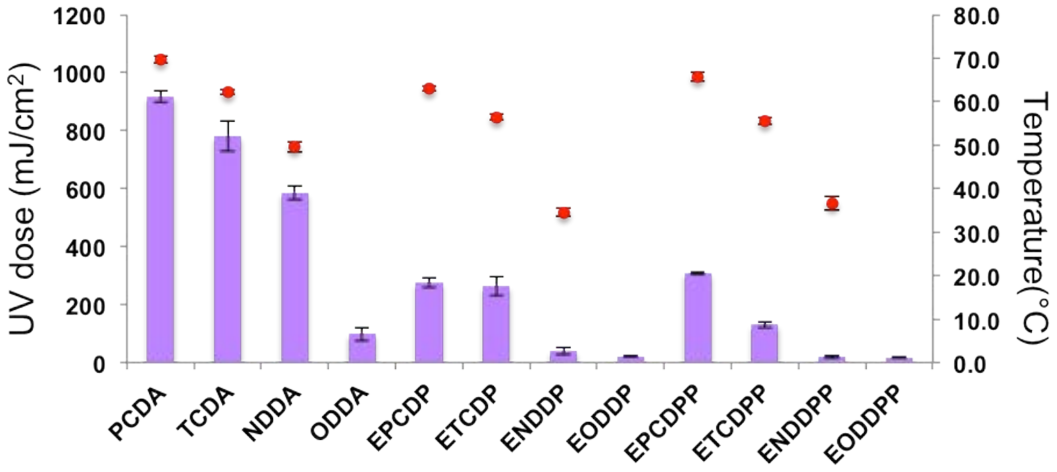

Figure 3.10 Color transition temperatures (●) and UV-doses (■) of diacetylene-based paper sensors. The plots are the average data obtained from 3 independent samples with the error bars representing the standard deviation.

To gain insight mechanism of the blue-to-red color transition induced by the UV irradiation, the color transition UV-doses (purple bars) of the PDAs were plotted in the same chart (Figure 3.10) with the color transition temperatures. Within each series, the chart shows the same trend of the color transition temperature and color transition UV-doses. This similarity suggests that the photo-induced thermochromism [42] is responsible for the sensitivity trend of the PDAs with the same side chain head groups observed during the UV irradiation. However, the comparison of thermal sensitivity between the series is not well correlated with their UV sensitivity. For example, the blue-to-red transition of EPCDP, a monopropanamide derivative, was observed at a much lower UV dose comparing with TCDA while both of them showed very similar color transition temperature. This difference is even more pronounced when comparing EPCDPP, a dipropanamide derivative, with TCDA; the less thermally sensitive EPCDPP is significantly more UV sensitive than TCDA. The results demonstrated that the color transition caused by UV irradiation is not solely driven by the photo-induced thermochromism. The blue-to-red transition during the UV irradiation of some PDAs has also been attributed to the conformational change caused by the propagation of the polymer chain [44,55,56]

3.3.4 Morphology change of PDAs upon heating

For SEM micrographs, the morphologies of polydiacetylene thermal indicators are shown in Figure 3.11. The red phase of diacetylene containing carboxylic acid head group showed PDA film rupture (Figure 3.11d) after being heated to 90 °C similar to that observed in the photo process (Figure 3.7d). Moreover, there are no morphology changes observed upon the thermochromic transition of PDAs with mono- and diamide groups (Figure 3.11 e and f).

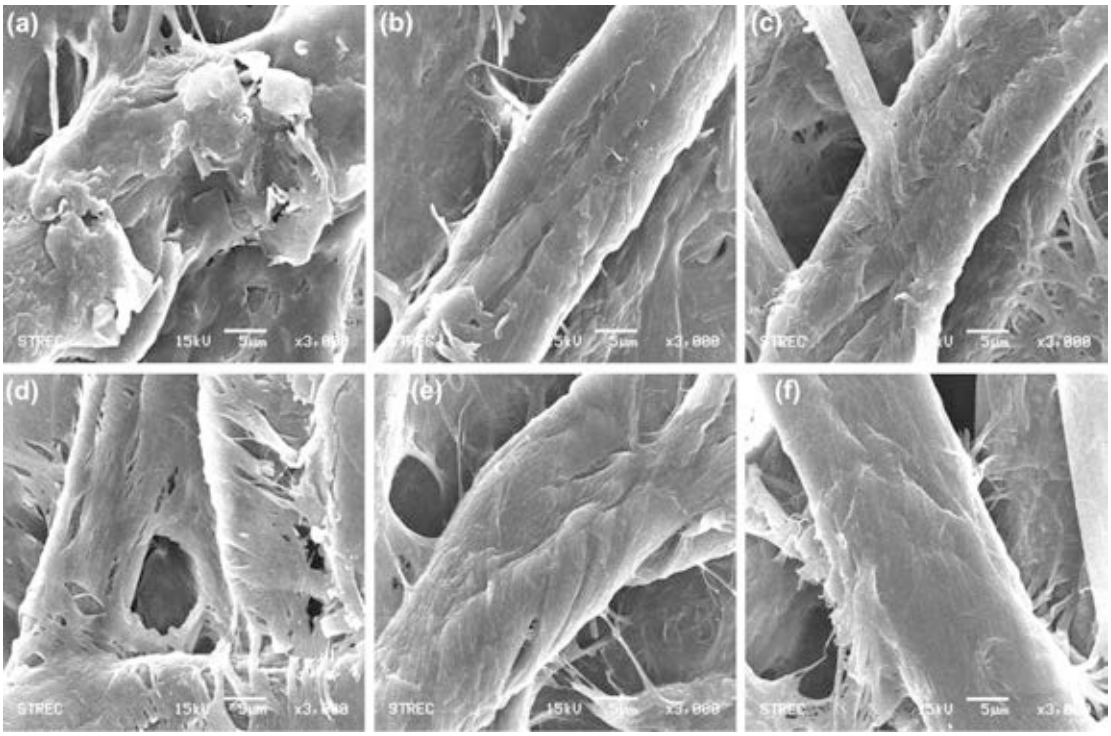

Figure 3.11 SEM (15 kV) micrographs of the filter paper coated with PDAs before heating: (a) PCDA (b) EPCDP (c) EPCDPP, and after heating: (d) PCDA (red) (e) EPCDP (red) (f) EPCDPP (purple).

3.4 Solvent sensing study

As PDAs are known to have solvatochromism, a color change upon a solvent contact, the PDAs from 6 monomers i.e. TCDA, PCDA, ETCDP, EPCDP, ETCDPP and EPCDPP were investigated for fabrication of an indicator array for solvent detection and identification. The indicators were prepared on filter paper by dip-coating technique from the diacetylene monomer solutions. The diacetylene coated paper strips were irradiated with 254 nm UV light to obtain the blue PDA indicators. To test the solvent sensing properties, the indicators were soaked with 14 solvents for 1 minute and allowed to dry in the air for 10 minutes. The color images of the indicators before and after solvent testing were recorded by a commercial scanner to determine the extent of their colorimetric responses.

As shown in Figure 3.12, the 6 PDA indicators show an array of colorimetric responses upon the contact with various solvents. The RGB values of the color images were evaluated by image processing software to provide a set of 756 RGB numerical data (3 RGB values × 14 solvents × 6 indicators × 3 replicates) as tabulated in Table D1-D6. These data were analyzed by principal component analysis (PCA) to generate clusters of PCA scores as shown in Figure 3.13. The PC score plot showed that the first and second components (PC1, PC2, PC3) accounted for 98.68%, 0.75% and 0.27% of the data variance, respectively. To evaluate the classification accuracy, linear discriminant analysis (LDA) was applied on the PC scores to cross validate the discriminating ability using a leave-one-out technique. The LDA cross validation gave 74% classification accuracy indicating relatively low discriminating ability of this indicator array for the 14 solvents. With careful inspection of the cross validation results, the problematic solvents, which cannot be discriminated, are ethylacetate, acetone and toluene.

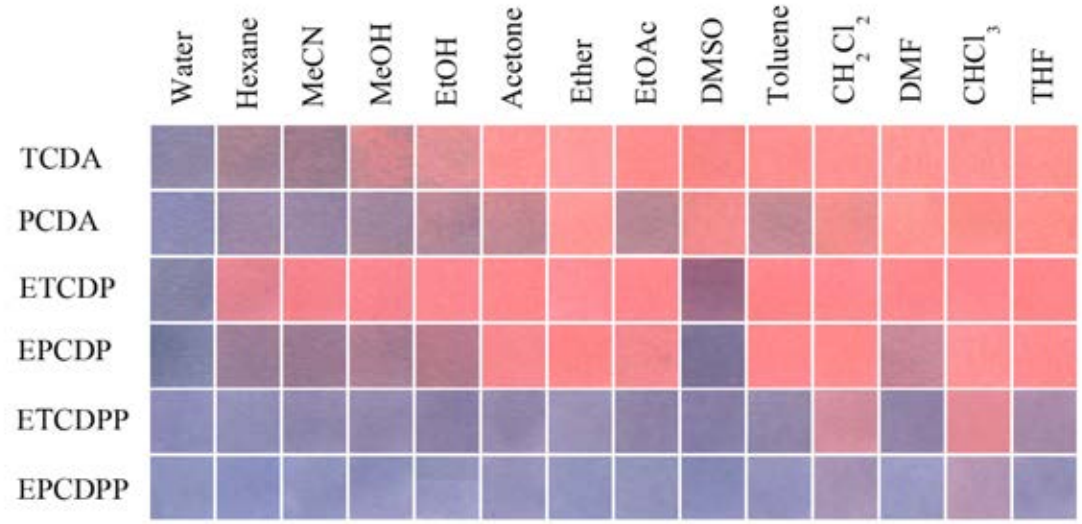

Figure 3.12 Color images of PDA indicators obtained after exposure to different solvents.

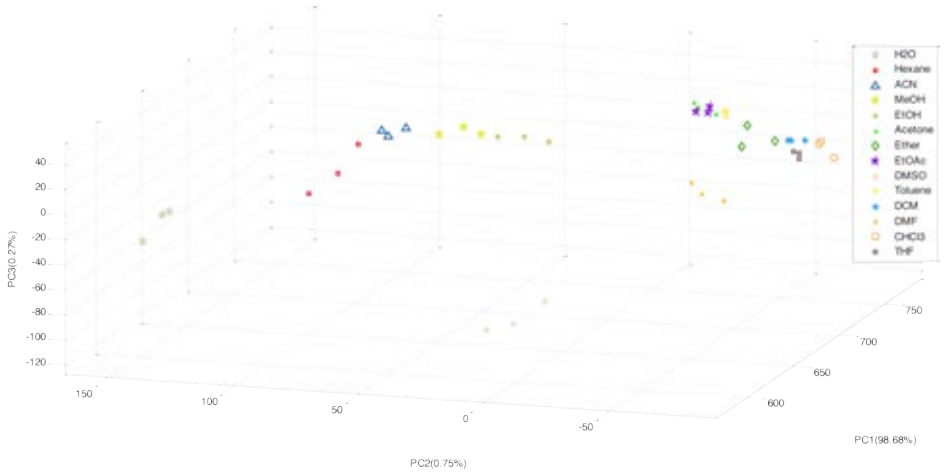

Figure 3.13 PCA score plots of the RGB values obtained from water (control) and 13 organic solvents tested by a sensing array PDA indicators.

3.5 Humidity indicators

The designs of paper-based PDA humidity indicators are based on the alkalinochromism of acidic PDAs using carbonate salts as the source of alkalinity. Two carbonate salts, Na_2CO_3 and K_2CO_3 were tested with two acidic diacetylene monomers, PCDA and TCDA. Three methods for the monomer and carbonate salt deposition on filter paper (Whatman No. 3), i.e. 1) single coating of diacetylene

carboxylate salts, 2) layer-by-layer coating of diacetylene carboxylic acid/carbonate salt and 3) zone coating of diacetylene carboxylic acid and carbonate salt, were investigated.

3.5.1 Single coating of diacetylene carboxylate salts

The diacetylene carboxylate salt was prepared by sonication of TCDA in a carbonate salt solution (Na_2CO_3 or K_2CO_3) until a milky solution was formed. The solution was left overnight at room temperature. The solution was then dropped on the filter paper, dried and irradiated by UV light. The paper coated with TCDA-Na^+ turned into sporadic black spots (Figure 3.14) while those of TCDA-K^+ indicators showed uneven purple spots. After exposed to the ambient humidity, the TCDA-Na^+ indicator did not show any apparent change while the color of TCDA-K^+ indicator changed from purple to red. It seems that the TCDA-K^+ salt may be useful as a moisture sensitive material, however this single coating of diacetylene carboxylate salt did not give uniform color on the filter paper. Better fabrication technique is needed.

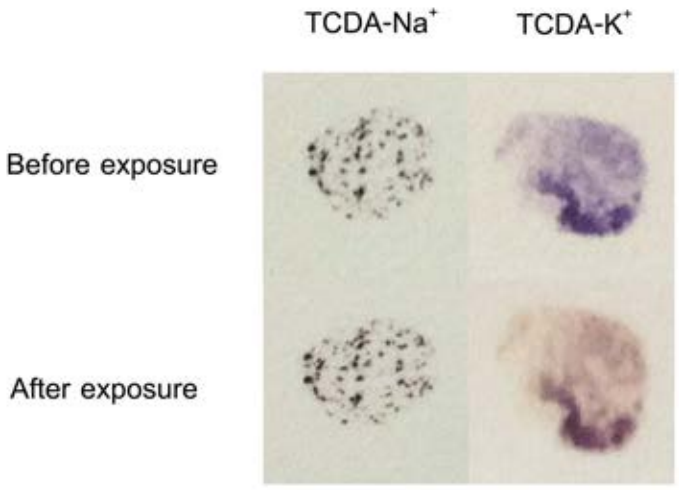

Figure 3.14 Images of indicators prepared from a single coating of TCDA carboxylate salts before and after exposed to the ambient humidity for 24 h.

3.5.2 Layer-by-layer coating of diacetylene carboxylic acid/carbonate salt

The layer-by-layer coating of diacetylene carboxylic acid/carbonate salt was performed in two ways. In the first method, TCDA was deposited on the filter paper

first and followed by the deposition of carbonate salt (Na_2CO_3 or K_2CO_3). The second method utilized the opposite deposition sequences, the carbonate salt followed by TCDA. After the layer-by-layer deposition, the coated paper was irradiated with UV 254 nm for 1 min. In the first method, TCDA with Na_2CO_3 did not polymerize (Figure 3.15) while that with K_2CO_3 polymerized to give a purple spot. After the exposure to the ambient humidity, there was no change for the indicators with Na_2CO_3 but the indicators with K_2CO_3 became more reddish. In the second method, TCDA with Na_2CO_3 gave a red spot while that with K_2CO_3 gave a purple spot after the UV irradiation. The indicator with Na_2CO_3 did not change its color while that with K_2CO_3 became more reddish after the exposure to the ambient humidity. All the results suggest that the K_2CO_3 salt is more appropriate for preparation of humidity indicators. However, the color transition from purple to reddish-purple was not satisfactory to indicate the change of humidity. Therefore, another fabrication method was attempted as described in the next section.

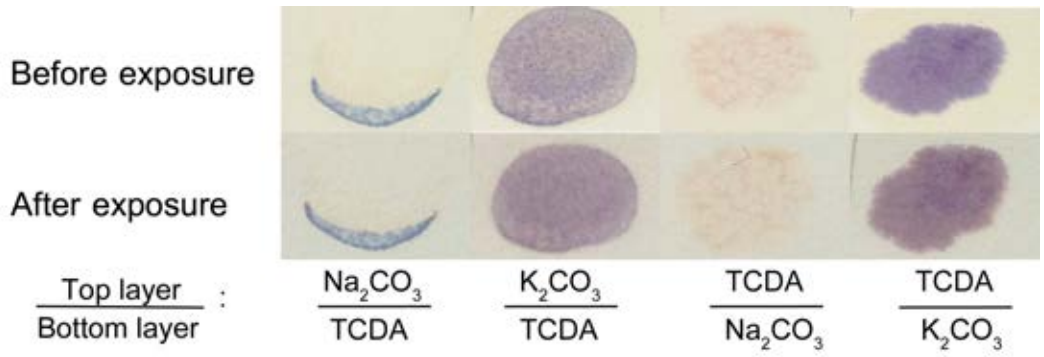

Figure 3.15 Images of indicators prepared by layer-by-layer coating of TCDA and carbonate salt before and after exposed to the ambient humidity for 24 h.

3.5.3 Zone coating of diacetylene carboxylic acid and carbonate salt

In this final preparation method, a filter paper strip was divided into 2 zones. The first zone was coated with carbonate salt and the second zone was coated with TCDA monomer. The filter paper strip was dipped into a saturated aqueous solution of the carbonate salt and dried at 100 ℃. Then, the other end of the filter paper strip was dipped into a TCDA solution in CH_2Cl_2 and the filter paper was dried in a desiccator. The coated paper was irradiated with 254 nm UV light to generate a

humidity indicator with blue PDA zone on one end and off-white zone of the carbonate salt on the other end. The dipping process was performed with care to make sure that these two zones are separated by 3 mm (See Scheme 3.3 for the preparation steps).

To test the humidity sensitivity, the indicator samples were placed in the chamber of which relative humidity (%RH) was controlled by a saturated NaBr solution. The color images of the indicators were recorded by a webcam (1.4 Mpixel). The %RH within the chamber was monitored with a hygrometer which showed relatively constant humidity of 62±1 %RH throughout the entire experimental period of 24 h. The color image of the blue zone was cropped and processed to obtain the RGB values for further analysis of the color transition time.

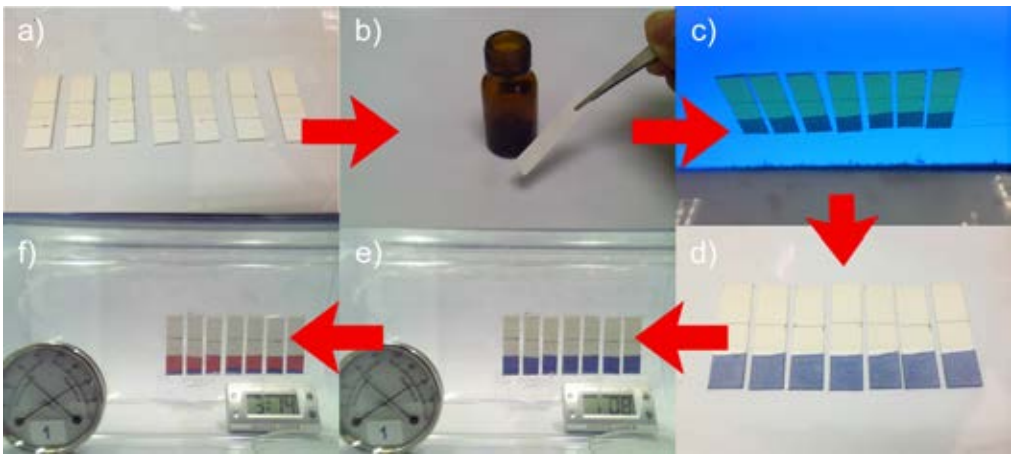

Scheme 3.3 Steps in preparation and humidity indicators from TCDA and carbonate salt using zone coating technique: a) dry filter paper strip coated with saturated carbonate solution, b) dip-coating of TCDA solution, c) UV irradiation of the TCDA zone, d) blue PDA zone appearance after UV irradiation, e) apparatus set-up for humidity sensing study, f) color change of the indicators captured by a webcam.

In Figure 3.16, the blue TCDA zone fabricated next to Na_2CO_3 did not change its color within 24 hours of the humidity exposure. On the other hand, the blue TCDA zone with K_2CO_3 started to turn red from the edge near the carbonate zone after 3 hours and the red color gradually expanded to fill the entire TCDA zone within 24 h.

An intersection point was observed in the plot of %R and %B against the exposure time for the indicator coated with K_2CO_3 around 6 h but not for the indicator using Na_2CO_3 salt (Figure 3.17). This allows the determination of the color transition time at specific relative humidity. The different colorimetric responses of the PDA to the different carbonate salts may be rationalized by the fact that Na_2CO_3 is less hygroscopic than K_2CO_3 [57] or the indicators fabricated with K_2CO_3, the filter paper became dampen after the humidity test while those fabricated with Na_2CO_3 remained relatively dry. Furthermore, the blue TCDA zone fabricated next to K_2CO_3 in 75% RH changed their color from blue to red within 3 h while those in 42% RH did not change their color (Figure 3.18). The crossing point of the plot of %R and %B against the exposure time in 75% RH for the indicator coated with K_2CO_3 was around 6 h but not for the indicator in 42% (Figure 3.19). Comparing the different PDA, the PCDA indicator with K_2CO_3 can change their color from blue to red in 62% RH and the plots of %R and %B against time showed that the indicator prepared from PCDA had similar humidity sensitivity as that from TCDA (Figure 3.20). After K_2CO_3 absorbs moisture in the air, the base gradually diffused toward the less concentrated area and attracted more moisture to the dry interface. By this mechanism and the alkalinochromism effect, the blue color of the PDA turned into red color with good time dependence. This time dependent colorimetric transition is highly desirable to indicate when the moisture-protected products have unintentionally exposed to the ambient humidity for an unacceptable period.

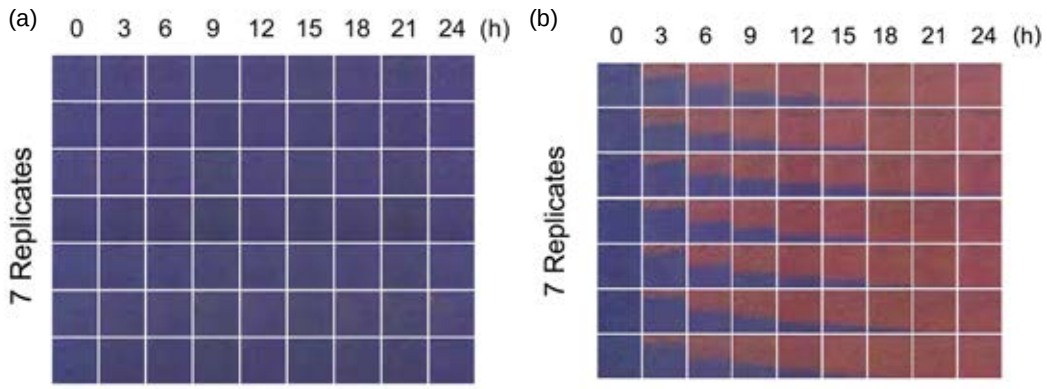

Figure 3.16 Color images of TCDA zone of the humidity indicators prepared with (a) Na_2CO_3 and (b) K_2CO_3 captured at different exposure times in a closed chamber having 62±1%RH.

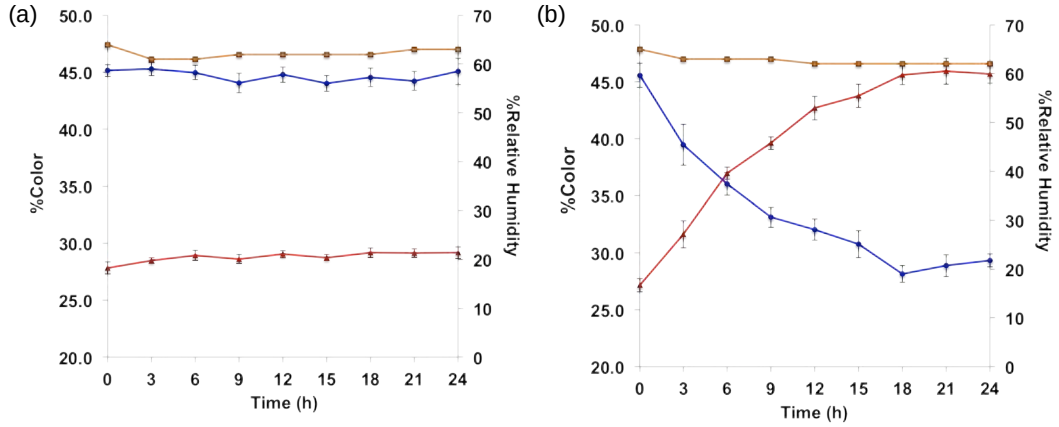

Figure 3.17 Plots of %R (▲) and %B (●) of the TCDA indicators with (a) Na_2CO_3 and (b) K_2CO_3 against exposure times under controlled %RH (■). Error bars represent standard deviations.

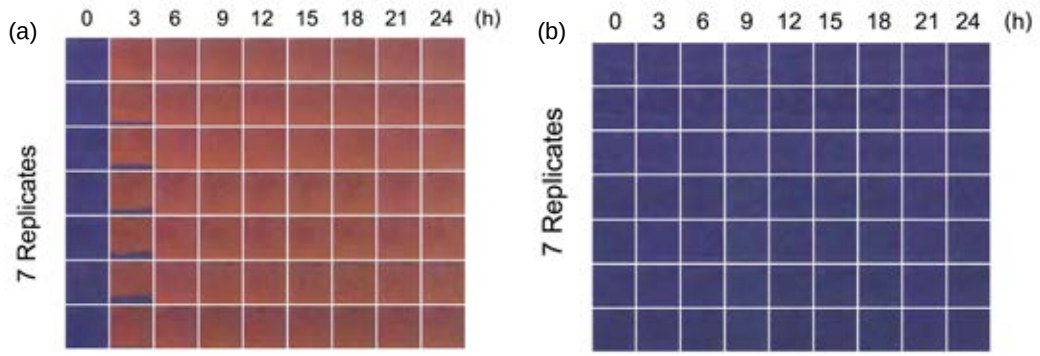

Figure 3.18 Color images of TCDA zone of the humidity indicators prepared with K_2CO_3 captured at different exposure times in a closed chamber having (a) 75±2% RH and (b) 42±2% RH.

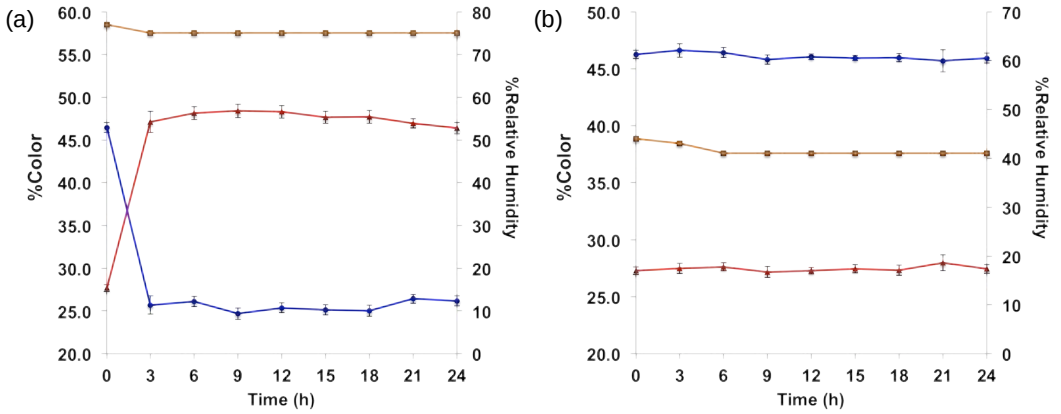

Figure 3.19 Plots of %R (▲) and %B (●) of the TCDA indicators with K_2CO_3 against exposure times under controlled %RH (■) by (a) NaCl (75±2% RH) and (b) $MgCl_2$ (42±2% RH). Error bars represent standard deviations.

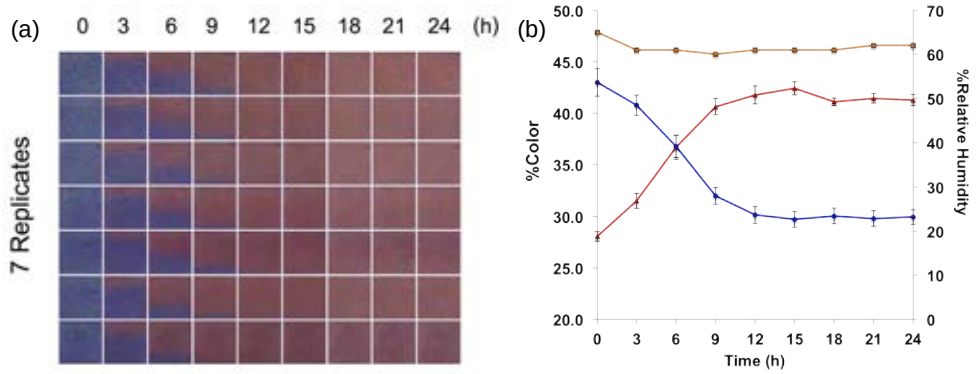

Figure 3.20 (a) Color images of PCDA zone of the humidity indicators prepared with K_2CO_3 captured at different exposure times in a closed chamber having 62±3% RH and (b) Plots of %R (▲) and %B (●) of the PCDA indicators with K_2CO_3 against exposure times under controlled %RH (■) by NaBr (62±3% RH).

CHAPTER IV

CONCLUSION

In conclusion, a novel series of diacetylene lipid monomers containing mono- and di-β-alanine ethyl ester with various length of methylene spacers were successfully synthesized. The diacetylene lipids were fabricated onto filter paper and photopolymerized by 254 nm UV light. The indicators were studied for 4 types of applications i.e. UV-dose indicators, temperature indicators, solvent indicators and humidity indicators. The color transitions of the indicators were determined from their color images using the RGB color system in which the crossing point of %B and %R curves from their plots against the independent variables such as time and temperature.

In UV sensing study, the coarse tuning of the UV sensitivity was achieved by converting the lipid head group from carboxylic acid to the amide or diamide, which ably affects the photochromism sensitivity, while the fine tuning was possible by varying the aliphatic chain length, which progressively affects the photo-induced thermochromism sensitivity. The conversions of the head groups from the carboxylic acid to the amide groups alter the intermolecular interaction and orientation in the monomer assembly.

In the thermal sensing study, the color transition temperature of the indicator increased with the aliphatic chain length. The carboxylic acid series (PCDA, TCDA, NDDA and ODDA) generally gave higher color transition temperature than those of the corresponding monoamide (EPCDP, ETCDP, ENDDP and EODDP) and diamide (EODDPP, ENDDPP, ETCDPP and EPCDPP). Comparing between different functional groups, thermal sensitivity was not always in line with UV sensitivity that demonstrated other mechanisms beyond the photo-induced thermochromism for the blue-to-red color transition induced by UV light.

In the solvent sensing study, 6 PDAs were used in the construction of the indicator array for detecting and identifying 14 solvents. The colorimetric responses were evaluated using RGB color system and analyzed by principal component

analysis (PCA). The 756 RGB numerical values (3 RGB values × 14 solvents × 6 indicators × 3 replicates) were transformed into clusters of PCA scores corresponding to each solvent. However, the LDA cross validation gave only 74% accuracy indicating relatively low discriminating ability of this array for classification of all 14 solvents.

In humidity sensing study, the humidity indicator was successfully fabricated by zone coating of TCDA and K_2CO_3. The edge of blue PDA zone next to the K_2CO_3 zone started to turn red after 3 hours and the red color gradually expanded to fill the entire PDA zone within 24 h at 62% RH. The indicator exhibited faster color transition at 75% RH where the entire PDA zone turned the color from blue to red within 3 h while the indicator became essentially insensitive at 42% RH. The plots of %R and %B against time showed that the indicator prepared from PCDA had similar humidity sensitivity as that from TCDA. The humidity sensitivity is governed by the alkalinochromism effect that depends on the rate of moisture absorption and diffusion on the filter paper coated with the carbonate salt. This time dependent colorimetric transition is highly desirable to indicate when the moisture-protected products have unintentionally exposed to the ambient humidity for an unacceptable period.

The monomer structures, sensor preparation and evaluation techniques devised in this dissertation should serve as guidelines for systematic study of PDA paper-based indicators toward the development of economical and reliable colorimetric sensors for various applications.

REFERENCES

[1] McQuade, D. T.; Pullen, A. E.; Swager, T. M. Conjugated polymer-based chemical sensors. *Chem. Rev.* 100 (2000): 2537-2574.

[2] Ahn, D. J.; Lee, S.; Kim, J. M. Rational design of conjugated polymer supramolecules with tunable colorimetric responses. *Adv. Funct. Mater.* 19 (2009): 1483-1496.

[3] Potisatityuenyong, A.; Rojanathanes, R.; Tumcharern, G.; Sukwattanasinitt, M. Electronic absorption spectroscopy probed side-chain movement in chromic transitions of polydiacetylene vesicles. *Langmuir* 24 (2008): 4461-4463.

[4] Wacharasindhu, S.; Montha, S.; Boonyiseng, J.; Potisatityuenyong, A.; Phollookin, C.; Tumcharern, G.; Sukwattanasinitt, M. Tuning of thermochromic properties of polydiacetylene toward universal temperature sensing materials through amido hydrogen bonding. *Macromolecules* 43 (2010): 716-724.

[5] Phollookin, C.; Wacharasindhu, S.; Ajavakom, A.; Tumcharern, G.; Ampornpun, S.; Eaidkong, T.; Sukwattanasinitt, M. Tuning down of color transition temperature of thermochromically reversible bisdiynamide polydiacetylenes. *Macromolecules* 43 (2010): 7540-7548.

[6] Song, J.; Cheng, Q.; Kopta, S.; Stevens, R. C. Modulating artificial membrane morphology: pH-induced chromatic transition and nanostructural transformation of a bolaamphiphilic conjugated polymer from blue helical ribbons to red Nanofibers. *J. Amer. Chem. Soc.* 123 (2001): 3205-3213.

[7] Shimizu, T.; Masuda, M.; Minamikawa, H. Supramolecular nanotube architectures based on amphiphilic molecules. *Chem. Rev.* 105 (2005): 1401-1443.

[8] Park, K. H.; Lee, J. S.; Park, H.; Oh, E. H.; Kim, J. M. Vancomycin-induced morphological transformation of self-assembled amphiphilic diacetylene supramolecules. *Chem. Commun.* 4 (2007): 410-412.

[9] Okada, S.; Peng, S.; Spevak, W.; Charych, D. Color and chromism of polydiacetylene vesicles. *Acc. Chem. Res.* 31 (1998): 229-239.

[10] Frankel, D. A.; Obrien, D. F. Supramolecular assemblies of diacetylenic aldonamides. *J. Amer. Chem. Soc.* 116 (1994): 10057-10069.

[11] Jonas, U.; Shah, K.; Norvez, S.; Charych, D. H. Reversible color switching and unusual solution polymerization of hydrazide-modified diacetylene lipids. *J. Amer. Chem. Soc.* 121 (1999): 4580-4588.

[12] Charych, D. H.; Nagy, J. O.; Spevak, W.; Bednarski, M. D. Direct colorimetric detection of a receptor-ligand interaction by a polymerized bilayer assembly. *Science* 261 (1993): 585-588.

[13] Van den Heuvel, M.; Lowik, D.; van Hest, J. C. M. Self-assembly and polymerization of diacetylene-containing peptide amphiphiles in aqueous solution. *Biomacromolecules* 9 (2008): 2727-2734.

[14] Champaiboon, T.; Tumcharern, G.; Potisatityuenyong, A.; Wacharasindhu, S.; Sukwattanasinitt, M. A polydiacetylene multilayer film for naked eye detection of aromatic compounds. *Sensor. Actuat-B.* 139 (2009): 532-537.

[15] Chen, X.; Yoon, J. A thermally reversible temperature sensor based on polydiacetylene: Synthesis and thermochromic properties. *Dyes. Pigments.* 89 (2011): 194-198.

[16] Eo, S. H.; Song, S.; Yoon, B.; Kim, J. M., A microfluidic conjugated-polymer sensor chip. *Adv. Mater.* 20 (2008): 1690-1694.

[17] Martinez, A. W.; Phillips, S. T.; Carrilho, E.; Thomas, S. W.; Sindi, H.; Whitesides, G. M. Simple telemedicine for developing regions: Camera phones and paper-based microfluidic devices for real-time, off-site diagnosis. *Anal. Chem.* 80 (2008): 3699-3707.

[18] Apilux, A.; Dungchai, W.; Siangproh, W.; Praphairaksit, N.; Henry, C. S.; Chailapakul, O., Lab-on-Paper with Dual Electrochemical/Colorimetric Detection for Simultaneous Determination of Gold and Iron. *Anal. Chem.* 82 (2010): 1727-1732.

[19] Pumtang, S.; Siripornnoppakhun, W.; Sukwattanasinitt, M.; Ajavakom, A. Solvent colorimetric paper-based polydiacetylene sensors from diacetylene lipids. *J. Colloid Interface Sci.* 364 (2011): 366-372.

[20] Thongmalai, W.; Eaidkong, T.; Ampornpun, S.; Mungkarndee, R.; Tumcharern, G.; Sukwattanasinitt, M.; Wacharasindhu, S., Polydiacetylenes carrying amino groups for colorimetric detection and identification of anionic surfactants. *J. Mater. Chem.* 21 (2011): 16391-16397.

[21] Eaidkong, T.; Mungkarndee, R.; Phollookin, C.; Tumcharern, G.; Sukwattanasinitt, M.; Wacharasindhu, S. Polydiacetylene paper-based colorimetric sensor array for vapor phase detection and identification of volatile organic compounds. *J. Mater. Chem.* 22 (2012): 5970-5977.

[22] Jung, Y. K.; Park, H. G.; Kim, J. M. Polydiacelylene (PDA)-based colorimetric detection of biotin-streptavidin interactions. *Biosensors Bioelectronics* 21 (2006): 1536-1544.

[23] http://www.nobelprize.org/nobel_prizes/physics/laureates/2009/press.html (accessed Jun 7, 2012)].

[24] Friedman, S.; Kolusheva, S.; Volinsky, R.; Zeiri, L.; Schrader, T.; Jelinek, R. Lipid/polydiacetylene films for colorimetric protein surface-charge analysis. *Anal. Chem.* 80 (2008): 7804-7811.

[25] Volinsky, R.; Kliger, M.; Sheynis, T.; Kolusheva, S.; Jelinek, R. Glass-supported lipid/polydiacetylene films for colour sensing of membrane-active compounds. *Biosensors Bioelectronics* 22 (2007): 3247-3251.

[26] Kim, J. M.; Lee, J. S.; Choi, H.; Sohn, D.; Ahn, D. J. Rational design and in-situ FTIR analyses of colorimetrically reversibe polydiacetylene supramolecules. *Macromolecules* 38 (2005): 9366-9376.

[27] Tajima, K.; Aida, T. Controlled polymerizations with constrained geometries *Chem. Commun.* 24 (2000): 2399-2412.

[28] Baughman, R. H.; Yee, K. C. Solid-state polymerization of linear and cyclic acetylenes *J. Polym. Sci. Macromol. Rev.* 13 (1978) 219-239.

[29] Enkelmann, V. Structural aspects of the topochemical polymerization of diacetylenes *Adv. Polym. Sci*. 63 (1984) 91-136. [30] Itoh, T.; Shichi, T.; Yui, T.; Takahashi, H.; Inui, Y.; Takagi, K. Reversible Color Changes in Lamella Hybrids of Poly(diacetylenecarboxylates) Incorporated in Layered Double Hydroxide Nanosheets. *J. Phys. Chem. B.* 109 (2005): 3199.

[30] Reppy, M.A.; Pindzola, B.A. Biosensing with polydiacetylene materials: structures, optical properties and applications *Chem. Commu*n, (2007) 4137-4338.

[31] Yoon, J.; Chae, S.; Kim, J. Colorimetric sensors for volatile organic compounds (VOCs) based on conjugated polymer-embedded electrospun fibers *J. Am. Chem. Soc.* 129 (2007) 3038-3039.

[32] Rangin, M.; Basu, A., Lipopolysaccharide identification with functionalized polydiacetylene liposome sensors. *J. Am. Chem. Soc.* 126 (2004): 5038-5039.

[33] Yoon, B.; Lee, S.; Kim, J. M. Recent conceptual and technological advances in polydiacetylene-based supramolecular chemosensors. *Chem. Soc. Rev.* 38 (2009): 1958-1968.

[34] Su, Y. L.; Li, J. R.; Jiang, L., Chromatic immunoassay based on polydiacetylene vesicles. *Colloids Surf.B.* 38 (2004): 29-33.

[35] http://en.wikipedia.org/wiki/RGB_color_model (accessed April 17, 2013)].

[36] Kuriyama, K.; Kikuchi, H.; and Kajiyama, T. Chromatic Phase of Polydiacetylene Langmuir-Blodgett Film. *Langmuir* 14 (1998): 1130-1138.

[37] Fujita, N.; Sakamoto, Y.; Shirakawa, M.; Ojima, M.; Fujii, A.; Ozaki, M.; Shinkai, S., Polydiacetylene nanofibers created in low-molecular-weight gels by post modification: Control of blue and red phases by the odd-even effect in alkyl chains. *J. Am. Chem. Soc.* 129 (2007): 4134-4135.

[38] Ampornpun, S.; Montha, S.; Tumcharern, G.; Vchirawongkwin, V.; Sukwattanasinitt, M.; Wacharasindhu, S. Odd-Even and Hydrophobicity

Effects of Diacetylene Alkyl Chains on Thermochromic Reversibility of Symmetrical and Unsymmetrical Diyndiamide Polydiacetylenes. *Macromolecules* 45 (2012): 9038-9045.

[39] Chanakul, A.; Traiphol, N.; Traiphol, R. Controlling the reversible thermochromism of polydiacetylene/zinc oxide nanocomposites by varying alkyl chain length. *J. Colloid Interface Sci.* 389 (2013): 106-114.

[40] Kanetake, T.; Tokura, Y.; Koda, T. Photo and thermochromism in vacuum deposited polydiacetylene films. *Solid State Commun.* 56 (1985): 803-807.

[41] Tokura, Y. Photochromism and photoinduced bond-structure change in the conjugated polymer polydiacetylene. *Phys. Rev. B.* 36 (1987): 2913-2915.

[42] Wenzel, M.; Atkinson, G. H.; Chromatic Properties of Polydiacetylene Films. *J. Am. Chem. Soc.* 111 (1989): 6123-6121.

[43] Peng, J. C. Photochromism and its mechanism polydiacetylene crystals. *Acta Phisica Sinica* 6 (1997): 140-150.

[44] Huo, Q.; Russell, K. C.; Leblanc, R. M. Chromatic studies of a polymerizable diacetylene hydrogen bonding self-assembly: A "self-folding" process to explain the chromatic changes of polydiacetylenes. *Langmuir* 15 (1999): 3972-3980.

[45] Song, J.; Cisar, J. S.; Bertozzi, C. R. Functional self-assembling bolaamphiphilic polydiacetylenes as colorimetric sensor scaffolds. *J. Am. Chem. Soc.* 126 (2004): 8459-8465.

[46] Yuan, W. F.; Jiang, G. Y.; Song, Y. L.; Jiang, L. Micropatterning of polydiacetylene based on a photoinduced chromatic transition and mechanism study. *J. Appl. Pol. Sci.* 103 (2007): 942-946.

[47] Sung, X. M.; Chen, T.; Huang, S. Q.; Cai, F. J.; Chen, X. L.; Yang, Z. B.; Li, L.; Cao, H.; Lu, Y. F.; Peng, H. S., UV-Induced Chromatism of Polydiacetylenic Assemblies. *J. Phys. Chem. B* 114 (2010): 2379-2382.

[48] Yoon, J.; Jung, Y. S.; Kim, J. M. A Combinatorial Approach for Colorimetric Differentiation of Organic Solvents Based on Conjugated Polymer-Embedded Electrospun Fibers. *Advanced Functional Materials* 19 (2009): 209-214.

[49] Jiang, H.; Wang, Y. L.; Ye, Q.; Zou, G.; Su, W.; Zhang, Q. J. Polydiacetylene-based colorimetric sensor microarray for volatile organic compounds. *Sensors Actuat-B.* 143 (2010): 789-794.

[50] Wu, S.; Zhang, Q. J.; Bubeck, C. Solvent Effects on Structure, Morphology, and Photophysical Properties of an Azo Chromophore-Functionalized Polydiacetylene. *Macromolecules* 43 (2010): 6142-6151.

[51] Cheng, Q.; Stevens, C. Charge-induced chromatic transition of amino acid-derivatized polydiacetylene liposomes. *Langmuir* 14 (1998): 1974.

[52] Charoenthai, N.; Pattanatornchai, T.; Wacharasindhu, S.; Sukwattanasinitt, M.; Traiphol, R., Roles of head group architecture and side chain length on colorimetric response of polydiacetylene vesicles to temperature, ethanol and pH. *J. Colloid Interface Sci.* 360 (2011): 565-573.

[53] Jiwpanich, S. Effect of substituents on salicylimine catalysts on enantioselectivity of asymmetric strecker reaction, Degree of Master of Science in Chemistry, Faculty of Science, Chulalongkorn University (2002)

[54] Li, L. S.; Stupp, S. I., Two-dimensional supramolecular assemblies of a polydiacetylene .2. Morphology, structure, and chromic transitions. *Macromolecules* 30 (1997): 5313-5320.

[55] Huo, Q.; Wang, S. P.; Pisseloup, A.; Verma, D.; Leblanc, R. M. Unusual chromatic properties observed from polymerized dipeptide diacetylenes. *Chem. Commun.* 16 (1999): 1601-1602.

[56] Hsu, L.; Cvetanovich, G. L.; Stupp, S. I. Peptide amphiphile nanofibers with conjugated polydiacetylene backbones in their core. *J. Amer. Chem. Soc.* 12 (2008): 3892-3899.

[57] Greenspun, L. Humidity fixed points of binary saturated aqueous solutions. *J. res. Nat. Bur. Stand*-A. 81 (1977): 89-96.

APPENDICES

APPENDIX A

NMR SPECTRA

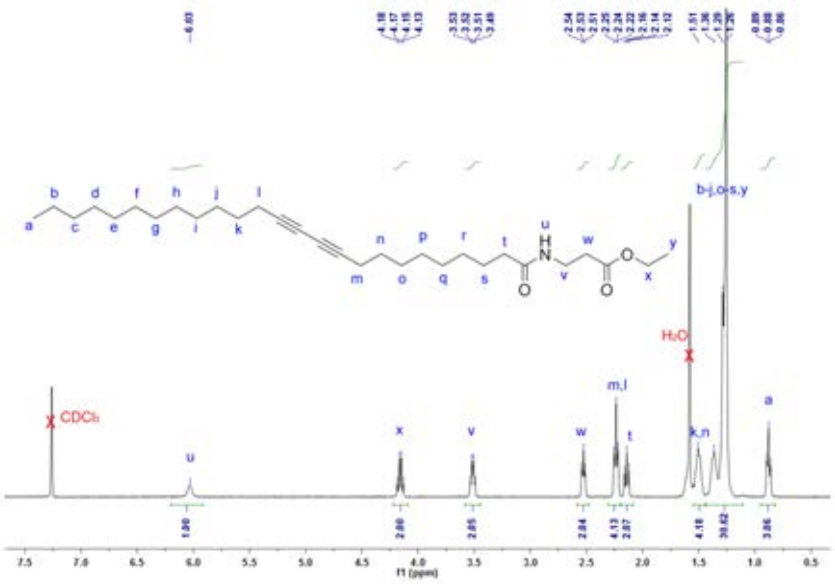

Figure A1 ^{1}H spectrum of Ethyl 3-(pentacosa-10,12-diynamido)propanoate (EPCDP) in $CDCl_3$.

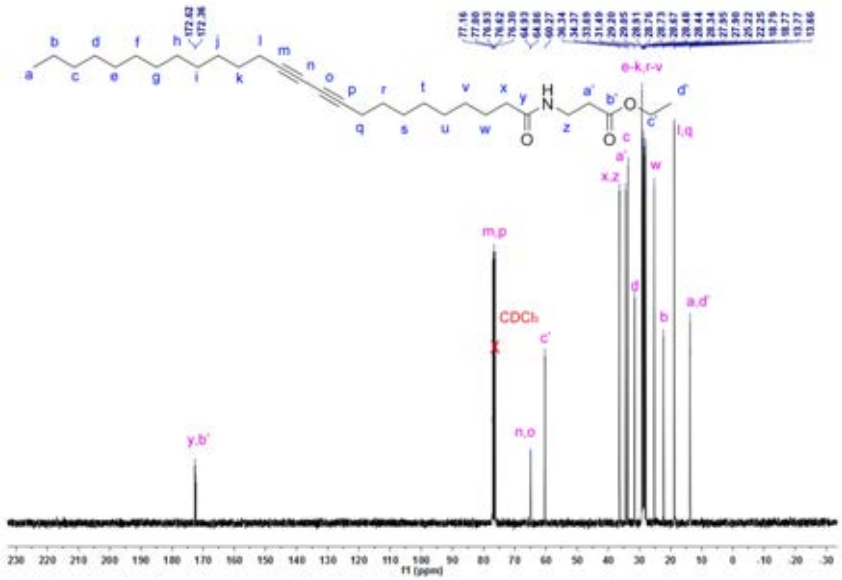

Figure A2 ^{13}C spectrum of Ethyl 3-(pentacosa-10,12-diynamido)propanoate (EPCDP) in $CDCl_3$.

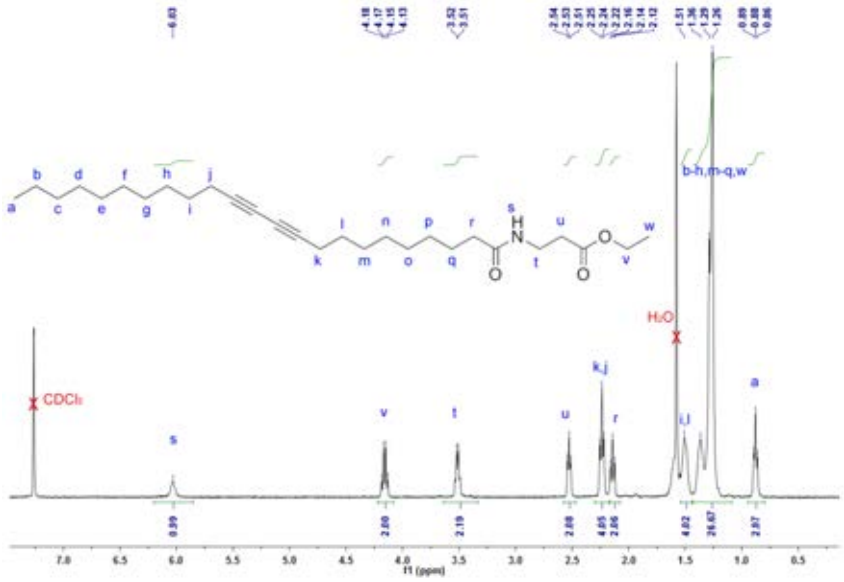

Figure A3 ^{1}H spectrum of Ethyl 3-tricosa-10,12-diynamidopropanoate (ETCDP) in $CDCl_3$.

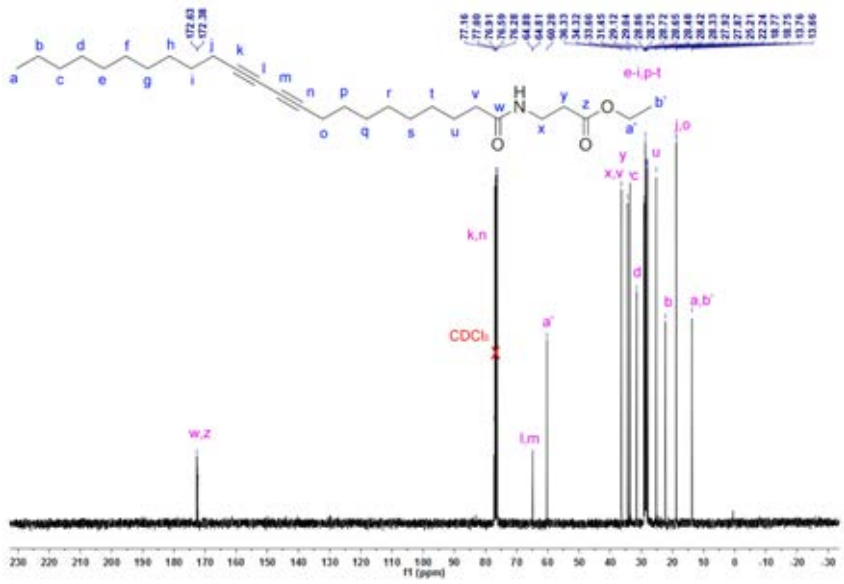

Figure A4 ^{13}C spectrum of Ethyl 3-tricosa-10,12-diynamidopropanoate (ETCDP) in $CDCl_3$.

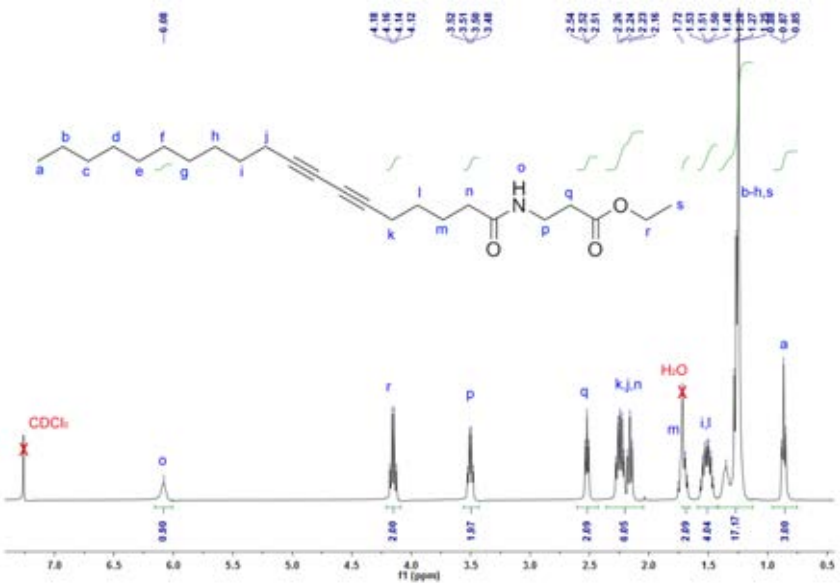

Figure A5 ^{1}H spectrum of Ethyl 3-nonadeca-6,8-diynamidopropanoate (ENDDP) in $CDCl_3$.

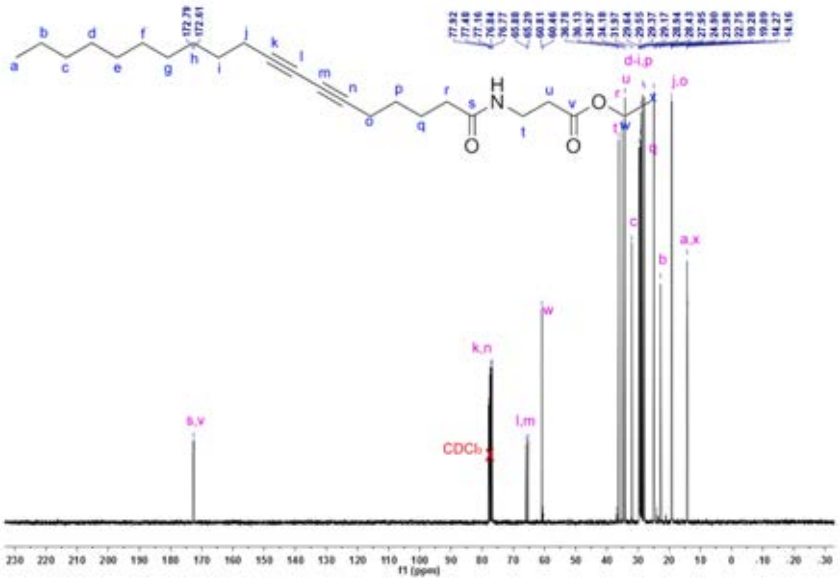

Figure A6 ^{13}C spectrum of Ethyl 3-nonadeca-6,8-diynamidopropanoate (ENDDP) in $CDCl_3$.

Figure A7 ^{1}H spectrum of Ethyl 3-octadeca-5,7-diynamidopropanoate (EODDP) in $CDCl_3$.

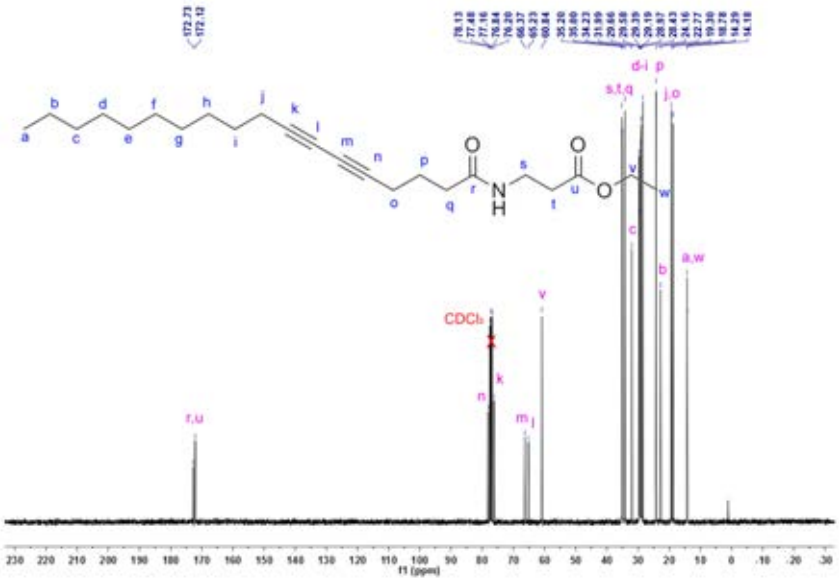

Figure A8 ^{13}C spectrum of Ethyl 3-octadeca-5,7-diynamidopropanoate (EODDP) in $CDCl_3$.

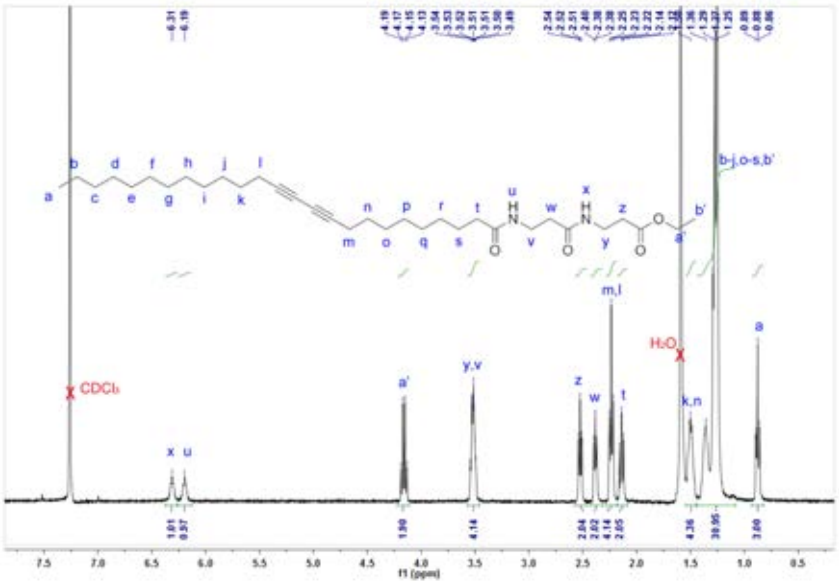

Figure A9 ^{1}H spectrum of Ethyl 3-(3-pentacosa-10,12-diynamidopropanamido)propanoate (EPCDPP) in $CDCl_3$.

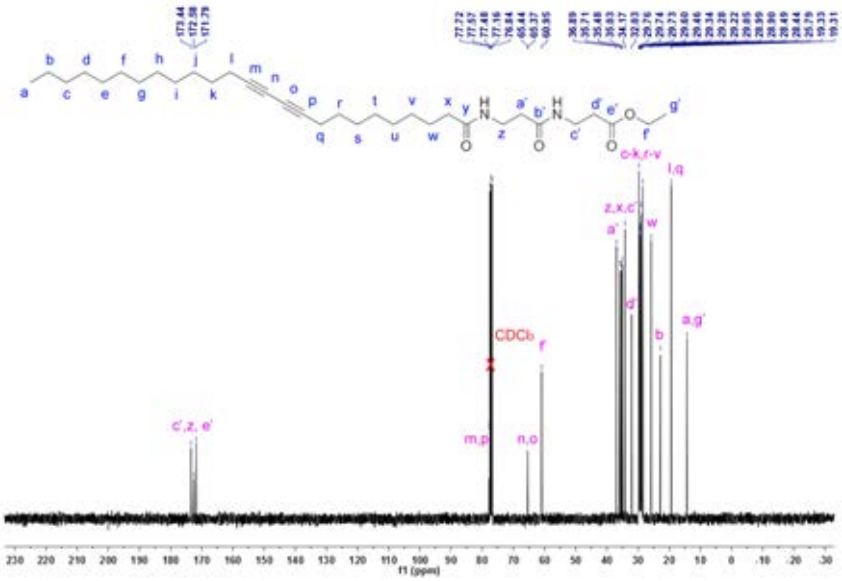

Figure A10 ^{13}C spectrum of Ethyl 3-(3-pentacosa-10,12-diynamidopropanamido)propanoate (EPCDPP) in $CDCl_3$.

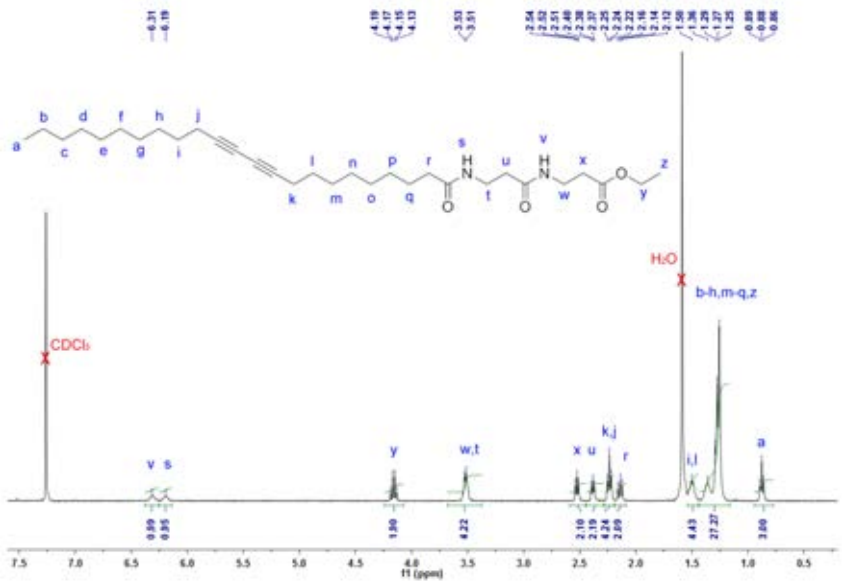

Figure A11 ^{1}H spectrum of Ethyl 3-(3-tricosa-10, 12-diynamidopropanamido) propanoate (ETCDPP) in $CDCl_3$.

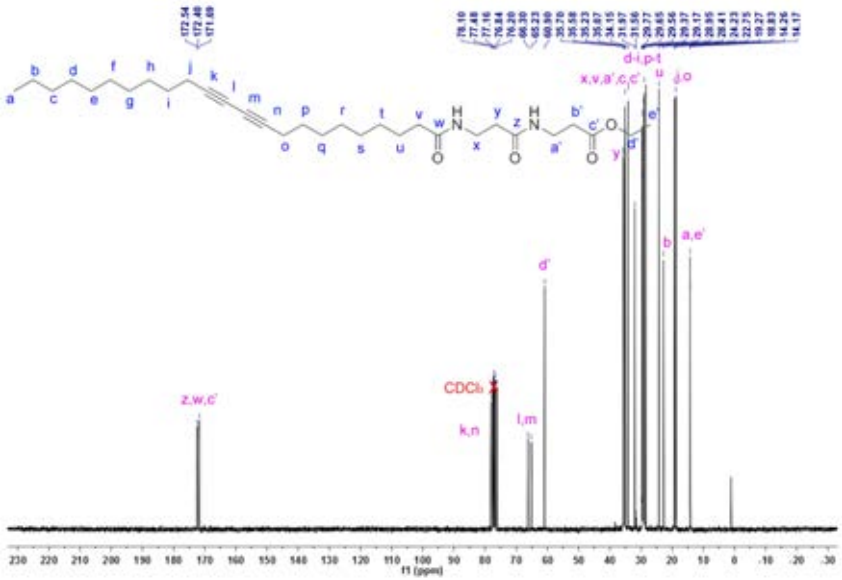

Figure A12 ^{13}C spectrum of Ethyl 3-(3-tricosa-10, 12-diynamidopropanamido) propanoate (ETCDPP) in $CDCl_3$.

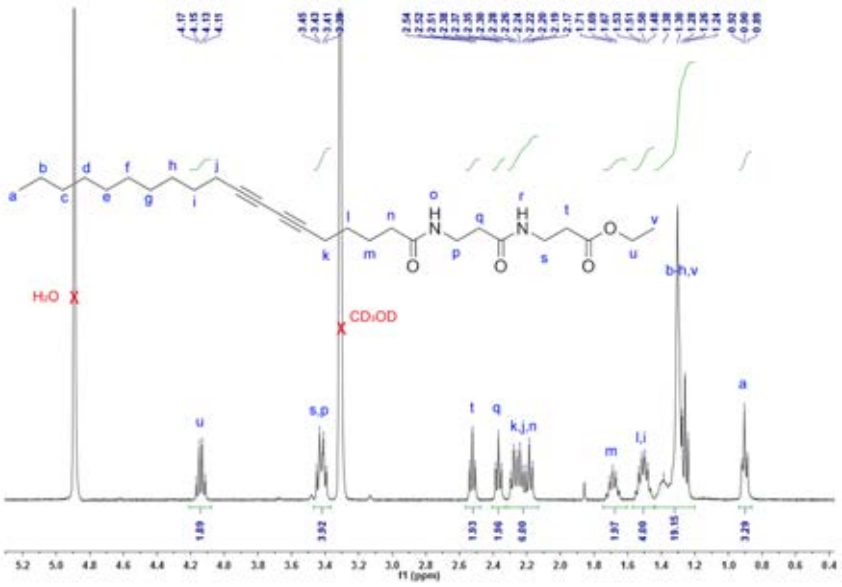

Figure A13 ^{1}H spectrum of Ethyl 3-(3-nonadeca-6,8-diynamidopropanamido) propanoate (ENDDPP) in CD_3OD.

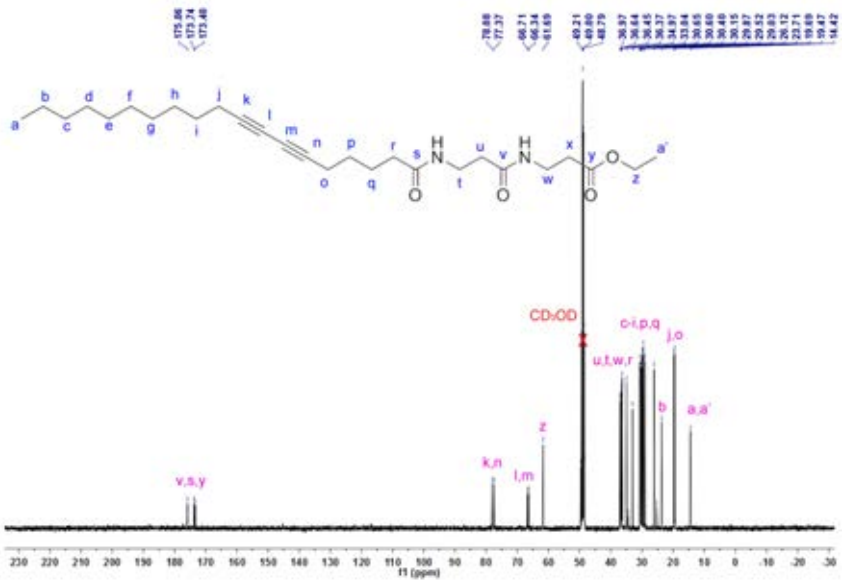

Figure A14 ^{13}C spectrum of Ethyl 3-(3-nonadeca-6,8-diynamidopropanamido) propanoate (ENDDPP) in CD_3OD.

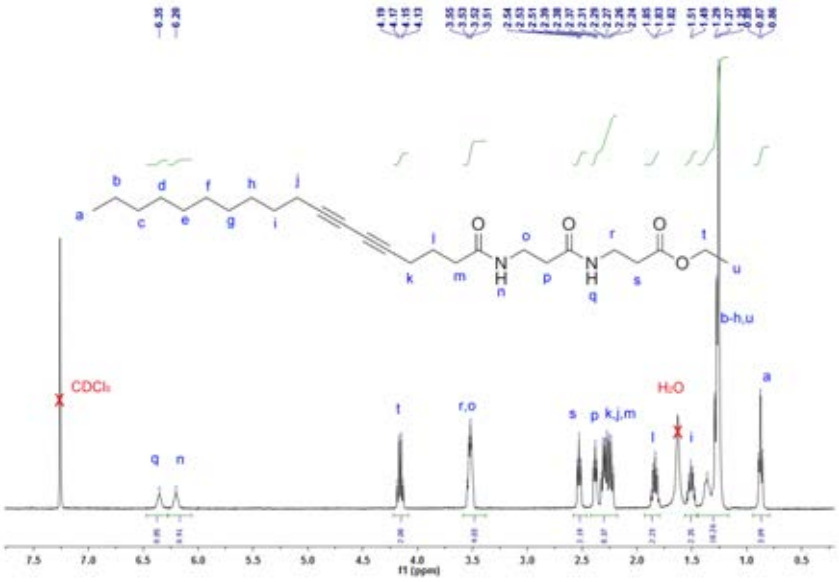

Figure A15 ^{1}H spectrum of Ethyl 3-(3-octadeca-5, 7-diynamidopropanamido) propanoate(EODDPP) in $CDCl_3$.

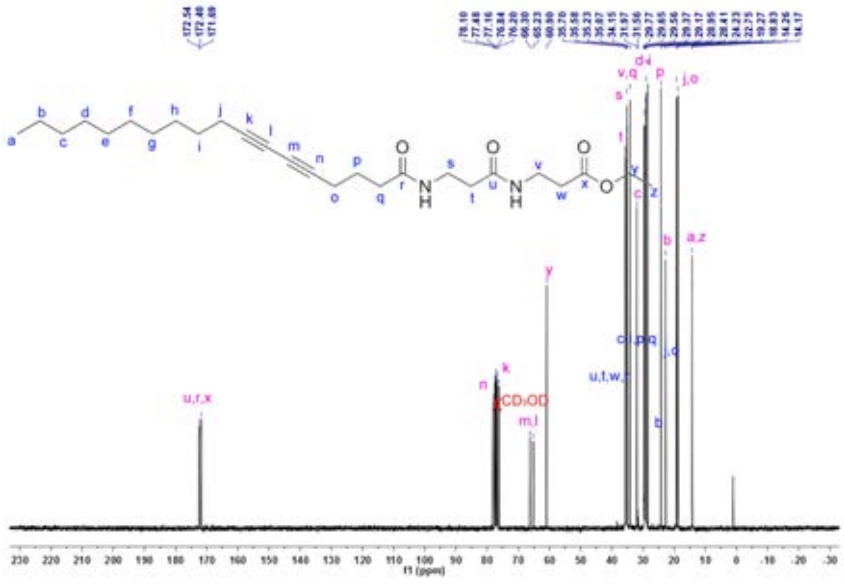

Figure A16 ^{13}C spectrum of Ethyl 3-(3-octadeca-5, 7-diynamidopropanamido) propanoate(EODDPP) in $CDCl_3$.

APPENDIX B

UV SENSING STUDY

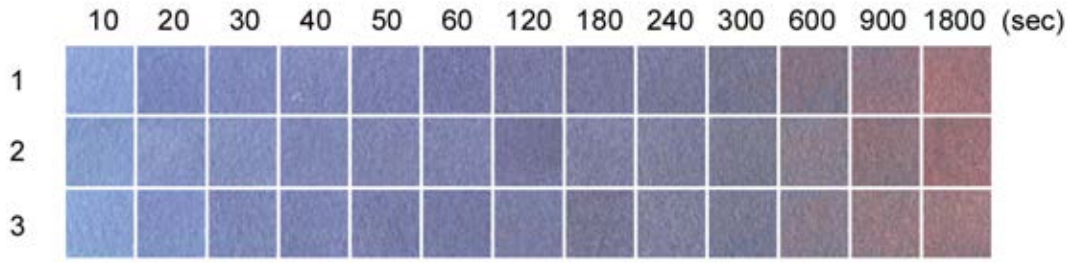

Figure B1 Photographs of UV sensing of PCDA indicators.

Table B1 RGB values of PCDA indicators at various UV doses (3 independent experiments)

UV dose (mJ/cm^2)	1				UV dose (mJ/cm^2)	2				UV dose (mJ/cm^2)	3			
	R	G	B	Sum		R	G	B	Sum		R	G	B	Sum
14	140	162	212	514	14	134	157	203	494	14	138	163	211	512
28	123	136	188	447	28	138	152	197	487	28	130	146	197	473
42	128	138	187	453	42	133	144	188	465	42	126	137	182	445
56	130	139	185	454	56	127	135	179	441	56	125	133	178	436
70	124	130	176	430	70	128	133	173	434	70	120	126	167	413
84	118	121	164	403	84	128	132	172	432	84	118	122	162	402
168	121	124	161	406	168	117	117	152	386	168	122	127	162	411
252	119	121	155	395	252	127	128	160	415	252	120	120	147	387
336	121	122	153	396	336	125	128	155	408	336	128	129	155	412
420	120	119	143	382	420	124	123	145	392	420	122	122	145	389
840	130	117	133	380	840	138	127	141	406	840	136	125	139	400
1260	142	118	132	392	1260	140	117	126	383	1260	149	123	132	404
2520	161	118	123	402	2520	151	114	119	384	2520	156	123	134	413

Table B2 %RGB values of PCDA indicators at various UV doses (3 independent experiments)

UV dose (mJ/cm^2)	1			UV dose (mJ/cm^2)	2			UV dose (mJ/cm^2)	3		
	%R	%G	%B		%R	%G	%B		%R	%G	%B
14	27.2	31.5	41.2	14	27.1	31.8	41.1	14	27.0	31.8	41.2
28	27.5	30.4	42.1	28	28.3	31.2	40.5	28	27.5	30.9	41.6
42	28.3	30.5	41.3	42	28.6	31.0	40.4	42	28.3	30.8	40.9
56	28.6	30.6	40.7	56	28.8	30.6	40.6	56	28.7	30.5	40.8
70	28.8	30.2	40.9	70	29.5	30.6	39.9	70	29.1	30.5	40.4
84	29.3	30.0	40.7	84	29.6	30.6	39.8	84	29.4	30.3	40.3
168	29.8	30.5	39.7	168	30.3	30.3	39.4	168	29.7	30.9	39.4
252	30.1	30.6	39.2	252	30.6	30.8	38.6	252	31.0	31.0	38.0
336	30.6	30.8	38.6	336	30.6	31.4	38.0	336	31.1	31.3	37.6
420	31.4	31.2	37.4	420	31.6	31.4	37.0	420	31.4	31.4	37.3
840	34.2	30.8	35.0	840	34.0	31.3	34.7	840	34.0	31.3	34.8
1260	36.2	30.1	33.7	1260	36.6	30.5	32.9	1260	36.9	30.4	32.7
2520	40.0	29.4	30.6	2520	39.3	29.7	31.0	2520	37.8	29.8	32.4

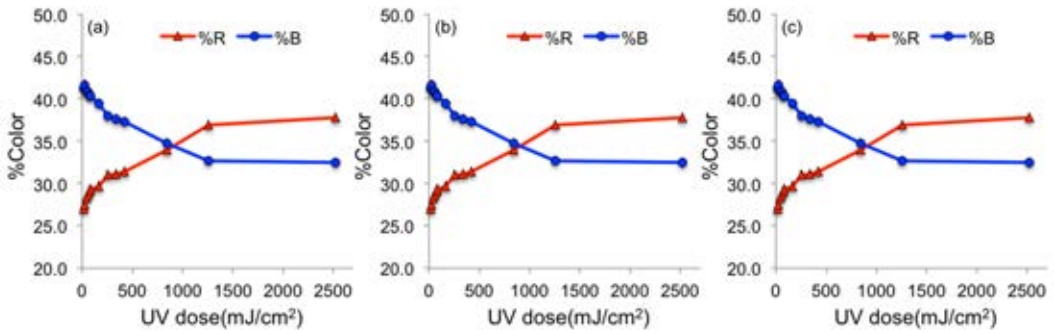

Figure B2 Plots of %RGB value of 3 independent PCDA indicators against UV dose to determine the color transition UV dose.

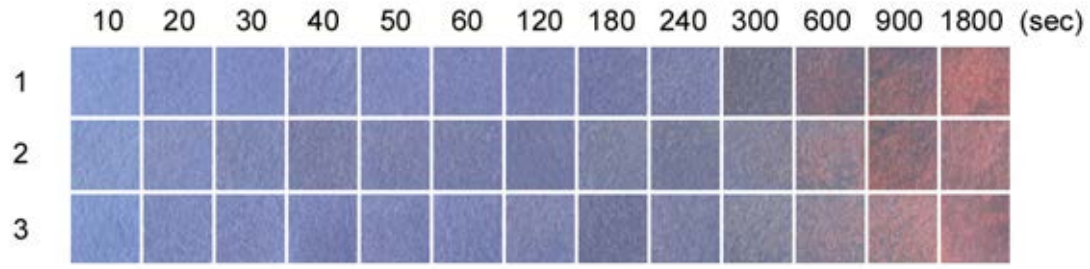

Figure B3 Photographs of UV sensing of TCDA indicators.

Table B3 RGB values of TCDA indicators at various UV doses (3 independent experiments)

UV dose (mJ/cm^2)	1				UV dose (mJ/cm^2)	2				UV dose (mJ/cm^2)	3			
	R	G	B	Sum		R	G	B	Sum		R	G	B	Sum
14	134	154	207	495	14	136	154	200	490	14	128	149	201	478
28	127	141	193	461	28	133	144	188	465	28	127	139	188	454
42	127	138	192	457	42	128	136	180	444	42	129	138	186	453
56	127	136	186	449	56	124	129	167	420	56	122	131	178	431
70	128	137	186	451	70	127	133	173	433	70	126	133	180	439
84	125	133	181	439	84	123	129	168	420	84	125	132	179	436
168	121	128	175	424	168	118	123	163	404	168	128	133	172	433
252	118	123	165	406	252	126	131	160	417	252	114	118	153	385
336	127	132	168	427	336	120	124	153	397	336	126	130	163	419
420	115	115	134	364	420	133	132	154	419	420	136	136	156	428
840	131	112	126	369	840	149	131	143	423	840	149	135	149	433
1260	136	111	122	369	1260	141	111	120	372	1260	170	135	144	449
2520	179	119	122	420	2520	170	125	133	428	2520	163	122	132	417

Table B4 %RGB values of TCDA indicators at various UV doses (3 independent experiments)

UV dose (mJ/cm^2)	1			UV dose (mJ/cm^2)	2			UV dose (mJ/cm^2)	3		
	%R	%G	%B		%R	%G	%B		%R	%G	%B
14	27.1	31.1	41.8	14	27.8	31.4	40.8	14	26.8	31.2	42.1
28	27.5	30.6	41.9	28	28.6	31.0	40.4	28	28.0	30.6	41.4
42	27.8	30.2	42.0	42	28.8	30.6	40.5	42	28.5	30.5	41.1
56	28.3	30.3	41.4	56	29.5	30.7	39.8	56	28.3	30.4	41.3
70	28.4	30.4	41.2	70	29.3	30.7	40.0	70	28.7	30.3	41.0
84	28.5	30.3	41.2	84	29.3	30.7	40.0	84	28.7	30.3	41.1
168	28.5	30.2	41.3	168	29.2	30.4	40.3	168	29.6	30.7	39.7
252	29.1	30.3	40.6	252	30.2	31.4	38.4	252	29.6	30.6	39.7
336	29.7	30.9	39.3	336	30.2	31.2	38.5	336	30.1	31.0	38.9
420	31.6	31.6	36.8	420	31.7	31.5	36.8	420	31.8	31.8	36.4
840	35.5	30.4	34.1	840	35.2	31.0	33.8	840	34.4	31.2	34.4
1260	36.9	30.1	33.1	1260	37.9	29.8	32.3	1260	37.9	30.1	32.1
2520	42.6	28.3	29.0	2520	39.7	29.2	31.1	2520	39.1	29.3	31.7

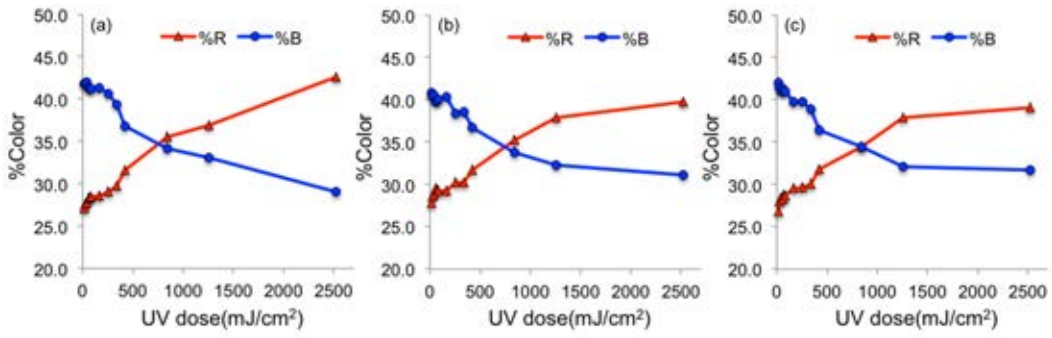

Figure B4 Plots of %RGB value of 3 independent TCDA indicators against UV dose to determine the color transition UV dose.

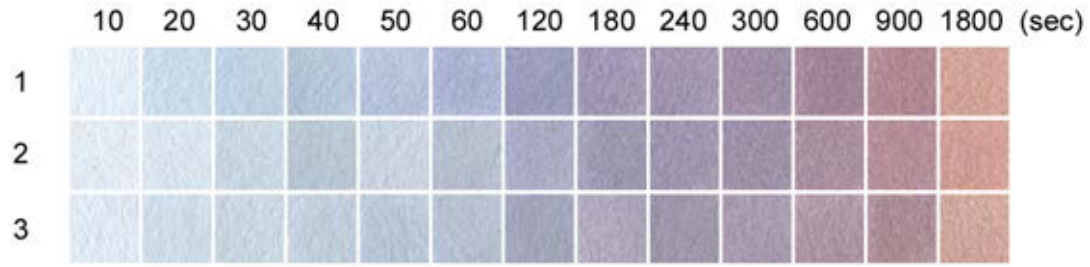

Figure B5 Photographs of UV sensing of NDDA indicators

Table B5 RGB values of NDDA indicators at various UV doses (3 independent experiments)

UV dose (mJ/cm^2)	1				UV dose (mJ/cm^2)	2				UV dose (mJ/cm^2)	3			
	R	G	B	Sum		R	G	B	Sum		R	G	B	Sum
14	228	238	247	713	14	227	235	242	704	14	223	230	242	695
28	202	218	233	653	28	217	228	238	683	28	206	220	231	657
42	191	209	227	627	42	201	215	226	642	42	201	215	225	641
56	181	197	217	595	56	184	198	209	591	56	192	206	218	616
70	182	196	217	595	70	201	211	223	635	70	185	197	214	596
84	169	179	210	558	84	181	192	206	579	84	183	193	208	584
168	156	157	187	500	168	170	171	195	536	168	161	165	186	512
252	161	152	180	493	252	157	153	176	486	252	175	169	187	531
336	162	150	176	488	336	159	150	172	481	336	160	151	171	482
420	158	142	166	466	420	158	145	166	469	420	169	155	175	499
840	161	131	151	443	840	170	144	159	473	840	175	150	163	488
1260	177	137	149	463	1260	180	143	152	475	1260	171	139	149	459
2520	209	163	153	525	2520	207	158	150	515	2520	207	168	157	532

Table B6 %RGB values of NDDA indicators at various UV doses (3 independent experiments)

UV dose (mJ/cm^2)	1			UV dose (mJ/cm^2)	2			UV dose (mJ/cm^2)	3		
	%R	%G	%B		%R	%G	%B		%R	%G	%B
14	32.0	33.4	34.6	14	32.2	33.4	34.4	14	32.1	33.1	34.8
28	30.9	33.4	35.7	28	31.8	33.4	34.8	28	31.4	33.5	35.2
42	30.5	33.3	36.2	42	31.3	33.5	35.2	42	31.4	33.5	35.1
56	30.4	33.1	36.5	56	31.1	33.5	35.4	56	31.2	33.4	35.4
70	30.6	32.9	36.5	70	31.7	33.2	35.1	70	31.0	33.1	35.9
84	30.3	32.1	37.6	84	31.3	33.2	35.6	84	31.3	33.0	35.6
168	31.2	31.4	37.4	168	31.7	31.9	36.4	168	31.4	32.2	36.3
252	32.7	30.8	36.5	252	32.3	31.5	36.2	252	33.0	31.8	35.2
336	33.2	30.7	36.1	336	33.1	31.2	35.8	336	33.2	31.3	35.5
420	33.9	30.5	35.6	420	33.7	30.9	35.4	420	33.9	31.1	35.1
840	36.3	29.6	34.1	840	35.9	30.4	33.6	840	35.9	30.7	33.4
1260	38.2	29.6	32.2	1260	37.9	30.1	32.0	1260	37.3	30.3	32.5
2520	39.8	31.0	29.1	2520	40.2	30.7	29.1	2520	38.9	31.6	29.5

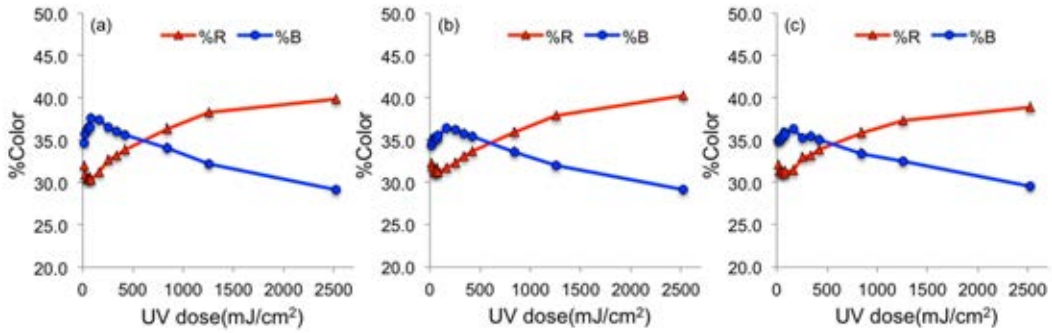

Figure B6 Plots of %RGB value of 3 independent NDDA indicators against UV dose to determine the color transition UV dose.

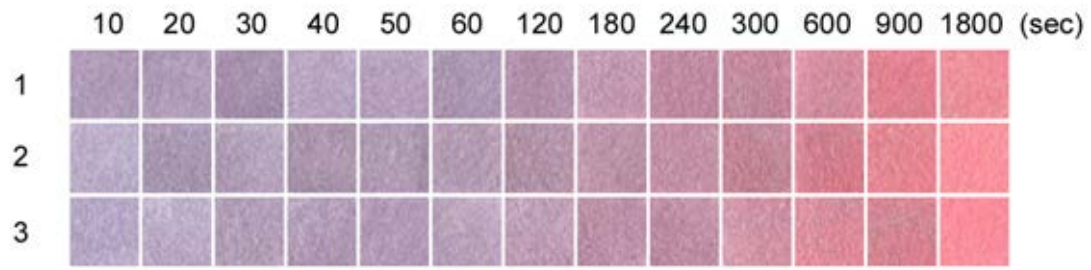

Figure B7 Photographs of UV sensing of ODDA indicators.

Table B7 RGB values of ODDA indicators at various UV doses (3 independent experiments)

UV dose (mJ/cm^2)	1				UV dose (mJ/cm^2)	2				UV dose (mJ/cm^2)	3			
	R	G	B	Sum		R	G	B	Sum		R	G	B	Sum
	R	G	B	Sum		R	G	B	Sum		R	G	B	Sum
14	176	154	183	513	14	188	174	201	563	14	182	167	197	546
28	176	156	184	516	28	167	150	175	492	28	189	173	200	562
42	168	146	174	488	42	180	162	187	529	42	178	159	184	521
56	185	165	193	543	56	174	152	174	500	56	179	156	184	519
70	182	160	186	528	70	178	156	180	514	70	178	154	182	514
84	172	152	179	503	84	180	155	179	514	84	186	163	187	536
168	177	144	169	490	168	178	147	167	492	168	191	159	182	532
252	194	153	177	524	252	188	148	167	503	252	188	145	168	501
336	192	138	161	491	336	194	145	164	503	336	190	141	163	494
420	194	138	158	490	420	194	133	151	478	420	208	148	166	522
840	211	141	160	512	840	210	127	142	479	840	218	140	156	514
1260	225	130	145	500	1260	229	134	148	511	1260	211	135	148	494

Table B8 %RGB values of ODDA indicators at various UV doses (3 independent experiments)

UV dose (mJ/cm^2)	1			UV dose (mJ/cm^2)	2			UV dose (mJ/cm^2)	3		
	%R	%G	%B		%R	%G	%B		%R	%G	%B
14	34.3	30.0	35.7	14	33.4	30.9	35.7	14	33.3	30.6	36.1
28	34.1	30.2	35.7	28	33.9	30.5	35.6	28	33.6	30.8	35.6
42	34.4	29.9	35.7	42	34.0	30.6	35.3	42	34.2	30.5	35.3
56	34.1	30.4	35.5	56	34.8	30.4	34.8	56	34.5	30.1	35.5
70	34.5	30.3	35.2	70	34.6	30.4	35.0	70	34.6	30.0	35.4
84	34.2	30.2	35.6	84	35.0	30.2	34.8	84	34.7	30.4	34.9
168	36.1	29.4	34.5	168	36.2	29.9	33.9	168	35.9	29.9	34.2
252	37.0	29.2	33.8	252	37.4	29.4	33.2	252	37.5	28.9	33.5
336	39.1	28.1	32.8	336	38.6	28.8	32.6	336	38.5	28.5	33.0
420	39.6	28.2	32.2	420	40.6	27.8	31.6	420	39.8	28.4	31.8
840	41.2	27.5	31.3	840	43.8	26.5	29.6	840	42.4	27.2	30.4
1260	45.0	26.0	29.0	1260	44.8	26.2	29.0	1260	42.7	27.3	30.0
2520	47.0	22.5	30.4	2520	45.3	26.4	28.4	2520	45.9	25.9	28.3

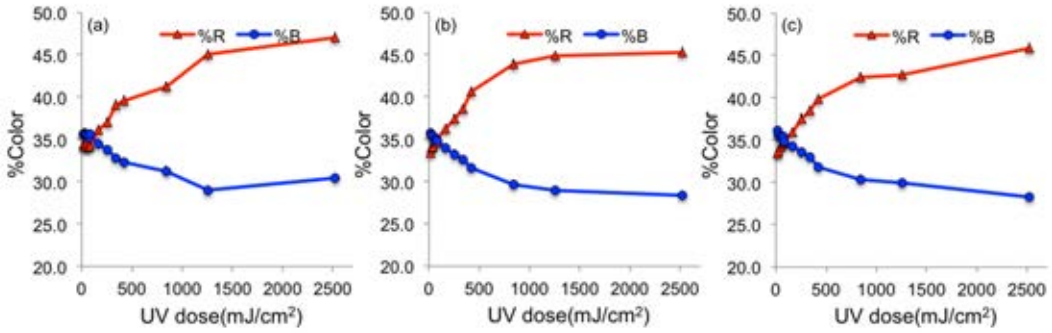

Figure B8 Plots of %RGB value of 3 independent ODDA indicators against UV dose to determine the color transition UV dose.

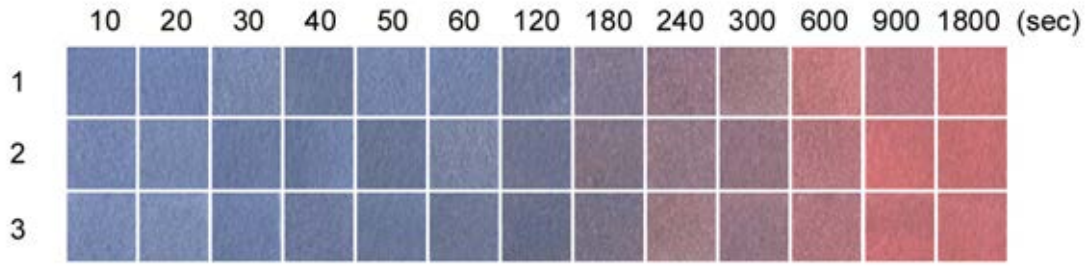

Figure B9 Photographs of UV sensing of EPCDP indicators

Table B9 RGB values of EPCDP indicators at various UV doses (3 independent experiments)

UV dose (mJ/cm^2)	1				UV dose (mJ/cm^2)	2				UV dose (mJ/cm^2)	3			
	R	G	B	Sum		R	G	B	Sum		R	G	B	Sum
14	114	130	173	417	14	117	133	175	425	14	121	137	176	434
28	114	131	173	418	28	120	136	172	428	28	123	139	176	438
42	121	136	171	428	42	107	123	160	390	42	110	126	164	400
56	107	121	153	381	56	109	124	161	394	56	109	121	155	385
70	117	132	168	417	70	106	118	147	371	70	106	119	151	376
84	117	131	166	414	84	124	133	161	418	84	110	119	147	376
168	114	121	151	386	168	110	115	141	366	168	102	109	135	346
252	130	122	143	395	252	129	116	130	375	252	121	113	131	365
336	147	118	132	397	336	146	120	132	398	336	155	122	130	407
420	159	125	134	418	420	147	116	128	391	420	150	118	131	399
840	193	123	128	444	840	177	118	126	421	840	174	118	126	418
1260	181	116	125	422	1260	203	114	117	434	1260	191	112	117	420
2520	198	116	119	433	2520	197	110	114	421	2520	198	114	118	430

Table B10 %RGB values of EPCDP indicators at various UV doses (3 independent experiments)

UV dose (mJ/cm^2)	1			UV dose (mJ/cm^2)	2			UV dose (mJ/cm^2)	3		
	%R	%G	%B		%R	%G	%B		%R	%G	%B
14	27.3	31.2	41.5	14	27.5	31.3	41.2	14	27.9	31.6	40.6
28	27.3	31.3	41.4	28	28.0	31.8	40.2	28	28.1	31.7	40.2
42	28.3	31.8	40.0	42	27.4	31.5	41.0	42	27.5	31.5	41.0
56	28.1	31.8	40.2	56	27.7	31.5	40.9	56	28.3	31.4	40.3
70	28.1	31.7	40.3	70	28.6	31.8	39.6	70	28.2	31.6	40.2
84	28.3	31.6	40.1	84	29.7	31.8	38.5	84	29.3	31.6	39.1
168	29.5	31.3	39.1	168	30.1	31.4	38.5	168	29.5	31.5	39.0
252	32.9	30.9	36.2	252	34.4	30.9	34.7	252	33.2	31.0	35.9
336	37.0	29.7	33.2	336	36.7	30.2	33.2	336	38.1	30.0	31.9
420	38.0	29.9	32.1	420	37.6	29.7	32.7	420	37.6	29.6	32.8
840	43.5	27.7	28.8	840	42.0	28.0	29.9	840	41.6	28.2	30.1
1260	42.9	27.5	29.6	1260	46.8	26.3	27.0	1260	45.5	26.7	27.9
2520	45.7	26.8	27.5	2520	46.8	26.1	27.1	2520	46.0	26.5	27.4

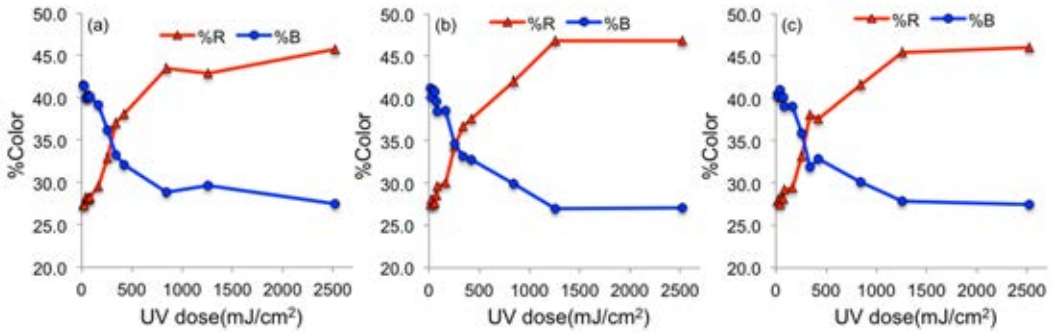

Figure B10 Plots of %RGB value of 3 independent EPCDP indicators against UV dose to determine the color transition UV dose.

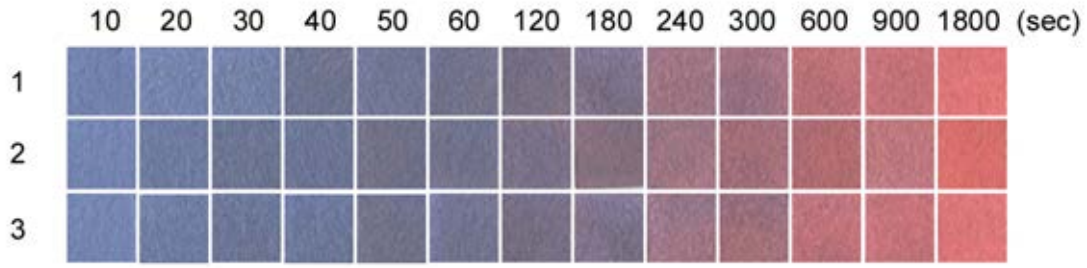

Figure B11 Photographs of UV sensing of ETCDP indicators.

Table B11 RGB values of ETCDP indicators at various UV doses (3 independent experiments)

UV dose (mJ/cm^2)	1				UV dose (mJ/cm^2)	2				UV dose (mJ/cm^2)	3			
	R	G	B	Sum		R	G	B	Sum		R	G	B	Sum
14	113	129	172	414	14	116	133	176	425	14	117	133	177	427
28	118	133	173	424	28	111	124	159	394	28	112	125	163	400
42	116	129	166	411	42	109	117	147	373	42	108	118	150	376
56	110	115	142	367	56	108	117	148	373	56	109	120	155	384
70	113	118	149	380	70	113	113	134	360	70	113	114	137	364
84	114	114	138	366	84	112	113	137	362	84	114	116	144	374
168	120	111	131	362	168	121	113	136	370	168	118	110	132	360
252	123	113	135	371	252	131	110	125	366	252	124	114	137	375
336	157	116	129	402	336	157	117	130	404	336	156	118	135	409
420	154	113	129	396	420	162	111	120	393	420	158	111	123	392
840	186	113	120	419	840	177	108	113	398	840	189	115	122	426
1260	194	114	120	428	1260	189	120	127	436	1260	197	115	122	434
2520	222	118	120	460	2520	216	110	108	434	2520	220	118	120	458

Table B12 %RGB values of ETCDP indicators at various UV doses (3 independent experiments)

UV dose (mJ/cm^2)	1			UV dose (mJ/cm^2)	2			UV dose (mJ/cm^2)	3		
	%R	%G	%B		%R	%G	%B		%R	%G	%B
14	27.3	31.2	41.5	14	27.3	31.3	41.4	14	27.4	31.1	41.5
28	27.8	31.4	40.8	28	28.2	31.5	40.4	28	28.0	31.3	40.8
42	28.2	31.4	40.4	42	29.2	31.4	39.4	42	28.7	31.4	39.9
56	30.0	31.3	38.7	56	29.0	31.4	39.7	56	28.4	31.3	40.4
70	29.7	31.1	39.2	70	31.4	31.4	37.2	70	31.0	31.3	37.6
84	31.1	31.1	37.7	84	30.9	31.2	37.8	84	30.5	31.0	38.5
168	33.1	30.7	36.2	168	32.7	30.5	36.8	168	32.8	30.6	36.7
252	33.2	30.5	36.4	252	35.8	30.1	34.2	252	33.1	30.4	36.5
336	39.1	28.9	32.1	336	38.9	29.0	32.2	336	38.1	28.9	33.0
420	38.9	28.5	32.6	420	41.2	28.2	30.5	420	40.3	28.3	31.4
840	44.4	27.0	28.6	840	44.5	27.1	28.4	840	44.4	27.0	28.6
1260	45.3	26.6	28.0	1260	43.3	27.5	29.1	1260	45.4	26.5	28.1
2520	48.3	25.7	26.1	2520	49.8	25.3	24.9	2520	48.0	25.8	26.2

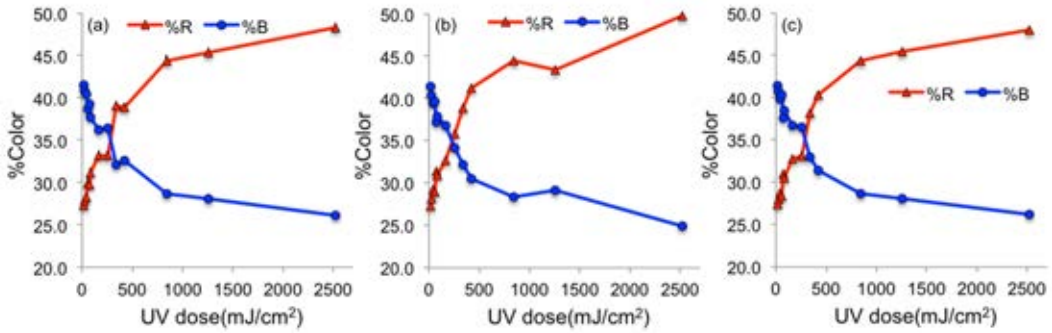

Figure B12 Plots of %RGB value of 3 independent ETCDP indicators against UV dose to determine the color transition UV dose.

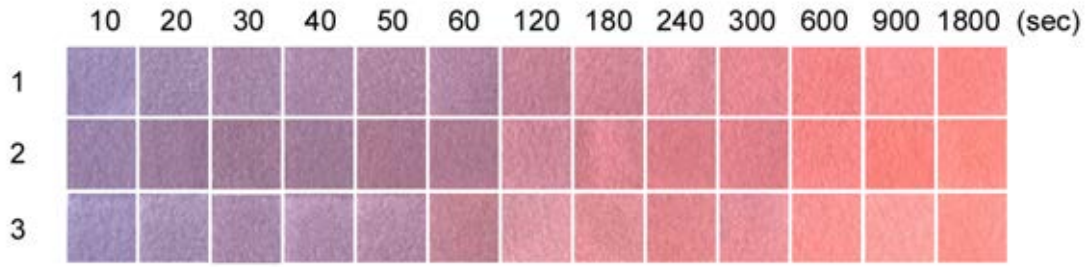

Figure B13 Photographs of UV sensing of ENDDP indicators

Table B13 RGB values of ENDDP indicators at various UV doses (3 independent experiments)

UV dose (mJ/cm^2)	1				UV dose (mJ/cm^2)	2				UV dose (mJ/cm^2)	3			
	R	G	B	Sum		R	G	B	Sum		R	G	B	Sum
14	157	141	182	480	14	155	131	168	454	14	161	146	186	493
28	161	140	172	473	28	156	125	155	436	28	166	145	178	489
42	165	137	167	469	42	157	123	149	429	42	167	137	168	472
56	172	137	167	476	56	158	123	151	432	56	176	142	172	490
70	173	133	160	466	70	169	121	145	435	70	182	142	169	493
84	176	133	161	470	84	173	123	146	442	84	191	131	146	468
168	196	130	151	477	168	206	137	153	496	168	222	153	166	541
252	211	134	150	495	252	223	137	149	509	252	221	141	150	512
336	223	140	152	515	336	218	126	135	479	336	225	136	142	503
420	233	137	145	515	420	223	128	139	490	420	231	145	154	530
840	244	132	134	510	840	246	136	135	517	840	249	149	148	546
1260	248	142	143	533	1260	250	132	127	509	1260	250	161	158	569
2520	250	137	134	521	2520	252	141	132	525	2520	252	150	142	544

Table 14 %RGB values of ENDDP indicators at various UV doses (3 independent experiments)

UV dose (mJ/cm^2)	1			UV dose (mJ/cm^2)	2			UV dose (mJ/cm^2)	3		
	%R	%G	%B		%R	%G	%B		%R	%G	%B
14	32.7	29.4	37.9	14	34.1	28.9	37.0	14	32.7	29.6	37.7
28	34.0	29.6	36.4	28	35.8	28.7	35.6	28	33.9	29.7	36.4
42	35.2	29.2	35.6	42	36.6	28.7	34.7	42	35.4	29.0	35.6
56	36.1	28.8	35.1	56	36.6	28.5	35.0	56	35.9	29.0	35.1
70	37.1	28.5	34.3	70	38.9	27.8	33.3	70	36.9	28.8	34.3
84	37.4	28.3	34.3	84	39.1	27.8	33.0	84	40.8	28.0	31.2
168	41.1	27.3	31.7	168	41.5	27.6	30.8	168	41.0	28.3	30.7
252	42.6	27.1	30.3	252	43.8	26.9	29.3	252	43.2	27.5	29.3
336	43.3	27.2	29.5	336	45.5	26.3	28.2	336	44.7	27.0	28.2
420	45.2	26.6	28.2	420	45.5	26.1	28.4	420	43.6	27.4	29.1
840	47.8	25.9	26.3	840	47.6	26.3	26.1	840	45.6	27.3	27.1
1260	46.5	26.6	26.8	1260	49.1	25.9	25.0	1260	43.9	28.3	27.8
2520	48.0	26.3	25.7	2520	48.0	26.9	25.1	2520	46.3	27.6	26.1

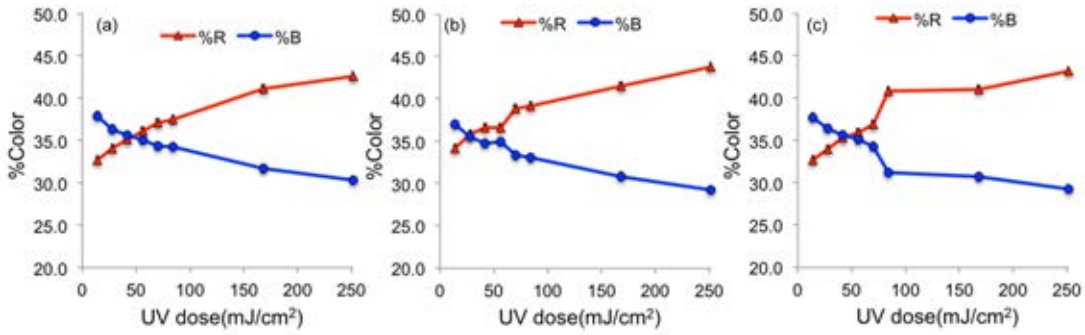

Figure B14 Plots of %RGB value of 3 independent ENDDP indicators against UV dose to determine the color transition UV dose.

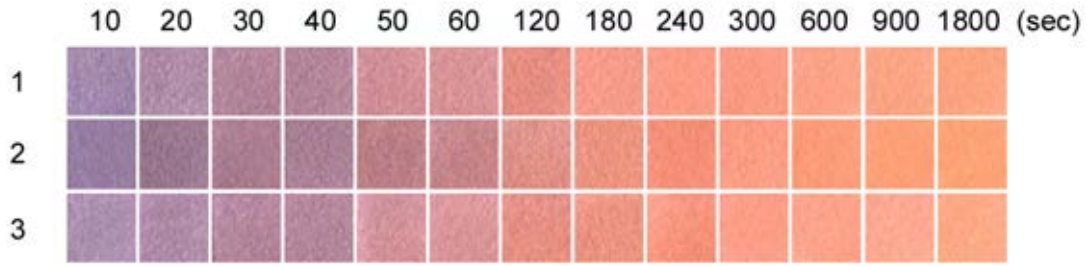

Figure B15 photographs of UV sensing of EODDP indicators

Table B15 RGB values of EODDP indicators at various UV doses (3 independent experiments)

UV dose (mJ/cm^2)	1				UV dose (mJ/cm^2)	2				UV dose (mJ/cm^2)	3			
	R	G	B	Sum		R	G	B	Sum		R	G	B	Sum
14	164	138	173	475	14	149	125	160	434	14	171	143	175	489
28	176	140	169	485	28	154	120	143	417	28	174	138	167	479
42	178	133	154	465	42	172	125	144	441	42	180	135	157	472
56	179	134	154	467	56	170	128	150	448	56	180	135	155	470
70	209	144	150	503	70	186	127	133	446	70	210	147	155	512
84	218	149	151	518	84	198	133	139	470	84	219	151	155	525
168	230	142	129	501	168	225	147	137	509	168	231	144	132	507
252	247	156	138	541	252	238	148	127	513	252	237	148	132	517
336	252	157	133	542	336	245	143	118	506	336	248	149	130	527
420	251	156	130	537	420	251	157	132	540	420	252	158	126	536
840	252	163	134	549	840	253	156	121	530	840	252	163	139	554
1260	252	165	132	549	1260	253	160	119	532	1260	252	169	145	566
2520	252	164	127	543	2520	253	163	118	534	2520	252	170	134	556

Table B16 %RGB values of EODDP indicators at various UV doses (3 independent experiments)

UV dose (mJ/cm^2)	1			UV dose (mJ/cm^2)	2			UV dose (mJ/cm^2)	3		
	%R	%G	%B		%R	%G	%B		%R	%G	%B
14	32.7	29.4	37.9	14	34.1	28.9	37.0	14	35.0	29.2	35.8
28	34.0	29.6	36.4	28	35.8	28.7	35.6	28	36.3	28.8	34.9
42	35.2	29.2	35.6	42	36.6	28.7	34.7	42	38.1	28.6	33.3
56	36.1	28.8	35.1	56	36.6	28.5	35.0	56	38.3	28.7	33.0
70	37.1	28.5	34.3	70	38.9	27.8	33.3	70	41.0	28.7	30.3
84	37.4	28.3	34.3	84	39.1	27.8	33.0	84	41.7	28.8	29.5
168	41.1	27.3	31.7	168	41.5	27.6	30.8	168	45.6	28.4	26.0
252	42.6	27.1	30.3	252	43.8	26.9	29.3	252	45.8	28.6	25.5
336	43.3	27.2	29.5	336	45.5	26.3	28.2	336	47.1	28.3	24.7
420	45.2	26.6	28.2	420	45.5	26.1	28.4	420	47.0	29.5	23.5
840	47.8	25.9	26.3	840	47.6	26.3	26.1	840	45.5	29.4	25.1
1260	46.5	26.6	26.8	1260	49.1	25.9	25.0	1260	44.5	29.9	25.6
2520	48.0	26.3	25.7	2520	48.0	26.9	25.1	2520	45.3	30.6	24.1

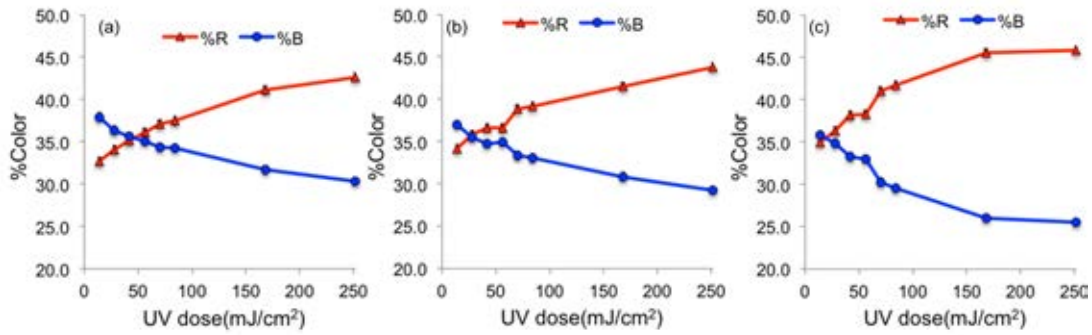

Figure B16 Plots of %RGB value of 3 independent EODDP indicators against UV dose to determine the color transition UV dose.

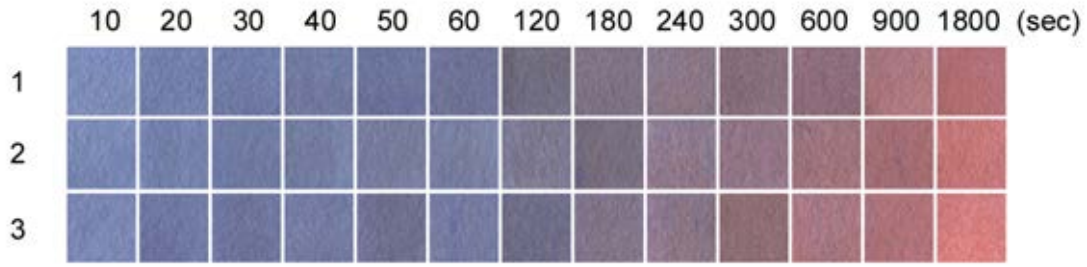

Figure B17 Photographs of UV sensing of EPCDPP indicators.

Table B17 RGB values of EPCDPP indicators at various UV doses (3 independent experiments)

UV dose (mJ/cm^2)	1				UV dose (mJ/cm^2)	2				UV dose (mJ/cm^2)	3			
	R	G	B	Sum		R	G	B	Sum		R	G	B	Sum
14	125	139	184	448	14	121	135	179	435	14	122	134	180	436
28	114	127	170	411	28	115	128	170	413	28	110	119	162	391
42	112	124	167	403	42	112	123	163	398	42	110	116	155	381
56	113	122	161	396	56	116	125	161	402	56	116	124	162	402
70	108	117	155	380	70	118	123	156	397	70	111	112	141	364
84	110	115	150	375	84	121	127	159	407	84	117	122	161	400
168	112	108	127	347	168	124	120	143	387	168	110	108	134	352
252	127	115	132	374	252	119	109	125	353	252	129	116	136	381
336	138	119	135	392	336	142	121	139	402	336	139	118	136	393
420	134	110	121	365	420	146	117	133	396	420	142	109	117	368
840	141	108	122	371	840	158	115	124	397	840	167	109	112	388
1260	172	118	126	416	1260	161	108	115	384	1260	174	113	121	408
2520	178	110	116	404	2520	197	119	119	435	2520	213	127	127	467

Table B18 %RGB values of EPCDPP indicators at various UV doses (3 independent experiments)

UV dose (mJ/cm^2)	1			UV dose (mJ/cm^2)	2			UV dose (mJ/cm^2)	3		
	%R	%G	%B		%R	%G	%B		%R	%G	%B
14	27.9	31.0	41.1	14	27.8	31.0	41.1	14	28.0	30.7	41.3
28	27.7	30.9	41.4	28	27.8	31.0	41.2	28	28.1	30.4	41.4
42	27.8	30.8	41.4	42	28.1	30.9	41.0	42	28.9	30.4	40.7
56	28.5	30.8	40.7	56	28.9	31.1	40.0	56	28.9	30.8	40.3
70	28.4	30.8	40.8	70	29.7	31.0	39.3	70	30.5	30.8	38.7
70	29.3	30.7	40.0	84	29.7	31.2	39.1	84	29.3	30.5	40.3
70	32.3	31.1	36.6	168	32.0	31.0	37.0	168	31.3	30.7	38.1
70	34.0	30.7	35.3	252	33.7	30.9	35.4	252	33.9	30.4	35.7
70	35.2	30.4	34.4	336	35.3	30.1	34.6	336	35.4	30.0	34.6
70	36.7	30.1	33.2	420	36.9	29.5	33.6	420	38.6	29.6	31.8
70	38.0	29.1	32.9	840	39.8	29.0	31.2	840	43.0	28.1	28.9
70	41.3	28.4	30.3	1260	41.9	28.1	29.9	1260	42.6	27.7	29.7
70	44.1	27.2	28.7	2520	45.3	27.4	27.4	2520	45.6	27.2	27.2

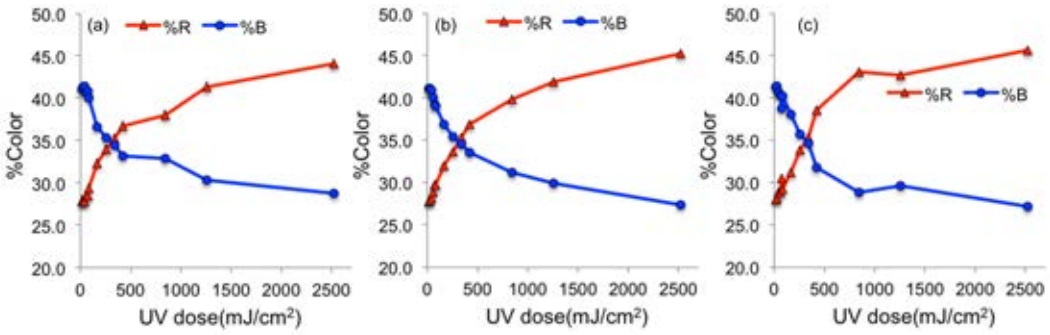

Figure B18 Plots of %RGB value of 3 independent EPCDPP indicators against UV dose to determine the color transition UV dose.

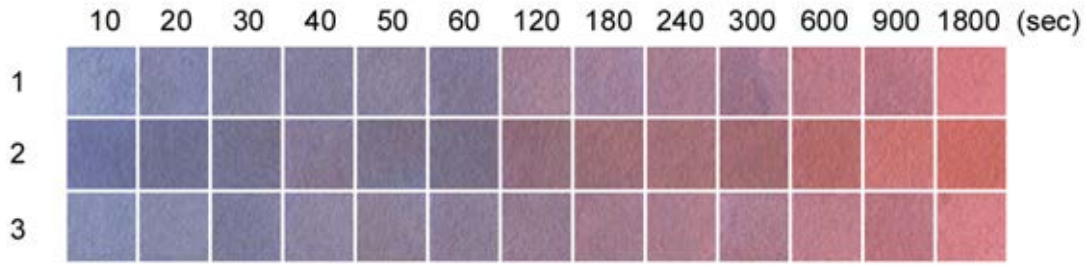

Figure B19 Photographs of UV sensing of ETCDPP indicators

Table B19 RGB values of ETCDPP indicators at various UV doses (3 independent experiments)

UV dose (mJ/cm^2)	1				UV dose (mJ/cm^2)	2				UV dose (mJ/cm^2)	3			
	R	G	B	Sum		R	G	B	Sum		R	G	B	Sum
14	132	143	183	458	14	109	115	157	381	14	133	142	177	452
28	129	133	167	429	28	112	113	146	371	28	135	137	168	440
42	130	128	156	414	42	117	114	143	374	42	124	123	153	400
56	131	127	155	413	56	132	121	145	398	56	142	133	160	435
70	139	130	155	424	70	124	115	137	376	70	140	128	150	418
84	129	120	147	396	84	120	111	136	367	84	139	125	148	412
168	161	131	150	442	168	145	110	124	379	168	150	124	143	417
252	159	129	154	442	252	157	112	120	389	252	160	124	141	425
336	165	125	144	434	336	163	112	121	396	336	170	125	142	437
420	160	119	140	419	420	161	107	113	381	420	171	126	143	440
840	186	123	136	445	840	179	106	107	392	840	188	126	139	453
1260	184	117	132	433	1260	201	117	117	435	1260	184	118	129	431
2520	212	123	130	465	2520	202	108	103	413	2520	213	129	136	478

Table B20 %RGB values of ETCDPP indicators at various UV doses (3 independent experiments)

UV dose (mJ/cm^2)	1			UV dose (mJ/cm^2)	2			UV dose (mJ/cm^2)	3		
	%R	%G	%B		%R	%G	%B		%R	%G	%B
14	28.8	31.2	40.0	14	28.6	30.2	41.2	14	29.4	31.4	39.2
28	30.1	31.0	38.9	28	30.2	30.5	39.4	28	30.7	31.1	38.2
42	31.4	30.9	37.7	42	31.3	30.5	38.2	42	31.0	30.8	38.3
56	31.7	30.8	37.5	56	33.2	30.4	36.4	56	32.6	30.6	36.8
70	32.8	30.7	36.6	70	33.0	30.6	36.4	70	33.5	30.6	35.9
84	32.6	30.3	37.1	84	32.7	30.2	37.1	84	33.7	30.3	35.9
168	36.4	29.6	33.9	168	38.3	29.0	32.7	168	36.0	29.7	34.3
252	36.0	29.2	34.8	252	40.4	28.8	30.8	252	37.6	29.2	33.2
336	38.0	28.8	33.2	336	41.2	28.3	30.6	336	38.9	28.6	32.5
420	38.2	28.4	33.4	420	42.3	28.1	29.7	420	38.9	28.6	32.5
840	41.8	27.6	30.6	840	45.7	27.0	27.3	840	41.5	27.8	30.7
1260	42.5	27.0	30.5	1260	46.2	26.9	26.9	1260	42.7	27.4	29.9
2520	45.6	26.5	28.0	2520	48.9	26.2	24.9	2520	44.6	27.0	28.5

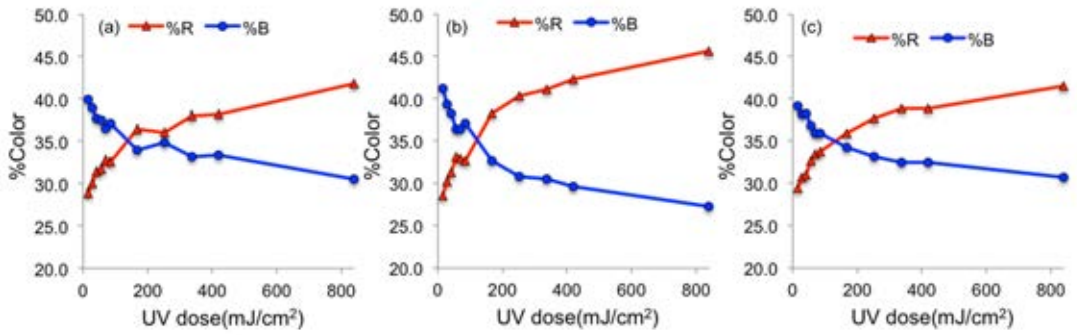

Figure B20 Plots of %RGB value of 3 independent ETCDPP indicators against UV dose to determine the color transition UV dose.

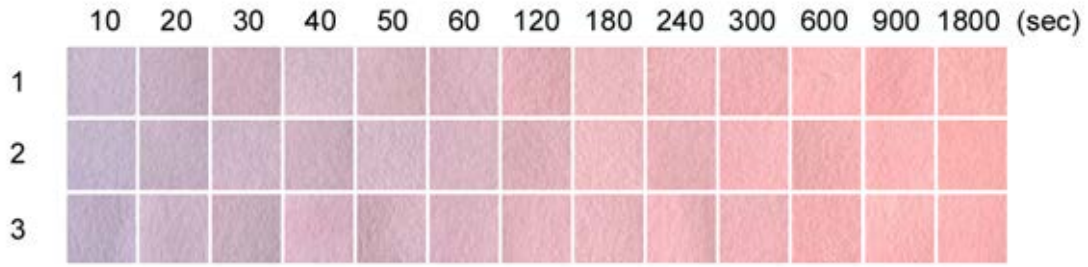

Figure B21 Photographs of UV sensing of ENDDPP indicators

Table B21 RGB values of ENDDPP indicators at various UV doses (3 independent experiments)

UV dose (mJ/cm^2)	1				UV dose (mJ/cm^2)	2				UV dose (mJ/cm^2)	3			
	R	G	B	Sum		R	G	B	Sum		R	G	B	Sum
14	199	184	204	587	14	195	181	203	579	14	194	178	195	567
28	197	174	191	562	28	197	178	194	569	28	202	178	194	574
42	204	173	188	565	42	207	182	199	588	42	196	171	183	550
56	212	185	197	594	56	205	175	191	571	56	209	181	193	583
70	213	179	189	581	70	213	185	198	596	70	211	180	190	581
84	219	181	193	593	84	218	182	195	595	84	216	179	189	584
168	224	174	182	580	168	221	176	185	582	168	212	175	179	566
252	234	185	190	609	252	239	189	196	624	252	232	177	183	592
336	238	179	185	602	336	231	177	183	591	336	239	181	186	606
420	241	176	181	598	420	246	182	189	617	420	232	173	176	581
840	249	184	186	619	840	240	175	178	593	840	251	184	187	622
1260	246	172	173	591	1260	249	182	184	615	1260	250	182	182	614
2520	249	180	179	608	2520	251	177	176	604	2520	251	187	185	623

Table B22 %RGB values of ENDDPP indicators at various UV doses (3 independent experiments)

UV dose (mJ/cm^2)	1			UV dose (mJ/cm^2)	2			UV dose (mJ/cm^2)	3		
	%R	%G	%B		%R	%G	%B		%R	%G	%B
14	33.9	31.3	34.8	14	33.7	31.3	35.1	14	34.2	31.4	34.4
28	35.1	31.0	34.0	28	34.6	31.3	34.1	28	35.2	31.0	33.8
42	36.1	30.6	33.3	42	35.2	31.0	33.8	42	35.6	31.1	33.3
56	35.7	31.1	33.2	56	35.9	30.6	33.5	56	35.8	31.0	33.1
70	36.7	30.8	32.5	70	35.7	31.0	33.2	70	36.3	31.0	32.7
84	36.9	30.5	32.5	84	36.6	30.6	32.8	84	37.0	30.7	32.4
168	38.6	30.0	31.4	168	38.0	30.2	31.8	168	37.5	30.9	31.6
252	38.4	30.4	31.2	252	38.3	30.3	31.4	252	39.2	29.9	30.9
336	39.5	29.7	30.7	336	39.1	29.9	31.0	336	39.4	29.9	30.7
420	40.3	29.4	30.3	420	39.9	29.5	30.6	420	39.9	29.8	30.3
840	40.2	29.7	30.0	840	40.5	29.5	30.0	840	40.4	29.6	30.1
1260	41.6	29.1	29.3	1260	40.5	29.6	29.9	1260	40.7	29.6	29.6
2520	41.0	29.6	29.4	2520	41.6	29.3	29.1	2520	40.3	30.0	29.7

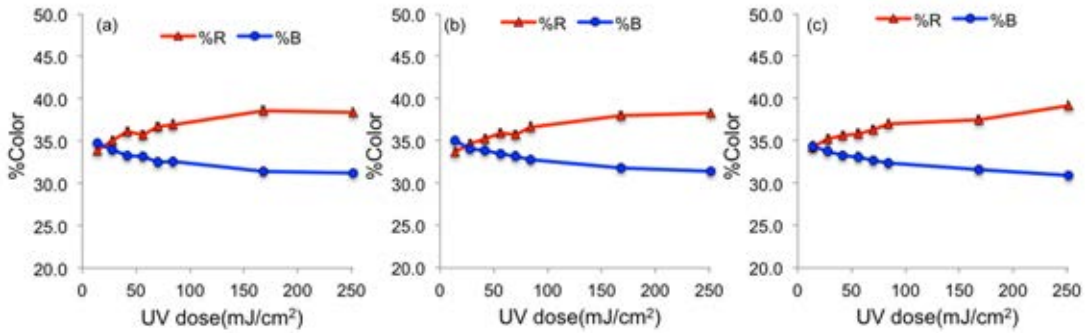

Figure B22 Plots of %RGB value of 3 independent ENDDPP indicators against UV dose to determine the color transition UV dose.

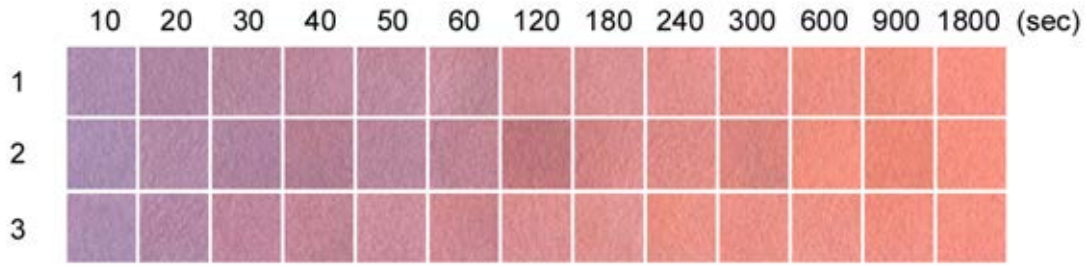

Figure B23 Photographs of UV sensing of EODDPP indicators.

Table B23 RGB values of EODDPP indicators at various UV doses (3 independent experiments)

UV dose (mJ/cm^2)	1				UV dose (mJ/cm^2)	2				UV dose (mJ/cm^2)	3			
	R	G	B	Sum		R	G	B	Sum		R	G	B	Sum
14	172	141	176	489	14	170	142	177	489	14	172	142	175	489
28	174	134	162	470	28	178	139	166	483	28	178	136	164	478
42	180	136	160	476	42	174	132	159	465	42	190	135	155	480
56	186	138	157	481	56	180	127	147	454	56	194	134	150	478
70	189	139	158	486	70	183	135	156	474	70	202	142	158	502
84	193	139	154	486	84	190	133	150	473	84	205	135	144	484
168	210	138	143	491	168	191	119	125	435	168	218	144	147	509
252	218	145	148	511	252	214	136	135	485	252	223	147	145	515
336	226	144	142	512	336	223	139	135	497	336	235	146	135	516
420	232	143	134	509	420	217	133	128	478	420	234	144	134	512
840	237	145	132	514	840	242	145	129	516	840	237	147	136	520
1260	239	125	125	489	1260	237	137	119	493	1260	242	143	130	515
2520	247	132	132	511	2520	246	145	128	519	2520	245	146	133	524

Table B24 %RGB values of EODDPP indicators at various UV doses (3 independent experiments)

UV dose (mJ/cm^2)	1			UV dose (mJ/cm^2)	2			UV dose (mJ/cm^2)	3		
	%R	%G	%B		%R	%G	%B		%R	%G	%B
14	35.2	28.8	36.0	14	34.8	29.0	36.2	14	35.2	29.0	35.8
28	37.0	28.5	34.5	28	36.9	28.8	34.4	28	37.2	28.5	34.3
42	37.8	28.6	33.6	42	37.4	28.4	34.2	42	39.6	28.1	32.3
56	38.7	28.7	32.6	56	39.6	28.0	32.4	56	40.6	28.0	31.4
70	38.9	28.6	32.5	70	38.6	28.5	32.9	70	40.2	28.3	31.5
84	39.7	28.6	31.7	84	40.2	28.1	31.7	84	42.4	27.9	29.8
168	42.8	28.1	29.1	168	43.9	27.4	28.7	168	42.8	28.3	28.9
252	42.7	28.4	29.0	252	44.1	28.0	27.8	252	43.3	28.5	28.2
336	44.1	28.1	27.7	336	44.9	28.0	27.2	336	45.5	28.3	26.2
420	45.6	28.1	26.3	420	45.4	27.8	26.8	420	45.7	28.1	26.2
840	46.1	28.2	25.7	840	46.9	28.1	25.0	840	45.6	28.3	26.2
1260	48.9	25.6	25.6	1260	48.1	27.8	24.1	1260	47.0	27.8	25.2
2520	48.3	25.8	25.8	2520	47.4	27.9	24.7	2520	46.8	27.9	25.4

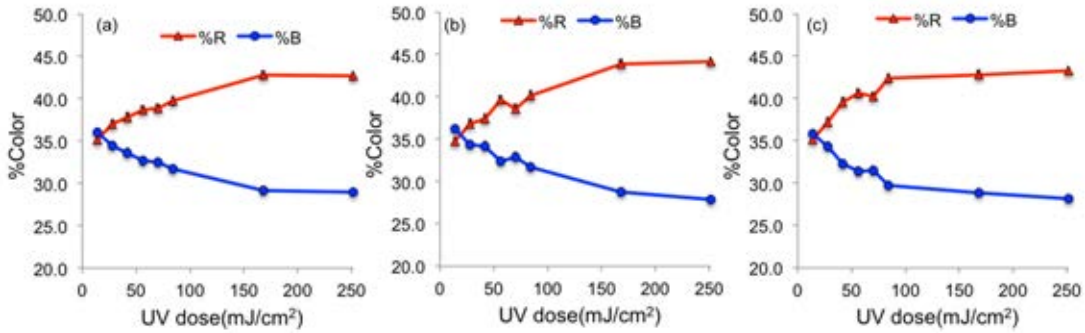

Figure B24 Plots of %RGB value of 3 independent EODDPP indicators against UV dose to determine the color transition UV dose.

APPENDIX C
THERMAL SENSING STUDY

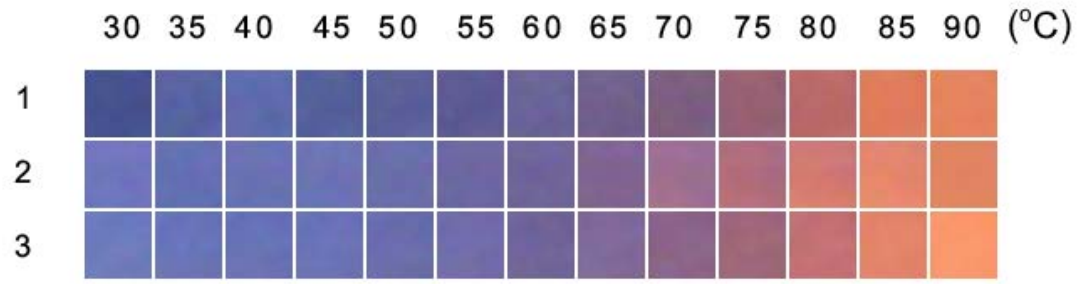

Figure C1 Photographs of Thermal sensing of PCDA indicators

Table C1 RGB values of PCDA indicators at various Temperatures (3 independent experiments)

T(°C)	1				T(°C)	2				T(°C)	3			
	R	G	B	Sum		R	G	B	Sum		R	G	B	Sum
30	70	81	143	294	30	112	117	189	418	30	109	122	189	420
35	86	99	162	347	35	99	111	180	390	35	105	116	184	405
40	95	107	172	374	40	106	113	179	398	40	104	114	182	400
45	83	95	155	333	45	108	115	180	403	45	106	114	183	403
50	89	96	153	338	50	106	109	171	386	50	105	108	172	385
55	91	89	147	327	55	109	103	163	375	55	113	108	170	391
60	105	100	151	356	60	110	100	153	363	60	111	99	154	364
65	112	96	139	347	65	128	99	146	373	65	128	105	153	386
70	124	94	128	346	70	157	111	146	414	70	139	100	138	377
75	150	97	115	362	75	176	108	125	409	75	159	103	121	383
80	185	104	105	394	80	210	122	114	446	80	196	112	116	424
85	224	122	92	438	85	230	134	109	473	85	227	132	105	464
90	229	131	95	455	90	225	132	97	454	90	250	151	107	508

Table C2 %RGB values of PCDA indicators at various temperatures (3 independent experiments)

T(°C)	1			T(°C)	2			T(°C)	3		
	%R	%G	%B		%R	%G	%B		%R	%G	%B
30	23.8	27.6	48.6	30	26.8	28.0	45.2	30	26.0	29.0	45.0
35	24.8	28.5	46.7	35	25.4	28.5	46.2	35	25.9	28.6	45.4
40	25.4	28.6	46.0	40	26.6	28.4	45.0	40	26.0	28.5	45.5
45	24.9	28.5	46.5	45	26.8	28.5	44.7	45	26.3	28.3	45.4
50	26.3	28.4	45.3	50	27.5	28.2	44.3	50	27.3	28.1	44.7
55	27.8	27.2	45.0	55	29.1	27.5	43.5	55	28.9	27.6	43.5
60	29.5	28.1	42.4	60	30.3	27.5	42.1	60	30.5	27.2	42.3
65	32.3	27.7	40.1	65	34.3	26.5	39.1	65	33.2	27.2	39.6
70	35.8	27.2	37.0	70	37.9	26.8	35.3	70	36.9	26.5	36.6
75	41.4	26.8	31.8	75	43.0	26.4	30.6	75	41.5	26.9	31.6
80	47.0	26.4	26.6	80	47.1	27.4	25.6	80	46.2	26.4	27.4
85	51.1	27.9	21.0	85	48.6	28.3	23.0	85	48.9	28.4	22.6
90	50.3	28.8	20.9	90	49.6	29.1	21.4	90	49.2	29.7	21.1

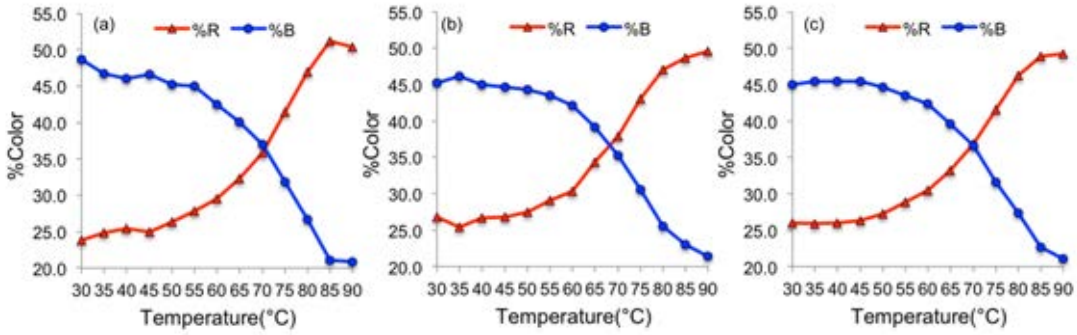

Figure C2 Plots of %RGB value of 3 independent PCDA indicators against temperature to determine the color transition temperature.

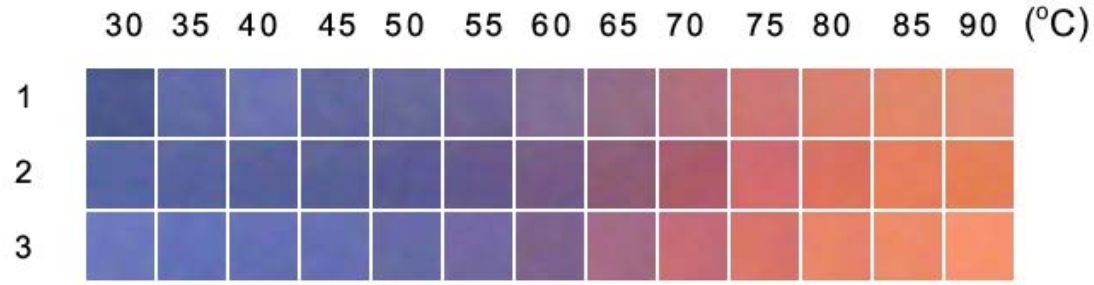

Figure C3 Photographs of Thermal sensing of TCDA indicators.

Table C3 RGB values of TCDA indicators at various Temperatures (3 independent experiments)

T(°C)	1				T(°C)	2				T(°C)	3			
	R	G	B	Sum		R	G	B	Sum		R	G	B	Sum
30	77	90	143	310	30	88	102	163	353	30	107	119	188	414
35	97	107	166	370	35	89	100	158	347	35	99	113	185	397
40	109	116	176	401	40	88	96	154	338	40	98	111	180	389
45	98	104	158	360	45	90	98	151	339	45	101	110	178	389
50	103	105	153	361	50	90	90	149	329	50	102	106	165	373
55	111	100	148	359	55	101	88	141	330	55	115	104	161	380
60	129	111	150	390	60	117	90	134	341	60	124	98	140	362
65	147	107	132	386	65	142	92	118	352	65	164	106	133	403
70	177	111	124	412	70	171	91	107	369	70	198	107	118	423
75	206	117	116	439	75	208	107	111	426	75	217	116	104	437
80	218	126	108	452	80	220	113	95	428	80	232	131	104	467
85	225	134	105	464	85	231	126	92	449	85	238	138	105	481
90	226	138	112	476	90	230	126	87	443	90	246	146	110	502

Table C4 %RGB values of TCDA indicators at various temperatures (3 independent experiments)

T(°C)	1			T(°C)	2			T(°C)	3		
	%R	%G	%B		%R	%G	%B		%R	%G	%B
30	24.8	29.0	46.1	30	24.9	28.9	46.2	30	25.8	28.7	45.4
35	26.2	28.9	44.9	35	25.6	28.8	45.5	35	24.9	28.5	46.6
40	27.2	28.9	43.9	40	26.0	28.4	45.6	40	25.2	28.5	46.3
45	27.2	28.9	43.9	45	26.5	28.9	44.5	45	26.0	28.3	45.8
50	28.5	29.1	42.4	50	27.4	27.4	45.3	50	27.3	28.4	44.2
55	30.9	27.9	41.2	55	30.6	26.7	42.7	55	30.3	27.4	42.4
60	33.1	28.5	38.5	60	34.3	26.4	39.3	60	34.3	27.1	38.7
65	38.1	27.7	34.2	65	40.3	26.1	33.5	65	40.7	26.3	33.0
70	43.0	26.9	30.1	70	46.3	24.7	29.0	70	46.8	25.3	27.9
75	46.9	26.7	26.4	75	48.8	25.1	26.1	75	49.7	26.5	23.8
80	48.2	27.9	23.9	80	51.4	26.4	22.2	80	49.7	28.1	22.3
85	48.5	28.9	22.6	85	51.4	28.1	20.5	85	49.5	28.7	21.8
90	47.5	29.0	23.5	90	51.9	28.4	19.6	90	49.0	29.1	21.9

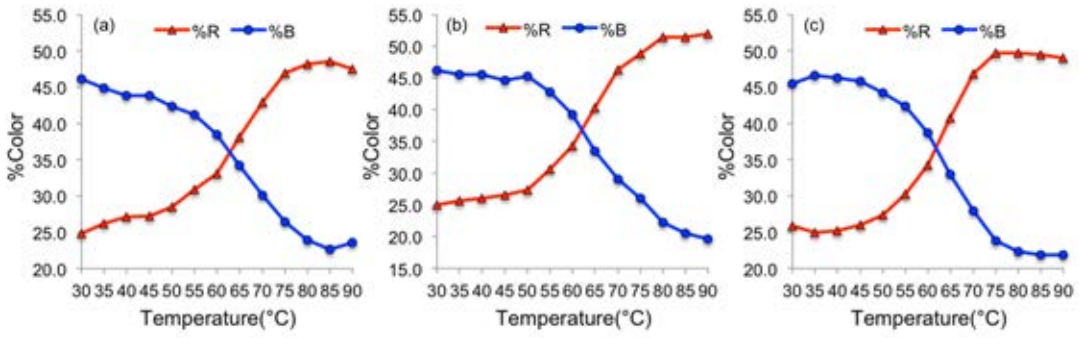

Figure C4 Plots of %RGB value of 3 independent TCDA indicators against temperature to determine the color transition temperature.

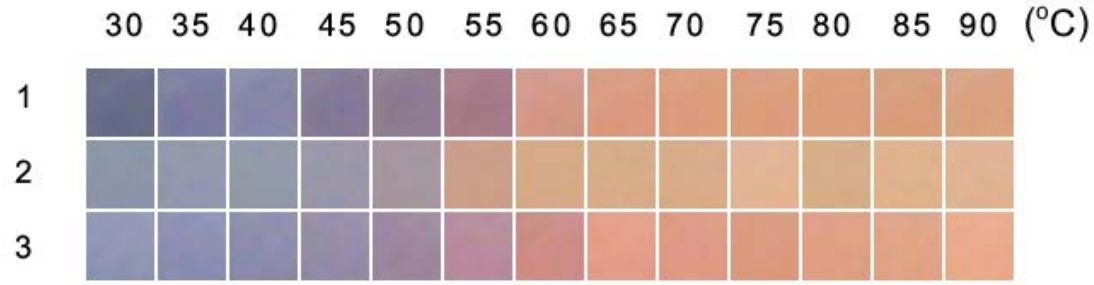

Figure C5 Photographs of Thermal sensing of NDDA indicators.

Table C5 RGB values of NDDA indicators at various Temperatures (3 independent experiments)

T(°C)	1				T(°C)	2				T(°C)	3			
	R	G	B	Sum		R	G	B	Sum		R	G	B	Sum
30	105	109	138	352	30	140	149	169	458	30	146	150	180	476
35	124	124	161	409	35	147	151	174	472	35	141	143	178	462
40	136	134	169	439	40	147	153	169	469	40	141	141	172	454
45	130	122	151	403	45	154	151	169	474	45	150	141	169	460
50	141	123	145	409	50	165	150	159	474	50	158	135	158	451
55	166	122	136	424	55	204	158	138	500	55	185	139	157	481
60	212	152	137	501	60	214	170	135	519	60	205	141	134	480
65	218	155	129	502	65	215	172	135	522	65	228	158	137	523
70	220	156	126	502	70	218	171	137	526	70	223	154	134	511
75	219	158	126	503	75	228	181	148	557	75	219	154	126	499
80	219	157	123	499	80	215	174	138	527	80	223	159	132	514
85	216	158	126	500	85	224	178	141	543	85	225	164	134	523
90	218	162	128	508	90	224	179	147	550	90	235	170	140	545

Table C6 %RGB values of NDDA indicators at various temperatures (3 independent experiments)

T(°C)	1			T(°C)	2			T(°C)	3		
	%R	%G	%B		%R	%G	%B		%R	%G	%B
30	29.8	31.0	39.2	30	30.6	32.5	36.9	30	30.7	31.5	37.8
35	30.3	30.3	39.4	35	31.1	32.0	36.9	35	30.5	31.0	38.5
40	31.0	30.5	38.5	40	31.3	32.6	36.0	40	31.1	31.1	37.9
45	32.3	30.3	37.5	45	32.5	31.9	35.7	45	32.6	30.7	36.7
50	34.5	30.1	35.5	50	34.8	31.6	33.5	50	35.0	29.9	35.0
55	39.2	28.8	32.1	55	40.8	31.6	27.6	55	38.5	28.9	32.6
60	42.3	30.3	27.3	60	41.2	32.8	26.0	60	42.7	29.4	27.9
65	43.4	30.9	25.7	65	41.2	33.0	25.9	65	43.6	30.2	26.2
70	43.8	31.1	25.1	70	41.4	32.5	26.0	70	43.6	30.1	26.2
75	43.5	31.4	25.0	75	40.9	32.5	26.6	75	43.9	30.9	25.3
80	43.9	31.5	24.6	80	40.8	33.0	26.2	80	43.4	30.9	25.7
85	43.2	31.6	25.2	85	41.3	32.8	26.0	85	43.0	31.4	25.6
90	42.9	31.9	25.2	90	40.7	32.5	26.7	90	43.1	31.2	25.7

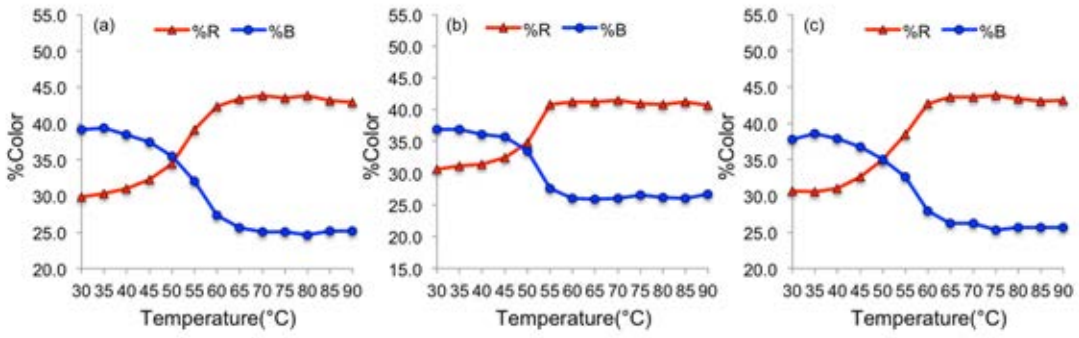

Figure C6 Plots of %RGB value of 3 independent NDDA indicators against temperature to determine the color transition temperature.

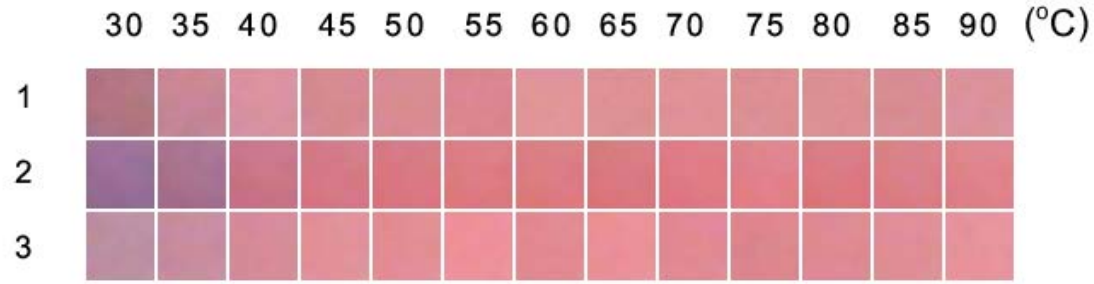

Figure C7 Photographs of Thermal sensing of ODDA indicators

Table C7 RGB values of ODDA indicators at various Temperatures (3 independent experiments)

T(°C)	1				T(°C)	2				T(°C)	3			
	R	G	B	Sum		R	G	B	Sum		R	G	B	Sum
30	178	118	129	425	30	153	110	151	414	30	187	143	161	491
35	199	133	149	481	35	168	114	143	425	35	199	140	158	497
40	218	146	160	524	40	202	118	136	456	40	214	139	152	505
45	214	137	145	496	45	212	121	135	468	45	226	144	152	522
50	216	140	145	501	50	217	120	131	468	50	226	141	147	514
55	219	134	144	497	55	220	124	131	475	55	238	144	154	536
60	225	149	153	527	60	220	124	131	475	60	226	137	145	508
65	222	145	149	516	65	217	121	129	467	65	234	144	151	529
70	223	145	150	518	70	223	123	132	478	70	226	137	147	510
75	220	143	148	511	75	225	129	139	493	75	221	134	140	495
80	220	143	147	510	80	219	121	130	470	80	223	137	146	506
85	217	140	148	505	85	219	128	137	484	85	224	141	150	515
90	219	145	156	520	90	223	131	140	494	90	231	147	156	534

Table C8 %RGB values of ODDA indicators at various temperatures (3 independent experiments)

T(°C)	1			T(°C)	2			T(°C)	3		
	%R	%G	%B		%R	%G	%B		%R	%G	%B
30	41.9	27.8	30.4	30	37.0	26.6	36.5	30	38.1	29.1	32.8
35	41.4	27.7	31.0	35	39.5	26.8	33.6	35	40.0	28.2	31.8
40	41.6	27.9	30.5	40	44.3	25.9	29.8	40	42.4	27.5	30.1
45	43.1	27.6	29.2	45	45.3	25.9	28.8	45	43.3	27.6	29.1
50	43.1	27.9	28.9	50	46.4	25.6	28.0	50	44.0	27.4	28.6
55	44.1	27.0	29.0	55	46.3	26.1	27.6	55	44.4	26.9	28.7
60	42.7	28.3	29.0	60	46.3	26.1	27.6	60	44.5	27.0	28.5
65	43.0	28.1	28.9	65	46.5	25.9	27.6	65	44.2	27.2	28.5
70	43.1	28.0	29.0	70	46.7	25.7	27.6	70	44.3	26.9	28.8
75	43.1	28.0	29.0	75	45.6	26.2	28.2	75	44.6	27.1	28.3
80	43.1	28.0	28.8	80	46.6	25.7	27.7	80	44.1	27.1	28.9
85	43.0	27.7	29.3	85	45.2	26.4	28.3	85	43.5	27.4	29.1
90	42.1	27.9	30.0	90	45.1	26.5	28.3	90	43.3	27.5	29.2

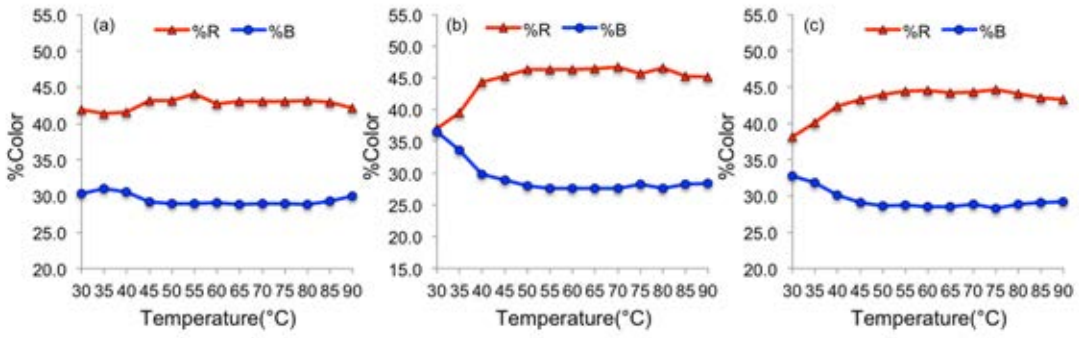

Figure C8 Plots of %RGB value of 3 independent ODDA indicators against temperature to determine the color transition temperature.

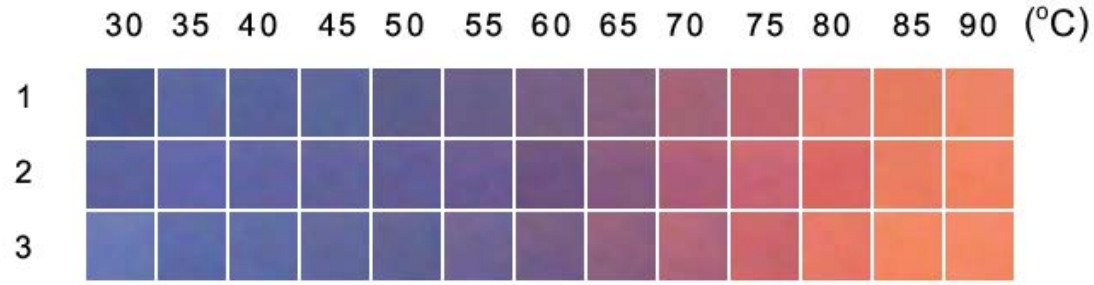

Figure C9 Photographs of Thermal sensing of EPCDP indicators.

Table C9 RGB values of EPCDP indicators at various Temperatures (3 independent experiments)

T(°C)	1				T(°C)	2				T(°C)	3			
	R	G	B	Sum		R	G	B	Sum		R	G	B	Sum
30	75	86	140	301	30	93	98	158	349	30	105	120	180	405
35	92	102	161	355	35	98	102	171	371	35	93	107	168	368
40	89	99	154	342	40	96	100	161	357	40	95	107	164	366
45	91	102	154	347	45	98	98	155	351	45	97	103	156	356
50	93	93	139	325	50	98	93	150	341	50	97	99	146	342
55	104	94	137	335	55	106	91	147	344	55	111	100	147	358
60	117	94	131	342	60	110	83	129	322	60	118	94	133	345
65	134	97	126	357	65	133	91	127	351	65	144	97	126	367
70	164	98	118	380	70	174	94	120	388	70	178	103	122	403
75	191	100	109	400	75	200	101	116	417	75	202	101	108	411
80	224	118	107	449	80	219	102	98	419	80	231	119	102	452
85	230	123	94	447	85	235	125	98	458	85	243	135	96	474
90	238	131	100	469	90	242	130	97	469	90	245	136	102	483

Table C10 %RGB values of EPCDP indicators at various temperatures (3 independent experiments)

T(°C)	1			T(°C)	2			T(°C)	3		
	%R	%G	%B		%R	%G	%B		%R	%G	%B
30	24.9	28.6	46.5	30	26.6	28.1	45.3	30	25.9	29.6	44.4
35	25.9	28.7	45.4	35	26.4	27.5	46.1	35	25.3	29.1	45.7
40	26.0	28.9	45.0	40	26.9	28.0	45.1	40	26.0	29.2	44.8
45	26.2	29.4	44.4	45	27.9	27.9	44.2	45	27.2	28.9	43.8
50	28.6	28.6	42.8	50	28.7	27.3	44.0	50	28.4	28.9	42.7
55	31.0	28.1	40.9	55	30.8	26.5	42.7	55	31.0	27.9	41.1
60	34.2	27.5	38.3	60	34.2	25.8	40.1	60	34.2	27.2	38.6
65	37.5	27.2	35.3	65	37.9	25.9	36.2	65	39.2	26.4	34.3
70	43.2	25.8	31.1	70	44.8	24.2	30.9	70	44.2	25.6	30.3
75	47.8	25.0	27.3	75	48.0	24.2	27.8	75	49.1	24.6	26.3
80	49.9	26.3	23.8	80	52.3	24.3	23.4	80	51.1	26.3	22.6
85	51.5	27.5	21.0	85	51.3	27.3	21.4	85	51.3	28.5	20.3
90	50.7	27.9	21.3	90	51.6	27.7	20.7	90	50.7	28.2	21.1

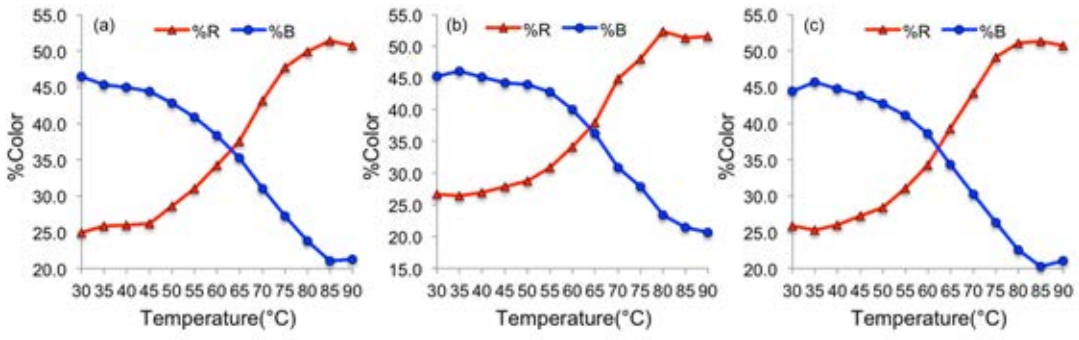

Figure C10 Plots of %RGB value of 3 independent EPCDP indicators against temperature to determine the color transition temperature.

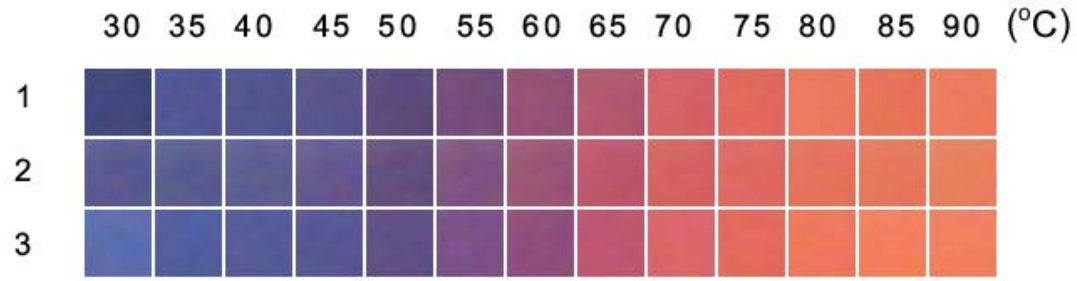

Figure C11 Photographs of Thermal sensing of ETCDP indicators.

Table C11 RGB values of ETCDP indicators at various Temperatures (3 independent experiments)

T(°C)	1				T(°C)	2				T(°C)	3			
	R	G	B	Sum		R	G	B	Sum		R	G	B	Sum
30	66	72	124	262	30	90	89	145	324	30	92	109	173	374
35	82	86	149	317	35	90	93	144	327	35	81	94	159	334
40	82	85	143	310	40	94	94	146	334	40	86	91	154	331
45	88	85	140	313	45	101	89	144	334	45	88	87	149	324
50	93	74	124	291	50	100	80	127	307	50	96	81	135	312
55	117	78	122	317	55	127	85	131	343	55	123	81	136	340
60	151	81	116	348	60	155	86	119	360	60	143	78	123	344
65	178	88	111	377	65	189	86	108	383	65	190	87	114	391
70	213	97	102	412	70	214	97	98	409	70	218	102	106	426
75	225	105	94	424	75	223	104	97	424	75	228	106	94	428
80	236	120	95	451	80	230	113	93	436	80	238	118	94	450
85	231	116	88	435	85	230	120	92	442	85	243	126	95	464
90	238	122	95	455	90	231	128	94	453	90	242	127	96	465

Table C12 %RGB values of ETCDP indicators at various temperatures (3 independent experiments)

T(°C)	1			T(°C)	2			T(°C)	3		
	%R	%G	%B		%R	%G	%B		%R	%G	%B
30	25.2	27.5	47.3	30	27.8	27.5	44.8	30	24.6	29.1	46.3
35	25.9	27.1	47.0	35	27.5	28.4	44.0	35	24.3	28.1	47.6
40	26.5	27.4	46.1	40	28.1	28.1	43.7	40	26.0	27.5	46.5
45	28.1	27.2	44.7	45	30.2	26.6	43.1	45	27.2	26.9	46.0
50	32.0	25.4	42.6	50	32.6	26.1	41.4	50	30.8	26.0	43.3
55	36.9	24.6	38.5	55	37.0	24.8	38.2	55	36.2	23.8	40.0
60	43.4	23.3	33.3	60	43.1	23.9	33.1	60	41.6	22.7	35.8
65	47.2	23.3	29.4	65	49.3	22.5	28.2	65	48.6	22.3	29.2
70	51.7	23.5	24.8	70	52.3	23.7	24.0	70	51.2	23.9	24.9
75	53.1	24.8	22.2	75	52.6	24.5	22.9	75	53.3	24.8	22.0
80	52.3	26.6	21.1	80	52.8	25.9	21.3	80	52.9	26.2	20.9
85	53.1	26.7	20.2	85	52.0	27.1	20.8	85	52.4	27.2	20.5
90	52.3	26.8	20.9	90	51.0	28.3	20.8	90	52.0	27.3	20.6

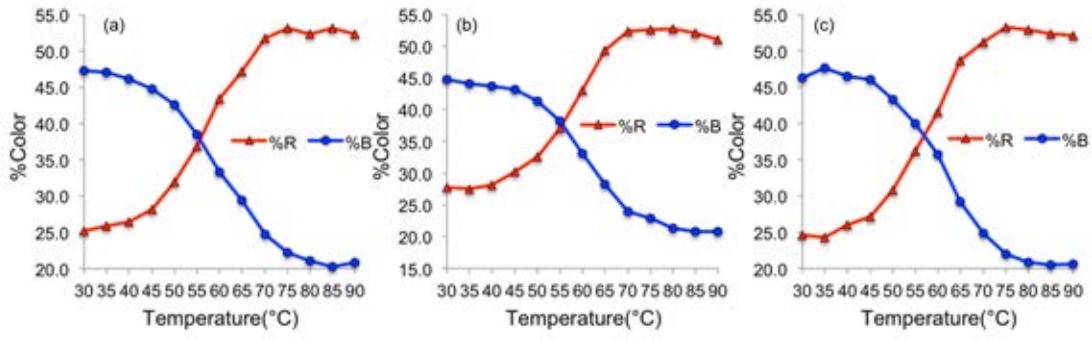

Figure C12 Plots of %RGB value of 3 independent ETCDP indicators against temperature to determine the color transition temperature.

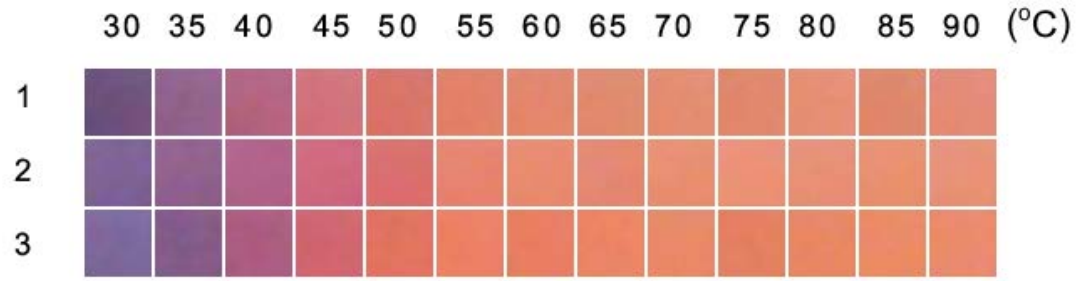

Figure C13 Photographs of Thermal sensing of ENDDP indicators.

Table C13 RGB values of ENDDP indicators at various Temperatures (3 independent experiments)

T(°C)	1				T(°C)	2				T(°C)	3			
	R	G	B	Sum		R	G	B	Sum		R	G	B	Sum
30	110	81	125	316	30	126	98	150	374	30	125	105	157	387
35	145	99	140	384	35	145	97	142	384	35	132	91	138	361
40	179	100	128	407	40	178	98	138	414	40	172	92	128	392
45	209	114	123	446	45	208	105	127	440	45	208	101	112	421
50	217	116	106	439	50	218	111	111	440	50	225	115	96	436
55	227	128	105	460	55	231	131	112	474	55	236	128	102	466
60	227	134	107	468	60	232	138	112	482	60	233	126	98	457
65	224	139	110	473	65	228	136	115	479	65	237	132	100	469
70	227	141	113	481	70	232	143	113	488	70	233	137	104	474
75	225	135	109	469	75	236	145	119	500	75	229	128	98	455
80	229	143	116	488	80	231	144	118	493	80	233	135	101	469
85	222	135	108	465	85	234	144	112	490	85	235	138	103	476
90	228	139	119	486	90	232	145	120	497	90	235	138	110	483

Table C14 %RGB values of ENDDP indicators at various temperatures (3 independent experiments)

T(°C)	1			T(°C)	2			T(°C)	3		
	%R	%G	%B		%R	%G	%B		%R	%G	%B
30	34.8	25.6	39.6	30	33.7	26.2	40.1	30	32.3	27.1	40.6
35	37.8	25.8	36.5	35	37.8	25.3	37.0	35	36.6	25.2	38.2
40	44.0	24.6	31.4	40	43.0	23.7	33.3	40	43.9	23.5	32.7
45	46.9	25.6	27.6	45	47.3	23.9	28.9	45	49.4	24.0	26.6
50	49.4	26.4	24.1	50	49.5	25.2	25.2	50	51.6	26.4	22.0
55	49.3	27.8	22.8	55	48.7	27.6	23.6	55	50.6	27.5	21.9
60	48.5	28.6	22.9	60	48.1	28.6	23.2	60	51.0	27.6	21.4
65	47.4	29.4	23.3	65	47.6	28.4	24.0	65	50.5	28.1	21.3
70	47.2	29.3	23.5	70	47.5	29.3	23.2	70	49.2	28.9	21.9
75	48.0	28.8	23.2	75	47.2	29.0	23.8	75	50.3	28.1	21.5
80	46.9	29.3	23.8	80	46.9	29.2	23.9	80	49.7	28.8	21.5
85	47.7	29.0	23.2	85	47.8	29.4	22.9	85	49.4	29.0	21.6
90	46.9	28.6	24.5	90	46.7	29.2	24.1	90	48.7	28.6	22.8

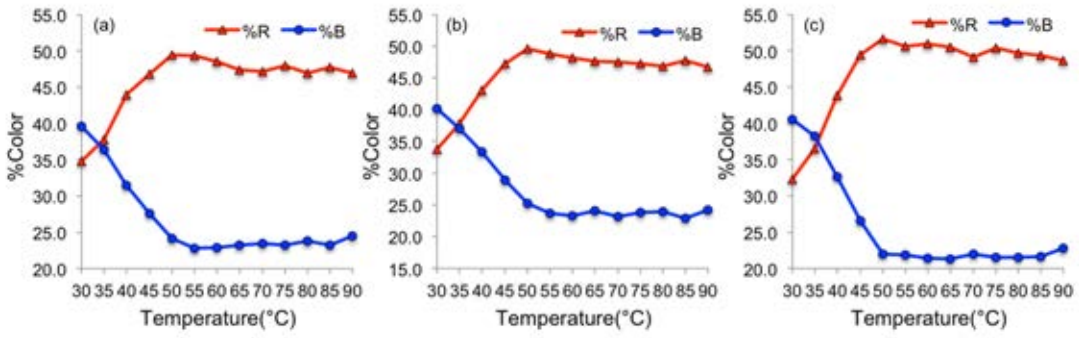

Figure C14 Plots of %RGB value of 3 independent ENDDP indicators against temperature to determine the color transition temperature.

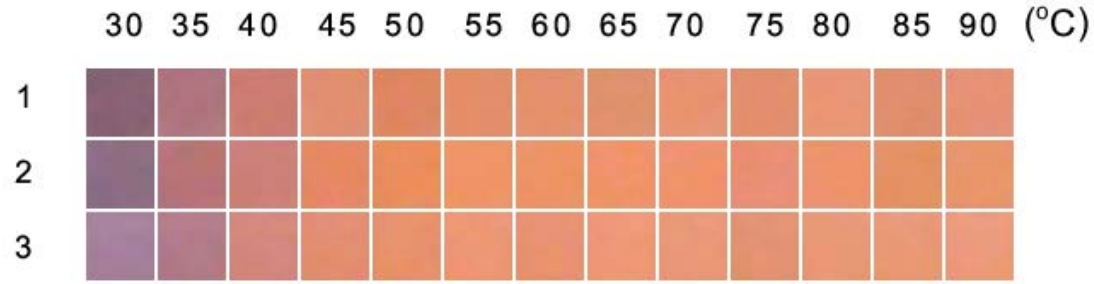

Figure C15 Photographs of Thermal sensing of EODDP indicators.

Table C15 RGB values of EODDP indicators at various Temperatures (3 independent experiments)

T(°C)	1				T(°C)	2				T(°C)	3			
	R	G	B	Sum		R	G	B	Sum		R	G	B	Sum
30	136	98	114	348	30	140	108	131	379	30	166	128	157	451
35	175	116	127	418	35	183	115	118	416	35	179	122	136	437
40	205	123	112	440	40	204	127	119	450	40	211	135	126	472
45	225	142	112	479	45	231	135	99	465	45	227	142	113	482
50	223	133	98	454	50	235	141	93	469	50	232	146	108	486
55	228	141	104	473	55	239	148	103	490	55	238	151	117	506
60	228	144	108	480	60	237	147	102	486	60	233	146	113	492
65	224	145	108	477	65	241	147	106	494	65	239	151	119	509
70	233	146	112	491	70	240	146	107	493	70	233	152	120	505
75	224	142	110	476	75	234	142	118	494	75	227	146	115	488
80	234	149	117	500	80	238	146	107	491	80	233	151	118	502
85	224	141	110	475	85	228	145	99	472	85	233	152	117	502
90	231	145	117	493	90	233	150	108	491	90	237	154	124	515

Table C16 %RGB values of EODDP indicators at various temperatures (3 independent experiments)

T(°C)	1			T(°C)	2			T(°C)	3		
	%R	%G	%B		%R	%G	%B		%R	%G	%B
30	39.1	28.2	32.8	30	36.9	28.5	34.6	30	36.8	28.4	34.8
35	41.9	27.8	30.4	35	44.0	27.6	28.4	35	41.0	27.9	31.1
40	46.6	28.0	25.5	40	45.3	28.2	26.4	40	44.7	28.6	26.7
45	47.0	29.6	23.4	45	49.7	29.0	21.3	45	47.1	29.5	23.4
50	49.1	29.3	21.6	50	50.1	30.1	19.8	50	47.7	30.0	22.2
55	48.2	29.8	22.0	55	48.8	30.2	21.0	55	47.0	29.8	23.1
60	47.5	30.0	22.5	60	48.8	30.2	21.0	60	47.4	29.7	23.0
65	47.0	30.4	22.6	65	48.8	29.8	21.5	65	47.0	29.7	23.4
70	47.5	29.7	22.8	70	48.7	29.6	21.7	70	46.1	30.1	23.8
75	47.1	29.8	23.1	75	47.4	28.7	23.9	75	46.5	29.9	23.6
80	46.8	29.8	23.4	80	48.5	29.7	21.8	80	46.4	30.1	23.5
85	47.2	29.7	23.2	85	48.3	30.7	21.0	85	46.4	30.3	23.3
90	46.9	29.4	23.7	90	47.5	30.5	22.0	90	46.0	29.9	24.1

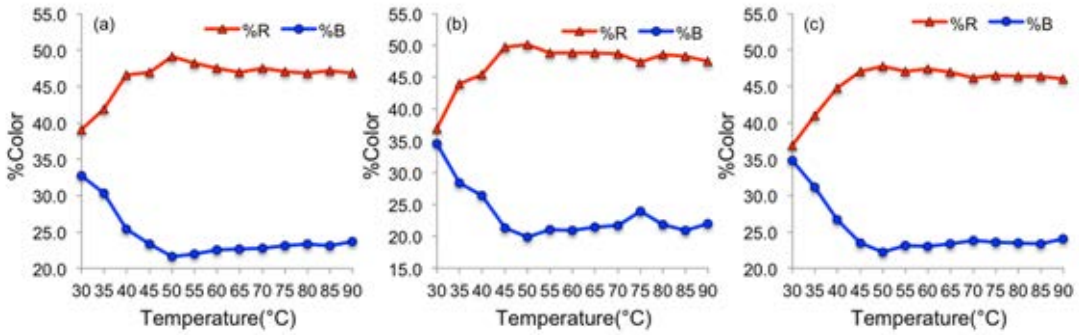

Figure C16 Plots of %RGB value of 3 independent EODDP indicators against temperature to determine the color transition temperature.

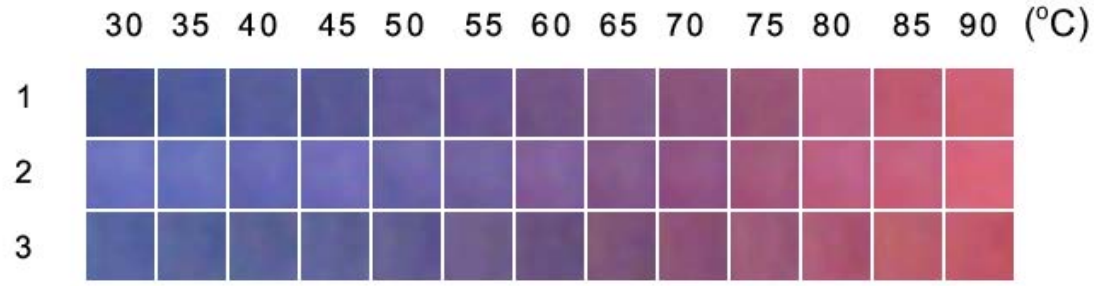

Figure C17 Photographs of Thermal sensing of EPCDPP indicators.

Table C17 RGB values of EPCDPP indicators at various Temperatures (3 independent experiments)

T(°C)	1				T(°C)	2				T(°C)	3			
	R	G	B	Sum		R	G	B	Sum		R	G	B	Sum
30	70	81	141	292	30	107	114	190	411	30	86	101	161	451
35	81	92	157	330	35	104	114	186	404	35	88	99	154	437
40	87	94	155	336	40	102	104	179	385	40	90	97	149	472
45	88	88	147	323	45	114	109	184	407	45	93	97	149	482
50	100	89	151	340	50	108	101	167	376	50	97	92	145	486
55	103	85	147	335	55	113	99	158	370	55	111	93	139	506
60	114	84	133	331	60	130	96	155	381	60	103	81	126	492
65	129	90	134	353	65	132	91	138	361	65	123	83	121	509
70	138	83	124	345	70	145	84	132	361	70	138	80	118	505
75	151	85	116	352	75	164	90	124	378	75	156	90	121	488
80	182	95	128	405	80	188	96	132	416	80	170	87	114	502
85	190	89	112	391	85	198	97	126	421	85	188	96	108	502
90	206	96	114	416	90	216	101	122	439	90	194	87	105	515

Table C18 %RGB values of EPCDPP indicators at various temperatures (3 independent experiments)

T(°C)	1			T(°C)	2			T(°C)	3		
	%R	%G	%B		%R	%G	%B		%R	%G	%B
30	24.0	27.7	48.3	30	26.0	27.7	46.2	30	19.1	22.4	35.7
35	24.5	27.9	47.6	35	25.7	28.2	46.0	35	20.1	22.7	35.2
40	25.9	28.0	46.1	40	26.5	27.0	46.5	40	19.1	20.6	31.6
45	27.2	27.2	45.5	45	28.0	26.8	45.2	45	19.3	20.1	30.9
50	29.4	26.2	44.4	50	28.7	26.9	44.4	50	20.0	18.9	29.8
55	30.7	25.4	43.9	55	30.5	26.8	42.7	55	21.9	18.4	27.5
60	34.4	25.4	40.2	60	34.1	25.2	40.7	60	20.9	16.5	25.6
65	36.5	25.5	38.0	65	36.6	25.2	38.2	65	24.2	16.3	23.8
70	40.0	24.1	35.9	70	40.2	23.3	36.6	70	27.3	15.8	23.4
75	42.9	24.1	33.0	75	43.4	23.8	32.8	75	32.0	18.4	24.8
80	44.9	23.5	31.6	80	45.2	23.1	31.7	80	33.9	17.3	22.7
85	48.6	22.8	28.6	85	47.0	23.0	29.9	85	37.5	19.1	21.5
90	49.5	23.1	27.4	90	49.2	23.0	27.8	90	37.7	16.9	20.4

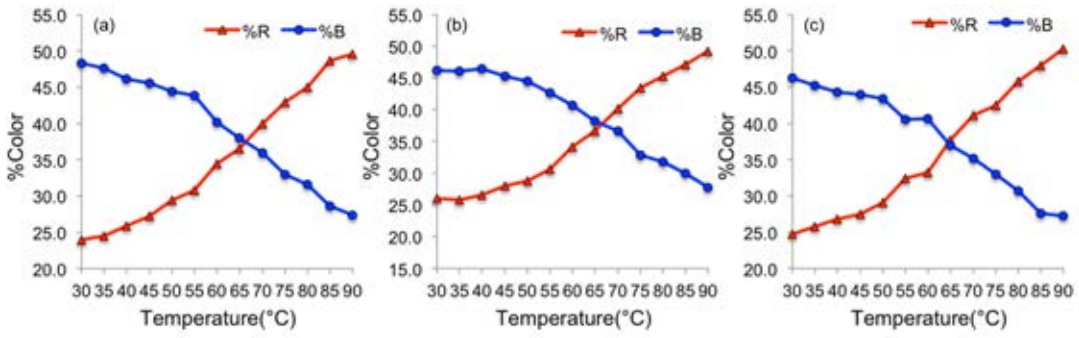

Figure C18 Plots of %RGB value of 3 independent EPCDPP indicators against temperature to determine the color transition temperature.

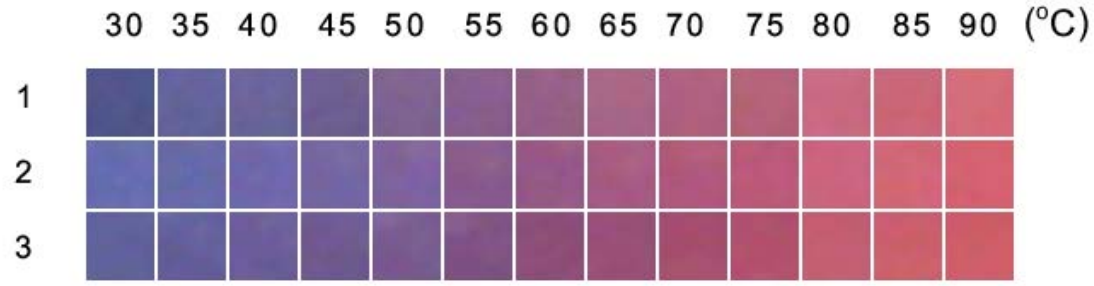

Figure C19 Photographs of Thermal sensing of ETCDPP indicators

Table C19 RGB values of ETCDPP indicators at various Temperatures (3 independent experiments)

T(°C)	1				T(°C)	2				T(°C)	3			
	R	G	B	Sum		R	G	B	Sum		R	G	B	Sum
30	81	85	138	304	30	102	108	176	386	30	96	98	155	349
35	99	99	155	353	35	102	106	168	376	35	100	95	154	349
40	106	101	154	361	40	112	103	171	386	40	108	94	154	356
45	110	94	144	348	45	116	103	162	381	45	111	89	144	344
50	127	98	144	369	50	127	99	157	383	50	122	91	144	357
55	136	95	142	373	55	137	91	140	368	55	128	83	133	344
60	149	96	134	379	60	151	88	135	374	60	141	77	120	338
65	168	102	135	405	65	168	92	130	390	65	152	80	118	350
70	175	96	127	398	70	177	89	124	390	70	166	78	110	354
75	181	98	121	400	75	188	89	123	400	75	178	80	108	366
80	201	106	130	437	80	202	100	127	429	80	195	94	113	402
85	203	102	118	423	85	209	103	119	431	85	204	96	107	407
90	212	108	121	441	90	213	98	112	423	90	206	93	104	403

Table C20 %RGB values of ETCDPP indicators at various temperatures (3 independent experiments)

T(°C)	1			T(°C)	2			T(°C)	3		
	%R	%G	%B		%R	%G	%B		%R	%G	%B
30	26.6	28.0	45.4	30	26.4	28.0	45.6	30	27.5	28.1	44.4
35	28.0	28.0	43.9	35	27.1	28.2	44.7	35	28.7	27.2	44.1
40	29.4	28.0	42.7	40	29.0	26.7	44.3	40	30.3	26.4	43.3
45	31.6	27.0	41.4	45	30.4	27.0	42.5	45	32.3	25.9	41.9
50	34.4	26.6	39.0	50	33.2	25.8	41.0	50	34.2	25.5	40.3
55	36.5	25.5	38.1	55	37.2	24.7	38.0	55	37.2	24.1	38.7
60	39.3	25.3	35.4	60	40.4	23.5	36.1	60	41.7	22.8	35.5
65	41.5	25.2	33.3	65	43.1	23.6	33.3	65	43.4	22.9	33.7
70	44.0	24.1	31.9	70	45.4	22.8	31.8	70	46.9	22.0	31.1
75	45.3	24.5	30.3	75	47.0	22.3	30.8	75	48.6	21.9	29.5
80	46.0	24.3	29.7	80	47.1	23.3	29.6	80	48.5	23.4	28.1
85	48.0	24.1	27.9	85	48.5	23.9	27.6	85	50.1	23.6	26.3
90	48.1	24.5	27.4	90	50.4	23.2	26.5	90	51.1	23.1	25.8

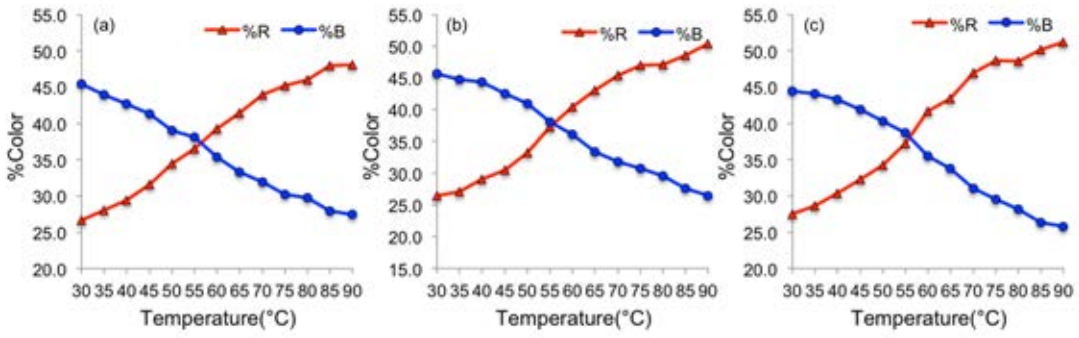

Figure C20 Plots of %RGB value of 3 independent ETCDPP indicators against temperature to determine the color transition temperature.

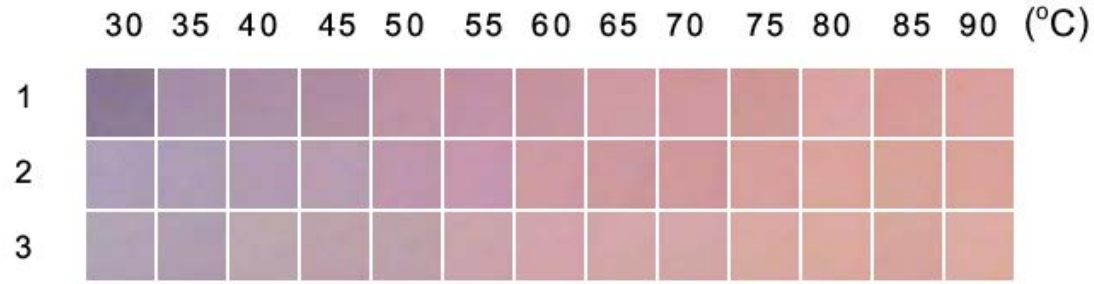

Figure C21 Photographs of Thermal sensing of ENDDPP indicators.

Table C21 RGB values of EPCDP indicators at various Temperatures (3 independent experiments)

T(°C)	1				T(°C)	2				T(°C)	3			
	R	G	B	Sum		R	G	B	Sum		R	G	B	Sum
30	138	120	148	406	30	182	167	184	533	30	176	163	180	519
35	166	143	169	478	35	181	166	182	529	35	176	157	176	509
40	171	143	166	480	40	184	164	179	527	40	187	166	175	528
45	175	142	162	479	45	188	168	179	535	45	189	161	170	520
50	190	146	165	501	50	194	161	177	532	50	189	161	169	519
55	193	144	165	502	55	199	159	178	536	55	202	164	171	537
60	198	147	160	505	60	203	163	167	533	60	212	163	172	547
65	208	154	163	525	65	202	161	163	526	65	211	167	167	545
70	208	151	156	515	70	205	159	160	524	70	211	167	167	545
75	206	151	150	507	75	209	165	163	537	75	217	168	160	545
80	218	163	164	545	80	216	169	163	548	80	219	169	160	548
85	214	156	152	522	85	211	170	159	540	85	215	164	157	536
90	218	160	158	536	90	216	170	164	550	90	211	171	162	544

Table C22 %RGB values of ENDDPP indicators at various temperatures (3 independent experiments)

T(°C)	1			T(°C)	2			T(°C)	3		
	%R	%G	%B		%R	%G	%B		%R	%G	%B
30	34.0	29.6	36.5	30	34.1	31.3	34.5	30	33.9	31.4	34.7
35	34.7	29.9	35.4	35	34.2	31.4	34.4	35	34.6	30.8	34.6
40	35.6	29.8	34.6	40	34.9	31.1	34.0	40	35.4	31.4	33.1
45	36.5	29.6	33.8	45	35.1	31.4	33.5	45	36.3	31.0	32.7
50	37.9	29.1	32.9	50	36.5	30.3	33.3	50	36.4	31.0	32.6
55	38.4	28.7	32.9	55	37.1	29.7	33.2	55	37.6	30.5	31.8
60	39.2	29.1	31.7	60	38.1	30.6	31.3	60	38.8	29.8	31.4
65	39.6	29.3	31.0	65	38.4	30.6	31.0	65	38.7	30.6	30.6
70	40.4	29.3	30.3	70	39.1	30.3	30.5	70	38.7	30.6	30.6
75	40.6	29.8	29.6	75	38.9	30.7	30.4	75	39.8	30.8	29.4
80	40.0	29.9	30.1	80	39.4	30.8	29.7	80	40.0	30.8	29.2
85	41.0	29.9	29.1	85	39.1	31.5	29.4	85	40.1	30.6	29.3
90	40.7	29.9	29.5	90	39.3	30.9	29.8	90	38.8	31.4	29.8

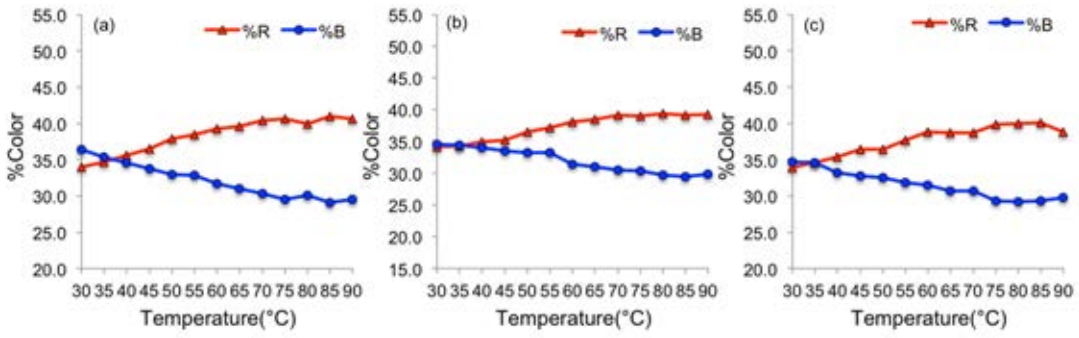

Figure C22 Plots of %RGB value of 3 independent ENDDPP indicators against temperature to determine the color transition temperature.

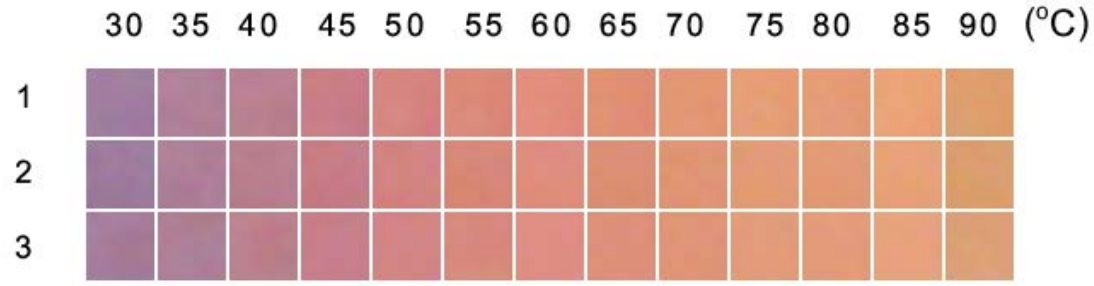

Figure C23 Photographs of Thermal sensing of EODDPP indicators.

Table C23 RGB values of EODDPP indicators at various Temperatures (3 independent experiments)

T(°C)	1				T(°C)	2				T(°C)	3			
	R	G	B	Sum		R	G	B	Sum		R	G	B	Sum
30	160	125	159	444	30	157	122	156	435	30	164	123	153	440
35	175	128	152	455	35	174	125	151	450	35	173	127	150	450
40	185	128	145	458	40	183	126	142	451	40	188	126	140	454
45	200	124	134	458	45	199	123	134	456	45	200	126	140	466
50	214	132	129	475	50	211	132	130	473	50	211	132	134	477
55	219	137	120	476	55	215	135	119	469	55	215	136	125	476
60	226	141	124	491	60	223	140	127	490	60	223	141	131	495
65	224	143	115	482	65	219	142	116	477	65	221	144	121	486
70	227	150	115	492	70	224	148	117	489	70	223	148	120	491
75	230	157	118	505	75	226	154	117	497	75	227	155	123	505
80	229	154	119	502	80	226	153	117	496	80	227	154	122	503
85	234	163	120	517	85	232	161	121	514	85	232	161	125	518
90	222	158	109	489	90	218	158	111	487	90	221	159	119	499

Table C24 %RGB values of EODDPP indicators at various temperatures (3 independent experiments)

T(°C)	1			T(°C)	2			T(°C)	3		
	%R	%G	%B		%R	%G	%B		%R	%G	%B
30	36.0	28.2	35.8	30	36.1	28.0	35.9	30	37.3	28.0	34.8
35	38.5	28.1	33.4	35	38.7	27.8	33.6	35	38.4	28.2	33.3
40	40.4	27.9	31.7	40	40.6	27.9	31.5	40	41.4	27.8	30.8
45	43.7	27.1	29.3	45	43.6	27.0	29.4	45	42.9	27.0	30.0
50	45.1	27.8	27.2	50	44.6	27.9	27.5	50	44.2	27.7	28.1
55	46.0	28.8	25.2	55	45.8	28.8	25.4	55	45.2	28.6	26.3
60	46.0	28.7	25.3	60	45.5	28.6	25.9	60	45.1	28.5	26.5
65	46.5	29.7	23.9	65	45.9	29.8	24.3	65	45.5	29.6	24.9
70	46.1	30.5	23.4	70	45.8	30.3	23.9	70	45.4	30.1	24.4
75	45.5	31.1	23.4	75	45.5	31.0	23.5	75	45.0	30.7	24.4
80	45.6	30.7	23.7	80	45.6	30.8	23.6	80	45.1	30.6	24.3
85	45.3	31.5	23.2	85	45.1	31.3	23.5	85	44.8	31.1	24.1
90	45.4	32.3	22.3	90	44.8	32.4	22.8	90	44.3	31.9	23.8

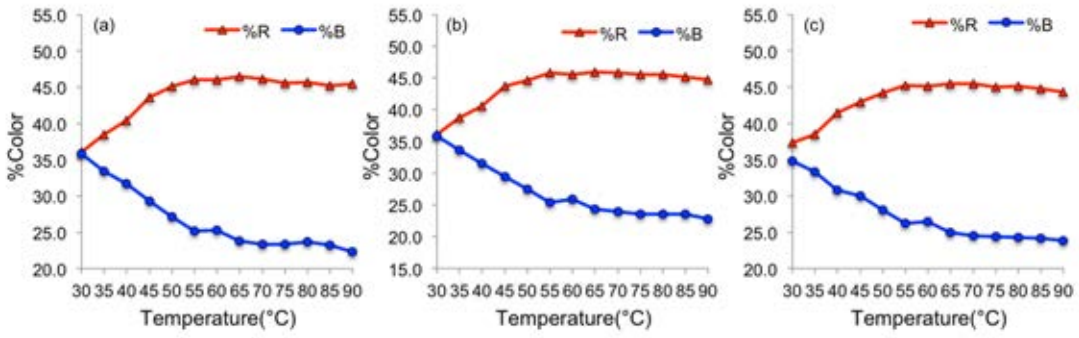

Figure C24 Plots of %RGB value of 3 independent EODDPP indicators against temperature to determine the color transition temperature.

APPENDIX D

SOLVENT SENSING STUDY

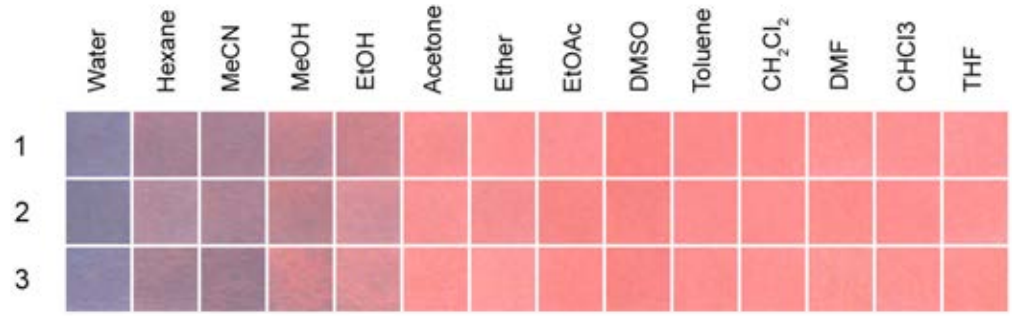

Figure D1 Color images of TCDA indicators obtained after exposure to different solvents.

Table D1 RGB values of TCDA indicators obtained after exposure to different solvents (3 independent experiments)

Solvent	1				Solvent	2				Solvent	3			
	R	G	B	sum		R	G	B	sum		R	G	B	sum
Water	138	132	160	430	Water	134	128	155	417	Water	143	135	166	444
Hexane	163	129	148	440	Hexane	176	140	158	474	Hexane	162	130	146	438
MeCN	167	130	148	445	MeCN	173	134	149	456	MeCN	159	125	142	426
MeOH	191	131	142	464	MeOH	186	131	141	458	MeOH	211	136	142	489
EtOH	205	133	141	479	EtOH	211	143	154	508	EtOH	222	145	151	518
Acetone	248	144	144	536	Acetone	249	147	150	546	Acetone	254	148	148	550
Ether	254	145	146	545	Ether	245	143	145	533	Ether	254	155	155	564
EtOAc	253	145	147	545	EtOAc	249	135	133	517	EtOAc	254	140	140	534
DMSO	252	131	130	513	DMSO	248	133	131	512	DMSO	249	135	134	518
Toluene	252	138	139	529	Toluene	253	141	142	536	Toluene	254	143	143	540
CH_2Cl_2	254	141	142	537	CH_2Cl_2	254	143	144	541	CH_2Cl_2	254	146	147	547
DMF	254	147	147	548	DMF	254	142	140	536	DMF	254	150	149	553
$CHCl_3$	254	145	148	547	$CHCl_3$	254	143	144	541	$CHCl_3$	254	148	148	550
THF	254	149	150	553	THF	254	147	148	549	THF	254	147	145	546

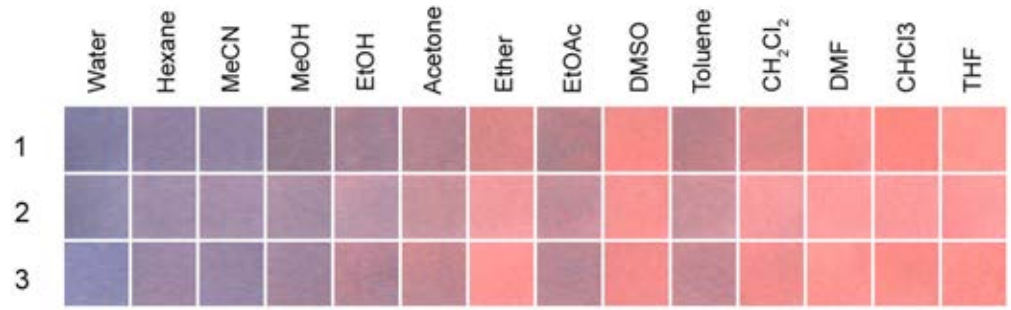

Figure D2 Color images of PCDA indicators obtained after exposure to different solvents.

Table D2 RGB values of PCDA indicators obtained after exposure to different solvents (3 independent experiments)

Solvent	1				Solvent	2				Solvent	3			
	R	G	B	sum		R	G	B	sum		R	G	B	sum
Water	130	126	159	415	Water	140	135	165	440	Water	142	139	179	460
Hexane	145	139	161	445	Hexane	158	141	170	469	Hexane	157	136	166	459
MeCN	146	132	161	439	MeCN	165	143	169	477	MeCN	153	135	164	452
MeOH	148	124	143	415	MeOH	169	142	162	473	MeOH	161	134	157	452
EtOH	162	130	149	441	EtOH	188	150	167	505	EtOH	182	134	150	466
Acetone	179	132	143	454	Acetone	200	146	155	501	Acetone	196	137	146	479
Ether	216	137	138	491	Ether	240	155	158	553	Ether	254	152	151	557
EtOAc	185	130	137	452	EtOAc	194	141	152	487	EtOAc	184	135	148	467
DMSO	249	139	135	523	DMSO	248	143	147	538	DMSO	244	141	141	526
Toluene	186	129	136	451	Toluene	206	146	156	508	Toluene	195	137	147	479
CH_2Cl_2	218	137	138	493	CH_2Cl_2	248	156	160	564	CH_2Cl_2	242	141	142	525
DMF	253	144	141	538	DMF	253	157	158	568	DMF	254	152	149	555
$CHCl_3$	253	138	131	522	$CHCl_3$	252	154	155	561	$CHCl_3$	250	141	137	528
THF	254	152	146	552	THF	254	154	155	563	THF	254	145	141	540

Figure D3 Color images of ETCDP indicators obtained after exposure to different solvents.

Table D3 RGB values of ETCDP indicators obtained after exposure to different solvents (3 independent experiments)

Solvent	1				Solvent	2				Solvent	3			
	R	G	B	sum		R	G	B	sum		R	G	B	sum
Water	129	127	162	418	Water	127	124	158	409	Water	134	132	165	431
Hexane	181	125	149	455	Hexane	187	119	135	441	Hexane	226	130	145	501
MeCN	231	123	130	484	MeCN	250	135	146	531	MeCN	245	131	141	517
MeOH	251	135	143	529	MeOH	253	138	146	537	MeOH	248	133	144	525
EtOH	248	132	140	520	EtOH	253	137	146	536	EtOH	254	136	145	535
Acetone	254	137	142	533	Acetone	253	133	139	525	Acetone	254	136	140	530
Ether	254	138	143	535	Ether	254	138	141	533	Ether	254	143	151	548
EtOAc	254	136	143	533	EtOAc	254	137	142	533	EtOAc	254	135	141	530
DMSO	167	121	142	430	DMSO	186	123	145	454	DMSO	152	102	130	384
Toluene	254	137	144	535	Toluene	254	143	152	549	Toluene	254	133	138	525
CH_2Cl_2	254	135	139	528	CH_2Cl_2	253	136	144	533	CH_2Cl_2	254	137	143	534
DMF	254	141	148	543	DMF	253	136	142	531	DMF	253	135	140	528
$CHCl_3$	254	136	142	532	$CHCl_3$	254	134	140	528	$CHCl_3$	254	137	143	534
THF	254	139	142	535	THF	254	136	142	532	THF	254	134	139	527

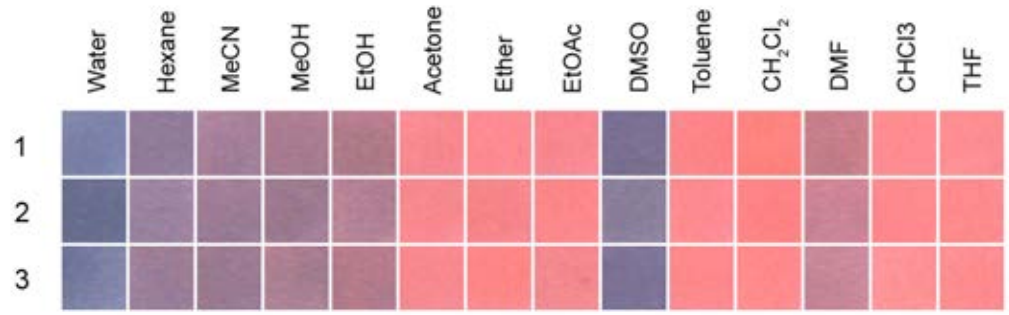

Figure D4 Color images of EPCDP indicators obtained after exposure to different solvents.

Table D4 RGB values of EPCDP indicators obtained after exposure to different solvents (3 independent experiments)

Solvent	1				Solvent	2				Solvent	3			
	R	G	B	sum		R	G	B	sum		R	G	B	sum
Water	123	129	167	419	Water	105	110	143	358	Water	123	127	162	412
Hexane	145	123	154	422	Hexane	155	131	158	444	Hexane	153	125	152	430
MeCN	164	127	153	444	MeCN	157	125	149	431	MeCN	155	122	145	422
MeOH	171	124	147	442	MeOH	157	121	143	421	MeOH	168	126	145	439
EtOH	174	121	136	431	EtOH	180	129	148	457	EtOH	181	123	140	444
Acetone	248	136	141	525	Acetone	247	136	141	524	Acetone	248	137	142	527
Ether	254	139	146	539	Ether	246	132	137	515	Ether	254	134	134	522
EtOAc	248	135	144	527	EtOAc	252	135	138	525	EtOAc	243	136	141	520
DMSO	124	113	147	384	DMSO	137	126	154	417	DMSO	124	114	150	388
Toluene	253	131	134	518	Toluene	254	138	144	536	Toluene	254	137	140	531
CH_2Cl_2	254	131	129	514	CH_2Cl_2	254	130	132	516	CH_2Cl_2	254	138	139	531
DMF	196	125	137	458	DMF	204	132	149	485	DMF	200	136	152	488
$CHCl_3$	254	139	145	538	$CHCl_3$	254	137	142	533	$CHCl_3$	254	147	151	552
THF	254	141	145	540	THF	254	138	141	533	THF	254	139	143	536

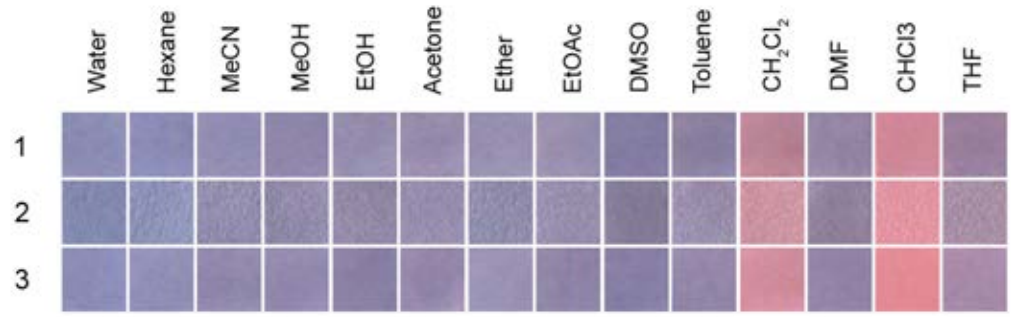

Figure D5 Color images of ETCDPP indicators obtained after exposure to different solvents.

Table D5 RGB values of ETCDPP indicators obtained after exposure to different solvents (3 independent experiments)

Solvent	1				Solvent	2				Solvent	3			
	R	G	B	sum		R	G	B	sum		R	G	B	sum
Water	140	141	179	460	Water	130	137	174	441	Water	140	140	183	463
Hexane	137	138	179	454	Hexane	142	147	183	472	Hexane	145	143	182	470
MeCN	144	140	177	461	MeCN	147	143	175	465	MeCN	144	136	172	452
MeOH	142	133	170	445	MeOH	147	139	170	456	MeOH	146	135	172	453
EtOH	148	139	172	459	EtOH	147	137	166	450	EtOH	137	127	163	427
Acetone	149	137	170	456	Acetone	150	141	173	464	Acetone	146	133	169	448
Ether	151	143	176	470	Ether	144	141	171	456	Ether	156	146	179	481
EtOAc	148	140	173	461	EtOAc	152	142	172	466	EtOAc	143	131	165	439
DMSO	131	124	161	416	DMSO	130	122	150	402	DMSO	135	127	165	427
Toluene	141	129	160	430	Toluene	153	142	172	467	Toluene	149	135	169	453
CH_2Cl_2	183	130	148	461	CH_2Cl_2	171	204	148	523	CH_2Cl_2	208	141	157	506
DMF	149	133	164	446	DMF	143	128	155	426	DMF	146	130	165	441
$CHCl_3$	208	135	151	494	$CHCl_3$	226	148	162	536	$CHCl_3$	227	138	149	514
THF	153	127	155	435	THF	168	143	166	477	THF	168	138	168	474

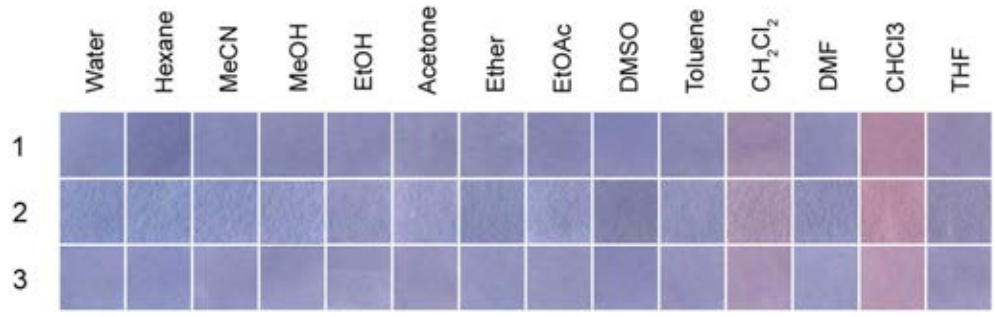

Figure D6 Color images of EPCDPP indicators obtained after exposure to different solvents.

Table D6 RGB values of EPCDPP indicators obtained after exposure to different solvents (3 independent experiments)

Solvent	1				Solvent	2				Solvent	3			
	R	G	B	sum		R	G	B	sum		R	G	B	sum
Water	137	142	186	465	Water	134	146	191	471	Water	142	148	190	480
Hexane	116	121	167	404	Hexane	137	150	194	481	Hexane	137	144	191	472
MeCN	132	138	181	451	MeCN	140	149	194	483	MeCN	144	147	188	479
MeOH	134	136	178	448	MeOH	146	152	196	494	MeOH	145	146	189	480
EtOH	139	140	182	461	EtOH	146	149	190	485	EtOH	150	151	189	490
Acetone	144	143	182	469	Acetone	155	157	197	509	Acetone	149	146	185	480
Ether	140	141	180	461	Ether	135	141	182	458	Ether	146	149	189	484
EtOAc	132	134	176	442	EtOAc	145	150	192	487	EtOAc	147	148	186	481
DMSO	129	132	177	438	DMSO	126	128	165	419	DMSO	136	138	182	456
Toluene	137	139	179	455	Toluene	146	147	185	478	Toluene	148	146	187	481
CH_2Cl_2	154	136	168	458	CH_2Cl_2	164	145	174	483	CH_2Cl_2	166	146	178	490
DMF	140	138	180	458	DMF	155	142	141	438	DMF	156	155	195	506
$CHCl_3$	174	135	161	470	$CHCl_3$	183	142	165	490	$CHCl_3$	180	150	180	510
THF	146	138	176	460	THF	146	140	175	461	THF	150	144	182	476

APPENDIX E

HUMIDITY SENSING STUDY

Table E1 RGB values of TCDA indicators with Na_2CO_3 after exposure at 62% RH for 24 h (7 independent experiments)

Time (h)	1				Time (h)	2				Time (h)	3				Time (h)	4			
	R	G	B	Sum		R	G	B	Sum		R	G	B	Sum		R	G	B	Sum
0	79	77	129	285	0	77	73	126	276	0	80	75	125	280	0	74	70	119	263
3	79	73	125	277	3	76	69	121	266	3	77	71	122	270	3	72	68	113	253
6	80	72	124	276	6	77	69	121	267	6	78	72	121	271	6	75	67	111	253
9	77	75	121	273	9	74	71	117	262	9	76	74	114	264	9	70	70	107	247
12	80	73	125	278	12	77	70	120	267	12	79	71	120	270	12	74	68	113	255
15	78	75	120	273	15	75	71	117	263	15	76	73	115	264	15	71	69	107	247
18	80	73	124	277	18	77	70	120	267	18	80	72	119	271	18	74	68	110	252
21	79	73	121	273	21	76	69	117	262	21	77	71	115	263	21	72	68	105	245
24	81	74	127	282	24	78	70	124	272	24	81	72	123	276	24	76	69	115	260

Time (h)	5				Time (h)	6				Time (h)	7			
	R	G	B	Sum		R	G	B	Sum		R	G	B	Sum
0	76	76	126	278	0	78	77	123	278	0	71	72	120	263
3	75	72	120	267	3	78	74	118	270	3	71	68	112	251
6	76	72	120	268	6	79	73	117	269	6	72	68	112	252
9	76	73	116	265	9	78	76	112	266	9	71	70	106	247
12	77	73	118	268	12	80	74	116	270	12	74	68	113	255
15	76	74	115	265	15	77	75	111	263	15	71	70	108	249
18	77	73	118	268	18	81	75	115	271	18	73	69	110	252
21	75	73	115	263	21	78	74	111	263	21	72	68	108	248
24	79	74	112	265	24	82	75	119	276	24	74	69	116	259

Table E2 %RGB values of TCDA indicators with Na_2CO_3 after exposure at 62% RH for 24 h (7 independent experiments)

Time (h)	1			Time (h)	2			Time (h)	3			Time (h)	4		
	R	G	B		R	G	B		R	G	B		R	G	B
0	27.7	27.0	45.3	0	27.9	27.9	45.7	0	28.6	26.8	44.6	0	28.1	26.6	45.2
3	28.5	26.4	45.1	3	28.6	28.6	45.5	3	28.5	26.3	45.2	3	28.5	26.9	44.7
6	29.0	26.1	44.9	6	28.8	28.8	45.3	6	28.8	26.6	44.6	6	29.6	26.5	43.9
9	28.2	27.5	44.3	9	28.2	28.2	44.7	9	28.8	28.0	43.2	9	28.3	28.3	43.3
12	28.8	26.3	45.0	12	28.8	28.8	44.9	12	29.3	26.3	44.4	12	29.0	26.7	44.3
15	28.6	27.5	44.0	15	28.5	28.5	44.5	15	28.8	27.7	43.6	15	28.7	27.9	43.3
18	28.9	26.4	44.8	18	28.8	28.8	44.9	18	29.5	26.6	43.9	18	29.4	27.0	43.7
21	28.9	26.7	44.3	21	29.0	29.0	44.7	21	29.3	27.0	43.7	21	29.4	27.8	42.9
24	28.7	26.2	45.0	24	28.7	28.7	45.6	24	29.3	26.1	44.6	24	29.2	26.5	44.2
Time (h)	5			Time (h)	6			Time (h)	7						
	R	G	B		R	G	B		R	G	B				
0	27.3	27.3	45.3	0	28.1	27.7	44.2	0	27.0	27.4	45.6				
3	28.1	27.0	44.9	3	28.9	27.4	43.7	3	28.3	27.1	44.6				
6	28.4	26.9	44.8	6	29.4	27.1	43.5	6	28.6	27.0	44.4				
9	28.7	27.5	43.8	9	29.3	28.6	42.1	9	28.7	28.3	42.9				
12	28.7	27.2	44.0	12	29.6	27.4	43.0	12	29.0	26.7	44.3				
15	28.7	27.9	43.4	15	29.3	28.5	42.2	15	28.5	28.1	43.4				
18	28.7	27.2	44.0	18	29.9	27.7	42.4	18	29.0	27.4	43.7				
21	28.5	27.8	43.7	21	29.7	28.1	42.2	21	29.0	27.4	43.5				
24	29.8	27.9	42.3	24	29.7	27.2	43.1	24	28.6	26.6	44.8				

Table E3 RGB values of TCDA indicators with K_2CO_3 after exposure at 62% RH for 24 h (7 independent experiments)

Time (h)	1				Time (h)	2				Time (h)	3				Time (h)	4			
	R	G	B	Sum		R	G	B	Sum		R	G	B	Sum		R	G	B	Sum
0	82	83	128	293	0	78	77	126	281	0	73	70	122	265	0	69	70	121	260
3	105	91	123	319	3	102	86	116	304	3	90	78	120	288	3	88	77	122	287
6	123	91	119	333	6	122	87	113	322	6	111	81	114	306	6	112	78	113	303
9	131	92	109	332	9	130	89	103	322	9	116	81	104	301	9	119	79	102	300
12	133	85	102	320	12	137	80	96	313	12	119	73	97	289	12	126	71	90	287
15	149	91	102	342	15	144	86	99	329	15	128	79	99	306	15	137	77	93	307
18	149	92	92	333	18	146	87	89	322	18	134	80	88	302	18	139	77	81	297
21	151	91	97	339	21	146	85	92	323	21	136	79	90	305	21	139	76	83	298
24	155	92	101	348	24	151	87	98	336	24	144	80	95	319	24	145	77	91	313
Time (h)	5				Time (h)	6				Time (h)	7								
	R	G	B	Sum		R	G	B	Sum		R	G	B	Sum					
0	82	83	128	293	0	78	77	126	281	0	73	70	122	265					
3	105	91	123	319	3	102	86	116	304	3	90	78	120	288					
6	123	91	119	333	6	122	87	113	322	6	111	81	114	306					
9	131	92	109	332	9	130	89	103	322	9	116	81	104	301					
12	133	85	102	320	12	137	80	96	313	12	119	73	97	289					
15	149	91	102	342	15	144	86	99	329	15	128	79	99	306					
18	149	92	92	333	18	146	87	89	322	18	134	80	88	302					
21	151	91	97	339	21	146	85	92	323	21	136	79	90	305					
24	155	92	101	348	24	151	87	98	336	24	144	80	95	319					

Table E4 %RGB values of TCDA indicators with K_2CO_3 after exposure at 62% RH for 24 h (7 independent experiments)

Time (h)	1			Time (h)	2			Time (h)	3			Time (h)	4		
	R	G	B		R	G	B		R	G	B		R	G	B
0	28.0	28.3	43.7	0	27.8	27.8	44.8	0	27.5	26.4	46.0	0	26.5	26.9	46.5
3	32.9	28.5	38.6	3	33.6	33.6	38.2	3	31.3	27.1	41.7	3	30.7	26.8	42.5
6	36.9	27.3	35.7	6	37.9	37.9	35.1	6	36.3	26.5	37.3	6	37.0	25.7	37.3
9	39.5	27.7	32.8	9	40.4	40.4	32.0	9	38.5	26.9	34.6	9	39.7	26.3	34.0
12	41.6	26.6	31.9	12	43.8	43.8	30.7	12	41.2	25.3	33.6	12	43.9	24.7	31.4
15	43.6	26.6	29.8	15	43.8	43.8	30.1	15	41.8	25.8	32.4	15	44.6	25.1	30.3
18	44.7	27.6	27.6	18	45.3	45.3	27.6	18	44.4	26.5	29.1	18	46.8	25.9	27.3
21	44.5	26.8	28.6	21	45.2	45.2	28.5	21	44.6	25.9	29.5	21	46.6	25.5	27.9
24	44.5	26.4	29.0	24	44.9	44.9	29.2	24	45.1	25.1	29.8	24	46.3	24.6	29.1

Time (h)	5			Time (h)	6			Time (h)	7		
	R	G	B		R	G	B		R	G	B
0	26.8	26.8	46.3	0	26.6	27.0	46.5	0	26.8	28.0	45.1
3	31.2	27.0	41.8	3	30.2	27.3	42.4	3	31.6	27.7	40.8
6	37.1	25.8	37.1	6	36.5	26.0	37.5	6	37.1	27.1	35.8
9	39.9	27.0	33.1	9	39.6	27.0	33.4	9	39.9	27.7	32.4
12	43.0	25.4	31.7	12	42.6	25.5	31.9	12	42.9	26.1	31.0
15	44.2	25.4	30.4	15	43.3	26.0	30.7	15	45.0	26.7	28.3
18	46.5	26.3	27.3	18	45.5	26.7	27.7	18	46.0	27.2	26.8
21	47.5	25.4	27.1	21	46.5	25.9	27.6	21	46.5	26.7	26.7
24	46.6	24.9	28.4	24	46.0	25.4	28.6	24	46.2	25.8	28.0

Table E5 RGB values of TCDA indicators with K_2CO_3 after exposure at 75% RH for 24 h (7 independent experiments)

Time (h)	1				Time (h)	2				Time (h)	3				Time (h)	4			
	R	G	B	Sum		R	G	B	Sum		R	G	B	Sum		R	G	B	Sum
0	76	69	126	271	0	74	68	124	266	0	71	66	123	260	0	70	66	117	253
3	159	86	82	327	3	150	83	81	314	3	148	80	81	309	3	140	79	79	298
6	158	88	90	336	6	159	85	86	330	6	164	85	85	334	6	156	83	83	322
9	156	89	85	330	9	158	86	79	323	9	162	87	78	327	9	154	84	78	316
12	157	89	87	333	12	159	85	83	327	12	162	86	81	329	12	156	84	79	319
15	156	92	87	335	15	156	88	82	326	15	160	89	80	329	15	153	87	79	319
18	155	92	86	333	18	155	89	81	325	18	160	89	80	329	18	153	87	77	317
21	159	93	94	346	21	156	90	88	334	21	161	90	87	338	21	156	87	87	330
24	160	98	96	354	24	159	94	89	342	24	163	95	88	346	24	158	93	88	339

Time (h)	5				Time (h)	6				Time (h)	7			
	R	G	B	Sum		R	G	B	Sum		R	G	B	Sum
0	70	65	116	251	0	71	67	115	253	0	65	63	113	241
3	135	77	79	291	3	129	77	82	288	3	136	75	76	287
6	153	80	80	313	6	151	81	84	316	6	141	76	80	297
9	151	83	76	310	9	147	83	76	306	9	139	78	75	292
12	150	82	79	311	12	149	82	78	309	12	139	77	76	292
15	151	84	78	313	15	145	84	78	307	15	138	79	76	293
18	151	86	75	312	18	144	85	76	305	18	136	79	73	288
21	151	86	83	320	21	149	86	82	317	21	140	79	80	299
24	155	90	84	329	24	151	91	85	327	24	143	85	83	311

Table E6 %RGB values of TCDA indicators with K_2CO_3 after exposure at 75% RH for 24 h (7 independent experiments)

Time (h)	1			Time (h)	2			Time (h)	3			Time (h)	4		
	R	G	B		R	G	B		R	G	B		R	G	B
0	28.0	25.5	46.5	0	27.8	27.8	46.6	0	27.3	25.4	47.3	0	27.7	26.1	46.2
3	48.6	26.3	25.1	3	47.8	47.8	25.8	3	47.9	25.9	26.2	3	47.0	26.5	26.5
6	47.0	26.2	26.8	6	48.2	48.2	26.1	6	49.1	25.4	25.4	6	48.4	25.8	25.8
9	47.3	27.0	25.8	9	48.9	48.9	24.5	9	49.5	26.6	23.9	9	48.7	26.6	24.7
12	47.1	26.7	26.1	12	48.6	48.6	25.4	12	49.2	26.1	24.6	12	48.9	26.3	24.8
15	46.6	27.5	26.0	15	47.9	47.9	25.2	15	48.6	27.1	24.3	15	48.0	27.3	24.8
18	46.5	27.6	25.8	18	47.7	47.7	24.9	18	48.6	27.1	24.3	18	48.3	27.4	24.3
21	46.0	26.9	27.2	21	46.7	46.7	26.3	21	47.6	26.6	25.7	21	47.3	26.4	26.4
24	45.2	27.7	27.1	24	46.5	46.5	26.0	24	47.1	27.5	25.4	24	46.6	27.4	26.0
Time (h)	5			Time (h)	6			Time (h)	7						
	R	G	B		R	G	B		R	G	B				
0	27.9	25.9	46.2	0	28.1	26.5	45.5	0	27.0	26.1	46.9				
3	46.4	26.5	27.1	3	44.8	26.7	28.5	3	47.4	26.1	26.5				
6	48.9	25.6	25.6	6	47.8	25.6	26.6	6	47.5	25.6	26.9				
9	48.7	26.8	24.5	9	48.0	27.1	24.8	9	47.6	26.7	25.7				
12	48.2	26.4	25.4	12	48.2	26.5	25.2	12	47.6	26.4	26.0				
15	48.2	26.8	24.9	15	47.2	27.4	25.4	15	47.1	27.0	25.9				
18	48.4	27.6	24.0	18	47.2	27.9	24.9	18	47.2	27.4	25.3				
21	47.2	26.9	25.9	21	47.0	27.1	25.9	21	46.8	26.4	26.8				
24	47.1	27.4	25.5	24	46.2	27.8	26.0	24	46.0	27.3	26.7				

Table E7 RGB values of TCDA indicators with K_2CO_3 after exposure at 42% RH for 24 h (7 independent experiments)

Time (h)	1				Time (h)	2				Time (h)	3				Time (h)	4			
	R	G	B	Sum		R	G	B	Sum		R	G	B	Sum		R	G	B	Sum
0	71	68	120	259	0	69	66	117	252	0	70	67	121	258	0	68	65	113	246
3	72	67	119	258	3	69	64	117	250	3	71	66	121	258	3	69	64	115	248
6	74	67	123	264	6	70	64	116	250	6	71	66	118	255	6	68	65	113	246
9	76	72	124	272	9	70	70	120	260	9	73	71	121	265	9	68	69	117	254
12	71	68	118	257	12	68	65	114	247	12	70	67	117	254	12	65	65	111	241
15	72	67	118	257	15	68	65	113	246	15	69	66	115	250	15	66	65	111	242
18	72	68	117	257	18	67	65	114	246	18	70	66	116	252	18	67	66	111	244
21	75	68	112	255	21	71	64	118	253	21	73	66	121	260	21	70	64	116	250
24	73	68	118	259	24	69	65	117	251	24	70	68	116	254	24	67	66	114	247
Time (h)	5				Time (h)	6				Time (h)	7								
	R	G	B	Sum		R	G	B	Sum		R	G	B	Sum					
0	65	66	113	244	0	66	65	112	243	0	65	63	108	236					
3	67	65	120	252	3	67	65	114	246	3	66	63	109	238					
6	68	64	117	249	6	66	64	111	241	6	63	63	106	232					
9	71	71	117	259	9	67	70	114	251	9	65	68	109	242					
12	67	66	113	246	12	64	64	109	237	12	62	63	104	229					
15	67	66	111	244	15	64	65	109	238	15	63	63	105	231					
18	67	67	112	246	18	64	65	110	239	18	62	64	105	231					
21	69	66	117	252	21	67	64	114	245	21	66	62	111	239					
24	68	67	112	247	24	65	65	109	239	24	63	64	106	233					

Table E8 %RGB values of TCDA indicators with K_2CO_3 after exposure at 42% RH for 24 h (7 independent experiments)

Time (h)	1			Time (h)	2			Time (h)	3			Time (h)	4		
	R	G	B		R	G	B		R	G	B		R	G	B
0	27.4	26.3	46.3	0	27.4	27.4	46.4	0	27.1	26.0	46.9	0	27.6	26.4	45.9
3	27.9	26.0	46.1	3	27.6	27.6	46.8	3	27.5	25.6	46.9	3	27.8	25.8	46.4
6	28.0	25.4	46.6	6	28.0	28.0	46.4	6	27.8	25.9	46.3	6	27.6	26.4	45.9
9	27.9	26.5	45.6	9	26.9	26.9	46.2	9	27.5	26.8	45.7	9	26.8	27.2	46.1
12	27.6	26.5	45.9	12	27.5	27.5	46.2	12	27.6	26.4	46.1	12	27.0	27.0	46.1
15	28.0	26.1	45.9	15	27.6	27.6	45.9	15	27.6	26.4	46.0	15	27.3	26.9	45.9
18	28.0	26.5	45.5	18	27.2	27.2	46.3	18	27.8	26.2	46.0	18	27.5	27.0	45.5
21	29.4	26.7	43.9	21	28.1	28.1	46.6	21	28.1	25.4	46.5	21	28.0	25.6	46.4
24	28.2	26.3	45.6	24	27.5	27.5	46.6	24	27.6	26.8	45.7	24	27.1	26.7	46.2
Time (h)	5			Time (h)	6			Time (h)	7						
	R	G	B		R	G	B		R	G	B				
0	26.6	27.0	46.3	0	27.2	26.7	46.1	0	27.5	26.7	45.8				
3	26.6	25.8	47.6	3	27.2	26.4	46.3	3	27.7	26.5	45.8				
6	27.3	25.7	47.0	6	27.4	26.6	46.1	6	27.2	27.2	45.7				
9	27.4	27.4	45.2	9	26.7	27.9	45.4	9	26.9	28.1	45.0				
12	27.2	26.8	45.9	12	27.0	27.0	46.0	12	27.1	27.5	45.4				
15	27.5	27.0	45.5	15	26.9	27.3	45.8	15	27.3	27.3	45.5				
18	27.2	27.2	45.5	18	26.8	27.2	46.0	18	26.8	27.7	45.5				
21	27.4	26.2	46.4	21	27.3	26.1	46.5	21	27.6	25.9	46.4				
24	27.5	27.1	45.3	24	27.2	27.2	45.6	24	27.0	27.5	45.5				

Table E9 RGB values of PCDA indicators with K_2CO_3 after exposure at 62% RH for 24 h (7 independent experiments)

Time (h)	1				Time (h)	2				Time (h)	3				Time (h)	4			
	R	G	B	Sum		R	G	B	Sum		R	G	B	Sum		R	G	B	Sum
0	71	68	120	259	0	69	66	117	252	0	70	67	121	258	0	68	65	113	246
3	72	67	119	258	3	69	64	117	250	3	71	66	121	258	3	69	64	115	248
6	74	67	123	264	6	70	64	116	250	6	71	66	118	255	6	68	65	113	246
9	76	72	124	272	9	70	70	120	260	9	73	71	121	265	9	68	69	117	254
12	71	68	118	257	12	68	65	114	247	12	70	67	117	254	12	65	65	111	241
15	72	67	118	257	15	68	65	113	246	15	69	66	115	250	15	66	65	111	242
18	72	68	117	257	18	67	65	114	246	18	70	66	116	252	18	67	66	111	244
21	75	68	112	255	21	71	64	118	253	21	73	66	121	260	21	70	64	116	250
24	73	68	118	259	24	69	65	117	251	24	70	68	116	254	24	67	66	114	247
Time (h)	5				Time (h)	6				Time (h)	7								
	R	G	B	Sum		R	G	B	Sum		R	G	B	Sum					
0	65	66	113	244	0	66	65	112	243	0	65	63	108	236					
3	67	65	120	252	3	67	65	114	246	3	66	63	109	238					
6	68	64	117	249	6	66	64	111	241	6	63	63	106	232					
9	71	71	117	259	9	67	70	114	251	9	65	68	109	242					
12	67	66	113	246	12	64	64	109	237	12	62	63	104	229					
15	67	66	111	244	15	64	65	109	238	15	63	63	105	231					
18	67	67	112	246	18	64	65	110	239	18	62	64	105	231					
21	69	66	117	252	21	67	64	114	245	21	66	62	111	239					
24	68	67	112	247	24	65	65	109	239	24	63	64	106	233					

Table E10 %RGB values of PCDA indicators with K_2CO_3 after exposure at 62% RH for 24 h (7 independent experiments)

Time (h)	1			Time (h)	2			Time (h)	3			Time (h)	4		
	R	G	B		R	G	B		R	G	B		R	G	B
0	27.4	26.3	46.3	0	27.4	27.4	46.4	0	27.1	26.0	46.9	0	27.6	26.4	45.9
3	27.9	26.0	46.1	3	27.6	27.6	46.8	3	27.5	25.6	46.9	3	27.8	25.8	46.4
6	28.0	25.4	46.6	6	28.0	28.0	46.4	6	27.8	25.9	46.3	6	27.6	26.4	45.9
9	27.9	26.5	45.6	9	26.9	26.9	46.2	9	27.5	26.8	45.7	9	26.8	27.2	46.1
12	27.6	26.5	45.9	12	27.5	27.5	46.2	12	27.6	26.4	46.1	12	27.0	27.0	46.1
15	28.0	26.1	45.9	15	27.6	27.6	45.9	15	27.6	26.4	46.0	15	27.3	26.9	45.9
18	28.0	26.5	45.5	18	27.2	27.2	46.3	18	27.8	26.2	46.0	18	27.5	27.0	45.5
21	29.4	26.7	43.9	21	28.1	28.1	46.6	21	28.1	25.4	46.5	21	28.0	25.6	46.4
24	28.2	26.3	45.6	24	27.5	27.5	46.6	24	27.6	26.8	45.7	24	27.1	26.7	46.2

Time (h)	5			Time (h)	6			Time (h)	7		
	R	G	B		R	G	B		R	G	B
0	26.6	27.0	46.3	0	27.2	26.7	46.1	0	27.5	26.7	45.8
3	26.6	25.8	47.6	3	27.2	26.4	46.3	3	27.7	26.5	45.8
6	27.3	25.7	47.0	6	27.4	26.6	46.1	6	27.2	27.2	45.7
9	27.4	27.4	45.2	9	26.7	27.9	45.4	9	26.9	28.1	45.0
12	27.2	26.8	45.9	12	27.0	27.0	46.0	12	27.1	27.5	45.4
15	27.5	27.0	45.5	15	26.9	27.3	45.8	15	27.3	27.3	45.5
18	27.2	27.2	45.5	18	26.8	27.2	46.0	18	26.8	27.7	45.5
21	27.4	26.2	46.4	21	27.3	26.1	46.5	21	27.6	25.9	46.4
24	27.5	27.1	45.3	24	27.2	27.2	45.6	24	27.0	27.5	45.5

APPENDIX F

AWARD

Figure F1 Winning the 2nd award from 5th Sci & Tech initiative and Sustainability Award by The Thai Institute of Chemical Engineering and Applied Chemistry, SCG Chemicals and Dow Chemical (From left to right : Mr. Jettapong Klaharn, Mr. Natdanai Suta, Mr. Pracharat Sa-ngadsup and Mr. Watcharin Ngampeungpis) ("System for real time monitoring of environmental parameters via optical responses")

APPENDIX G
MANUSCRIPT

UV Sensors with Tunable Sensitivity from Diacetylenes

Watcharin Ngampeungpis [a], Gamolwan Tumcharern [b] ,Prompong Pienpinijtham [c], Mongkol Sukwattanasinitt [d,*]

[a] *Program of Petrochemistry, Faculty of Science, Chulalongkorn University, Bangkok 10330, Thailand*

[b] *Thailand National Nanotechnology Center, National Science and Technology Development Agency, Pathumthanee 12120, Thailand*

[c] *Sensor Research Unit, Department of Chemistry, Faculty of Science, Chulalongkorn University, Bangkok 10330, Thailand*

[d] *Organic Synthesis Unit, Department of Chemistry, Faculty of Science and Nanotec-CU Center of Excellence on Food and Agriculture Chulalongkorn University, Bangkok 10330, Thailand.*

*Corresponding author. Tel.: +662-218-7620; Fax: +66-2-2187634.

E-mail: mongkol.s@chula.ac.th (M. Sukwattanasinitt).

Abstract

A series of paper-based polydiacetylene UV sensors containing with β-alanine ethyl ester and di-β-alanine ethyl ester were fabricated and investigated by photo scanner and analyzed by an image processing software. The tuning of the UV sensitivity was achieved by converting the lipid head group from carboxylic acid to the amide or diamide.

KEYWORDS: Polydiacetylene, UV Sensor, RGB

1. Introduction

Ultraviolet radiation is a very useful electromagnetic wave, which is commonly applied in germicidal and chemical curing processes of many products such as foods,

medicines, polymers and printing materials. On the other hand, excessive UV exposure is very harmful to human health, animals and plant life. For useful applications and hazardous precaution, the amount of radiation or so-called UV dose should be monitored and controlled. Therefore, development of a tool which can detect and record UV doses in real time is of importance. Currently, available techniques used in UV dose determination include photoelectric measurement [1] and colorimetric methods. The colorimetric method offers an attractive feature in the possibility for instrumentless naked eye detection or warning labels. Classes of compounds commonly used in colorimetric display of UV doses are spiropyran or spirooxazine [2]. This type of compounds change from colorless to darker color upon exposure to UV radiation that is not easily judged for the critical UV dose [3]. Furthermore, tunable sensitivity of the sensing materials is highly desirable but it has not been well established for such compounds.

Diacetylenes are a promising class of colorimetric UV responsive compounds due to their distinct color change with tunable sensitivity [4]. Color transitions of polydiacetylenes (PDAs) by heat [5], solvent [6], mechanical stress [7], molecular recognition [8], and pH [9] have been extensively investigated and PDAs have been applied as sensing materials in various form [10]. Self-assembled amphiphilic diacetylene lipids are readily polymerized to form conjugated PDAs with intense color. Although the color change of PDAs from blue to red by prolong UV irradiation have been noted, their color transition mechanism remains a topic under debate [11] and their applications for UV dose sensors have not been directed. Here, we would like to report our study on two series of diacetylene amido lipids (Figure 1) containing mono- and diamide head groups with variable lengths of methylene spacers in comparison with their diacetylene fatty acid analogue aiming for tunable colorimetric UV responsive materials.

2. Experimental

2.1 Materials and equipment

10,12-Pentacosadynoic acid (PCDA), 10,12-tricosadiynoic acid (TCDA), 6,8-nonadecadiynoic acid (NDDA) and 5,7-octadecadiynoic acid (ODDA) were purchased from GFS Chemicals USA, and other reagents were purchased from Sigma-Aldrich and Fluka. Analytical grade solvents were used without further purification. For extraction and chromatography, solvents were commercial grade and they were distilled prior to use. Column chromatography was performed on Merck silica gel 60 (70-230 mesh). Thin layer chromatography (TLC) was carried out using Merck 60 F254 plates with a thickness of 0.25 mm. All diacetylene monomers were dissolved in chloroform and filtered before use, to remove the unintentionally polymerized monomers. The ^{1}H and ^{13}C NMR spectra were collected on a 400 MHz NMR spectrometer (Murcury 400, Varian). The color transitions of PDAs were monitored and recorded by a scanner (Epson Perfection V33) for UV sensing or a webcam (ICON228, 14M pixels) linked to a commercial laptop computer.

2.2 Synthesis of diacetylene monomers

2.2.1 Ethyl 3-(pentacosa-10,12-diynoylamido)propanoate (EPCDP)

10,12-Pentacosadiynoic acid (0.38g, 1.0 mmol) and 1-hydroxybenzotriazole hydrate (HOBt•H_2O; 0.20 g, 1.5 mmol) were stirred to dissolve in CH_2Cl_2 (3 mL). The solution was then added with a solution of 1-ethyl-3-(3-dimethylaminopropyl)carbodiimide (EDC; 0.29 g, 1.5 mmol) in CH_2Cl_2 (5 mL) and stirred for 1 h. The mixture of ethyl 3-aminopropanoate hydrochloride (0.18 g, 1.2 mmol) and triethylamine (0.56 mL, 4.0 mmol) in CH_2Cl_2 (5 mL) was added dropwise into the mixture at 0 ℃. The resulting mixture was stirred at room temperature for 3 h. The mixture was evaporated and the crude product was eluted through a silica gel column using hexane and ethyl acetate (1:1 v/v) as the eluent. After the solvent removal, ethyl-3-pentacosa-10,12-diynamidopropanoate (EPCDP) was obtained as a white solid (0.41 g, 87% yield).

2.3 Preparation of paper-based diacetylene indicator and UV sensing study

A piece of filter paper (Whatman No.1) (1 × 5 cm^2) was dipped in a solution of diacetylene monomer with designated concentration (10 mM) in CH_2Cl_2 and dried in the air for 2 h. Then, it was stored at 4 ℃ for overnight. The indicators were irradiated by 254 nm UV light with the UV energy power of 1.4-1.5 mW/cm^2 for various periods of time. Their color images of the indicators were recorded by a commercial scanner and the RGB values were determined from the centered crop area of 50 × 50 pixels by an image-processing program.

2.4 Preparation of paper-based diacetylene indicator and thermal sensing study

A piece of filter paper (Whatman No.1) (1 × 5 cm^2) was dipped in a diacetylene monomer solution (10 mM) in CH_2Cl_2 and dried in the air for 2 h. Then, the indicators were irradiated by 254 nm UV light for specific periods of time depended on the time required for obtaining the maximum blue phase, typically 10 sec to 2 min. The indicators were attached on the outside of a glass beaker 600 mL filled with 400 mL of water. The beaker was gradually heated from 30 ℃ to 90 ℃ while their color images were monitored by webcam and the RGB values were determined from the centered crop area of 15 × 15 pixels by an image-processing program.

Results and discussion

The diacetylene fatty acids i.e. ODDA, NDDA, TCDA and PCDA (Figure 1) were commercially available. The ethyl-3-amidopropanoate derivatives (EODDP, ENDDP, ETCDP and EPCDP) and the corresponding diamides (EODDPP, ENDDPP, ETCDPP and EPCDPP) of the diacetylene fatty acids were synthesized from the carboxyl/amino condensation between the fatty acids and the mono- and di-β-alanine ethyl esters using 1-ethyl-3-(3-dimethylaminopropyl)carbodiimide (EDC) and hydroxybenzotriazole hydrate (HOBt) as the coupling reagents (Scheme S1). For portable and disposable applications,

paper is a very practical substrate for preparation of colorimetric sensors as it is omnipresent in white color, inexpensive and easy to be stored, transported and handled [12]. We have successfully fabricated PDA paper-based sensors by simple dipping filter paper (Whatman No.1) into the diacetylene monomer solutions (10 mM) followed by UV irradiation [13]. In this work, after an air dry, the monomer coated paper strips were stored at 4 °C for at least 12 h before their UV sensing properties were studied at 26.5±1.5 °C by irradiation with a 254 nm UV lamp at a power intensity of 1.40±0.05 mW/cm^2. At designated time intervals, the paper strips were removed from the irradiation zone and their colors were recorded by a photo scanner (300 dpi). The white diacetylenes coated paper initially turned blue or purple within ten seconds of the irradiation (Figure 2) signifying efficient topopolymerization of the diacetylene monomers to form the corresponding blue phase PDAs [14]. Extending the UV exposure time, the blue color changed to red at different irradiation time depending on the diacetylene structures. It is important to mention here that UV-vis absorption spectroscopy is not applicable for paper based sensors although it is a standard technique for colorimetric analysis of transparent samples of PDAs [15]. The related UV reflectance technique also did not give reproducible measurements for these rough surface samples. We thus opted to use a commercial photo scanner, which has a capability of wide image area capturing that gave more reproducible color data.

The RGB color system has been successfully used to analyze digital images of various colorimetric paper-based sensors [12,16]. The color images of the PDA sensors were thus converted to the RGB values by an image-processing program. With the numerical RGB data in hand, we would also like to propose here a method to translate the RGB values for sensitivity evaluation of the PDA paper-based sensors. The R, G and B values represent the extent of the red, green and blue components in the image. The values are varied from 0 to 255 that the greater the value is the higher the extent of the hue. For better comparison of the

colorimetric responses, the effects from the background light and color depth were evened out by using the percentage value of each RGB component calculated according to the following equation below, instead of its absolute value.

$$\%R \text{ (or \%G or \%B)} = \ (R \ (or\ G\ or\ B))/(R+G+B)\times 100$$

The plot of %R and %B against the UV dose clearly showed the increase of %R in the expense of %B (Figure 3) while %G remained relatively constant (Figure S17). The small error bars in the plots confirmed high reproducibility of the indicator preparation and color measurement.

To apply the RGB values for the sensitivity evaluation, we assigned the UV dose required at the intersection between %R and %B curves as the color transition UV dose. According to this assignment, the color transition point corresponds to a purple color. The diacetylene that turns to this color with less UV exposure dose is more UV sensitive. For examples, TCDA, ETCDP and ETCDPP required the exposure doses of 780±52 mJ/cm^2, 264±32 mJ/cm^2 and 130±9 mJ/cm^2, respectively, that represent the sensitivity order of TCDA < ETCDP < ETCDPP. The UV doses required for color transition of all paper-based sensors from all 12 diacetylene monomers were determined (Table S1) and plotted into a bar chart as shown in Figure 4. Within the series of the same head group, the diacetylenes with shorter alkyl chain (lower n or m numbers), either between the diyne and carboxyl group or in the lipid tail, required lower UV doses to cause the blue-to-red color transition indicating their greater UV sensitivity. The photo-induced thermochromism has been proposed for the blue-to-red color transition of several PDAs under prolong UV exposure [17]. In thermochromism, the role of the alkyl side chains on the temperature sensitivity has been attributed to the increase of their hydrophobic interaction, which in turn stabilizes the π-conjugated backbone [4,15,18]. We therefore conducted a thermochromism study of the blue PDAs obtained from all 12 monomers (see supporting information for detail experiments of the thermochromism

study). The blue-to-red color transition temperatures of the PDAs, depicted as the dots in Figure 4, within each series gave the same trend with the color transition UV doses. The results suggested that, the photo-induced thermochromism is responsible for the sensitivity trend of the PDAs with the same side chain head groups observed during the UV irradiation. Comparing between the series of different head groups, the UV doses required for the color transition of the fatty acid series (PCDA, TCDA, NDDA and ODDA) are generally greater than those of the corresponding monopropanamide (EPCDP, ETCDP, ENDDP and EODDP) and dipropanamide (EODDPP, ENDDPP, ETCDPP and EPCDPP). Interestingly, the comparison of UV sensitivity between the series is not well correlated with their thermal sensitivity. For example, the blue-to-red transition of EPCDP, a monopropanamide derivative, was observed at a much lower UV dose comparing with TCDA while both of them showed very similar color transition temperature. This difference is even more pronounced when comparing EPCDPP, a dipropanamide derivative, with TCDA; the less thermally sensitive EPCDPP is more UV sensitive than TCDA. The results demonstrated that the color transition caused by UV irradiation is not solely driven by the photo-induced thermochromism. The blue-to-red transition during the UV irradiation of some PDAs has also been attributed to the conformational change caused by the propagation of the polymer chain [19]. The orientation and strength of hydrogen bonding among the head groups in the molar self-assemblies of the diacetylene amido lipids are likely to be quite different from those of the diacetylene containing carboxylic acid groups. Since the blue-to-red transition of the amide series is faster in the UV irradiation but not in the heating process, their molecular assemblies are thus more readily to undergo the conformational alteration during the topopolymerization process.

Scanning electron microscopy (SEM) of the blue and red PDA coated on cellulose fibers of the filter paper strips revealed interesting microscopic phenomena. The diacetylene

containing carboxylic acid head group showed PDA film rupture upon the color transition from blue to red (Figure 5a and d). However, no significant change was observed for the PDAs obtained from the diacetylene containing mono- and diamide head groups. Similar results were also observed in the thermochromic color transition (Fig. S25). The rupture denoted that the blue-to-red color transition was accompanied with a major and sudden change in the molecular assembly [20]

Conclusion

At room temperature, both photo-induced thermochromism and direct photochromism cooperate in the UV-induced blue-to-red color transition of the PDAs generated from the diacetylene lipids containing carboxylic acid and amide head groups. The coarse tuning of the UV sensitivity was achieved by converting the lipid head group from carboxylic acid to the amide or diamide, which ably affects the photochromism sensitivity, while the fine tuning was possible by varying the aliphatic chain length, which progressively affects the photo-induced thermochromism sensitivity. The conversions of the head groups from the carboxylic acid to the amide groups alter the intermolecular interaction and orientation in the monomer assembly. The monomer structures, sensor preparation and evaluation techniques devised in this work should serve as guidelines for systematic study of solid-state chromic materials toward the development of economical and reliable colorimetric sensors.

Acknowledgement

This study was financially supported by the grants from the Thailand Nanotechnology Center (NANOTEC, NSTDA), the IIAC Chulalongkorn University Centenary Academic Development Project, the National Research University Project of Thailand, Office of the Higher Education Commission (AM1006A), the 90th Anniversary Fund of CU, the Thai

Government Stimulus Package 2 (TKK2555, SP2) and the Thailand Graduate Institute of Science and Technology (TGIST) for student scholarships.

Appendix A. Supplementary data

Supplementary data associated with this article can be found, in the online version, at doiXXXX.

References

[1] X. Z. Kong, C. X. Liu, W. Dong, X. D. Zhang, C. Tao, L. Shen, J. R. Zhou, Y. F. Fei, S. P. Ruan, Appl. Phys. Lett. 94 (2009) 123502.

[2] (a) M. I. Zakharova, C. Coudret, V. Pimienta, J. C. Micheau, S. Delbaere, G. Vermeersch, A. V. Metelitsa, N. Voloshin, V. I. Minkin, Photochem. Photobio. Sci. 9 (2010) 199-207. (b) G. K. Such, R. A. Evans, T. P. Davis, Macromolecules 39 (2006) 1391-1396.

[3] G. Berkovic, V. Krongauz and V. Weiss, Chemical Reviews 100 (2000) 1741-1753.

[4] C. Phollookin, S. Wacharasindhu, A. Ajavakom, G. Tumcharern, S. Ampornpun, T. Eaidkong, M. Sukwattanasinitt, Macromolecules 43 (2010) 7540-7548.

[5] (a) H. S. Peng, J. Tang, L. Yang, J. B. Pang, H. S. Ashbaugh, C. J. Brinker, Z. Z. Yang, Y. F. Lu, J. Am. Chem. Soc. 128 (2006) 5304-5305. (b) X. Y. Wang, J. E. Whitten, D. J. Sandman, J. Chem. Phys. 126 (2007) 184905.

[6] J. M. Kim, Y. B. Lee, D. H. Yang, J. S. Lee, G. S. Lee, D. J. Ahn, J. Am. Chem. Soc. 127 (2005) 17580-17581.

[7] R. A. Nallicheri, M. F. Rubner, Macromolecules 24 (1991) 517–525.

[8] D. H. Charych, J. O. Nagy, W. Spevak, M. D. Bednarski, Science 261 (1993) 585-588.

[9] U. Jonas, K. Shah, S. Norvez, D. H. Charych, J. Am. Chem. Soc. 121 (1999) 4580-4588. (b) Q. Cheng, M. Yamamoto, R. C. Stevens, Langmuir 16 (2000) 5333-5342.

[10] B. Yoon, S. Lee, J. M. Kim, Chem. Soc. Rev. 38 (2009) 1958-1968. (b) J. Yoon, S. K. Chae, J. M. Kim, J. Am. Chem. Soc. 129 (2007) 3038-3039. (c) M. van den Heuvel, D. Lowik, J. C. M. van Hest, Biomacromolecules 11 (2010) 1676-1683.

[11] (a) B. Tieke, G. Lieser, G. Wegner, J. Polym. Sci. Part A: Polym. Chem. 17 (1979) 1631-1644. (b) W. F. Yuan, G. Y. Jiang, Y. L. Song, L. Jiang, J. Appl. Polym. Sci. 103 (2007) 942-946. (c) T. Kanetake, Y. Tokura and T. Koda, Solid State Commun. 56 (1985) 803-807. (d) G. N. Patel, Radiat. Phys. Chem. 18 (1981) 913–925. (e) J. Song, J. S. Cisar, C. R. Bertozzi, J. Am. Chem. Soc. 126 (2004) 8459-8465. (f) A. A. Abdel-Fattah, F. Abdel-Rehim, Y. S. Soliman, Radiat. Phys. Chem. 81 (2012) 70-76.

[12] W. Martinez, S. T. Phillips, E. Carrilho, S. W. Thomas, H. Sindi, G. M. Whitesides, Anal. Chem. 80 (2008) 3699-3707.

[13] T. Eaidkong, R. Mungkarndee, C. Phollookin, G. Tumcharern, M. Sukwattanasinitt, S. Wacharasindhu, J. Mater. Chem. 22 (2012) 5970-5977.

[14] G. Wegner, Makromol. Chem. 154 (1972) 35-48.

[15] S. Okada, S. Peng, W. Spevak and D. Charych, Acc. Chem. Res. 31 (1998) 229-239.

[16] S. Friedman, S. Kolusheva, R. Volinsky, L. Zeiri, T. Schrader, R. Jelinek, Anal. Chem. 80 (2008) 7804-7811.

[17] M. Wenzel, G. H. Atkinson, J. Am. Chem. Soc. 111 (1989) 6123-6127.

[18] N. Fujita, Y. Sakamoto, M. Shirakawa, M. Ojima, A. Fujii, M. Ozaki, S. Shinkai, J. Am. Chem. Soc. 129 (2007) 4134-4135.

[19] (a) Q. Huo, K. C. Russell, R. M. Leblanc, Langmuir 15 (1999) 3972-3980. (b) L. Hsu, G. L. Cvetanovich, S. I. Stupp, J. Am. Chem. Soc. 130 (2008) 3892-3899. (c) Q. Huo, S. P. Wang, A. Pisseloup, D. Verma, R. M. Leblanc, Chem. Commun. (1999) 1601-1602.

[20] L. S. Li and S. I. Stupp, Macromolecules 30 (1997) 5313-5320.

Figures

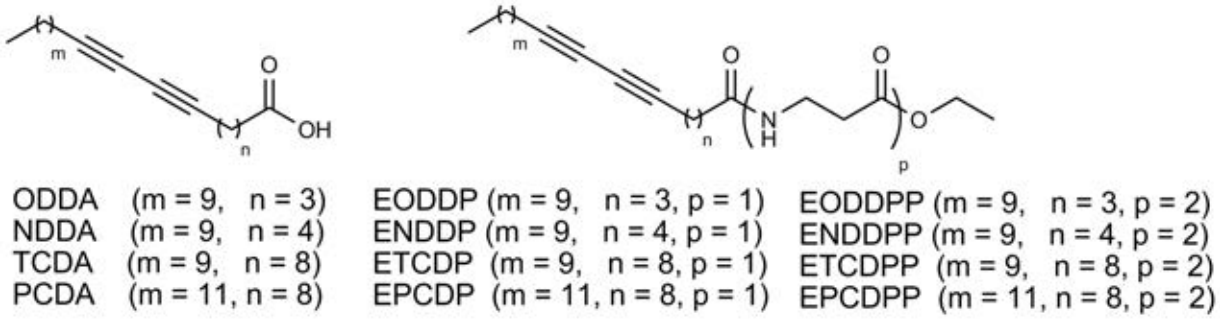

Fig. 1 Structures of diacetylene fatty acids and diacetylene amidolipids

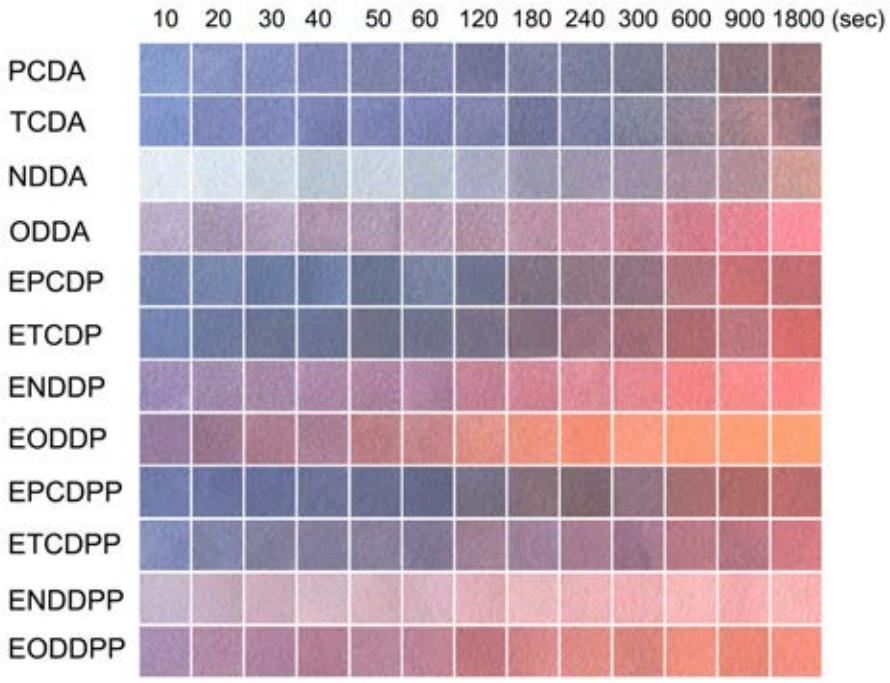

Fig. 2 The photographs of UV sensing of PDA indicators

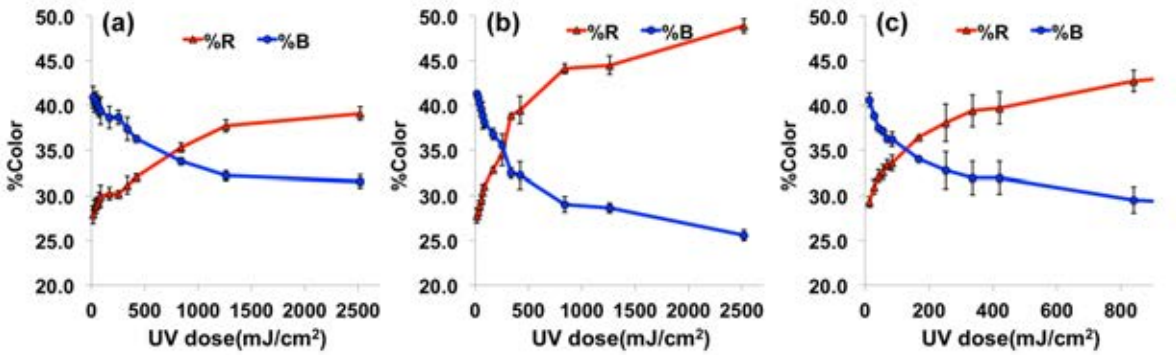

Fig. 3 Plots of %R and %B of paper coated with three representative diacetylenes, (a) TCDA, (b) ETCDP and (c) ETCDPP, upon UV-irradiation. The plots are the average data obtained from 3 independent samples with the error bars representing the standard deviation.

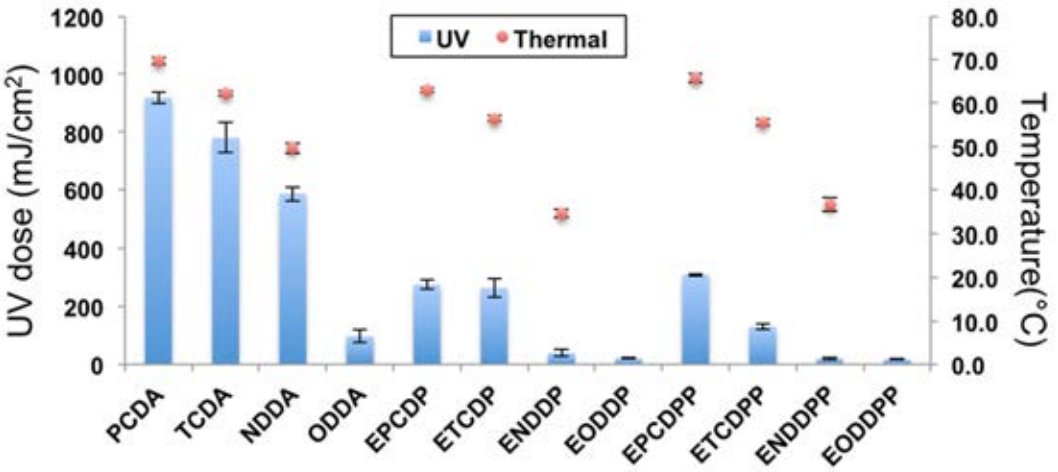

Fig. 4 Bar chart of UV doses required for causing blue-to-red color transition of diacetylene-based paper sensors comparing to their color transition temperatures (dot). The plots are the average data obtained from 3 independent samples with the error bars representing the standard deviation.

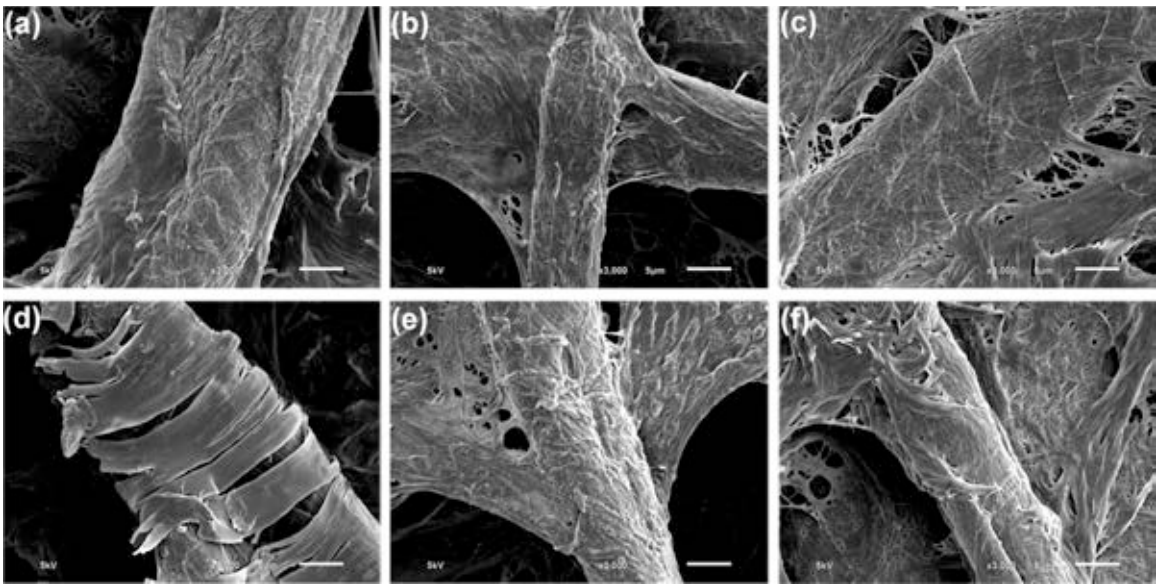

Fig. 5 SEM (5 kV) micrographs of filter paper coated with blue PDAs (a) PCDA (b) EPCDP (c) EPCDPP and red PDAs of (d) PCDA (e) EPCDP (f) EPCDPP. The scale bars represent 5 μm.

APPENDIX H

PATENT

รายละเอียดการประดิษฐ์

ชื่อที่แสดงถึงการประดิษฐ์

กระบวนการระบุการเปลี่ยนแปลงสีของอินดิเคเตอร์โดยใช้เทคโนโลยีประมวลผลภาพ

สาขาวิทยาการที่เกี่ยวข้องกับการประดิษฐ์

เป็นการประดิษฐ์ที่เกี่ยวข้องกับวิธีการประมวลผลภาพ (Digital Image Processing) โดยนำมาใช้ในการระบุการเปลี่ยนแปลงของอินดิเคเตอร์

ภูมิหลังของศิลปะหรือวิทยาการที่เกี่ยวข้อง

ปัจจุบันมีการพัฒนาอินดิเคเตอร์ต่าง ๆ เพื่อใช้ในชีวิตประจำวันและในอุตสาหกรรม เช่น การตรวจวัดอุณหภูมิ ความชื้น และรังสียูวี เป็นต้น ซึ่งจะใช้ในการตรวจวัดสภาพแวดล้อมของการจัดเก็บผลิตภัณฑ์ต่าง ๆ เช่น ยา อุปกรณ์อิเล็กโทรนิค และอาหาร เพราะถ้ามีการเก็บรักษาผลิตภัณฑ์อย่างไม่ถูกต้อง จะทำให้เกิดความเสียหายต่อผลิตภัณฑ์นั้น ๆ เช่น ยาอาจเกิดการสลายตัวหรือเสื่อมสภาพเมื่อเก็บไว้ในบริเวณที่มีอุณหภูมิสูง อุปกรณ์อิเล็กโทรนิคต่าง ๆ อาจจะเกิดความเสียหายเมื่อเก็บไว้ในบริเวณที่มีความชื้นสูง ซึ่งโดยทั่วไป อินดิเคเตอร์จะมีการเปลี่ยนแปลงจะมีการเปลี่ยนแปลงสีซึ่งสามารถสังเกตการเปลี่ยนแปลงได้ด้วยตาเปล่าแต่อาจจะไม่สามารถบอกการเปลี่ยนแปลงในเชิงปริมาณได้
จึงจำเป็นต้องใช้เครื่องมือช่วยในการตรวจวัดการดูดกลืนแสง เช่น เครื่องยูวีวิซิเบิลสเปกโตรมิเตอร์ (UV-Visible Spectrometer) และรายงานผลออกมาอยู่ในรูปความยาวคลื่น ซึ่งบอกสีได้คร่าว ๆ โดยสีที่ตามองเห็นจะเป็นสีตรงข้ามกับสีที่ถูกดูดกลืน
ซึ่งมีงานวิจัยที่เสนอการรายงานผลการเปลี่ยนสีของอินดิเคเตอร์จะให้ค่าออกมาในรูปของ %CR (รูปที่ 1) [Charych และคณะ Direct Colorimetric Detection of a Receptor-Ligand Interaction by a Polymerized Bilayer Assembly, *Science*, **1993**, 261, 585-588] ซึ่งสามารถหาได้จากสมการ

$$\%CR = (PB_0 - PB_1)/PB_0 \times 100\%$$

ซึ่ง $PB = A_{blue}/(A_{blue}+A_{red})$ และ A_{blue} และ A_{red} คือค่าการดูดกลืนแสงที่ 640 nm และ 540 nm
ซึ่งยากต่อการบอกจุดเปลี่ยนแปลงของอินดิเคเตอร์ นอกจากนี้
สารตัวอย่างส่วนใหญ่จะต้องใช้ในรูปของเหลวและไม่สามารถวัดตัวอย่างที่มีลักษณะทึบแสงได้

ต่อมาได้มีงานวิจัยที่นำระบบประมวลผลทางภาพมาใช้ในการวัดค่าการเปลี่ยนสีเพื่อบอกการเปลี่ยนแปลงของอินดิเคเตอร์ซึ่งสัมพันธ์กับปริมาณสารที่ต้องการตรวจวัด เช่น Martinez และคณะ [Simple telemedicine for developing regions: camera phones and paper-based microfluidic devices for real-time, off-site diagnosis, *Anal. Chem.* **2008**, 80, 3699–3707] ได้เตรียมอุปกรณ์ไมโครฟลูอิดิกบนกระดาษ เพื่อตรวจวิเคราะห์สารหลาย ๆ ชนิดในเวลาเดียวกัน เพื่อตรวจวัดหาปริมาณความเข้มข้นของกลูโคสและโปรตีนในน้ำปัสสาวะเทียมโดยใช้กล้องดิจิตอล

หรือสแกนเนอร์บันทึกภาพสีของอุปกรณ์กระดาษแล้วส่งข้อมูลไปยังห้องปฏิบัติการวิเคราะห์ผ่านระบบเครือข่ายโทรศัพท์ไร้สายเพื่อนำภาพไปวิเคราะห์เปรียบเทียบความเข้มของสีเทียบกับกราฟมาตราฐาน (Calibration curve) ซึ่งนับได้ว่าเป็นแนวคิดทางเลือกใหม่ในการตรวจสุขภาพที่สะดวก ราคาไม่แพง และเหมาะกับการตรวจนอกโรงพยาบาล หรือ ณ สถานพยาบาลที่ห่างไกล

นอกจากนี้ ในอุตสาหกรรม มีการประยุกต์ใช้ระบบประมวลภาพในกระบวนการผลิตต่าง ๆ เช่น สิทธิบัตรอเมริกาเลขที่ 5533628 ได้ประดิษฐ์อุปกรณ์เพื่อใช้สำหรับเรียงวัตถุตามสีและขนาด ซึ่งมีการใช้ระบบประมวลผลทางภาพ ระบบสี HSI เพื่อช่วยในการแยกฉากหลังออกจากวัตถุ จากนั้น ค่าสีในช่องสัญญาณสี H จะถูกนำมาใช้เรียงมะเขือเทศ จากแดง เหลือง เขียว และขนาดวัดได้จากการนับจำนวนพิกเซลของแต่ละวัตถุที่ทำการแยกออกจากฉากหลังได้

สิทธิบัตรอเมริกาเลขที่ 2008/0285848 A1 ได้คิดค้นวิธีหาค่าสีที่สนใจ โดยใช้อัตราส่วนคัลเลอร์สเปซ (color space) ซึ่งหาจากนำค่าองค์ประกอบสีของแต่ละพิกเซลในรูป แล้วหารด้วยค่าสีที่มากที่สุด ของแต่ละพิกเซลแล้วจะสามารถสังเกตการเปลี่ยนแปลงของสีที่สนใจได้ โดยมีจุดเด่นคือสามารถหาสีของวัตถุที่สนใจซึ่งอยู่ในสิ่งแวดล้อมที่มีแสงไม่เท่ากันได้ เช่น อยู่กลางแสงแดด หรืออยู่ในห้องมืด ด้วยกล้องเวปแคมซึ่งมีราคาถูก

ในปีค.ศ. 2008 Friedman และคณะ [Lipid/polydiacetylene films for colorimetric protein surface-charge analysis, *Anal. Chem.* **2008**, 80, 7804–7811] ได้เสนอวิธีวิเคราะห์หาประจุบนพื้นผิวของโปรตีนวิธีใหม่ โดยใช้ระบบประมวลผลทางภาพ โดยการปรับแรงกระทำระหว่างโปรตีนกับ poly(10, 12-tricosadiynoic acid) ในรูปฟิล์มบนแผ่นกระจกโดยวิธีแลง-เมียร์-เชเฟอร์(Langmuir-Shaefer method) เมื่อเติมโปรตีนที่มีประจุบวก
โปรตีนจะไปจับกับประจุลบของหมู่คาร์บอกซิลลิกของพอลิไดแอเซทิลีน
ทำให้เกิดการเปลี่ยนสีจากสีน้ำเงินเป็นสีแดง
และสามารถวิเคราะห์เชิงปริมาณได้โดยวัดค่าความเข้มสีแดงที่เพิ่มขึ้นในรูป
โดยรายงานผลเป็น %RCS ซึ่งหาได้จากสมการ

$$\%RCS = \frac{(r_{sample} - r_0)}{r_{max} - r_0} \times 100\%$$

โดยที่ r_{sample} คือ ค่าสีแดงของสารตัวอย่าง

r_0 คือ ค่าสีแดงเริ่มต้นของแบลงค์(Blank)

net RCS = RCS_1-RCS_0

ทำให้สามารถระบุเอกลักษณ์ของประจุบนพื้นผิวของโปรตีนได้

ในปี 2012 Eaidkong และคณะ ได้ศึกษาเกี่ยวกับพอลิไดแอเซทิลีนอินดิเคเตอร์เพื่อใช้ในการตรวจวัดไอของตัวทำละลายอินทรีย์ ซึ่งได้นำระบบสี RGB มาใช้ในการบอกปริมาณของการเปลี่ยนแปลงของสี จากนั้นนำไปใช้แยกชนิดของตัวทำละลายอินทรีย์โดยการใช้โปรแกรมทางสถิติพีซีเอ (PCA, principal component analysis) ซึ่งวิธีนี้ได้ใช้ค่า RGB โดยตรง จึงอาจจะมีผลของแสงสภาวะแวดล้อม ทำให้ผลวิเคราะห์ที่ได้ผิดพลาดได้

ในปี 2012 Abdel-Fattah และคณะ [A new label dosimetry system based on pentacosa-diynoic acid monomer for low dose applications, *Radiation Physics and Chemistry*, **2012**, 81, 70-76] ได้นำระบบสี Lab มาใช้ในการบอกปริมาณการเปลี่ยนแปลงของพอลิไดแอเซทิลีนที่จะนำมาใช้เป็นอินดิเคเตอร์ในการตรวจวัดปริมาณรังสีแกมม่า โดยใช้ช่องสี b ที่ลดลงเป็นตัวบอกปริมาณของสีน้ำเงินที่เพิ่มขึ้น

จากงานวิจัยและสิทธิบัตรเกี่ยวกับการใช้การประมวลผลทางภาพมาใช้ในการวิเคราะห์เชิงปริมาณของอินดิเคเตอร์ ซึ่งการเปลี่ยนแปลงสียังไม่สามารถบอกจุดเปลี่ยนสีที่แม่นยำ และต้องใช้เครื่องมือที่มีราคาแพง

ลักษณะและความมุ่งหมายของการประดิษฐ์

การประดิษฐ์นี้ได้นำเสนอวิธีที่ใช้ในบอกจุดเปลี่ยนแปลงสีด้วยเทคโนโลยีประมวลผลภาพ เพื่อใช้กับอินดิเคเตอร์ที่มีการเปลี่ยนแปลงสีสำหรับการตรวจวัดต่าง ๆ โดยจะเก็บภาพการเปลี่ยนแปลงสีของอินดิเคเตอร์ ด้วยกล้องถ่ายภาพกล้องเวปแคมหรือสแกนเนอร์ จากนั้นทำการหาค่าสี RGB และนำไปคำนวณเป็นค่าเปอร์เซ็นต์ของแต่ละองค์ประกอบสี และนำไปแสดงผลให้อยู่ในรูปกราฟเส้น ซึ่งจะให้ผลที่ระบุช่วงการเปลี่ยนสีที่แคบ ชัดเจนมากขึ้น มีความแม่นยำสูง และลดผลกระทบจากแสงแวดล้อมได้ กระบวนการทำไม่ซับซ้อน

คำอธิบายรูปเขียนโดยย่อ

รูปที่ 1 แสดงกราฟเปอร์เซ็นต์คัลเลอริเมตริกเรสปอนส์ (Colorimetric Response, %CR) ของการเปลี่ยนแปลงสีของอินดิเคเตอร์ที่ใช้ในการตรวจไวรัส
รูปที่ 2 แสดงอุปกรณ์และส่วนประกอบเพื่อการตรวจวัดการเปลี่ยนสีของอินดิเคเตอร์
รูปที่ 3 แสดงขั้นตอนการตรวจวัดการเปลี่ยนแปลงสีของอินดิเคเตอร์โดยการประมวลผลภาพ
รูปที่ 4 การเปลี่ยนสีของอินดิเคเตอร์ตรวจวัดอุณหภูมิ
รูปที่ 5 แสดงกราฟระหว่างเปอร์เซ็นต์สีกับอุณหภูมิ
รูปที่ 6 การเปลี่ยนสีของอินดิเคเตอร์ตรวจวัดปริมาณรังสียูวี
รูปที่ 7 แสดงกราฟระหว่างเปอร์เซ็นต์สีกับปริมาณรังสียูวี
ตารางที่ 1 แสดงค่าองค์ประกอบสีของอินดิเคเตอร์กับอุณหภูมิ
ตารางที่ 2 แสดงค่าเปอร์เซ็นต์องค์ประกอบสีของอินดิเคเตอร์กับอุณหภูมิ
ตารางที่ 3 แสดงค่าองค์ประกอบสีของอินดิเคเตอร์กับปริมาณรังสียูวี
ตารางที่ 4 แสดงค่าเปอร์เซ็นต์องค์ประกอบสีของอินดิเคเตอร์กับปริมาณรังสียูวี

การเปิดเผยการประดิษฐ์โดยสมบูรณ์

เริ่มจากการนำภาพที่ได้จากสแกนเนอร์ กล้องถ่ายภาพ หรือกล้องเวปแคม มาประมวลผลทางภาพด้วยระบบสี RGB ซึ่งจะทำให้ได้องค์ประกอบของสีต่าง ๆ จากนั้นจะทำการคำนวณเปอร์เซนต์องค์ประกอบสีต่าง ๆ ดังสมการ

$$\%R = \frac{R}{R+G+B} \times 100 \qquad (1)$$

$$\%G = \frac{G}{R+G+B} \times 100 \qquad (2)$$

$$\%B = \frac{B}{R+G+B} \times 100 \qquad (3)$$

ซึ่งการคำนวณเป็นเปอร์เซนต์ มีข้อดีคือ ช่วยลดผลของแสงแวดล้อม เพราะถ้าใช้ค่า RGB จริงจะให้ค่าที่ผันผวนมากตามปริมาณของแสงแวดล้อม

จากนั้นนำค่า %R %G และ %B ไปสร้างกราฟเส้น จะได้ผลแสดงดังรูปที่ 5 จากกราฟเป็นอินดิเคเตอร์วัดอุณหภูมิที่เปลี่ยนสีจากสีน้ำเงินเป็นสีแดงเมื่ออุณหภูมิเพิ่มขึ้น ซึ่งเราจะกำหนดจุดสีม่วง (%R = %B) เป็นจุดเปลี่ยนสีของอินดิเคเตอร์ ซึ่งจะทำให้สามารถหาค่าอุณหภูมิที่ทำให้อินดิเคเตอร์เกิดการเปลี่ยนสี โดยดูจากจุดตัดระหว่าง %R และ %B

ตัวอย่าง

ตัวอย่างที่ 1 วิธีการระบุจุดเปลี่ยนสีของพอลิ(สิบ,สิบสอง เพนตะโคสะไดไอน์โนอิกแอซิด) (poly(10,12-pentacosadiynoic acid) ,PCDA) อินดิเคเตอร์เพื่อใช้ในการตรวจวัดอุณหภูมิ

พอลิ(สิบ, สิบสอง เพนตะโคสะไดไอน์โนอิกแอซิด) ถูกเตรียมเป็นอินดิเคเตอร์กระดาษซึ่งจะถูกนำมาติดกับด้านข้างของบีกเกอร์ขนาด 600 mL ซึ่งบรรจุน้ำอยู่ 400 mL อินดิเคเตอร์จะถูกให้ความร้อนจาก 30 °C ถึง 90 °C และถ่ายภาพโดยใช้กล้องเวบแคมที่ต่อกับคอมพิวเตอร์

จากนั้นนำรูปที่ได้จากกล้องเวปแคม นำมาประมวลผลทางภาพเพื่อหาค่าสี RGB ดังแสดงในตารางที่ 1 จากนั้นนำไปคำนวณหาค่า %R, %G, และ %B ดังแสดงในตารางที่ 2

จากตารางที่ 2 จะเห็นได้ว่าค่า %G ค่อนข้างคงที่ เพราะการเปลี่ยนสีของอินดิเคเตอร์เป็นการเปลี่ยนจากสีน้ำเงินเป็นสีแดง ดังนั้นเราจึงสามารถใช้จุดที่ %R เท่ากับ %B เป็นจุดเปลี่ยนสีของอินดิเคเตอร์ ซึ่งการหาจุดตัดจะหาจากสร้างสมการเส้นตรงสองเส้น ตามรูปที่ 5 จุดตัดจะอยู่ระหว่างอุณหภูมิ 70-75°C ซึ่งที่ 70°C จะมีค่า %R, %G, %B = 35.8, 27.2, 37.0 และที่ 75°C จะมีค่า %R, %G, %B = 41.4, 26.8, 31.8 ซึ่งจะนำ %R ที่ 70°C และ 75°C มาสร้างเป็นสมการเส้นตรงตามสมการ

$y = ((y_2-y_1)/(x_2-x_1))x+c$

$x_1 = 70$, $y_1 = 35.8$, $x_2 = 75$, $y_2 = 41.4$

จะได้ว่า $y = ((41.4-35.8)/(75-70))x + c$

$y = 1.12x - 42.6$

และในทำนองเดียวกันสร้างเส้นตรงจาก %B อีกหนึ่งเส้นจาก $x_1 = 70$, $y_1 = 37.0$, $x_2 = 75$, $y_2 = 31.8$

จะได้สมการ

$y = -1.05x + 110.2$

นำ สมการเส้นตรงสองเส้นมาหาจุดตัดโดยแก้สมการหาค่า x และ y จะได้จุดตัดที่ x = 70.5, y = 36.4 หมายความว่า พอลิไดแอเซทิลีนอินดิเคเตอร์ชนิดนี้สามารถเปลี่ยนเป็นสีม่วงเมื่อมีอุณหภูมิ 70.5 °C

ตัวอย่างที่ 2 เอทิล-3-ไตรโคสะ-สิบ, สิบสอง-ไดไอนามิโดโพรพาโนเอต poly(Ethyl-3-tricosa-10,12-diynamidopropanoate) อินดิเคเตอร์เพื่อใช้ในการตรวจวัดปริมาณรังสียูวี

เอทิล-3-ไตรโคสะ-สิบ, สิบสอง-ไดไอนามิโดโพรพาโนเอตถูกเตรียมเป็นอินดิเคเตอร์กระดาษ ซึ่งจะถูกฉายแสงด้วยรังสียูวี 254 nm ที่เวลาต่าง ๆ จากนั้นเก็บข้อมูลโดยใช้สแกนเนอร์ที่ต่อกับคอมพิวเตอร์

จากนั้นนำรูปที่ได้จากสแกนเนอร์ นำมาประมวลผลทางภาพเพื่อหาค่าสี RGB ดังแสดงในตารางที่ 3 จากนั้นนำไปคำนวณหาค่า %R, %G, และ %B ดังแสดงในตารางที่ 4 จากนั้นหาจุดตัดจะหาจากสร้างสมการเส้นตรงสองเส้น ตามรูปที่ 7 จุดตัดจะอยู่ระหว่างปริมาณรังสียูวี 252-336 mJ/cm^2 ซึ่งที่ 252 mJ/cm^2 มีค่า %R, %G, %B = 33.2, 30.5, 36.4 และที่ 336 mJ/cm^2 มีค่า %R, %G, %B = 39.1, 28.9, 32.1

ซึ่งมาสร้างเป็นสมการเส้นตรงตามสมการ

$y = ((y_2-y_1)/(x_2-x_1))x+c$

$x_1 = 252$, $y_1 = 33.2$, $x_2 = 336$, $y_2 = 39.1$

จะได้ว่า $y = 0.07x – 15.5$

และในทำนองเดียวกันสร้างเส้นตรงจาก %B อีกหนึ่งเส้นจาก $x_1 = 252$, $y_1 = 36.4$, $x_2 = 336$, $y_2 = 32.1$

จะได้สมการ

$y = -0.05x + 49.3$

นำ สมการเส้นตรงสองเส้นมาหาจุดตัดโดยแก้สมการหาค่า x และ y จะได้จุดตัดที่ x = 278.6, y = 35.37

หมายความว่า
พอลิไดแอเซทิลีนอินดิเคเตอร์ชนิดนี้สามารถเปลี่ยนเป็นสีม่วงเมื่อได้รับปริมาณรังสียูวี 278.6 mJ/cm^2

5 **วิธีการในการประดิษฐ์ที่ดีที่สุด**

ตามที่ได้กล่าวไว้แล้วในหัวข้อการเปิดเผยการประดิษฐ์โดยสมบูรณ์

การใช้การประดิษฐ์ในการผลิตทางอุตสาหกรรม หัตถกรรม เกษตรกรรม หรือ พาณิชยกรรม

อุตสาหกรรม พาณิชยกรรม

บทสรุปการประดิษฐ์

การประดิษฐ์นี้เกี่ยวข้องกับการนำเสนอวิธีระบุจุดเปลี่ยนสีของอินดิเคเตอร์โดยใช้เทคโนโลยีประมวลผลภาพ โดยการนำภาพที่ได้จากเครื่องสแกนเนอร์ กล้องถ่ายภาพหรือกล้องเวปแคม มาหาค่าสีโดยใช้ระบบสี RGB จากนั้นจะนำค่าองค์ประกอบสีต่าง ๆ มาคำนวณเป็นเปอร์เซ็นต์เพื่อลดผลกระทบของแสงแวดล้อม และสร้างเป็นกราฟเพื่อหาจุดตัดของระหว่างองค์ประกอบของสี ซึ่งถือว่าเป็นจุดเปลี่ยนแปลงของอินดิเคเตอร์

ข้อถือสิทธิ

1. การระบุจุดเปลี่ยนแปลงสีของอินดิเคเตอร์โดยใช้เทคโนโลยีประมวลผลภาพ ที่ประกอบด้วย

    - สแกนเนอร์(200) กล้องถ่ายภาพหรือกล้องเวปแคม(240) สำหรับการรับภาพอินดิเคเตอร์ (ที่ต้องการหาการเปลี่ยนสี)

    - หน่วยประมวลผล (220) ซึ่งรับข้อมูลภาพที่ได้จากสแกนเนอร์ กล้องถ่ายภาพหรือกล้องเวปแคมที่ใช้ในการบันทึกการเปลี่ยนแปลงสี

    - ส่วนแสดงผล(230) สำหรับแสดงผลการวิเคราะห์ที่ได้จากหน่วยประมวลผลดังกล่าว โดยกระบวนการหาจุดเปลี่ยนแปลงสีของอินดิเคเตอร์ดังกล่าว มี**ลักษณะเฉพาะ**คือ การนำภาพที่ได้มาประมวลผลเป็นค่าสี RGB และคำนวณให้อยู่ในรูปเปอร์เซนต์ เพื่อลดผลกระทบของแสงแวดล้อม และนำไปสร้างเป็นกราฟเส้นโดยกำหนดให้ค่าเปอร์เซนต์ของสีที่เท่ากันเป็นจุดเปลี่ยนแปลงของอินดิเคเตอร์

2. ตามข้อถือสิทธิ์ที่ 1 จากกราฟ ที่จุดที่มีค่าสีเท่ากัน สามารถใช้กับสารที่เปลี่ยนแปลงอื่น ๆ หรือการตรวจวัดการเปลี่ยนแปลงอื่น ๆได้

3. ตามข้อถือสิทธิ์ที่ 1 สามารถใช้ระบบสีอื่น ๆ นอกจาก RGB ได้

4. ตามข้อถือสิทธิ์ที่ 1 สามารถใช้กับค่าสีโดยไม่ต้องคำนวณเป็นเปอร์เซนต์

5. ตามข้อถือสิทธิ์ที่ 1 สามารถใช้กับอุปกรณ์วัดค่าสีต่าง ๆ โดยไม่ได้ผ่านหน่วยประมวลผลที่เป็นคอมพิวเตอร์

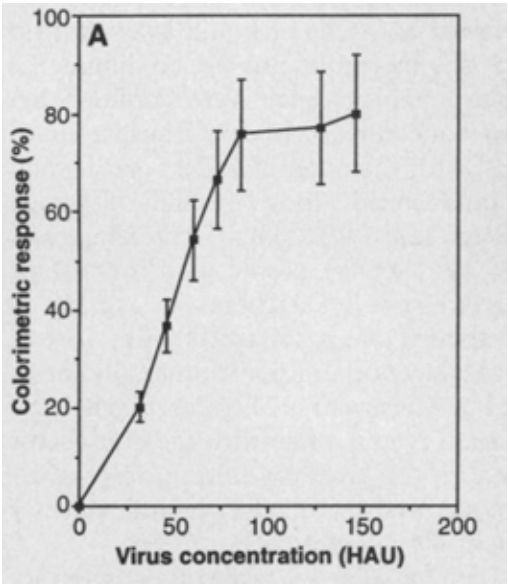
A
Colorimetric response (%)
Virus concentration (HAU)
0
20
40
60
80
100
0
50
100
150
200

รูปที่ 1

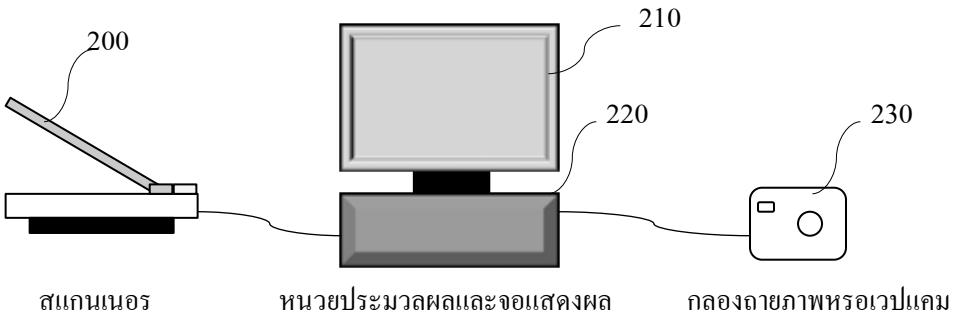
200
210
220
230
สแกนเนอร
หนวยประมวลผลและจอแสดงผล
กลองถายภาพหรอเวปแคม

รูปที่ 2

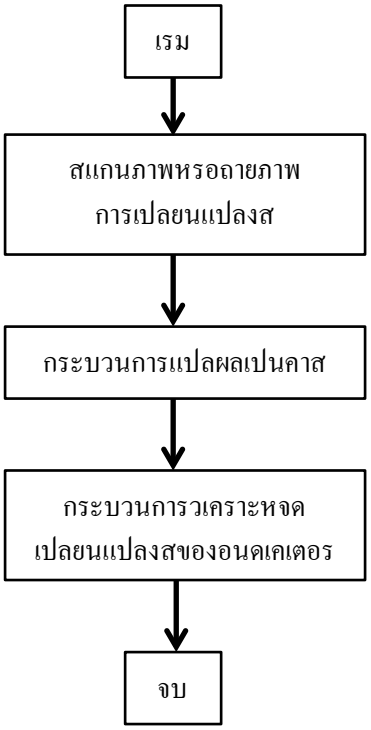
เรม
สแกนภาพหรอถายภาพ
การเปลยนแปลงส
กระบวนการแปลผลเปนคาส
กระบวนการวเคราะหจด
เปลยนแปลงสของอนดเคเตอร
จบ

รูปที่ 3

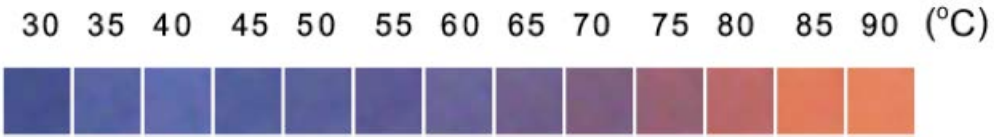
30 35 40 45 50 55 60 65 70 75 80 85 90 (°C)

รูปที่ 4

T(°C)	Color			
	R	G	B	Sum
30	70	81	143	294
35	86	99	162	347
40	95	107	172	374
45	83	95	155	333
50	89	96	153	338
55	91	89	147	327
60	105	100	151	356
65	112	96	139	347
70	124	94	128	346
75	150	97	115	362
80	185	104	105	394
85	224	122	92	438
90	229	131	95	455

ตารางที่ 1

T(°C)	%Color		
	%R	%G	%B
30	23.8	27.6	48.6
35	24.8	28.5	46.7
40	25.4	28.6	46.0
45	24.9	28.5	46.5
50	26.3	28.4	45.3
55	27.8	27.2	45.0
60	29.5	28.1	42.4
65	32.3	27.7	40.1
70	35.8	27.2	37.0
75	41.4	26.8	31.8
80	47.0	26.4	26.6
85	51.1	27.9	21.0
90	50.3	28.8	20.9

ตารางที่ 2

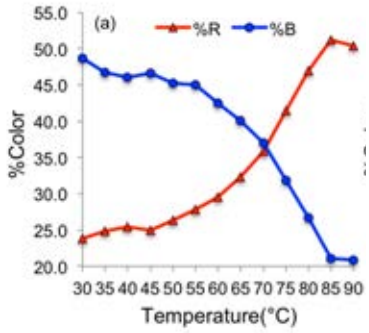

รูปที่ 5

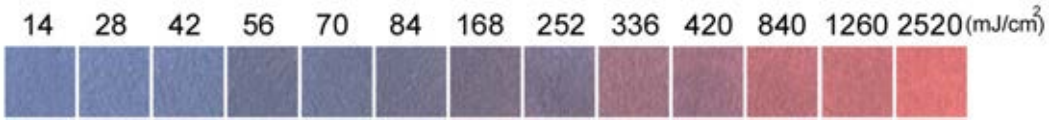

รูปที่ 6 การเปลี่ยนสีของอินดิเคเตอร์ตรวจวัดปริมาณรังสียูวี

UV dose (mJ/cm^2)	Color			
	R	G	B	Sum
14	113	129	172	414
28	118	133	173	424
42	116	129	166	411
56	110	115	142	367
70	113	118	149	380
84	114	114	138	366
168	120	111	131	362
252	123	113	135	371
336	157	116	129	402
420	154	113	129	396
840	186	113	120	419
1260	194	114	120	428
2520	222	118	120	460

ตารางที่ 3

UV dose (mJ/cm^2)	%color		
	%R	%G	%B
14	27.3	31.2	41.5
28	27.8	31.4	40.8
42	28.2	31.4	40.4
56	30.0	31.3	38.7
70	29.7	31.1	39.2
84	31.1	31.1	37.7
168	33.1	30.7	36.2
252	33.2	30.5	36.4
336	39.1	28.9	32.1
420	38.9	28.5	32.6
840	44.4	27.0	28.6
1260	45.3	26.6	28.0
2520	48.3	25.7	26.1

ตารางที่ 4

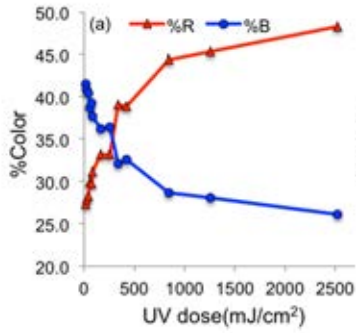

รูปที่ 7

VITAE

Mr. Watcharin Ngampeungpis was born on April 10, 1983 in Bangkok, Thailand. He graduated with Bachelor's Degree in Chemistry from Faculty of Science, Chulalongkorn University in 2005. For Master 's Degree, he graduated in Inorganic Chemistry in Department of Chemistry, Faculty of Science, Chulalongkorn University in 2008. After graduated in Master degree, he worked at Mahaphant fiber-cement public company as a researcher and then he continued his study in a Ph.D degree in program of Petrochemistry at Chulalongkorn University in academic year and completed in 2012. His current address is 162 Soi Wachirathumsathit 28, Sukhumvit 101/1 road, Bangna, Bangna, Bangkok, 10260.